

**CUADERNOS**  
de  
**INVESTIGACIÓN GEOGRÁFICA**  
*GEOGRAPHICAL RESEARCH LETTERS*



**Tomo 49 (2)**

**2023**

**ISSN: 1697-9540**

**UNIVERSIDAD DE LA RIOJA**  
**LOGROÑO (ESPAÑA)**

# CUADERNOS DE INVESTIGACIÓN GEOGRÁFICA

## GEOGRAPHICAL RESEARCH LETTERS

### Editor Principal / Editor-in-Chief

José Arnáez (Universidad de La Rioja)

### Editores Adjuntos / Associate Editors

Jorge Lorenzo-Lacruz (Universidad de La Rioja)

Amelia Gómez-Villar (Universidad de León)

Noemí Lana-Renault Monreal (Universidad de La Rioja)

Purificación Ruiz-Flaño (Universidad de La Rioja)

### Consejo Editorial / Editorial Board

- S. Beguería (Estación Experimental de Aula Dei, CSIC)  
*Spatial analysis, Climate change, Water resources management, Environmental hydrology*
- E. Cammeraat (Universiteit van Amsterdam, Holanda)  
*Geomorphology, Soil Science, Soil Conservation*
- S.R. Fassnacht (Colorado State University, EEUU)  
*Environmental hydrology, Snow hydrology, Hydrological Modeling*
- H. Holzmann (Universität für Bodenkultur Wien, Austria)  
*Hydrological modeling, Surface hydrology, Soil hydrology, Snow Hydrology, Climate change*
- P. Hughes (University of Manchester, Reino Unido)  
*Glacial and Periglacial Geomorphology, Climate change*
- V. Jomelli (Université Paris I, Francia)  
*Climate change, Climatology, Paleoclimatology, Glaciology, Periglacial Geomorphology*
- J.J. Keizer (Universidade de Aveiro, Portugal)  
*Ecological impact of wildfire, Soil erosion, Wind erosion*
- M.A. Lenzi (Università di Padova, Italia)  
*Fluvial geomorphology, Natural hazards, Sedimentology*
- M. López-Vicente (Universidad de Jaén)  
*Sustainability, Water Resources Management, Soils, Hydrological modelling*
- Y. Onda (University of Tsukuba, Japón)  
*Water Quality, Hydrology, Soil Science, Freshwater Ecology, Soil erosion, Geomorphology*
- J.L. Peña (Universidad de Zaragoza)  
*Geomorphology, Geoarchaeology, Natural hazards, Holocene*
- D. Palacios (Universidad Complutense de Madrid)  
*Palaeoclimatology, Glaciology*
- J. Poesen (Katholieke Universiteit Leuven, Alemania)  
*Geomorphology, Soil erosion, Badland geomorphology, Environmental change*
- J.B. Ries (Universität Trier, Alemania)  
*Water resources management, Soil erosion, Land degradation*
- M.A. Romero Díaz (Universidad de Murcia)  
*Soil erosion, Badland geomorphology, Reforestation, Piping geomorphology*
- E. Serrano Cañadas (Universidad de Valladolid)  
*Geomorphology, Glacial and periglacial environments, Quaternary*
- M. Vanmaercke (Katholieke Universiteit Leuven, Alemania)  
*Soil erosion, Sediment Transport, Geomorphology*
- S. Vicente-Serrano (Instituto Pirenaico de Ecología, CSIC)  
*Climatology, Droughts, Climate change, Environmental hydrology, Remote sensing*
- L. Vázquez Selem (Universidad Nacional Autónoma de México, México)  
*Paleoclimatology, Glacial geomorphology, Volcanoes, Natural Hazards*
- G-L. Wu (Northwest Agriculture & Forestry University, Chinese Academy of Sciences, China)  
*Soil and Water Conservation, Soil erosion, Land degradation, Desertification*

**Cuadernos de Investigación Geográfica = Geographical Research Letters (ISSN: 0211-6820)** is a scientific journal that publishes two issues per year. It includes papers on Physical Geography and other related environmental sciences (Hydrology, Ecology, Climatology). Interdisciplinary studies with Human Geography are also welcome. The peer review and publication of articles in *Cuadernos de Investigación Geográfica* is free of charge, in agreement with the policy of the journal of making accessible the advances in Physical Geography to the scientific community. All papers are subject to full peer review.

Since 2015 **Cuadernos de Investigación Geográfica = Geographical Research Letters** has been included in the Emerging Sources Citation Index (ESCI) of Clarivate Analytics, a new edition of the Web of Science, within the subject category of *Geography (Physical)*. The journal is also indexed in SCOPUS and SCIMAGO Journal & Country Rank within the subject categories of Geography, Planning and Development, Environmental Sciences, and Earth and Planetary Sciences.

**Fotografía de portada / Cover photo:** Bancales abandonados en Enciso, Sistema Ibérico, La Rioja, España / *Abandoned terraces in Enciso, Sistema Ibérico, La Rioja, Spain.* Autor / Author: J. Arnáez

**CUADERNOS DE INVESTIGACIÓN GEOGRÁFICA  
GEOGRAPHICAL RESEARCH LETTERS**

ISSN 1697-9540

**Tomo 49 (2) 2023**

**CONTENIDO / CONTENT**

*Número monográfico: Riesgos de degradación del suelo: temas clave para afrontar en el mundo*

**Special issue: Land Degradation Risks: Key Topics to be faced over the world**

Editores invitados / *Guest Editors*

**Jesús Rodrigo-Comino, Casandra Muñoz-Gómez, Mohammad Reza Rahdari, Luca Salvati**

**Jesús Rodrigo-Comino, Casandra Muñoz-Gómez, Mohammad Reza Rahdari, Luca Salvati.** Land degradation risks: Key topics to be faced over the world

*Riesgos de degradación del suelo: temas clave para afrontar en el mundo* ..... 3

**Masoud Masoudi, Elham Asrari, Somaye Razaghi, Fatemeh Karimi, Artemi Cerdà.** A new proposed model of EMOLUP for assessing of ecological capability of different utilizations and land use planning in Sepidan Township, Iran

*Una nueva propuesta del modelo EMOLUP para la evaluación de la capacidad ecológica de diferentes manejo y planificación del uso del suelo en Sepidan, Irán*..... 5

**Jesús Rodrigo-Comino, José María Senciales-González, Ana Pérez Albarracín, Erick R. Bandala, Francisco Escrivá Saneugenio, Saskia D. Keesstra, Artemi Cerdà.** Circulation weather types as a key factor on runoff initiation and sediment detachment in Mediterranean shrublands

*Tipos de tiempo como factor clave en el inicio de la escorrentía y el arranque de sedimentos en matorrales mediterráneos* ..... 29

**Ahmed Abed Gatea Al-Shammary, Nabil Raheem Lahmod, Jesús Fernández-Gálvez, Andrés Caballero-Calvo.** Effect of tillage systems combined with plastic film mulches and fertilizers on soil physical properties in a wheat-agricultural site in southern Iraq

*Efecto de la combinación de sistemas de cultivo, cubiertas plásticas y fertilizantes sobre las propiedades físicas del suelo de un trigo del sur de Iraq* ..... 51

<b>Abdessamed Derdour, Antonio Jodar-Abellán, Amparo Melian-Navarro, Ryan Bailey.</b> Assessment of land degradation and droughts in an arid area using drought indices, modified soil-adjusted vegetation index and Landsat remote sensing data	
<i>Evaluación de la degradación del suelo y sequías en una región árida utilizando índices de sequía, índice de vegetación ajustado al suelo modificado y datos de sensores remotos Landsat</i> .....	65
<b>Pedro Simón Lamprea-Quiroga, Omar Jaramillo-Rodríguez, Wladimir Mejía Ayala.</b> Soil erosion due to rainfall and the impacts of climate change in an Andean Highland in Colombia	
<i>Erosión del suelo por lluvias e impactos del cambio climático en un altiplano andino en Colombia</i> .....	83
<b>Nazanin Mohammadzade Miyab, Ramin Fazloulou, Manouchehr Heidarpour, Ataollah Kavian, Jesús Rodrigo-Comino.</b> Surveying three-dimensional perspectives of the flow structure around the bridge pile depending on the vegetation pattern distribution	
<i>Estudio de las perspectivas tridimensionales de la estructura de flujo alrededor del pilote del puente en función de la distribución del patrón de vegetación</i> .....	101
<b>Rafael Córdoba Hernández, Federico Camerin.</b> Assessment of ecological capacity for urban planning and improving resilience in the European framework. An approach based on the Spanish case	
<i>Evaluación de la capacidad ecológica para la planificación urbana y la mejora de la resiliencia en el contexto europeo: un enfoque basado en el caso español</i> .....	119
<b>Vito Imbrenda, Casandra Muñoz Gomez, Mariagrazia D’Emilio, Caterina Samela, Luca Salvati, Nadia Matarazzo, Maria Lanfredi, Rosa Coluzzi.</b> Remote sensing and spatial databases for investigating latent urban-rural dynamics in rural, inland districts of Southern Italy	
<i>Sensores remotos y bases de datos espaciales para la investigación de la dinámica urbano-rural latente en distritos rurales del interior de Italia meridional</i> .....	143
<b>COMUNICACIONES CORTAS / SHORT COMMUNICATIONS</b>	
<b>Jesús Rodrigo-Comino, Juan Jesús Padilla Fernández, Artemi Cerdà.</b> Soil erosion triggered by the archeological excavation and conservation of trenches. The case of “Cerro de las trincheras” in Bailén (Jaén, Spain). An open discussion	
<i>Erosión del suelo provocado por la excavación arqueológica y conservación de trincheras. El caso del “Cerro de las Trincheras” (Bailén, Jaén, España). Una discusión abierta</i> .....	163
<b>RECENSIONES / BOOK REVIEW</b> .....	173



## LAND DEGRADATION RISKS: KEY TOPICS TO BE FACED OVER THE WORLD

### *RIESGOS DE DEGRADACIÓN DEL SUELO: TEMAS CLAVE PARA AFRONTAR EN EL MUNDO*

JESÚS RODRIGO-COMINO<sup>1</sup> , CASANDRA MUÑOZ-GÓMEZ<sup>2</sup>,  
MOHAMMAD REZA RAHDARI<sup>3</sup> , SAFWAN MOHAMMED<sup>4,5</sup> ,  
LUCA SALVATI<sup>6</sup>

*Guest Editors*

<sup>1</sup>*Departamento de Análisis Geográfico Regional y Geografía Física, Facultad de Filosofía y Letras,  
Campus Universitario de Cartuja, Universidad de Granada, 18071 Granada, Spain.*

<sup>2</sup>*Escuela Nacional de Ciencias de la Tierra, Universidad Nacional Autónoma de México.  
Av. Antonio Delfín Madrigal 300, C.U., Coyoacán, 04510 Ciudad de México, México.*

<sup>3</sup>*Faculty of Agriculture and Natural Resource, University of Torbat Heydarieh,  
Torbat Heydarieh, Iran.*

<sup>4</sup>*Institute of Land Use, Engineering and Precision Farming Technology,  
Faculty of Agricultural and Food Sciences and Environmental Management,  
University of Debrecen, Böszörményi 138, H-4032, Debrecen, Hungary.*

<sup>5</sup>*Institutes for Agricultural Research and Educational Farm, University of Debrecen,  
Böszörményi 138, H-4032, Debrecen, Hungary.*

<sup>6</sup>*Department of Methods and Models for Economics, Territory and Finance, Faculty of Economics,  
Sapienza University of Rome, Via del Castro Laurenziano 9, I-00161 Rome, Italy.*

Land degradation is threatening biodiversity, soil fertility, food and water security, as well as rural and urban economies. To address this issue, new policies should endorse innovative strategies and management approaches that target key processes such as erosion, soil and water pollution, and the loss of biodiversity. These efforts align to achieve the United Nations Sustainable Development Goals (SDGs) and attain land degradation neutrality during this convulse Anthropocene.

Across various regions worldwide, there is a growing focus on assessing the significant land degradation processes, ranging from hillslopes to catchment and regional scales. Through direct measurements, experimental methods, and modeling techniques, it becomes evident that land degradation is a formidable challenge for humanity. While the scientific literature provides a comprehensive understanding of land degradation processes in some areas, there is a notable

gap in information regarding the impact of land uses, climate scenarios, and soil-water management at different scales on a broader range of non-studied territories.

This special issue seeks to bring together in-depth analyses of past, present, and potential future land degradation processes, employing modeling techniques with Geographic Information Systems (GIS) and *in situ* measurements or experimental approaches. A total of eight research articles, one short communication and one book review delves into the impact of land degradation on human and natural ecosystems, along with strategies to confront these challenges. The interdisciplinary nature of these investigations incorporates economic, social, perceptual, and biophysical data to provide a holistic understanding of the complex issue of land degradation. Some examples of land degradation processes and main topics that can fall within these publications are: i) Soil degradation (erosion, sealing, pollution, etc.); ii) Soil quality indicators and land-use changes; iii) Land consumption and land amelioration; iv) Data monitoring and evaluation instruments; and v) Tools and strategies to achieve land degradation neutrality.



## A NEW PROPOSED MODEL OF EMOLUP FOR ASSESSING OF ECOLOGICAL CAPABILITY OF DIFFERENT UTILIZATIONS AND LAND USE PLANNING IN SEPIDAN TOWNSHIP, IRAN

MASOUD MASOUDI<sup>1\*</sup> , ELHAM ASRARI<sup>2</sup> , SOMAYE RAZAGHI<sup>1</sup>,  
FATEMEH KARIMI<sup>2</sup>, ARTEMI CERDÀ<sup>3</sup> 

<sup>1</sup>*Department of Natural Resources and Environmental Engineering,  
School of Agricultural, Shiraz University, Iran.*

<sup>2</sup>*Department of Civil Engineering, Payame Noor University, Tehran, Iran.*

<sup>3</sup>*Department of Geography, University of Valencia, Spain.*

**ABSTRACT.** The optimum use and appropriate management of renewable resources, with dynamic characteristics, needs to evaluate and classify the ecological capability of environment and its socio-economic conditions. Land use planning (LUP) is an iterative process based on the dialogue amongst all stakeholders aiming at the negotiation and decision for a sustainable form of land use in rural areas as well as initiating and monitoring its implementation. The main objective of this paper is the implementation of integration quantitative model namely EMOLUP (Eco-Socioeconomic Model of Land Use Planning) in Sepidan Township of the Fars province in Iran. Therefore, two main steps were prepared for the new model: I. Ecological capability evaluation of different land uses. This step is composed of the geometric mean method instead of the Boolean and MCE methods. II. Land use planning and prioritizing for the various uses. This step has been composed intersecting ecological capability maps and land use planning, based on two scenarios (economic and social). Then, it was compared with current qualitative and quantitative methods. Also, current land use is used for calibrating and modifying the proposed models. Results show using the geometric mean method is better than Boolean models, and the method of the calibrated geometric mean (with overall accuracy > 63 and kappa index > 0.39 for all land uses) is the best among different used models. Also, results of prioritizing and land use planning showed that quantitative method with two socio-economic scenarios (with an average of EPM erosion model = 0.31) is the best method for land use planning in the study area. We confirmed that the EMOLUP model can contribute to a better understand land use planning in different regions of the world.

***Una nueva propuesta del modelo EMOLUP para la evaluación de la capacidad ecológica de diferentes manejo y planificación del uso del suelo en Sepidan, Irán***

**RESUMEN.** El uso óptimo y la gestión adecuada de los recursos renovables, con características dinámicas, necesita evaluar y clasificar la capacidad ecológica del medio ambiente y sus condiciones socioeconómicas. La planificación del uso del suelo (LUP) es un proceso basado en el diálogo entre todas las partes interesadas con el objetivo de negociar y decidir una forma sostenible del uso del suelo en áreas rurales, así como iniciar y monitorear su implementación. El objetivo principal de este documento es la implementación del modelo cuantitativo de integración denominado EMOLUP (Modelo Eco-socioeconómico de Planificación del Uso del Suelo) en el municipio de Sepidan, en la provincia de Fars (Irán). En concreto, se prepararon dos pasos principales para el nuevo modelo: I. Evaluación de la capacidad ecológica de los diferentes usos del suelo. Este paso incluye el método de la media geométrica en lugar de los métodos booleano y MCE. II. Ordenamiento territorial y priorización de los distintos usos. Este paso considera la intersección de mapas de capacidades ecológicas y la planificación del uso del suelo, en base a dos escenarios (económico y social). Posteriormente, se comparó con métodos cualitativos

y cuantitativos actuales. Además, el uso actual del suelo se utilizó para calibrar y modificar los modelos propuestos. Los resultados muestran que usar el método de la media geométrica es mejor que los modelos booleanos, y el método de la media geométrica calibrada (con una precisión general  $>63$  y un índice kappa  $>0,39$  para todos los usos del suelo) es el mejor entre los diferentes modelos utilizados. Además, los resultados de la priorización y la planificación del uso del suelo mostraron que el método cuantitativo con dos escenarios socioeconómicos (con un modelo de erosión EPM promedio = 0,31) es el mejor método para la planificación del uso del suelo en el área de estudio. Confirmamos pues que el modelo EMOLUP puede contribuir a una mejor comprensión de la planificación del uso del suelo en diferentes regiones del mundo.

**Key Words:** EMOLUP model, geomean, boolean, Prioritizing, land use, capability.

**Palabras clave:** modelo EMOLUP, media geométrica, booleano, priorización, uso del suelo, capacidad.

Received: 23 April 2022

Accepted: 30 October 2022

\***Corresponding author:** Masoud Masoudi, Department of Natural Resources and Environmental Engineering, School of Agricultural, Shiraz University, Iran. *E-mail address:* masoudi@shirazu.ac.ir

## 1. Introduction

Land refers to earth's terrestrial surface and includes climate, soil, landform, water, plants, animals, human settlements and infrastructure. In biophysical land evaluation analysis and land performance assessment, there are two major trends: qualitative and quantitative. In general terms, a land evaluation system is considered qualitative when in its development the values of diagnostic properties define categories (Makhdoum, 2006). The system is considered quantitative when these values are combined mathematically to give an index on a sliding scale. Land use planning (LUP) is a procedure which leads to an optimal and sustainable use of the land and all its attributes (Sarvazad *et al.*, 2015; Yohannes and Soromessa, 2018; Nazari Viand *et al.*, 2019). Use of the land may take various forms, from intensive use such as settlements and irrigated agriculture to less intensive use such as livestock production, forestry or nature reserves (Alavi Panah *et al.*, 2001; Asadifard *et al.*, 2019). The same piece of land can be used for more than one purpose at the same time (e.g. forestry and livestock production) or have different uses during different periods of year (e.g. rainfed cropping during the wet season, followed by grazing during the dry season). Land use planning is not something new: it has been practiced from the time that humans domesticated animals for livestock production and started crop cultivation (O'Neill, 1989; Abu Hammad and Tumeizi, 2010; Benthem, 2013; Ayalew, 2015; Masoudi *et al.*, 2017; Jokar *et al.*, 2021). It should be noted that land use planning must deal with the understanding of all problems, of potentials and alternatives for land use in all areas of the planning unit. It cannot be concerned selectively with partial areas, which are particularly intact or degraded. The whole area used by the stakeholders has to be planned (Mokarram and Zarei, 2021). Hence, before the beginning of development, it is better to select the suitable developing site in terms of ecological capability and land use planning in order to prevent reduction of natural resources, which may happen for the reason of illogical usage (Nouri and Sharifpour, 2004; Masoudi, 2014; Hosseini, 2018).

A significant amount of literature and research has been dedicated to intelligent systems for land use and management. The study conducted by McHarg (1969), land suitability assessment has become a standard practice in land use planning. Land uses include both natural and man-made uses. The FAO (Food and Agriculture Organization of the United Nations) (1976) defined land evaluation as the process of assessment of land performance when used for specified purposes. In this way, land evaluation can

be useful for predicting the potential use of land based on its attributes (Rossiter, 1996). In such classic methods like the FAO, Storie (1987) made the classification quite strict based on maximum limitation. This is because, according to Boolean logic, only one low index is enough to reduce the suitability of land from a highly suitable class to a not suitable class (Masoudi, 2018). Also, computer-assisted overlay techniques such as the Geographic Information System (GIS) were developed as a response to the manual method's limitations in mapping and combining large datasets (Steinitz *et al.*, 1976; Najafinezhad *et al.*, 2013; Lahmian, 2016; Jahantigh *et al.*, 2019). Methods such as Multi-Criteria Decision Making (MCDM) and genetic algorithms have considerably advanced the conventional map overlay approaches to land use suitability analysis (Oyinloye and Kufoniyi, 2013; Safaripour and Naseri, 2019). However, it is well-known land use suitability analysis methods have one problem. They do not assure a spatial pattern with contiguity or compactness in land allocations for different types of land use. Also, these methods are complex to use (Masoudi, 2018).

Among leading models in the field of economic planning (prioritizing), the French and the Anglo-Saxon models can be mentioned (Kindleberger, 1967; Metze, 2002). Also, there is a model designed by Nakos (1984) in Greece related to land use planning. Fallahshamsi (2004) investigated the economic evaluation of different land uses in the kalibar-chai forest-covered watershed in Iran, using linear programming and the GIS (Geographic Information System), and based on the cost-benefit method. Najafinezhad *et al.* (2013) compared the efficiency of systematic and multi-objective land allocation (MOLA) methods for land use planning using the GIS. They found that the map obtained from MOLA was better in terms of land use allocation and also, for reducing erosion and sediment production as compared to that of the systematic method. Piran *et al.* (2013) had utilized AHP and GIS methods for assessing land suitability for forest at Bdresh county western Iran. Pan *et al.* (2021) conducted practical efficient regional land-use planning using constrained multi-objective genetic algorithm optimization for Dapeng, China. Results showed that the comprehensive model gave superior fitness compared to the contrast experiments.

Considering the above mentioned-lack the main goal of this paper is the implementation of accurate integration quantitative models in order to evaluate ecological suitability and prioritize different land uses including forest, rangeland, agriculture, conservation, and development. Our research will help to achieve the Sustainable Development Goals of the United Nations and the Land Degradation Neutrality challenges due to the soil and water proper management we propose (Keesstra *et al.*, 2018; Keesstra *et al.*, 2021). To achieve this goal, an experimental area including total area of Sepidan county placed in Fars Province, Iran was selected because of available data for this land evaluation and also different variation in climate and topographic condition.

## **2. Materials and methods**

### *2.1. Study Area*

Sepidan county is situated in Northwest of the Fars province of Iran with an area of 286,000 hectares. Sepidan city is located in 51° 59' east longitude and 30° 15' north latitude (Fig. 1). The population of this county was equal to 91,049 people based on the 2015 census. Its average rainfall thirty-years past is 758 mm, with 35% and 65% relatively in the form of snow and rain, respectively, evenly distributed. The weather is very cold in the winter and reach to -15°C and cool and mild in the summer with average daily temperature of 25°C. From the contemporary technicalities of climatic classification and general populace, this city is considered cool and moist to semi-dry (Goudarzian and Yazdani, 2015). A major part of this county is mountainous and covered with forest, and due to its climate, it is one of the important agricultural and animal husbandry areas of Fars province. This county has been successful in preparing and distributing meat outside the province. Walnut, peach, apple and cherry trees comprise the most products of the region. It should say that Sepidan is one of the most famous ecotourism regions in Fars province and Iran. The region's cool climate in summer and snow-

covered mountains in winter and the natural tourist attractions of the region and the existence of riding tracks and ski tracks and areas such as Tangheh-Tizab and Chalehgah have given a special boost to the tourism industry. Figure 1 shows the location of the study area.

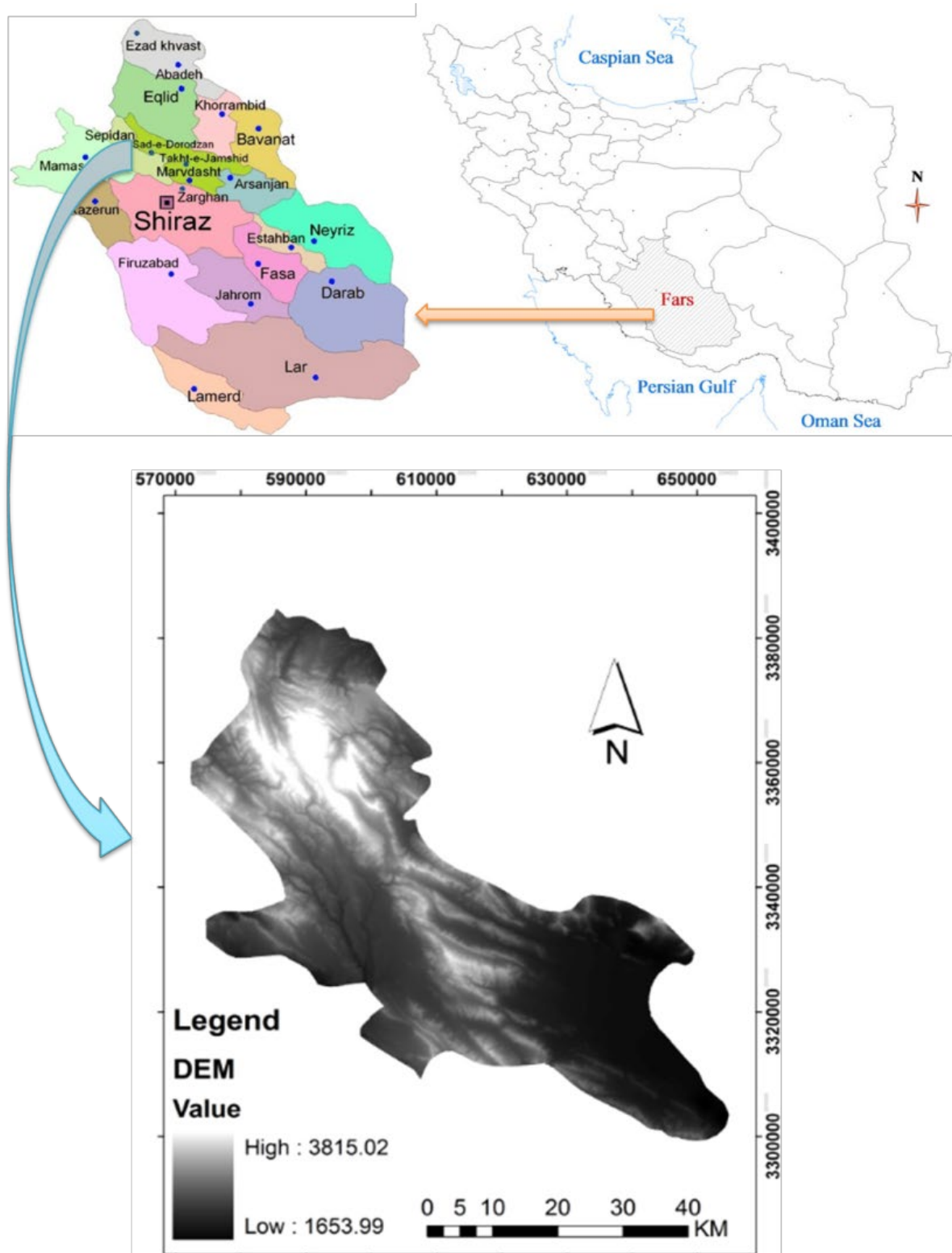


Figure 1. Location of the study area in Iran.

## 2.2. Ecological capability evaluation

### 2.2.1. Modeling Process for Ecological Capability Evaluation

The present paper aims to find a suitable model for land capability evaluation, for different land uses in the study area, using software like ArcGis9.3 (Produced by ESRI Company, USA), ENVI4.7, and Excel. Two types of data were obtained: numerical data and thematic maps, mainly in the map format. All such relevant data were obtained from the local and main offices and institutes of the Ministries of Agriculture and Energy in Iran. Figure 2 shows the platform structure of the designed model.

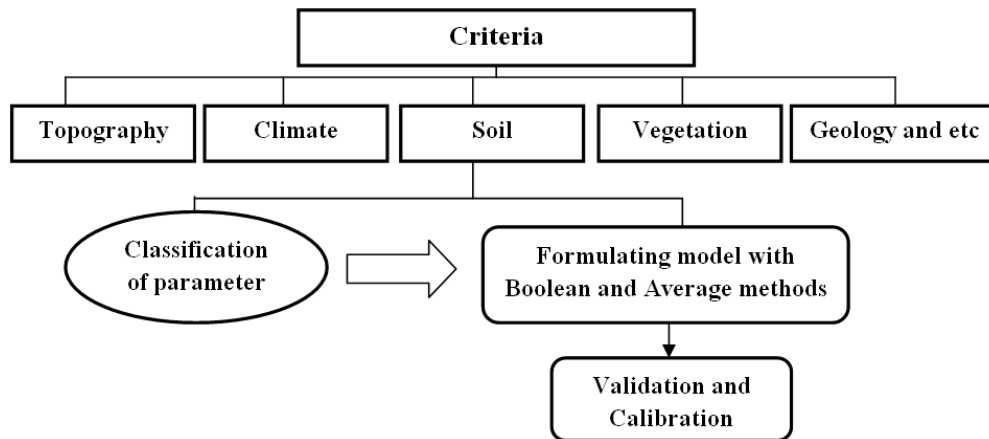


Figure 2. Flowchart showing the methodology adopted for ecological capability evaluation in this study.

### 2.2.2. Classification of Models

The Iranian Ecological Model (Makhdoum, 2006, Masoudi, 2018) is a land evaluation model for different land uses. For example, forestry (including 7 Classes), agriculture and rangeland management (including 7 Classes), development (including 3 Classes) and ecotourism (including 3 Classes). It should be noted that the ecological potential in every use reduces by increasing the capability number of the class. In the revised method, classes mentioned were reclassified (in order to make a standard classification). Accordingly, the uses of agriculture and natural resources (forest and rangeland) were reclassified into four Classes (Anex 1a) including: highly suitable (1), moderately suitable (2), poor (3), and not suitable (4). Human-made uses (development and ecotourism) were reclassified into 3 Classes including: highly suitable (1), moderately suitable (2), poor and not suitable (3) (Anex 1b). Also, environmental conservation uses or protected land was classified into 2 Classes including: suitable (1), not suitable (2) (Anex 1c).

### 2.2.3. Formulating Model

**Boolean Algebra:** Boolean logic has three basic operators: Intersection (logical term AND), Union (logical term OR), and Inverse (logical term NOT).

**Geometric Mean:** In the geometric mean method such as the MEDALUS model (Kosmas *et al.*, 1999; Zakerinejad and Masoudi, 2019) and according to criteria, in the uses with four classes, every indicator was given the weight between 0 and 3 (Anex 1). In this, 0 indicates the non-suitability of the ecological condition (Class 4) and 3 represents the most suitable ecological condition (Class 1) for a utilization like irrigation. Scores of 1 and 2 are given to the third and second classes, respectively. In uses like development with three classes, every indicator was given the weigh between 0 and 2 (Anex

1). In this, 0 stands for poor and non-suitable ecological condition (Class 3) and 2 stands for the most suitable ecological condition (Class 1).

Then every criterion (like topography) was calculated based on the geometric mean of indicators (Equation 1).

$$\text{Criterion\_X} = [(\text{Layer-1}) \times (\text{Layer-2}) \dots \times (\text{Layer-n})]^{1/n} \quad (\text{Equation 1})$$

In this, Criterion\_X is the defined criterion; Layer is the indicator map of criterion; and n is the number of used indicators. Then the criteria were multiplied through the geometric mean (Equation 2).

$$\text{Final Criterion} = [(\text{Layer-1}) \times (\text{Layer-2}) \dots \times (\text{Layer-n})]^{1/n} \quad (\text{Equation 2})$$

In this, Final Criterion is the final layer of ecological capability; n is the number of used criteria. Then classes of qualitative and suitable ecological capability were defined, for uses of three and four classes, in the study area in a GIS (Table 1).

Table 1. Suitability classes in capability maps and models for 4 classes' uses (a) and models for 3 classes' uses (b) regarding the scores of polygons.

(a)

	Suitability classes			
Their score	Good (1)	Moderate (2)	Poor (3)	Not suitable (4)
	2.5-3	1.5 - 2.5	0.5 - 1.5	< 0.5

(b)

	Suitability classes		
Their score	Good (1)	Moderate (2)	Poor & Not suitable (3)
	1.5-2	0.5-1.5	< 0.5

Note: The capability of conservation use was calculated based on the Boolean (OR) method.

Arithmetic Mean (Sum): In the arithmetic mean method, scores given to indicators were averaged (Tables 2 for classification).

MCE (WLC) method: In this paper, MCE was used for assessment. Accordingly, questionnaires were given to experts in the field of different uses for weighting the criteria and factors. Then calculation of weightings was done in Expert Choice software. Weight of criteria and factors was obtained with Consistency Ratio or CR<0.1. Then WLC (weighted linear combination) method used for the weighted overlay of the input data layers. With the weighted linear combination, factors are combined by first applying a weight to each factor and criteria (Equations 3), followed by a summation of the results to yield a suitability map (Equations 4). Finally, constraint factors (C<sub>i</sub>) were multiplied in map (Fallahshamsi, 2004).

$$[(W_1 \times \text{factor1}) + (W_2 \times \text{factor 2}) \dots + (W_n \times \text{factor})] \times C_i \quad (\text{Equation 3})$$

$$[(W_1 \times \text{Criteria1}) + (W_2 \times \text{Criteria2}) \dots + (W_n \times \text{Criteria})] \times C_i \quad (\text{Equation 4})$$

### 2.2.4. Validation and Calibration

Validation: In order to validate models, samples of ground reality (current land use map) were gathered by "Create Fishnet" algorithm (a systematic random sampling) in ArcGIS 9.3 environment (Congalton, 1991). Number of samples was based on importance of ground reality in every use. So, the

regions with more suitable condition for every use were sampled more than other regions (Fallahshamsi, 1997).

Then these points were overlaid to land capability maps. The obtained result is observed in a table named “Error Matrix” and by quantitative indices such as “Overall Accuracy, Kappa and Inclass Coefficients” (Fallahshamsi, 1997).

Calibration: To ensure the agreement of capability maps to current conditions (regarding omission and commission in errors and maps of parameters in the geometric mean method), quantitative ranges of suitability classes (Table 1) were slightly changed. For example, the range of Class 0.5-1.5 was changed to 0.5-1.85. This kind of calibration was done in other classifications like the MEDALUS method.

### 2.3. Prioritizing Different Land Uses

#### 2.3.1. Modeling Process

The present paper aims to find a land use planning model for prioritizing different land uses of the study area using ArcGis9.3. Every use with the best accuracy was intersected in a vector format in the ArcGIS software environment. Current land use was also applied. Figure 3 shows platforms structure of the designed model.

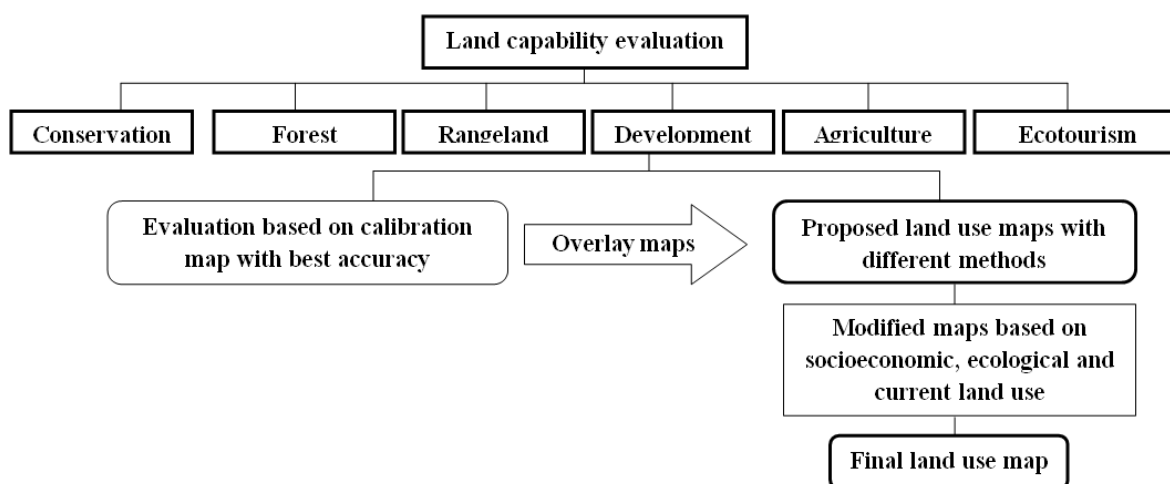


*Figure 3. The conceptual framework of land use planning for the proposed model.*

It should be noted that the land use planning process is based on selection of the best use in every polygon (unit). Hence, different methods were applied in order to select the best use.

Quantitative Method: Initially, the quantitative method developed by Nakos (1984) was used. Then it was revised (based on conditions in Iran) by Makhdoum (2006). To be more specific, four scenarios were developed for different land uses based on the regional information, including: current land use area, ecological scenario, economic scenario, and social scenario. Table 2 shows one example describing the four scenarios in a study area (as a planning unit).

The first scenario was ranked by evaluating the current land use. The land use with highest area in this region (forest) was given highest rank and the land use with least area in this region (protected zones) was given the least rank. But for other scenarios questionnaires was prepared. Experts of the study area were asked to rank different land uses for these other scenarios based on their knowledge and experience. Then all land uses were ranked for each scenario and given scores of 10 and below based

on their ranks (Table 2a) and classes of ecological capability (Table 2b). For example, if in one scenario in a land unit, the rank of forest is in third place and its ecological capability is in Class 2, then the score in its first step is 8, and one point is lowered for its capability reduction (Class 2), making the forest score 7. If ecological capability is in Class 3, the reduction in each scenario would be of two points.

To achieve a systematic analytical model, all layers of ecological capability maps were used by a vector format in GIS software environment. Then appropriate utilization of each land unit (polygon) was determined and prioritized. Appropriate utilizations are those that have a higher sum of scores among the used scenarios (Table 2b). Many of the units were seen to be fit for two appropriate uses by the quantitative model, considering the socio-economic status of the area, consistency of land uses and current land use.

Table 2. Example of scenarios designed for the study area (a) and Relative values (0-10) assigned to different land uses according to capability classes of the land with taking into consideration of different scenarios (b).

(a)

Scenario1	Rangeland >	Forest >	Agriculture >	Conservation >	Development
Scenario2	Conservation >	Rangeland >	Forest >	Agriculture >	Development
Scenario3	Development >	Agriculture >	Rangeland >	Conservation >	Forest
Scenario4	Development >	Agriculture >	Conservation >	Rangeland >	Forest
Weighted values	10	9	8	7	6

(b)

Capability class \ Scenario	Rangeland	Forest	Agriculture	Conservation	Development
	1	3	2	1	2
1	10	7	7	7	5
2	9	6	6	10	5
3	8	4	8	7	9
4	7	4	8	8	9
Sum	34	21	29	32	30
<b>Priority</b>	<b>1</b>	<b>5</b>	<b>4</b>	<b>2</b>	<b>3</b>

Modified Quantitative Method (four scenarios): Modifications were made in the process of work for assessing land use planning with a quantitative model. These modifications are described as follows:

- a. Each use was prioritized based on the highest score derived after summing up the scores of the scenarios. Of course, it is necessary to have appropriate capability (suitable or Classes 1 and 2) for the utilization with highest score.
- b. The compatibility of uses was considered. If uses are compatible together (for example, forest and conservation), they will be considered together. If uses are not compatible together (for example, development and forest), they will be considered based on economic needs (especially current land use).
- c. Current land use map was applied for assessment because of socio-economic compulsions of the population, especially in rural areas. The main modifications in this step are to hold the following land utilizations:
  - 1) Agricultural lands with suitable capability (classes 1 and 2).
  - 2) Settlement lands (urban, rural, and industrial areas).

- 3) Forest lands with a canopy cover of more than 25% (F<sub>1</sub> and F<sub>2</sub>) and those with conservational roles based on compatibility of uses.
- 4) Forest lands with a canopy cover of less than 25% (F<sub>3</sub>) that were prioritized as rangeland. They are prioritized as Forest – Rangeland based on compatibility of uses.
- 5) Rangelands with a canopy cover of more than 25% (R<sub>1</sub> and R<sub>2</sub>), F<sub>3</sub>, and ecotourism with suitable capability (Class 1) with taking into consideration of compatibility of uses.
- 6) Current protected lands with taking into consideration of compatibility of current land use (for example, natural resources) and holding man-made current land use in current protected lands (except core zones).
- 7) Lakes and river beds.
- 8) Lands not prioritized in earlier steps (with suitability Classes 3 and 4); their utilizations are retained.

In this study proposed land uses are defined with different codes including: F (Forest), E (Ecotourism), R (Rangeland), IF (Irrigated Farming), DF (Dry Farming), D (Settlement & Development), E (Ecotourism), C (Conservation), BL (Bare Land), L (Lake and water body).

Modified Quantitative Method (two scenarios): Due to problems in evaluation of the quantitative methods (4 scenarios) [a) the larger area of one utilization (for example, rangeland) as compared to the smaller area of another utilization, giving higher weight to the former; b) the existing ecological scenario in land ecological capability evaluation where experts may mistakenly prioritize the ecological scenario], the revised quantitative method was used based on two scenarios (economic and social) with mentioned modifications.

Qualitative and its Modified Method: Qualitative method (Makhdom, 2006; Khosravi *et al.*, 2012; Masoudi, 2018) keeps current utilizations with suitable capability (Classes 1 and 2) after intersecting ecological capability maps with the land use map. Other lands are prioritized based on utilizations that have better land capability. In modified qualitative method, some positive changes (mentioned in the modified quantitative method) were added.

### 2.3.2. Validation of Models

In order to validate models, the EPM (Erosion Potential Method) model was used (Gavrilovic, 1998). Based on the EPM model assigned with land uses, maps of proposed models were compared with the current land use map. The model close to good land uses assigned to the EPM model is considered to be the better model. The ranked land uses (agriculture and natural resources) assigned to the EPM model (with a little modification) were sorted based on their impact on soil protection (Table 3a). This ranking helps to compare land use planning maps to current land use. Based on Table 3a, if the optimized uses have better situations than current land use (A), positive (+1) score is given; if the optimized uses have worse situations than current land use (B), negative (-1) score is given; and if the optimized uses are the same as current land use (C), zero (0) score is given.

Point 1: If the current land use is kept and its ecological capability is in Class 1 (except protected lands), a positive (+1) score is given (D) due to its socio-economic importance.

Point 2: Converting a river bed to other uses is equivalent to a negative (-1) score.

It should be noted that the use of residential and industrial development has not been mentioned in the EPM model. Hence, a separate table (Table 3b) was made to compare current and optimized land

uses with regard to destructive out-site and in-site effects, and socio-economic special features for this use.

Also, for future (not current) environmental conservation, the score was considered to be positive due to land improvement and its protective role. Additionally, to convert areas of natural resources and agriculture to ecotourism, the rating -1 to +1 was used based on the capability degree of agriculture and ecotourism areas, and due to environmental and socio-economic special features for these uses.

Based on the above points, the proposed models were compared together. For this purpose, a certain number of points (1707) was scattered with the Create Fishnet algorithm in ArcGIS9.3 environment and was based on the study area (a systematic-random sampling). In the next step, proposed models were compared based on average ratings. So, the final number is between  $\pm 1$ . If the positive number obtained is larger, it represents the suitability of the prioritization process.

Table 3. Validation of proposed models by EPM model to compare with current land use (a) and validation of proposed models by comparing with current land use and development (b).

(a)

Order	Land use	Description
1	F <sub>1</sub> , F <sub>2</sub>	Current Dense and Semi dense Forest (capability classes of 1 and 2 in optimized use)
2	IF, DF with suitable capability (Classes of 1, 2)	Irrigated and Dry Farming with suitable capability (classes of 1 and 2)
3	F <sub>3</sub> , R <sub>1</sub>	Current Sparse Forest (capability class of 3 in optimized use), Current Dense Range (capability class of 1 in optimized use)
4	R <sub>2</sub>	Current Semi dense Range (capability class of 2 in optimized use)
5	IF, DF with none suitable capability (3, 4) and R <sub>3</sub>	Irrigated and Dry Farming with weak to none suitable capability (classes of 3 and 4) and Current Sparse Range (capability class of 3 in optimized use)
6	Desert (BL, SL)	Barren and Saline lands
Examples		Examples Code
R <sub>2</sub> (current) to F <sub>2</sub> (optimized)		A
F <sub>2</sub> (current) to R <sub>1</sub> (optimized)		B
F (current) to F (optimized)		C
IF (current) to IF (capability 1)		D

(b)

Current land use	Optimized Use	Score	Reason and Description
Development	Every use (e.g., range)	-1	Socio-economic conditions
Development	Development	0	No change
Every use	Development	-1 to +1	Based on capability degree of both uses

### 3. Results and discussion

#### 3.1. Ecological Capability Maps

The final results of validation for different uses are observed in Table 4. The final maps of ecological capability, with the best accuracy and suitability classes for different methods, are observed in Figure 4. The maps include methods of Iranian ecological model and maximum limit by Boolean algebra, MCE, arithmetic and geometric mean, and calibration of geometric mean.

Results (Table 4) generally show that the revised method using the geometric mean (with overall accuracy > 59 and kappa index > 0.39 for all land uses except for the natural resources area with kappa index < 0.2) is better than Boolean and MCE models. Of course, in the results of rainfed agriculture, development and natural resource uses there are not any difference between geometric mean and MCE (WLC) models. Also, the method of the calibrated geometric mean (with overall accuracy > 63 and kappa index > 0.39 for all land uses) is the best among different used models. It should be noted that the arithmetic mean (with overall accuracy 17 to 57% and kappa index < 0.01 for all land uses except for the natural resource area) have the lowest accuracy. In fact, the Boolean method (with overall accuracy 34 to 48 and kappa index = 0.0) is the worst suitable way in natural resources uses. Also, inclass coefficient was found to be the best to estimate suitable classes. These results are in good agreement with study results of Sanaee *et al.* (2010), Jokar and Masoudi (2016) and Asadifard (2016). In relation to natural resource utilizations, it was found that the calibration of geometric mean (with overall accuracy > 78 and kappa index > 0.64) has the best accuracy as compared to the other models like geometric mean evaluation and the difference in the results is almost significant. But between accuracy indices for geometric mean and their calibration in man-made utilizations like irrigated farming, development and etc. are not significant difference.

Table 4. Overall Accuracy, Inclass and Kappa coefficients in the used models.

Land Uses	Model Index	Boolean		Average			
		Ecological	Max limit	Arithmetic (Simple MCE)	MCE (WLC)	Geometric	Calibrated
Irrigated farming	Overall Accuracy	37.5	47.1	57.44	57.36	63.44	63.44
	Kappa Coefficient	0.17	0.29	0.02	0.09	0.39	0.39
	Inclass Coefficient	1.1	0.22	1.41	1.82	1.17	1.17
Rainfed farming	Overall Accuracy	74.59	66.4	38.4	78.68	78.37	79.4
	Kappa Coefficient	0.45	0.15	0	0.55	0.54	0.56
	Inclass Coefficient	0.9	0.14	0.62	1.33	1.25	1.3
Rangeland	Overall Accuracy	48.3	46.7	73.65	73.73	73.73	92.5
	Kappa Coefficient	0.05	0.03	0	0.004	0.004	0.79
	Inclass Coefficient	0.1	0.04	2.79	2.8	2.8	9.83
Forest	Overall Accuracy	33.81	41.3	53.71	59.29	59.29	77.6
	Kappa Coefficient	0.02	0.14	0	0.2	0.2	0.64
	Inclass Coefficient	0.05	0.07	1.16	1.34	1.37	3.08
Development <sup>8</sup>	Overall Accuracy	82	88	17	88	88	88
	Kappa Coefficient	0	0.46	0	0.46	0.46	0.46
	Inclass Coefficient	0	0.52	0.2	0.52	0.52	0.52
Ecotourism	Overall Accuracy	54	74	38	73	81	82
	Kappa Coefficient	0.2	0.56	0.09	0.59	0.7	0.72
	Inclass Coefficient	0	0	0.49	0.76	1.14	1.35

<sup>8</sup>Urban and industrial development

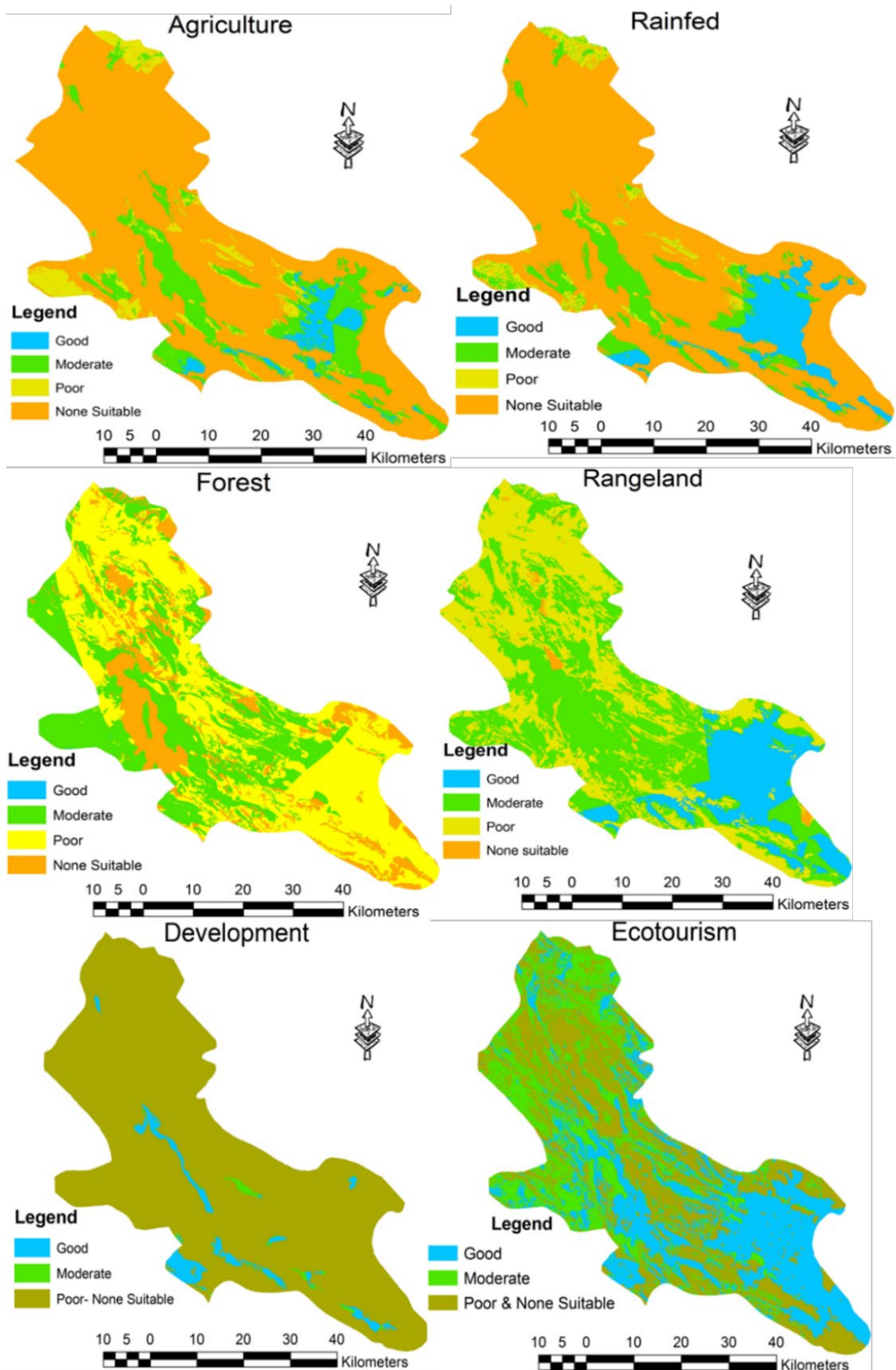


Figure 4. Ecological capability maps prepared with best accuracy.

Additionally, Figure 5 (for example ecotourism use) shows that the study area by the Simple MCE (arithmetic mean) methods tend to fall under good classes; Boolean methods tend to fall under not suitable classes; and the geometric mean and its calibration and WLC methods tend to be placed between the other methods. This indicates that the geometric mean and its calibration can be a useful and flexible model for finding the potential of use. This format of changes in the range of classes in different models for other uses in the region was also observed. These results are in good agreement with results of Elaalem *et al.* (2010), Najafinezhad *et al.* (2013), Jokar (2015) and Asadifard (2016) and are based on the same methods.

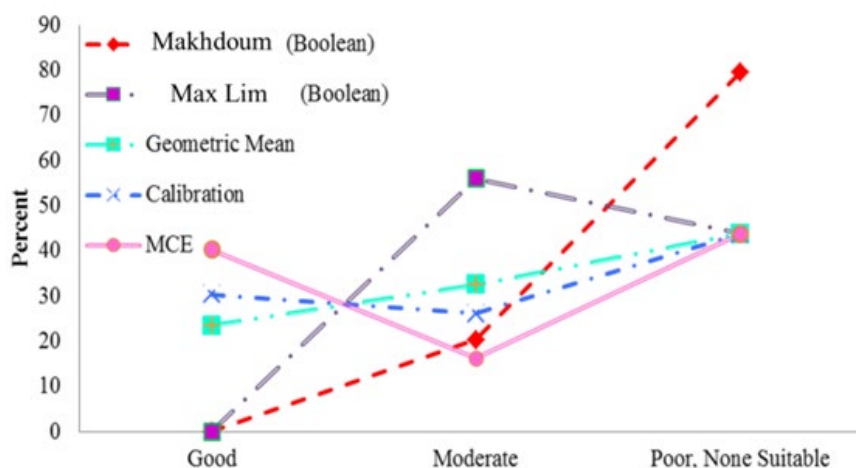


Figure 5. Percent of land under different capability classes for different methods of ecotourism use.

As a whole, AHP is a widely used method in WLC and was introduced by Saaty (Saaty, 1977; Saaty and Vargas, 2001). AHP is based on three principles: decomposition of the overall goal (suitability), comparative judgment of the criteria, and synthesis of the priorities (Baniya, 2008; Nazari Viand *et al.*, 2019). In contrast to above methodologies, this research showed that proposed method is easier than AHP and saves time and cost.

Also, the proposed method using geometric mean and different criteria reduces the high effect of certain criteria like soil with ten indicators as compared to other important criteria with fewer indicators. Therefore, climate and topography with only two indicators have an equal weight as the soil factor. Also, there is a range of ecological conditions that create restrictions in the land such as very severe salinity. By placing the number zero in an equation and multiplying, these regions were not considered to be suitable.

### 3.2. Land Use Planning Maps

Land use planning methods were applied in every polygon after intersecting ecological capability maps of different land uses with the current land use. Final results of validation for land use planning methods are observed in Table 5. The basic method is based on primary methods: Nakos (1984) and Makhdom (2006).

Table 5. Validation of land use planning methods.

Index \ Model	Basic		Modified		
	Qualitative	Quantitative	Qualitative	Quantitative	
				4 scenarios	2 scenarios
<b>EPM (Average)</b>	0.23	0.01	0.25	0.29	0.31

Results generally show that modified methods (with EPM index for modified qualitative = 0.25, for modified quantitative with 4 scenarios = 0.29 and for modified quantitative with 2 scenarios = 0.31) are better than basic models (with EPM index for basic qualitative = 0.23 and for basic quantitative with 4 scenarios = 0.01) due to reforms; and revised quantitative methods are better than qualitative models due to quantitative calculations, existing scenarios, and modifications. Also, the modified quantitative method with two scenarios (EPM index = 0.31) is the best among the different used models. Actually, the quantitative method with two scenarios is even better than the quantitative method with four scenarios. It shows that the area and ecological scenarios are not suitable for land use planning. These results agree well with Babae and Ownegh (2006), Jokar (2015), Asadifard (2016) and Masoudi *et al.* (2020). Additionally, it was found that the quantitative method with two scenarios (Figure 6) has more land for future conservation (in accordance to the mentioned regions). In other words, the existing scenarios of area and ecology led to the use of conservation being seen as less than range or forest (Masoudi and Jokar, 2015). The areas defined in Figure 6 represent future conservation. On the whole, Figure 6 and Table 5 show that 31% of the study area will be improved by the two scenarios method, using socio-economic and ecological information.

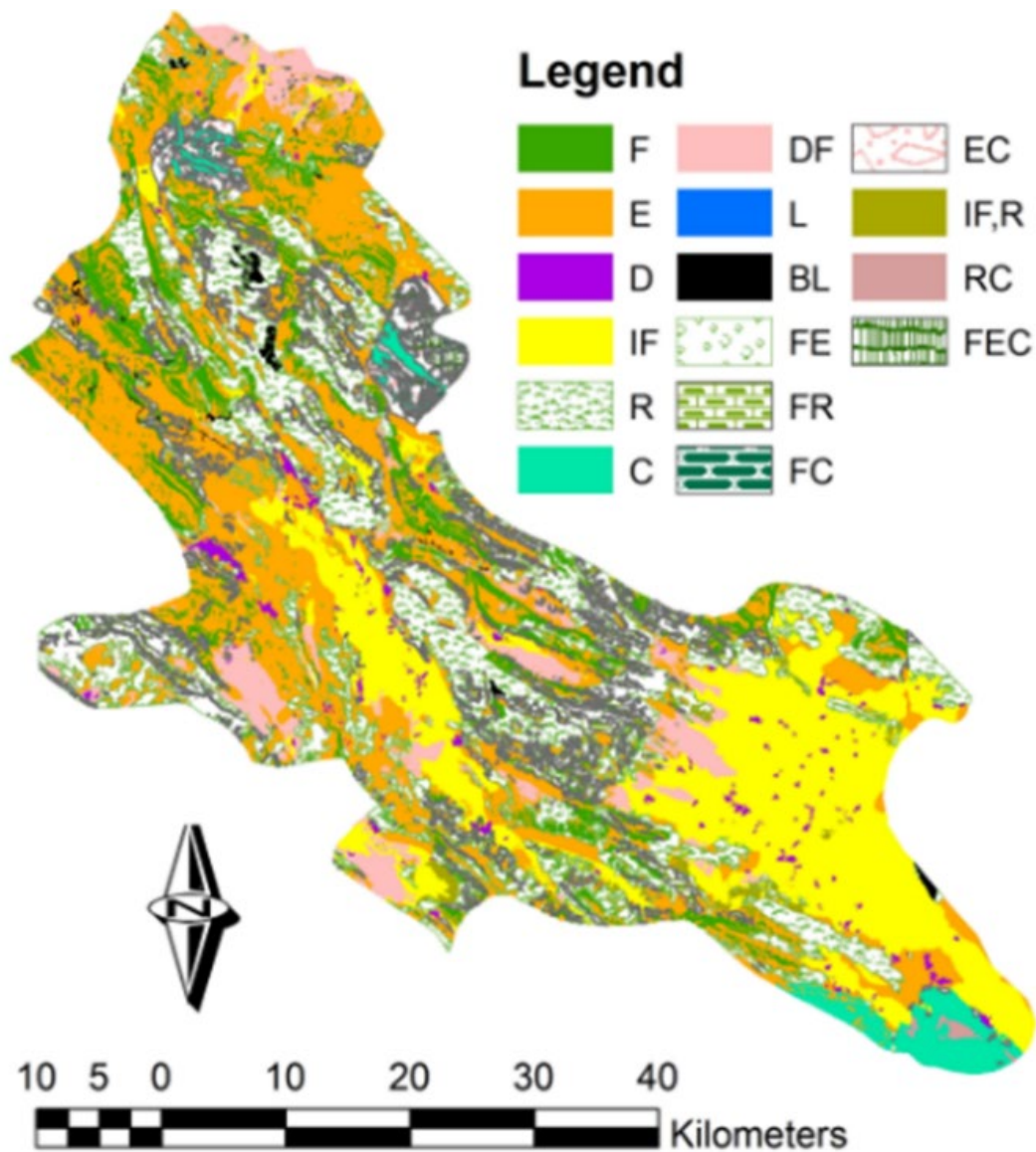


Figure 6. Final map of land use planning by two scenarios. [Note: Proposed land use: F (Forest), E (Ecotourism), R (Rangeland), IF (Irrigated Farming), DF (Dry Farming), D (Settlement & Development), E (Ecotourism), C (Conservation), BL (Bare Land), L (Lake and water body)].

The total results obtained in Table 6 are as follows:

1. To keep most forest lands and rangelands (especially R1, R2, and most of R3) in the optimized land use map.
2. To keep most irrigated lands in the optimized land use map.
3. To increase conservation lands in optimized land use as compared to current land use.
4. To increase development, use due to socio-economic issues, taking into consideration environmental conservation and EIA (Environmental impact assessment).
5. To convert few parts of deserts to natural resources in optimized land use.
6. To perform ecotourism in some forest lands.

*Table 6. Percent are of current and optimized land uses.*

<b>Land use</b>	<b>Current land use (%)</b>	<b>Optimized land use</b>
<b>Forest</b>	35.47	9.28 (F)
		0.25 (FC)
		0.56 (FEC)
		5.79 (FR)
		5.41 (FE)
<b>Rangeland</b>	24.12	16.04 (R)
		0.15 (RC)
<b>Irrigated farming</b>	27.41	20.35
<b>Ecotourism</b>	-	30.43
<b>Rainfed farming</b>	10.84	5.61
<b>Development</b>	1.12	1.22
<b>Desert</b>	0.68	0.52
<b>Conservation</b>	-	2.79 (C)
		1.48 (EC)
<b>Sum</b>	100	100

#### **4. Conclusion**

In this paper, different evaluation methods such as the Boolean and average were investigated. Results showed that the suitability of every use and the selection of suitable evaluation methods could be estimated by current land use. Since current land use is an important parameter, the socio-economic conditions in a region were stated (Di Gregorio and Jansen, 1998).

The modified classification of parameters has helped to increase the accuracy of the new model in land use planning. This indicates that in each specific area, a special classification appropriate to the conditions of the area is required. The geometric mean method has also improved the accuracy of the models, which shows this method has higher flexibility and accuracy. Another important advantage of this method is the simplicity of implementation compared to other methods.

In this paper, it was found that the quantitative method with two scenarios (social and economic) is the best method for land use planning. It should be noted that the proposed method considers ecological as well as socio-economic issues. Of course, if socio-economic information is not available, we can use the revised qualitative method.

We conclude that land management study based on geo-mean, its calibration and validation methods, and modification methods of land use planning (especially quantitative method with two

scenarios) are suggested to managers. Also, we denominate this kind of ecological capability evaluation and land use planning for different land uses with a proposed model of EMOLUP (Eco-Socioeconomic Model of Land Use Planning) to the scientific societies.

## Acknowledgements

We are also grateful to all of National offices and organizations for providing the data for monitoring the work. This work would not have been possible without the financial support of Shiraz University, Iran (Grant number: 95GRD1M75441; Grant recipient: Dr. Masoud Masoudi).

## Data Availability Statement

The datasets used and/or analyzed during the current study are available from the first author on reasonable request.

## References

- Abu Hammad, A., Tumeizi, A., 2010. Land degradation: socioeconomic and environmental causes and consequences in the Eastern Mediterranean. *Land Degradation and Development* 23, 216-226. <https://doi.org/10.1002/ldr.1069>
- Alavi Panah, S. K., De Dapper, M., Goossens, R., Masoudi, M., 2001. The Use of TM Thermal Band for Land Cover/Land Use Mapping in Two Different Environmental Conditions of Iran. *Journal of Agricultural Science and Technology* 3(1), 27-36.
- Asadifard, E., 2016. *Mapping of land use planning based on modification and quantitative method of current model (A case study: Firouzabad Township)*. M.Sc. Thesis, School of Agriculture, Shiraz University, Iran.
- Asadifard, E., Masoudi, M., Afzali, S.F., Fallah Shamsi, S.R., 2019. Evaluating the ecological potential for rangeland use by various land-use planning methods in Firozabad County. *Rangeland*, 13, 14-25.
- Ayalew, G., 2015. A geographic information system based physical land suitability evaluation to groundnut and sweet potato in East Amhara, highlands of Ethiopia. *Journal of Biology, Agriculture and Healthcare* 5(1), 33-38.
- Babae, A.R., Ownegh, M., 2006. Evaluation of Development Potential and Land Use Planning of Posht-e-Kooh Watershed. *J. Agric. Sci. Natur. Resour.* 13, 127-137.
- Baniya, N., 2008. Land suitability evaluation using GIS for vegetable crops in Kathmandu Valley, Nepal. [Available online]. <http://edoc.hu-berlin.de/dissertationen/baniya-nabarath-2008-10-13/PDF/baniya.pdf>.
- Benthem, R.V., 2013. Land evaluation for rain fed agriculture in the Mediterranean Peyne area, Southern France. M.Sc Thesis, Faculty of Geosciences, Utrecht University.
- Congalton, R. G., 1991. A Review of Assessing the Accuracy of Classifications of Remotely Sensed Data. *Remote Sensing of Environment* 37, 35-46. [https://doi.org/10.1016/0034-4257\(91\)90048-B](https://doi.org/10.1016/0034-4257(91)90048-B).
- Di Gregorio, A., Jansen, L.J.M., 1998. *Land Cover Classification System (LCCS): Classification Concepts and User Manual*. For software version 1.0. GCP/RAF/287/ITA Africover – East Africa Project in cooperation with AGLS and SDRN. Nairobi, Rome.
- Elaalem, M., Comber, A., Fisher, P., 2010. *Land Suitability Analysis comparing Boolean logic with fuzzy analytic hierarchy process*. Accuracy 2010 Symposium, July 20-23, Leicester, UK. pp 245-247.
- Fallahshamsi, S.R., 1997. *Accuracy Assessment of Satellite Based Maps Using Sampling*. M.Sc Dissertation, Faculty of Natural Resources, University of Tehran, Iran.

- Fallahshamsi, S.R., 2004. *Economic Evaluation of Different Land uses in Kalibar - chai Forest -covered Watershed, Using Linear Programming and Geographical Information Systems*. Ph.D. Thesis Report, Natural Resource Faculty, Tehran University, Karaj.
- FAO, 1976. A framework for land evaluation. Food and Agriculture Organization of the United Nations, *Soils Bulletin* 32. FAO, Rome.
- Gavrilovic, Z., 1998. The use of empirical method (erosion potential method) for calculating sediment production and transportation in studied or torrential streams. *International Conference on River Regime. Paper 12*, John Wiley and sons.
- Gharakhlou, M. Pourkhabbaz, H.R., Amiri, M.J., Faraji Sabokbar, H., 2008. Ecological Capability Evaluation of Qazvin Region for Determining Urban Development Potential Points Using Geographic Information System. *Journal of Urban-Regional Studies and Research* 2, 51-68.
- Goudarzian, P., Yazdani, M.R., 2015. Climate diversity in line with agroforestry systems: studying technicalities of agroforestry systems and allied components in two diverse climatic regions (Warm climate vs. cold climate) (Case study: Kazeroun & Sepidan in Fars Province, I.R.Iran). *Desert* 20(2), 157-166.
- Hosseini, S., 2018. Comparison Ability Between FAO and Iran Ecological Models to Estimate of Capability Ecological land for Using Pasture (case study: Meydavood area in the east of Khuzestan). *Journal of Environmental Science and Technology* 18(1), 89-103.
- Jahantigh, H.R., Masoudi, M., Jokar, P., 2019. A quantitative approach to land use planning using GIS – A case study of Chabahar County, Iran. *European Journal of Environmental Sciences* 9(1), 12-20. <https://doi.org/10.14712/23361964.2019.2>
- Jokar, P., 2015. *Mapping of land use planning based on modification and quantitative method of current model. (A case study: Jahrom Township)*. M.Sc. Thesis, School of Agriculture, Shiraz University, Iran.
- Jokar, P., Masoudi, M., 2016. Land Suitability for Urban and Industrial Development by a Proposal Model, Case Study: Jahrom Township, Iran. *Journal of Environmental Studies* 42, 135-149.
- Jokar, P., Masoudi, M., Karimi, F., 2021. An MCE-based innovative approach to evaluating ecotourism suitability using GIS. *Cuadernos de Investigación Geográfica* 47 (2), 545-556. <https://doi.org/10.18172/cig.4291>
- Keesstra, S., Mol, G., de Leeuw, J., Okx, J., de Cleen, M., Visser, S., 2018. Soil-related sustainable development goals: Four concepts to make land degradation neutrality and restoration work. *Land* 7(4), 133. <https://doi.org/10.3390/land7040133>
- Keesstra, S., Sannigrahi, S., López-Vicente, M., Pulido, M., Novara, A., Visser, S., Kalantari, Z., 2021. The role of soils in regulation and provision of blue and green water. *Philosophical Transactions of the Royal Society B* 376(1834), 20200175. <https://doi.org/10.1098/rstb.2020.0175>
- Khosravi, Y., Kalantari, M., Kouhestani, N., 2012. Spatial analysis of the degree of land suitability for agricultural and natural resources activities using FAO Model and GIS. *Journal of Conservation and Utilization of Natural Resources* 1 (3): 9-29.
- Kindleberger, C.P., 1967. French Planning. In M.F. Milikan (ed), *National Economic Planning*, Columbia University Press, pp. 279-303, New York.
- Kosmas, C., Poesen, J., Briassouli, H., 1999. Key indicators of desertification at the Environmentally Sensitive Areas (ESA) scale. *The Medalus Project: Mediterranean Desertification and Land Use. Manual on Key Indicators of Desertification and Mapping Environmentally Sensitive Areas to Desertification*. Project report. European Commission.
- Lahmian, R., 2016. The use of geographical information system in identifying suitable locations for planting plants at risk of north of Iran. *Journal of Current Research Science* 4 (2), 27-30.
- Makhdoum, M., 2006. *Principles of Land use planning*. 7th ed., University of Tehran.
- Masoudi, M. (2014). Risk Assessment of Vegetation Degradation Using GIS. *Journal of Agricultural Science and Technology* 16, 1711-1722. <http://hdl.handle.net/123456789/4101>
- Masoudi, M., 2018. *Land Use Planning Using Computer*. Payame Noor University Publisher, Tehran, Iran.

- Masoudi, M., Jokar, P., 2015. Land-use planning using a quantitative model and geographic information system (GIS) in Shiraz Township, Iran. *Ecopersia* 3, 959-974.
- Masoudi, M., Jokar, P., Sadeghi M., 2017. Land Use Planning using a Quantitative model and Geographic Information System (GIS) in Darab County, Iran. *Journal of Materials and Environmental Sciences* 8, 2975-2985.
- Masoudi, M., Jokar, P., Ramazani Poor, E., 2020. A GIS-based quantitative model for land use planning in Larestan County, Iran. *EQA-International Journal of Environmental Quality* 40, 19-30. <https://doi.org/10.6092/issn.2281-4485/10433>
- McHarg, I.L., 1969. *Design with Nature*. Wiley, New York.
- Metze, M., 2002. Het einde van de Amerikanisering, in *Het Financieele Dagblad*, November 23d, 2002.
- Mokarram, M., Zarei, A.R., 2021. Determining prone areas to gully erosion and the impact of land-use change on it by using multiple-criteria decision-making algorithms in arid and semi-arid regions. *Geoderma* 403, 115379. <https://doi.org/10.1016/j.geoderma.2021.115379>
- Najafinezhad, A. Pishdad Soleimanabad, L. Salmanmahini, A., 2013. Comparison of the efficiency of systematic and multi objective land allocation methods for land use planning using Geographic Information System. *Journal of Applied RS & GIS Techniques in Natural Resource Science* 4, 1-11.
- Nakos, G., 1984. The land resource survey of Greece: a tool for land use planning and policy. In *Policy Analysis for Forestry Development*. Proceedings of the International Conference held in Thessaloniki, Greece (IUFRO-Division 4), pp. 439-450.
- Nazari Viand, F., Koohestani, H., Zarifian, Sh., Kazemich, F., 2019. Land Suitability Assessment for Agriculture Using Analytical Hierarchy Process in Northern Parts of Khalkhal County (Case Study: Mikaeel Abad catchment). *Journal of Agricultural Science and Sustainable Production* 30 (1), 225-239.
- Nouri, J., Sharifipour, R., 2004. Ecological Capability Evaluation of Rural Development by means of GIS. *Journal of Environmental Health Science & Engineering* 1(2), 81-90.
- O'Neill, R.V., 1989. Perspectives in hierarchy and scale. In: J. Rougharden, R.M. May, S.A. Levin (Eds.), *Perspectives in Ecological Theory*. Princeton University Press, Princeton, New Jersey.
- Oyinloye, M., Kufoniya, O., 2013. Application of IKONOS Satellite Images in Monitoring of Urban Landuse Change in Ikeja, GRA, Lagos, Nigeria. *International Journal of Engineering Science Invention* 2, 1-10.
- Pan, T., Zhang, Y., Su, F., Lyne, V., Cheng, F., Xiao, H., 2021. Practical Efficient Regional Land-Use Planning Using Constrained Multi-Objective Genetic Algorithm Optimization. *ISPRS International Journal of Geo-Information* 10 (2), 100. <https://doi.org/10.3390/ijgi10020100>
- Piran, H., Maleknia, R., Akbari, H., Soosani, J., Karami, O., 2013. Site selection for local forest park using analytic hierarchy process and geographic information system (case study: Badresh county). *International Research Journal of Applied and Basic Sciences* 6 (7), 930-935.
- Rossiter, D.G., 1996. A theoretical framework for land evaluation. *Geoderma* 72, 165-190. [https://doi.org/10.1016/0016-7061\(96\)00031-6](https://doi.org/10.1016/0016-7061(96)00031-6)
- Saaty, T.L., 1977. A scaling method for priorities in hierarchical structures. *Mathematical Psychology* 15: 231-281.
- Saaty, T.L., Vargas, L.G., 2001. *Models, methods, concepts and applications of the analytic hierarchy process*. *International series in operations research and management sciences*. Kluwer Academic Publisher.
- Safaripour, M. Naseri, D., 2019. Ecological Land Capability Evaluation for Agriculture and Range Management Using WLC Method (Case study: Onarchay watershed, Ardabil province). *Journal of Environmental Science and Technology* 21(8), 113-123. <https://doi.org/10.22034/jest.2020.22063.3120>
- Sanaee, M. Fallah Shamsi, S.R., Ferdowsi Asemanjerdi, H., 2010. Multi-criteria land evaluation, using WLC and OWA strategies to select suitable site of forage plantation (Case study: Zakherd, Fars). *Rangeland* 4, 216-227.

- Sarvazad, A., Qadykolayy, J.O., Nasi, S.M.H., 2015. Determining the potential of Bistoon forest park and locating tourism activities. *Advances in Bioresarch* 6 (3), 25-31.
- Steinitz, C., Parker, P., Jordan, L., 1976. Hand drawn overlays: their history and prospective uses. *Landscape Architecture* 9, 444-455.
- Storie, R., 1987. *Storie index soil rating*. OaHand University of California, Division of Agricultural Sciences, Special publication 32 (3), 10 pp.
- Yohannes, H., Soromessa, T., 2018. Land suitability assessment for major crops by using GIS-based multi-criteria approach in Andit Tid watershed, Ethiopia. *Cogent Food & Agriculture* 4(1), 147048. <https://doi.org/10.1080/23311932.2018.1470481>
- Zakerinejad, R., Masoudi, M., 2019. Quantitative mapping of desertification risk using the modified MEDALUS model: a case study in the Mazayejan Plain, Southwest Iran. *AUC GEOGRAPHICA* 54, 232-239. <https://doi.org/10.14712/23361980.2019.20>

*Anex 1. The indicators used in the model of land evaluation for agriculture and natural resources or four classes' models (a) and for Development and Ecotourism or three classes' models (b) and Conservation Use (c).*

(a)

Criteria	Parameter	Irrigated Farming	Rainfed Farming	Forest	Rangeland	Class	
Topography	Slope (%)	0-8 <sup>1</sup>	0-5	0-35	0-15	1	
		8-15	5-15	35-55	15-25	2	
		15-30	15-25	55-65	25-40	3	
		>30	>25	>65	>40 (in mountains)	4	
	Elevation (m) or Land type	Plain	Plain	0-1000	-	1	
		-	-	1000-1800		2	
		Hill	Hill	1800-2600		3	
Mountain		Mountain	>2600	4			
Climate	Drought	Slight	Slight	-	Slight	1	
		Moderate	Moderate		Moderate	2	
		Severe & very severe	Severe & very severe		Severe & very severe	3	
		-	-		-	4	
	Rain (mm)	-	>400	>800	>400	>400	1
			200-400	500-800	200-400	200-400	2
			50-200	200-500	50-200	50-200	3
			<50	<200	<50	<50	4
	Temperature (°c)	-	-	18 - 21	-	-	1
				<18, 21.1-30			2
				>30			3
				-			4
	Current state of climate	Semi-arid to Humid	-	-	-	-	1
		Arid					2
		Very arid					3
		-					4
Soil	Texture	Heavy, moderate, light	Heavy, moderate, light	Heavy, moderate, light	Heavy, moderate, light	1	
		Coarse	Coarse	Coarse, very coarse	Coarse	2	
		Very coarse	Very coarse	-	Very coarse	3	
		-	-	-	-	4	
	Depth (cm)	Deep (>80)	Deep (>80)	Deep (>80)	Semi deep to deep (>50)	1	
		Semi deep (50-80)	Semi deep (50-80)	Semi deep (50-80)	Shallow (25-50)	2	
		Shallow (25-50)	Shallow (25-50)	Shallow to very shallow (<50)	Very shallow (<25)	3	
		Very shallow to no soil (0-25)	Very shallow to no soil (0-25)	No soil (0)	No soil (0)	4	
	pH	6.1-8.5	≤ 8.5	4.2-7	≤ 9	1	
		4.2-6,8.5-9	8.5-9	7.1-8.5	-	2	
		9-9.5	9-9.5	8.6-10	>9	3	
		>9.5	>9.5	>10	-	4	
	Gravel percent	0-35	0-35	≥15	0-35	1	
		35-75	35-75	16-50	35-75	2	
		>75	-	>51	>75	3	
		-	>75	-	-	4	

	Drainage (cm/hr)	Good to moderate (0.1-25)	Good to moderate (0.1-25)	Good to moderate (0.1-25)	Good to moderate (0.1-25)	1
		Poor (<0.1, >25)	Poor (<0.1, >25)	Poor (<0.1, >25)	Poor (<0.1, >25)	2
		-	-	-	-	3
		-	-	-	-	4
	Erosion	None, slight	None, slight	None, slight	None, slight	1
		Moderate	Moderate	Moderate	Moderate	2
		Severe	Severe	Severe, very severe	Severe, very severe	3
		Very severe	Very severe	-	-	4
	Granulating	Fine to Moderate	Fine to Moderate	Fine	Fine to Moderate	1
		Coarse	Coarse	Moderate	Coarse	2
		-	-	Coarse	-	3
		-	-	-	-	4
	Evolution (Structure)	Perfect (granular)	-	Perfect (granular)	-	1
		Moderate		Moderate		2
		Low		Low		3
		None (no structure)		None (no structure)		4
	Salinity (EC in ds/m)	<8	<8	-	<8	1
		8-16	8-16		8-18	2
		16-32	16-32		18<	3
		>32	>32		-	4
	ESP	<15	<15	-	<15	1
		15-30	15-30		15-30	2
		30-50	30-50		>30	3
		>50	>50		-	4
	Fertility (organic matter %)	Good (>1.5)	Good to Moderate (>1)	Good (>1.5)	Good to Moderate (>1)	1
		Moderate (1-1.5)	Low (1)	Moderate (1-1.5)	Low (1)	2
		Low to Very Low (<1)	Very Low (<1)	Low (1)	Very Low (<1)	3
		-	-	Very Low (<1)	-	4
Geology	Geology	-	-	Limestone and Dolomite, Intermediate pyroclastic rocks of Eocene, Shale, Clay Stone, Conglomerate and marl type 1, Ophiolite of melange color, floodplain	-	1
				Granite, sandstone, loess, schist and gneiss and amphibolite		2
				marl Type 2, alluvial fans, alluvial terraces, sand dunes, continental shelf sediments		3

				Salt domes, gypsum dome, calcite and dolomite marble, quartzite		4		
Vegetation	Canopy Cover (%)	-	-	75-100	$\geq 50$	1		
				25-74	25-50	2		
				<25	5-25	3		
				-	<5	4		
	Wood Value <sup>2</sup>	-	-	-	Wood with grade 1	-	1	
					Wood with grade 2		2	
					Wood with grade 3		3	
					None Commercial		4	
	Vegetation Type	-	-	-	Forest lands	-	1	
					-		2	
					Rangelands		3	
					Poor Rangelands (canopy cover <25%), Desert		4	
	Annual Growth (m <sup>3</sup> ) <sup>3</sup>	-	-	-	>5	-	1	
					2.1-5		2	
					<2		3	
					-		4	
	Dry Forage (kg/ha)	-	-	-	>500	-	1	
					350-500		2	
					<350		3	
					-		4	
Water	Quantity of water (m <sup>3</sup> /year)		-	-	-	>3000 <sup>4</sup>	1	
						1500-3000	2	
						<1500	3	
						Without water resources	4	
	Lowering of water table(cm/y)			-	-	-	0-20	1
							20-30	2
							>30	3
							-	4
	EC( $\mu$ mhos/cm)			-	-	-	0-750	1
							750-2250	2
							>2250	3
							-	4
	SAR			-	-	-	0-18	1
							18-26	2
							>26	3
							-	4

(b)

Criteria	Parameter	Development	Ecotourism	Class <sup>5</sup>	
Topography	Slope (%)	0-15	0-15	1	
		15-30	15-30	2	
		>30	>30	3	
	Land type	Plains except of flood plains	-	-	1
		Plateau & upper terraces, alluvial- colluvial fans			2
		Mountains, Hills, Flood Plains			3

Climate	Rain (mm)	501-800	-	1
		51-500, >800		2
		<50		3
	Temperature <sup>6</sup> (°c)	18.1-24	21-24	1
		24.1-30, <18	18-21, 24-30	2
		>30	>30, <18	3
	Number of sunny days (in spring & summer months)	-	>15	1
			7-15	2
			<7	3
	Relative humid (%)	40.1-70	-	1
		<40, 70-80		2
		>80		3
Wind speed(km/h)	1-35	-	1	
	36-60		2	
	>60		3	
Soil	Texture	Moderate (often)	Usually moderate	1
		light(often)	Coarse, light, heavy	2
		Heavy(often), Regosols, Lithosols	Very heavy	3
	Depth	Deep	Deep	1
		Semi deep	Semi deep	2
		Shallow to very shallow	Shallow to very shallow	3
	Gravel percent	0-25	-	1
		26-50		2
		>50		3
	Drainage (cm/hr)	Good (2-6)	Good (2-6)	1
		Moderate (0.1-2, 6-25)	moderate to poor (0.1-2, 6-25)	2
		Poor (<0.1, >25)	Incomplete (<0.1, >25)	3
	Erosion	None, slight	-	1
		Moderate		2
		Severe, very severe		3
	Granulating	Moderate	-	1
		Fine, coarse		2
		Very fine		3
	Evolution (Structure)	Perfect (granular)	Perfect (granular)	1
		Moderate	Moderate	2
		Low	Low	3
Fertility (Organic matter %)	-	Good, moderate (>1)	1	
		Low (1)	2	
		Very low (<1)	3	
Geology	Lithology	Sandstone, Ophiolite of melange color, sediments of continental shelf	pyroclastic rocks, Granite Ophiolite of melange color, sand dunes, continental shelf sediments	1
		Limestone and Dolomite, Intermediate pyroclastic rocks of Eocene, Granite, alluvial fans, Shale, Clay Stone, Conglomerate, loess, alluvial terraces	Limestone and Dolomite, sandstone, loess, schist and gneiss and amphibolite, quartzite, alluvial fans, flood plain	2
		marl, schist and gneiss and amphibolite, sand dunes, Salt domes, Gypsum dome, calcite and dolomite marble, quartzite, floodplain, Buffer <sup>7</sup> (Fault, River)	marl, Shale, Clay Stone, Conglomerate, Salt domes, gypsum dome, calcite and dolomite marble	3

Vegetation	Canopy Cover (%)	0-25	Forest lands with canopy cover of 50-80 %	1
		26-50	Forest lands with canopy cover of 5-50%	2
		>50	Poor Rangelands, Forest lands with canopy cover>80%, Desert	3
Water	Quantity of water for everyone (Lit/day)	>225	>40	1
		150-225	12-39.9	2
		<150	<12	3
Conservation	Protected area	-	Forest park of Natural and planted, Nature Park, National Park, Protected Area, Biosphere Reserve, World Heritage, Historical artefacts and national and pilgrimage	1
		-	-	2
		-	Reserve forest, Wildlife Sanctuary, National natural monuments	3

(c)

Parameter		Class
Value of Species (Mammals)	Cheetah, Zebra, Fallow deer, Ibex, Chamois, Panther, gazelle, Chinkara, Wild goat, Ovis, Wolf, Sable, Wild Cats, Bear	Suitable
	Fox, Badger, Hyena, Weasel, Pig, Porcupine, Squirrel, Jackal, Pika, Hedgehog, Bat, Rabbit, Rodents	None Suitable
Species Biodiversity	≥5	Suitable
	<5	None Suitable
Sensitive Habitats	Mangroves, estuaries, ponds	Suitable
	Other	None Suitable
Protected Area	Reserve forest, Forest Park of Natural and planted, National Park, Nature Park, Protected Area, Biosphere Reserve, Wildlife refuges, National natural monuments	Suitable
	Other	None Suitable

<sup>1</sup> This slope classification is assigned for horticulture and Class 1: 0-5, Class 2: 5-8, Class 3: 8-15 and Class 4: >15 is assigned for Irrigated cultivation.

<sup>2</sup> It is evaluated for only Commercial Forestry suitability

<sup>3</sup> It is evaluated for only Commercial Forestry suitability

<sup>4</sup> This classification is assigned for horticulture and Class 1: >4000, Class 2: 1500-4000, Class 3: <1500 and class 4: Without water resources is assigned for Irrigated cultivation

<sup>5</sup> Poor & not suitable situation for third class

<sup>6</sup> For ecotourism in spring & summer seasons

<sup>7</sup> Major Fault= 1km, Minor Fault =300m; River= 1km (Gharakhlou *et al.*, 2008, based on guidelines of Department of Energy and Department of Housing and Urban Development in Iran)



## CIRCULATION WEATHER TYPES AS A KEY FACTOR ON RUNOFF INITIATION AND SEDIMENT DETACHMENT IN MEDITERRANEAN SHRUBLANDS

JESÚS RODRIGO-COMINO<sup>1\*</sup>, JOSÉ MARÍA SENCIALES-GONZÁLEZ<sup>2</sup>,  
ANA PÉREZ ALBARRACÍN<sup>3</sup>, ERICK R. BANDALA<sup>4</sup>,  
FRANCISCO ESCRIVÀ SANEUGENIO<sup>3</sup>, SASKIA D. KEESSTRA<sup>1,5</sup>,  
ARTEMI CERDÀ<sup>3</sup>

<sup>1</sup>*Departamento de Análisis Geográfico Regional y Geografía Física, Facultad de Filosofía y Letras, Campus Universitario de Cartuja, University of Granada, Granada, 18071, Spain.*

<sup>2</sup>*Department of Geography, Málaga University, Campus of Teatinos s/n, 29071 Málaga, Spain.*

<sup>3</sup>*Soil Erosion and Degradation Research Group. Department of Geography, Valencia University, Blasco Ibáñez, 28, 46010 Valencia, Spain.*

<sup>4</sup>*Division of Hydrologic Sciences, Desert Research Institute, 755 E. Flamingo Road, Las Vegas, Nevada, 89119, USA.*

<sup>5</sup>*Team Soil, Water and Land Use, Wageningen Environmental Research, Wageningen University & Research, Wageningen, Netherlands.*

**ABSTRACT.** In this research, the circulation weather types (CWTs) associated with individual surface pressure data at different atmospheric heights were used to correlate and quantify soil erosion events collecting soil loss ( $\text{g m}^{-2}$ ), runoff ( $\text{l m}^{-2}$ ) and sediment concentration ( $\text{g L}^{-1}$ ) using field plots and sediment collectors. Representative Mediterranean shrubland, located at Sierra de Enguera (Eastern Spain), was used as a case study where 213 rainfall episodes and related soil loss events were recorded for the 2010-2014 period. Average annual precipitation of 544 mm was registered, summarizing a total of 2,720.1 mm for the five years of the research period. A total of 34.4% of the registered precipitation events ranged from 10 to 29.9 mm, 23.5% from 30 to 49.9 mm, and 15.9% from 50 to 99.9 mm. The dynamic low-pressure with fronts (DLp+f) CWT was found to generate the highest precipitation amount reaching 60.6% of the total precipitation (105 of the 213 events). Over a third (35%) of the precipitation events occurred during Eastern CWT, which accounted for 48% of the total precipitation with average values of 17.6 mm per event. From the total runoff, 65.6% was related to the combined Eastern and cold drops (CD) CWT. The DLp+f CWT was found to produce 48.9% of sediment mobilization, of which 73.5% of this amount was generated by Eastern CWT. The highest sediment concentration event was found for the southern CWT under thermal low-pressure (TLp) reaching  $51.65 \text{ g L}^{-1}$ , followed by A (anticyclones) with the Eastern CWT ( $42.23 \text{ g L}^{-1}$ ). As a whole, the southern is the CWT generating the highest average sediment concentration ( $28.66 \text{ g L}^{-1}$ ), followed by Easter CWT. Our findings suggest that CWTs contribute to foreseeing the periods with the highest soil losses and may help to prevent them. We discuss the need to analyse the changes in soil erosion rates due to CWT to better characterize the soil erosion process and assess the soil erosion rates, improve the current soil erosion models and investigate how climate change is changing the role CWT plays in runoff initiation and sediment delivery.

## ***Tipos de tiempo como factor clave en el inicio de la escorrentía y el arranque de sedimentos en matorrales mediterráneos***

**RESUMEN.** En esta investigación, los tipos de tiempo (CWT, por sus siglas en inglés) asociados con datos de presión de superficie individuales a diferentes alturas atmosféricas se utilizaron para correlacionar y cuantificar los eventos de erosión del suelo que corresponden a la pérdida de suelo ( $\text{g m}^{-2}$ ), la escorrentía ( $\text{l m}^{-2}$ ) y la concentración de sedimentos ( $\text{g L}^{-1}$ ) utilizando parcelas de erosión y colectores. Se utilizó como estudio de caso una zona de matorral mediterráneo representativo, ubicado en la Sierra de Enguera (este de España), donde se registraron 213 eventos de precipitación y eventos relacionados de pérdida de suelo durante el período 2010-2014. Se registró una precipitación media anual promedio de 544 mm, sumando un total de 2.720,1 mm para los cinco años de investigación. El 34,4% de los eventos de precipitación registrados varió de 10 a 29,9 mm, el 23,5% de 30 a 49,9 mm y el 15,9% de 50 a 99,9 mm. Se encontró que la baja presión dinámica con frentes (DLp+f) generó la mayor cantidad de precipitación alcanzando el 60,6% de la precipitación total (105 de los 213 eventos). Más de un tercio (35%) de los eventos de precipitación ocurrieron durante el CWT del Este, lo que representó el 48% de la precipitación total con valores promedio de 17,6 mm por evento. Del total de la escorrentía, el 65,6% estuvo relacionado con el CWT combinado de gotas frías y tiempos del este (CD). Se encontró que el DLp+f producía el 48,9% de la movilización de sedimentos, de los cuales el 73,5% de esta cantidad fue generada por el CWT del Este. El evento de mayor concentración de sedimentos se encontró para el tipo de tiempo del Sur con baja presión térmica (TLp) alcanzando  $51,65 \text{ g L}^{-1}$ , seguido por A (anticiclones) del Este ( $42,23 \text{ g L}^{-1}$ ). En su conjunto, el sur es el CWT que genera la mayor concentración promedio de sedimentos ( $28,66 \text{ g L}^{-1}$ ), seguido del Este. Nuestros hallazgos sugieren que los CWT contribuyen a prever los períodos con mayores pérdidas de suelo y pueden ayudar a prevenirlos. Discutimos la necesidad de analizar los cambios en las tasas de erosión del suelo debido a cada tipo de tiempo para caracterizar mejor el proceso de erosión del suelo y evaluar las tasas de erosión del suelo, mejorar los modelos actuales e investigar cómo el cambio climático está cambiando el papel que juega los CWT en el inicio de la escorrentía y en la entrega de sedimentos.

**Keywords:** Precipitation, Soil erosion, Land management, Human-affected ecosystems, Regional issues.

**Palabras clave:** Precipitación, Erosión del suelo, Gestión de tierras, Ecosistemas afectados por el hombre, Temas regionales.

Received: 21 July 2022

Accepted: 6 February 2023

\*Corresponding author: Jesús Rodrigo-Comino, Departamento de Análisis Geográfico Regional y Geografía Física, Facultad de Filosofía y Letras, Campus Universitario de Cartuja, University of Granada, Granada, 18071, Spain. E-mail address: [jesusrc@ugr.es](mailto:jesusrc@ugr.es).

## **1. Introduction**

Understanding soils as an indispensable Earth resource is necessary to know how ecosystem services work and which human activities can take place in a specific land (Jónsson and Davíðsdóttir, 2016; Keesstra *et al.*, 2018a; Norman, 2020). For millennia, humans have used the soil to establish settlements and to obtain minerals or food (Altınbilek, 2004; Neville 2007). However, prolonged exploitation has generated serious issues affecting the quality and, subsequently, soil fertility (Rodrigo-Comino *et al.*, 2021). For decades, scientists have reported that soil is being affected by numerous land degradation processes such as soil compaction (Al-Dousari *et al.*, 2019; Drewry *et al.*, 2008), sealing (Larsen *et al.*, 2009; Munafò *et al.*, 2013), arson fires (Fernandez-Anez *et al.*, 2021) or contamination (Radziemska *et al.*, 2019; Rodríguez-Seijo *et al.*, 2018). Among them, anthropogenic soil erosion is one

of the land degradation processes threatening humankind's sustainability (Bork *et al.*, 2003; Brown, 1981; Panagos *et al.*, 2020) because it causes nutrient loss in agricultural fields, damages lowlands, increases desertification risk inducing biodiversity and generate productivity losses (An *et al.*, 2019; Di *et al.*, 2019; Xie *et al.*, 2019).

The Mediterranean belt is one of the most affected areas by soil losses due to the intensification of urbanization (Egidi *et al.*, 2021), agriculture (Mohammed *et al.*, 2020; Raclot *et al.*, 2009; Vanwalleghem *et al.*, 2011) or grazing (Kairis *et al.*, 2015; Minea *et al.*, 2019). Prospects regarding climate change trends are claiming that soil erosion is becoming more intense in the most vulnerable lands (Borrelli *et al.*, 2020; Nearing *et al.*, 2004), with the consequent higher risks of desertification (Martínez-Valderrama *et al.*, 2016) and deterioration of rural economy (Ashby, 1985; Bayu, 2020; Sobral *et al.*, 2015).

Soil erosion is a complex process involving numerous interrelated and inherent factors such as rock and vegetation cover, antecedent soil moisture, roughness, slope, soil management or soil properties (Auzet *et al.*, 2002; Sun *et al.*, 2013). It also depends on the weather conditions before and during erosive events and, for this reason, generating knowledge about weather conditions will allow the scientific community to foresee the negative consequences of soil erosion and develop efficient control measures (Rodrigo-Comino *et al.*, 2019). To achieve this goal, defining the different circulation weather types (CWTs) and the rainfall events that may produce runoff and soil loss is a significant need. The CWTs have been extensively used for different purposes and classifications (Brazel and Nickling, 1986; Hess and Brezowsky, 2010; Lamb, 1972; Schroeder *et al.*, 1964) but are mainly restricted to specific areas and focused on weather forecasting and historical climate research (Ramos *et al.*, 2015). Recent improvements, during the last two decades, in remote sensing techniques, satellite information and climate datasets have made it possible to conduct more accurate studies considering larger scales and longer periods (Cortesi *et al.*, 2014; Fernandez-Raga *et al.*, 2017; Kidson, 2000; Trigo and DaCamara, 2000).

The relationship between weather types and soil erosion was originally used to assess landslides close to river or mountain catchments (Nadal-Romero *et al.*, 2014; Pattison and Lane, 2012). These works suggested that it is possible to find a correlation using a large number of precipitation events. Other studies (Nadal-Romero *et al.*, 2015; Peña-Angulo *et al.*, 2020, 2019) analysed large datasets from the Mediterranean belt to correlate weather types and soil erosion rates (Peña-Angulo *et al.*, 2021). However, little information is available about the way that CWTs affect runoff generation at the pedon scale, and most of the research is carried out in agricultural or forestry landscapes. This paper assesses the sediment delivery and runoff yield which will give a wider view of the soil erosion process and the climatic factors involved when vegetation cover changes.

To our best knowledge, assessments at hillslope and pedon scales considering CWTs and soil erosion are scarce. Recently, our research group (Rodrigo-Comino *et al.*, 2020a, 2019) carried out studies on CWTs in vineyards in Southern and Eastern Spain, comparing active and abandoned vine plots, and conventional soil management systems. Both studies found key steps for designing soil erosion control measures to mitigate the negative impact of extreme rainfall and runoff considering atmospheric conditions. However, the need for new approaches to detect the amount of rainfall needed to activate soil losses and prevent erosive events remain, and this is relevant for shrublands and forest as most of the previous research comes from agricultural land. The main goal of this study is to assess the relationship between CWTs and soil erosion at the pedon scale. To achieve this goal, a representative hillslope located in the Mediterranean belt was selected as a case study to, specifically, i) analyse CWTs associated with individual surface pressure data at different atmospheric heights; ii) detect CWTs and individual surface pressure data generating soil losses; and iii) estimate how shrublands are affected by soil losses.

## 2. Materials and methods

### 2.1. Study area

A typical Mediterranean *maquia* ecosystem representing a large area of the Mediterranean climatic region was selected as a study case. The shrublands are widespread due to the degradation of the original forest covers and they are diverse in plant composition but with similar characteristics: lower biomass than forest land and adapted to forest fires due to sprouting and seedling strategies. The experimental soil erosion station of Sierra de Enguera is located in the Eastern Iberian Peninsula (60 Km from the coast) at an altitude of 758 m above sea level (Fig. 1). The climate is typically Mediterranean (Csa according to Köppen and Geiger (1930) and Kottek *et al.* (2006) with a mean annual temperature of 12.7°C, mean annual rainfall of 540 mm, and characterized by a long drought period (from June to September). Intense rainfall events usually bring daily rainfall amounts higher than 100 mm. Soils are classified as Inceptisols (Soil Survey Staff, 2014) and show rock outcrops and a cover of rock fragments. The vegetation is composed of a mixture of Mediterranean *maquia* species (*Ulex parviflorus* Pourr., *Pistacia lentiscus* L., *Erica multiflora* L., *Juniperus oxycedrus* Sibth. & Sm., *Quercus coccifera* L. and *Rosmarinus officinalis* L.). The experimental station was constructed in January 2010, and runoff information collection started in October 2010 and lasted 5 years (from October 2010 to September 2014). The data from January to October 2010 were not considered due to the disturbances created by the plot installation.

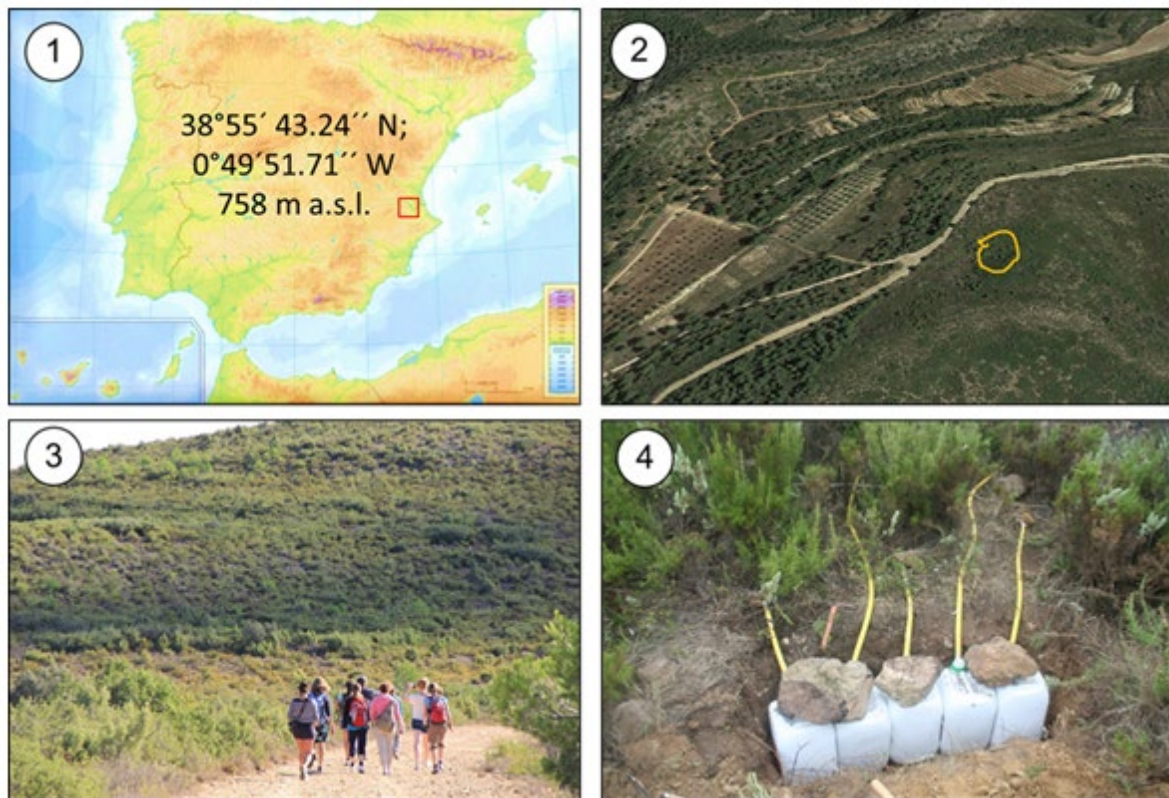


Figure 1. Localisation of the study area (1 and 2), landscape (3) and plots (4).

### 2.2. Assessment of CWTs

A total of 213 rainfall events were selected from the continuous rainfall records of the nearby meteorological station. A rainfall event is considered to have a minimum total rainfall value of 1 mm and is separated by a minimum of 6 continuous dry hours (Rodrigo-Comino *et al.*, 2020a). All single-

day (24 hours) events were counted. For multi-day events, only those retaining the same CWT, wind surface direction, or recorded no erosion, were counted.

In each event, individual surface pressure data (500 hPa) and dominant surface wind (intensity and direction) were recorded on the study experimental station. This study is aimed to identify and classify CWTs using synoptic maps. This assessment requires the use of a variety of downscaling procedures that attempt to relate circulation-scale variability (large scale) to precipitation variability at local scales (Jones *et al.*, 2013). To achieve this goal, we used the following meteorological sources: i) Wetter Zentrale (<https://www.wetterzentrale.de>); ii) Leeds University website (<http://homepages.see.leeds.ac.uk>); and, iii) the Spanish Agency of Meteorology (AEMET; <http://www.aemet.es/es/portada>).

Using the meteorological sources described before, the CWTs were catalogued and related to precipitation volumes and numbers of events, as well as their soil erosion results. The CWTs identified correspond to the following individual surface pressure data exhaustively described (Nadal-Romero *et al.*, 2015; Rodrigo-Comino *et al.*, 2020a): i) Dynamic low-pressure without fronts (DLp); ii) Thermal low-pressure (TLp); iii) Dynamic low-pressure with fronts (DLp+f); iv) Cold Drop (CD); v) Anticyclones with fronts (HP+f); vi) Anticyclones/Weak pressure (A). In another study, Rodrigo-Comino *et al.* (2020a) observed that other conditions that exhibited height inversion, related to coastal areas or arid and semi-arid lands close to the Iberian Peninsula. These conditions were excluded from this analysis because that classification was not adequate for soil erosion assessment. This assessment was based on how, and to what extent, the situation at 500 hPa affects the volume and the number of events that have an impact on soil erosion. The events have been classified according to the duration since this is how the runoff and soil loss values have been recorded.

### *2.3. Sampling plot strategy and soil erosion assessment*

Sixteen circular plots (from 0.33 to 0.45 m<sup>2</sup>, average 0.38 m<sup>2</sup>) were constructed with drainage connected to a 30 L container through a 40 mm diameter pipeline in the same slope, but under four different canopy cover (4 x 4 plots): *Quercus coccifera* L., *Pistacia lentiscus* L., *Ulex parviflorus* Pourr. and *Rosmarinus officinalis* L., to collect information about the detachment of sediments and runoff initiation. The runoff discharge and sediment concentration were collected, and plots borders, drainage, collectors, pipes and deposits were repaired after each rainfall event. Information on 150 erosive events was collected. Soil erosion rates and runoff coefficients were calculated for each rainfall event. Rainfall data was supplied by the Spanish Agency of Meteorology (AEMET) meteorological station located 5 Km from the study site. Sixty-four (four per plot) soil samples at 0-2 cm depth were collected to determine calcium carbonate content, grain size, organic matter, and bulk density. Soil organic matter was determined by the Walkley-Black method (Walkley and Black, 1934). Bulk density was measured using the ring method (Al-Shammary *et al.*, 2018) and calcium carbonate with the potassium dichromate method. The grain size was determined with the pipette method (Deshpande and Telang, 1950).

## **3. Results**

### *3.1. Soil characterization*

In Figure 2, the characterization of the soil properties obtained after sampling the study area is presented. Vegetation cover averaged 95% (maximum 98% and minimum 89%). Litter cover amounted to 31.1% (maximum 48 and minimum 19%). Rock fragment cover percentage was 19.8% (maximum 32% and minimum 13%) and gravel 6% (maximum 9.5% and minimum 2.7%). Organic matter in the samples was 6.12%, bulk density 1.01 gr cm<sup>-3</sup> and calcium carbonate 59.1%. Soil texture was identified as clay loam.

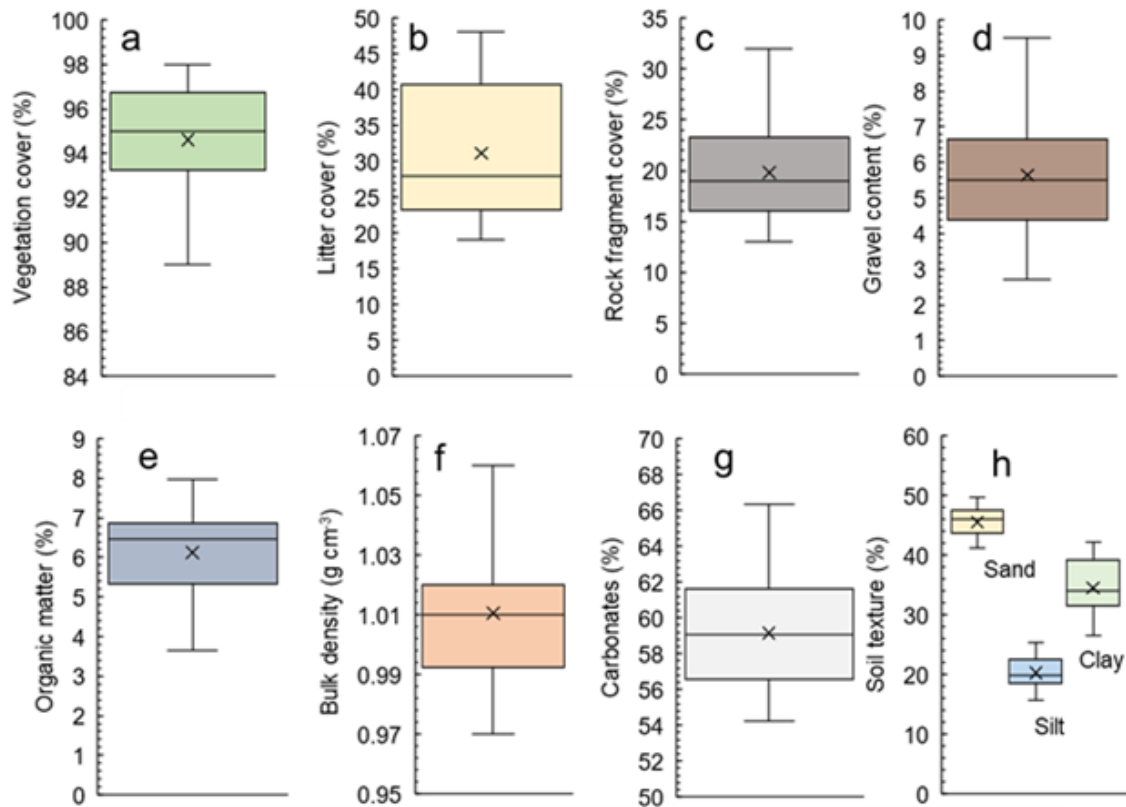


Figure 2. Soil properties and environmental characteristics within the studied plots.

### 3.2. Characterization of precipitation events (2010-2014)

A total of 213 precipitation events were identified during the studied period (Fig. 3). The mean annual precipitation was 544 mm (October to September). The yearly precipitation distribution was 554.2 mm in 2010; 590.4 mm in 2011; 593.7 mm in 2012; 560 mm in 2013; and 422.4 mm in 2014. The total accumulated rainfall was 2,720.1 mm. The three highest rainfall events recorded reached 176.8 (15/11/2012), 145.5 (23/11/2011) and 100.5 mm (25/04/2013).

Figure 4 shows the classification of each precipitation event in the base of the different individual surface pressure data described in Methods. The information was used to obtain the percentage of each rainfall related to the soil erosion events (top part) and the number of events considering each surface pressure data (bottom part). The 34.4% of the total events ranged from 10 to 29.9 mm, 23.5% from 30 to 49.9 mm and 15.9% from 50 to 99.9 mm. The highest precipitation amount was generated by DLp+f reaching 60.6% along 105 events, one of them higher than 100 mm and four in the 50-99.9 mm range. However, the highest number of events (85) generated precipitation values ranging from 1 to 4.9 mm (39.9%). A total of 55 events (25.8%) were recorded with precipitation values in the 10 to 29.9 mm interval, and 48 events (22.5%) ranged from 5 to 9.9 mm. The occurrence of HP+f (34 events) and CD (21 events) accumulated 13.0 and 11.6% of the total precipitations, respectively. It is worth highlighting that CD was able observed during one precipitation event within the 50-99.9 mm value range. In contrast, the mildest precipitation events (only one within the 29.9-50 mm range, and the rest lower) occurred with DLp (5.5%), A (4.8%) and TLp (4.4%), registering 18, 22, and 13 of the total set of events, respectively.

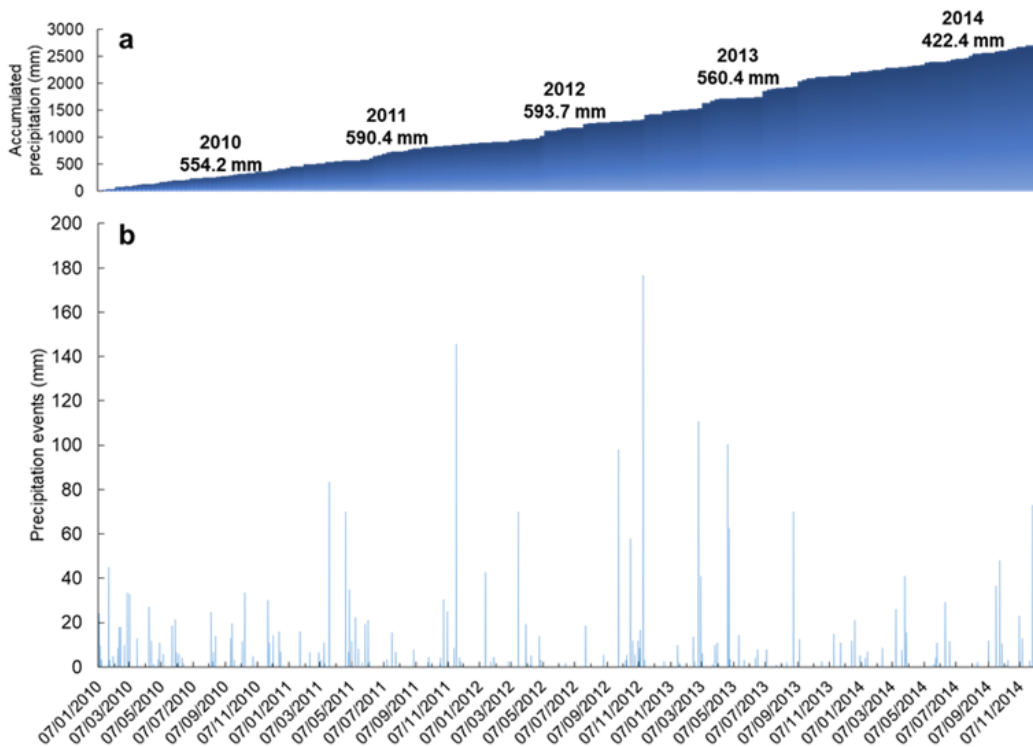


Figure 3. Temporal distribution and accumulated precipitation events during the studied period

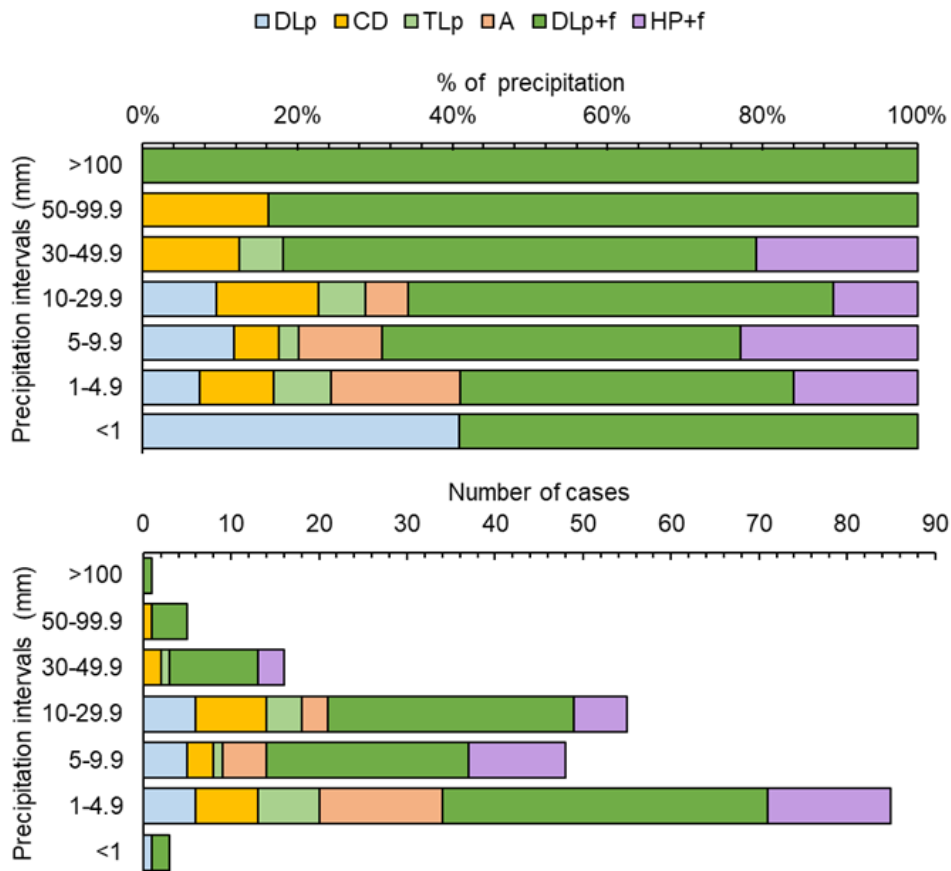


Figure 4. Classification of precipitation events per intervals considering each individual surface pressure data. i) Dynamic low-pressure without fronts (DLp); ii) Thermal low-pressure (TLp); iii) Dynamic low-pressure with fronts (DLp + f); iv) Cold Drop (CD); v) Anticyclones with fronts (HP + f); vi) Anticyclones/Weak pressure weather systems (A).

In Table 1 and Figure 5, the number of events distribution (%) and total precipitation of the events registered for the different CWTs are summarized. It was found that 35% of the precipitation events occurred during Eastern CWT, summarizing 48% of the total precipitation with an average precipitation value of 17.6 mm per event. Western and North CWT registered 17% and 13% of the events, respectively, but also the lowest precipitation amount (245.8 mm and 244.3 mm, respectively), and averages (6.6 and 8.8 mm, respectively). Southern CWT recorded 16% of total precipitation along 34 events averaging 11.9 mm. Finally, mixed atmospheric conditions accounted for 19% of the total precipitation, averaging 13 mm per event along 40 events.

Table 1. Number of events (n), total precipitation (mm), average total rainfall and standard deviation (S.D.) of the events recorded for the different weather types

Weather types	Total precipitation	N° of cases	Average	S.D.
N	94.2	9	10.5	14.4
N-NE	0	0	0	0
NE	673.6	28	24.1	30.9
E-NE	111	3	37	45.9
E	494.5	41	12.1	13.5
E-SE	26.5	2	13.3	0.4
SE	265.8	21	12.7	11.6
S-SE	0	0	0	0
S	138.6	13	10.7	9.6
S-SW	0	0	0	0
SW	71.2	9	7.9	6.1
W-SW	7.9	2	4.0	2.2
W	131.7	24	5.5	3.0
W-NW	35	2	17.5	7.8
NW	145.7	18	8.1	11.6
N-NW	5.4	1	5.4	0
Mixed	520	40	13.0	15.8

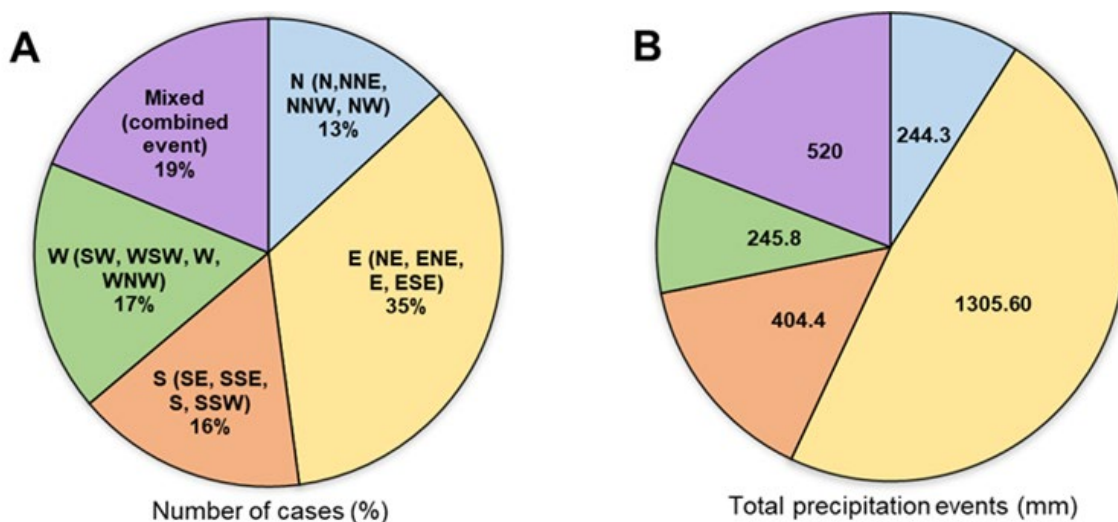


Figure 5. Distribution of the number of events (%) and total precipitation (mm) of the events registered for the different weather types.

### 3.3. Runoff generation depending on the weather types

Out of the 150 rainfall events, only 40 (less than one-third) registered runoff, suggesting that, in general, the longer the event lasts, the greater the volume per rainy day. In Table 2, runoff generation and total discharges are summarized for all the events recorded. It is worth highlighting that the most repeated rainfall events lasted one day (104 times). Similarly, the longer the event lasts, the higher the average runoff coefficient recorded, which implies a progressive saturation of the soil and runoff generation. Considering rainy days (Table 3), 37 of the 213 rainfall events registered runoff. Considering the specific CWT, Eastern CWT recorded most of the events and the highest percentage of runoff (50%), accounting for almost half of the events where runoff was recorded (37 out of 78).

Table 2. Number of runoff events used to assess runoff and soil loss generation, and sediment concentration classified per duration days

Duration (days)	Nº events	Total days	Total volume (mm)	mm/day	Runoff (l)	Runoff (mm)	Average runoff coefficient	Soil loss (g m <sup>2</sup> )	Sediment concentration (g l <sup>-1</sup> )
1	104	104	1154.4	11.1	23.4	63.3	2.0	1063.0	16.8
2	33	66	752.9	11.4	25.9	72.4	3.4	1987.6	27.5
3	11	33	567	17.2	29.8	81.1	5.3	2884.5	35.6
4	0	0	0	0	0	0	0	0	0
5	2	10	246.8	24.7	17.2	45.9	7.0	904.7	19.7
Total	150	213	2721.1					6839.2	

Table 3. Weather types and, runoff and soil loss characterization. i) weather type (WT); ii) number of cases (n); iii) precipitation (P); iv) Runoff estimated in liters (R); and v) average runoff coefficient (Av. Rc %)

WT	n	P(mm)	Av	R(l)	R (mm)	Av. Rc (%)	Cases with R	Events with R	Rc (%)	% of cases with R	SL (g)	SC (g l <sup>-1</sup> )
N	28	245.3	8.8	4.3	11.9	4.9	10	7	4.8	35.7	246.2	20.7
E	74	1305.6	17.6	70.7	198.1	20.2	37	19	15.2	50.0	5563.1	29.0
S	34	404.4	11.9	6.7	18.5	4.9	12	5	4.6	35.3	43.6	2.7
W	37	245.8	6.6	1.2	3.3	0.8	5	2	1.3	13.5	16.0	4.8
Mixed	40	520.0	13	10.9	31.3	3.7	14	7	6.0	35.0	971.0	31.1
Total	213	2721.1					78	40			6839.8	17.67

Considering the 40 events showing runoff (Table 4), 262.74 mm of precipitation was recorded (9.7% of the total precipitation), from which 54.8% correspond to DLp+f. CD summarized 25.3% of the total runoff volume while HP+f represented 11.8% of the runoff volume. The highest volume of runoff corresponds to weather types from the Eastern (78.5%). The remaining types of weather conditions account for 5.1% of the total events, and volumes are always below 5% of the total with a predominance of association with Eastern winds. However, there is an exception with the TLp, where the greater volume of runoff occurs with Southern weather types.

**Table 4.** Assessment of atmospheric conditions, rainfall events, runoff generation and weather types. i) Dynamic low-pressure without fronts (DLp); ii) Thermal low-pressure (TLp); iii) Dynamic low-pressure with fronts (DLp + f); iv) Cold Drop (CD); v) Anticyclones with fronts (HP + f); vi) Anticyclones/Weak pressure weather systems (A); vii) atmospheric situation (AS); viii) average (Av).

AS	l·m <sup>-2</sup>	N	E	S	W	Mixed	Total	%
DLp	Total	0.15	1.78	0	0.15	0.38	2.46	0.9
	Av.	0.15	1.78	0	0.15	0.38	0.49	
CD	Total	0	66.47	0	0	0	66.47	25.3
	Av.	0	5.57	0	0	0	1.11	
TLp	Total	0	0.09	7.87	0	0.09	8.05	3.1
	Av.	0	0.09	3.93	0	0.09	0.82	
A	Total	0	10.67	0.22	0	0	10.89	4.1
	Av.	0	3.56	0.22	0	0	0.76	
DLp+f	Total	11.72	94.40	8.89	3.16	25.69	143.87	54.8
	Av.	1.11	6.01	1.26	0.79	3.09	2.45	
HP+f	Total	0	24.35	1.55	0	5.11	31.01	11.8
	Av.	0	6.09	0.78	0	1.70	1.85	
Total		11.87	197.76	18.53	3.31	31.27	262.74	100
%		4.5	75.3	7.1	1.3	11.9	100.0	

### 3.4. Soil erosion rates depending on the weather types

The Eastern CWT was found to generate the highest volume of sediment discharge, both in total amount (g m<sup>-2</sup>) and concentration (g L<sup>-1</sup>), with 95.4% of the total mass.

Considering the 40 events that recorded runoff (Table 5), a total of 6.8 kg was collected, which implies 19,845.11 g m<sup>-2</sup> (considering 0.34 m<sup>2</sup> plots). It was found that DLp+f generated 48.9% of the mobilized sediments, and of this amount, 73.5% was generated by Eastern CWTs. CD registered 25.4% of the soil loss, all related to Eastern CWTs and HP+f, which represent 12.9% of the mobilized soil loss. The remaining CWTs supposed to be lower than 7% soil losses, all of them associated with Eastern CWT, except TLp, where most of all the mobilized mass was generated by Southern CWT.

**Table 5.** Assessment of atmospheric conditions, rainfall events, soil loss and weather types. i) Dynamic low-pressure without fronts (DLp); ii) Thermal low-pressure (TLp); iii) Dynamic low-pressure with fronts (DLp + f); iv) Cold Drop (CD); v) Anticyclones with fronts (HP + f); vi) Anticyclones/Weak pressure weather systems (A); vii) atmospheric situation (AS); viii) average (Av)

AS	g m <sup>-2</sup>	N	E	S	W	Mixed	Total	%
DLp	Total	2.68	42.42	0	2.68	12.80	60.57	0.3
	Av.	2.68	42.42	0	2.68	12.80	12.11	
CD	Total	0	5036.68	0	0	0	5036.68	25.4
	Av.	0	419.72	0	0	0	83.94	
TLp	Total	0	0.87	1179.07	0	0.87	1180.82	6
	Av.	0	0.87	589.54	0	0.87	118.26	
A	Total	0	1306.85	2.23	0	0	1309.09	6.6
	Av.	0	435.62	2.23	0	0	87.57	
DLp+f	Total	460.48	7133.22	320.26	125.86	1662.16	9701.99	48.9
	Av.	51.16	475.55	45.75	31.47	207.77	162.34	
HP+f	Total	0	2372.45	39.77	0	143.76	2555.98	12.9
	Av.	0	593.11	19.88	0	47.92	132.18	
Total		463.16	15892.49	1541.33	128.54	1819.58	19845.11	100
%		2.3	80.1	7.8	0.7	9.2	100.0	

Sediment concentration differed from total soil losses and runoff results (Table 6). DLp+f showed high sediment loads per unit volume ( $17.61 \text{ g l}^{-1}$ ), but not the highest values. TLp-Southern CWTs recorded the highest sediment concentration ( $51.65 \text{ g l}^{-1}$ ) followed by A-Eastern CWTs ( $42.23 \text{ g l}^{-1}$ ), and HP+f-Eastern WTs ( $33.58 \text{ g l}^{-1}$ ), suggesting that, as a whole, the Southern CWT generated the highest sediment concentration, followed by the Eastern CWT. The Western CWT of Atlantic Ocean origin generated the lowest sediment concentration.

Table 6. Assessment of atmospheric conditions, rainfall events, sediment concentration ( $\text{g l}^{-1}$ ) and weather types. i) Dynamic low-pressure without fronts (DLp); ii) Thermal low-pressure (TLp); iii) Dynamic low-pressure with fronts (DLp + f); iv) Cold Drop (CD); v) Anticyclones with fronts (HP + f); vi) Anticyclones/Weak pressure weather systems (A); vii) atmospheric situation (AS); viii) average (Av)

AS	N	E	S	W	Mixed	Av
DLp	6.21	8.23	0.00	6.21	11.59	6.45
CD	0.00	26.11	0.00	0.00	0.00	5.22
TLp	0.00	3.32	51.65	0.00	3.32	11.66
A	0.00	42.23	3.43	0.00	0.00	9.13
DLp+f	13.54	26.04	12.42	13.73	22.30	17.61
HP+f	0.00	33.58	8.84	0.00	9.70	10.42

## 4. Discussion

### 4.1. Soil erosion as a worldwide concern and the need for weather types research

Previous investigations conducted from the pedon scale (de Lima *et al.*, 2003; Telak *et al.*, 2021) to the regional or continent ones (Carretier *et al.*, 2018; Panagos *et al.*, 2015) concluded that soil erosion is a big concern for humankind due to the possible irreparable consequences on food security, biodiversity and natural resources. However, less attention is paid to responsible atmospheric factors at different heights (Fernández-González *et al.*, 2012; Jones *et al.*, 2013) than the methods used and the final consequences in form of soil and water losses. The main goal of this research was to understand how soils react after each precipitation event because of different barometric situations and diverse CWTs. Nowadays, this topic is poorly studied at the hillslope scale due to the elevated amount of data needed to establish a statistically considerable trend (Peña-Angulo *et al.*, 2021; Rodrigo-Comino *et al.*, 2019). The specific number has not been delimited and it is a key point to be stated in coming investigations. However, this difficult task will also depend on climate variations. Also, this research will be affected by the season monitored corresponding to the most representative years within the climatic trend of each region. In this study, a total of 213 precipitation events (rainfall and snow) were collected over 5 years. We can state that, despite the three extreme rainfall events higher than 100 mm, the precipitation was in line with the usual trend of Eastern Spain (Piñol *et al.*, 1998). In 2014, the rainfall amount was less than 500 mm, which also agrees with the occurrence of dry periods of the Mediterranean belt in the last decades studied by other scholars with clear ecological implications (Dong *et al.*, 2019; Guillot *et al.*, 2019; Vautard *et al.*, 2007; Vicente-Serrano *et al.*, 2004). Our research is a good example of the variability of the weather types that induce soil erosion, but also that few weather types are responsible for the high erosion rates in a location. To update the world knowledge on soil erosion and to plan future restoration and rehabilitation plans new studies on the weather types are necessary.

### 4.2. Weather type research. A need for standardization of the methods

We classified the total collected precipitation per interval. This allowed us to determine the most representative precipitation events and ranges and the least usual ones. Precipitations less than 50 mm were the most common reaching 57.9% in total volume. Only 16% was higher than that, which

originated from cold drops and DLp+f. Considering the CWTs, the Eastern WTs generated heavier precipitation events, coming from the Mediterranean Sea. This agrees with previous studies highlighting the connection between heavy rainfall events and the Eastern WT (Littmann, 2000; Senciales-González and Ruiz-Sinoga, 2020), and also, the difficult predictability (Alpert *et al.*, 2004; Hochman *et al.*, 2019). Also, several local publications informed about the rapid development of these extreme precipitation events when cold and warm air streams keep in contact with rapid interchanges (Benhamrouche and Martín Vide, 2011; Clar, 2017; Nuñez Mora, 2007). Eastern WTs and both cold drops and DLp+f were also responsible for the maximum runoff and erosion collected in the study area. These results coincide with other investigations made at the regional scale after comparing multiple plots and several years of monitoring (Nadal-Romero *et al.*, 2015; Peña-Angulo *et al.*, 2020, 2019). Also, in agricultural fields such as vineyards, the same WTs were able to generate the highest soil erosion rates and water losses. At larger scales, these high soil and water losses could even generate catastrophic events such as the ones of July 2021 in China and Western Europe. It is very common as other authors demonstrated in the past regarding urban flash floods, gully generation or landslides close to rivers without vegetation cover (Camarasa Belmonte and Segura Beltrán, 2001; Camarasa-Belmonte, 2016; Portugués-Mollá *et al.*, 2016). This is not only observed along the European Mediterranean belt, for example, the study conducted by Gilabert and Llasat (2018), highlighted that Eastern WTs under Mediterranean conditions may also generate extreme flood events, for example, in California (USA).

Once the scientific community accept that weather-type research should be developed at a world scale, we could better understand the soil erosion phenomenon. There is a key issue to be solved: the standardization of the methods. Right now, the three main concerns are to establish a range of rainfall intensity to be consistent from one study to the other. Upon different studies, we found that the ranges varied due to the different climates and, then, because of different rainfall intensities. This makes it difficult to compare results from one region to another, from one author to the other. It must be developed a rank for the rainfall intensities will be used by all the authors to allow us to make comparisons among study sites. Another key issue to improve the knowledge of weather types and soil erosion is to determine the main weather type during the measurements of the soil losses. We suggest here that the weather type should be considered multiple (different weather types in one rainfall event) when this will occur, but one should be the predominant weather type when the rainfall event will be characterized. The multiple weather types of rainfall events are a discussion topic for the future. And finally, another key methodological concern is to determine the period of rainfall (and soil erosion) event. We suggest that the rainfall events must be separated at least by 6 hours of dry weather and the rainfall events should be separated once this dry period takes place.

### 4.3. *Weather types and soil conservation*

From an applied and scientific perspective, it is necessary to consider potential environmental solutions to be applied in areas affected by extreme rainfall events concentrated in a few events- They are difficult to be predicted such as the catastrophic floods in China and Germany shown along with July 2021 and recurrent rainfall events that cause economic damages and casualties. Those rainfall events are found on different continents and in climatic conditions. Furl *et al.* (2018) found the Blanco River flood in South Texas an extreme event and Angillieri *et al.* (2017) in El Rodeo village, Northwestern Pampean Ranges in Argentina. Those extreme events are found in different climates, including the aridest ones such as the Atacama Desert where Izquierdo *et al.* (2021) researched catastrophic flood events with a mudflow. Or in temperate ones (Smith *et al.*, 1996). All those examples of extreme runoff and soil loss showed that research on the weather types is necessary to understand past events, manage the present ones and foresee the future ones to better manage them.

One of the solutions to the high erosion rates and corresponding flooding is the key relevance that vegetation cover plays on soil conservation, water infiltration capacity and retention (Collins, 2004; Martínez-Casasnovas *et al.*, 2009; Mohammed *et al.*, 2020). In abandoned areas or human-affected

ecosystems such as our study area, the conservation of a healthy vegetation cover is definitive to achieve sustainable soil erosion rates. Our research has shown that the shrubland is a highly protective vegetation cover, and this can be a solution for urban areas with a high level of impermeabilization and agricultural land also affected by high erosion rates (Novara *et al.*, 2019).

High soil erosion rates were found in this research during the eastern and cold drop atmospheric conditions, and this informs us that the soils should be covered with plants or mulches during the Autumn period when the highest soil losses take place. Previous research demonstrated that there are solutions to the millennia-old mismanagement of Mediterranean ecosystem types. Rodrigo-Comino *et al.* (2020b) used the cover of *Vicia sativa* Roth. to reduce the soil losses in vineyards. Cerdà *et al.* (2021a) applied weeds as cover crops in olive groves with success. Novara *et al.* (2019) cover crops in olive and vineyards and Cerdà *et al.* (2021b) in *Prunus persica* found that tillage or herbicides are the cause of the main soil degradation that use cause a reduction in the soil organic matter, aggregate stability and soil water retention capacity. This is why the use of control measures such as the ones applied in organic farming is recommended to restore soils in Mediterranean ecosystems (Baiamonte *et al.*, 2019).

Finding the causes of the soil losses will allow us to better find the right management. Determining the weather types and when they occur such as we did in this research will contribute to planning better restoration strategies. This is a worldwide benefit. High erosion rates are found in other regions of the Planet. Then, it is needed to apply sustainable management in many areas of the world due to the natural conditions (climate, sloping terrain, loss of forest or excessive tillage) and they must be designed upon the environmental conditions. This means that each region should develop weather types and soil erosion relationship studies to plan the most successful management for soil and water conservation. Madarász *et al.* (2021) found that conservation tillage is definitive to control the soil losses in Central Europe, and Klik and Rosner (2020) reviewed the long-term conservation experience in Austria and their impact on soil erosion. Rutebuka *et al.* (2021) demonstrated also the importance of terracing to reduce soil erosion rates. Chen *et al.* (2019) on the effect of vegetation coverage on soil erosion in a small watershed in China, and Kassawmar *et al.* (2018) and Negese *et al.* (2021) in Ethiopia. The two decades of research by Prasuhn (2020) demonstrate the impact of the conservation programs on soil losses in Switzerland. All this research will be highly beneficial from using a weather-type research approach that will inform when and which magnitude of soil erosion they are facing.

Understanding the influence of weather types on soil erosion is a key approach also to understanding the dynamics of soil erosion processes. The connectivity concept informs about how the sediment and water are transported and then connected from one scale to another (i.e. from pedon to watershed scale) and this is related to the intensity of the rainfall, and then to the weather type. The research of Keesstra *et al.* (2018b) showed that the connectivity of the sediments in a watershed or slope is highly dependent on the rainfall event characteristics. The weather types research approach should bring information about when and how long the soil erosion events take place. Zhao *et al.* (2020) assessed the sediment connectivity of a catchment in the Loess Plateau in China and confirmed the impact of afforestation and check dams reducing the connectivity, but also found that the rainfall volume and rainfall intensity are relevant. Weather types research will inform about the periods where the connectivity is higher. López-Vicente *et al.* (2021) also found that the sediment connectivity is determined by factors such as soil erosion barriers in a small basin recently affected by a forest fire; however, in both study sites the rainfall was considered the key factor, and then weather types contribute to better understand the soil erosion processes. The connectivity issue is highly related to conservation strategies that use to reduce soil losses due to the reduction in connectivity. This is found in agricultural land (Ares *et al.* 2020) but also in rangelands (Johnson *et al.* 2021). Climatic conditions always play a key role in connectivity, which can be assessed properly via the weather types research we developed here. We can now confirm that some weather types induce higher connectivity such as the East winds and some others such as the Western ones reduce the connectivity of the sediment and water under shrubland ecosystems.

The large dataset of weather types can help to improve the soil erosion models or complete other ones such as the recent improvements in soil biodiversity (Orgiazzi and Panagos, 2018), shallow water (Hajigholizadeh *et al.*, 2018), or the phosphorus in the sediments (Krasa *et al.*, 2019). Soil erosion modelling has been also reviewed for post-fire conditions by Lopes *et al.* (2021) and we found that the weather types contribute to a better understanding of the soil erosion processes and this should be incorporated into the models.

Even more relevant is that the large dataset of weather types must help to improve the soil erosion models. The information the weather types bring should also be used for the development of future soil erosion models that will take into account climate change. The climate change scenarios offer to the scientific research community information about the change in temperature and rainfall, but it will be also a change in the weather types and then soil erosion. Those research fields -weather types, soil erosion models and climate change- are new challenges that this paper shows as opportunities for future research directions and projects.

## 5. Conclusions

Circular Weather types (CWT) associated with individual surface pressure data at different atmospheric heights were analysed for 213 rainfall events (2010-2014) and soil and water losses were measured for the period to establish which kind of precipitation event related to each CWT can activate soil and water losses. Considering average annual precipitation of 544.0 mm and a total of 2720.1 mm during the study period, we concluded that a total of 34.4, 23.5 and 15.9% of the collected events ranged from 10 to 29.9 mm, 30 to 49.9 mm and 50 to 99.9 mm, respectively. The highest precipitation amount was generated by DLp+f (dynamic low-pressure with fronts) reaching 60.6% of the total precipitation, and 35% of the precipitation events occurring during eastern CWT (48% of the total precipitation). Most of the total runoff was collected during the Eastern CWT and cold drops (CD) summarizing 25.3% of the total runoff volume. Almost half of the mobilized sediments correspond again to DLp+f and 73.5% of this amount was generated from Eastern WTs too. Southern WTs under TLp (Thermal low-pressure) amounted to the highest sediment concentration reaching and the Southern WT the highest sediment concentration, followed by the Eastern ones.

## Acknowledgements

Artemi Cerdà thanks the Co-operative Research program from the OECD (Biological Resource Management for Sustainable Agricultural Systems) for its support with the 2016 CRP fellowship (OCDE TAD/CRP JA00088807), POSTFIRE Project (CGL2013-47862-C2-1 and 2-R) and POSTFIRE\_CARE Project (CGL2016-75178-C2-2-R) sponsored by the Spanish Ministry of Economy and Competitiveness and AEI/FEDER, UE. This paper was written as a result of the collaboration that was initiated due to COST ActionES1306: Connecting European Connectivity research and COST CA18135 FIRElinks: Fire in the Earth System. Science and Society. We wish to thank the Department of Geography secretariat team (Nieves Gómez, Nieves Dominguez and Susana Tomás) for their support over three decades to our research at the Soil Erosion and Degradation Research team (SEDER), with special thanks to the scientific researchers that as visitors from other research teams contributed to the SEDER research. The collaboration of the Geography and Environmental Sciences students was fruitful and enjoyable. Finally, we would like to thank the program “Visiting Scholars” of the Plan Propio de Investigación y Transferencia by the University of Granada (Granted to Jesús Rodrigo-Comino and Saskia Keesstra).

## References

- Al-Dousari, A.M., Alsaleh, A., Ahmed, M., Misak, R., Al-Dousari, N., Al-Shatti, F., Elrawi, M., William, T., 2019. Off-Road Vehicle Tracks and Grazing Points in Relation to Soil Compaction and Land Degradation. *Earth Systems and Environment* 3, 471-482. <https://doi.org/10.1007/s41748-019-00115-y>
- Alpert, P., Osetinsky, I., Ziv, B., Shafir, H., 2004. Semi-objective classification for daily synoptic systems: application to the eastern Mediterranean climate change. *International Journal of Climatology* 24, 1001-1011. <https://doi.org/10.1002/joc.1036>
- Al-Shammary, A.A.G., Kouzani, A.Z., Kaynak, A., Khoo, S.Y., Norton, M., Gates, W., 2018. Soil Bulk Density Estimation Methods: A Review. *Pedosphere* 28, 581-596. [https://doi.org/10.1016/S1002-0160\(18\)60034-7](https://doi.org/10.1016/S1002-0160(18)60034-7)
- Altinbilek, D., 2004. Development and management of the Euphrates–Tigris basin. *null* 20, 15-33. <https://doi.org/10.1080/07900620310001635584>
- An, H., Tang, Z., Keesstra, S., Shangguan, Z., 2019. Impact of desertification on soil and plant nutrient stoichiometry in a desert grassland. *Scientific Reports* 9. <https://doi.org/10.1038/s41598-019-45927-0>
- Angillieri, M.Y.E., Perucca, L., Vargas, N., 2017. Catastrophic flash flood triggered by an extreme rainfall event in El Rodeo village, January 2014. Northwestern Pampean Ranges of Argentina. *Geografiska Annaler: Series A, Physical Geography* 99, 72-84. <https://doi.org/10.1080/04353676.2016.1263022>
- Ares, M.G., Varni, M., Chagas, C., 2020. Runoff response of a small agricultural basin in the Argentine Pampas considering connectivity aspects. *Hydrological Processes* 34, 3102-3119. <https://doi.org/10.1002/hyp.13782>
- Ashby, J.A., 1985. *The social ecology of soil erosion in a Colombian farming system*. Rural sociology (USA).
- Auzet, A.V., Poesen, J., Valentin, C., 2002. Soil patterns as a key controlling factor of soil erosion by water. *Catena* 46, 85-87.
- Baiamonte, G., Minacapilli, M., Novara, A., Gristina, L., 2019. Time Scale Effects and Interactions of Rainfall Erosivity and Cover Management Factors on Vineyard Soil Loss Erosion in the Semi-Arid Area of Southern Sicily. *Water* 11, 978. <https://doi.org/10.3390/w11050978>
- Bayu, E.K., 2020. Determinant Variables for Women’s Participation in Soil and Water Conservation Practices in North Western Ethiopia: The Case of Shebel Berenta District (Woreda), East Gojjam Zone, Amhara National Regional State. *Air, Soil and Water Research* 13. <https://doi.org/10.1177/1178622120942199>
- Benhamrouche, A., Martín Vide, J., 2011. Distribución espacial de la concentración diaria de la precipitación en la provincia de Alicante. Spatial distribution of daily rainfall in the Region of Alicante. <https://doi.org/10.14198/INGEO2011.56.06>
- Bork, H.-R., Beckedahl, H.R., Dahlke, C., Geldmacher, K., Mieth, A., Li, Y., 2003. The world-wide explosion of soil erosion rates in the 20th century: The global soil erosion drama - Are we losing our food production base? *Petermanns Geographische Mitteilungen* 147, 16-29.
- Borrelli, P., Robinson, D.A., Panagos, P., Lugato, E., Yang, J.E., Alewell, C., Wuepper, D., Montanarella, L., Ballabio, C., 2020. Land use and climate change impacts on global soil erosion by water (2015-2070). *PNAS* 117, 21994-22001. <https://doi.org/10.1073/pnas.2001403117>
- Brazel, A.J., Nickling, W.G., 1986. The relationship of weather types to dust storm generation in Arizona (1965-1980). *Journal of Climatology* 6, 255-275. <https://doi.org/10.1002/joc.3370060303>
- Brown, L.R., 1981. World population growth, soil erosion, and food security. *Science* 214, 995-1002. <https://doi.org/10.1126/science.7302578>
- Camarasa Belmonte, A.M., Segura Beltrán, F., 2001. Flood events in Mediterranean ephemeral streams (ramblas) in Valencia region, Spain. *Catena* 45, 229-249. [https://doi.org/10.1016/S0341-8162\(01\)00146-1](https://doi.org/10.1016/S0341-8162(01)00146-1)
- Camarasa-Belmonte, A.M., 2016. Flash floods in Mediterranean ephemeral streams in Valencia Region (Spain). *Journal of Hydrology*, Flash floods, hydro-geomorphic response and risk management 541, 99-115. <https://doi.org/10.1016/j.jhydrol.2016.03.019>

- Carretier, S., Tolorza, V., Regard, V., Aguilar, G., Bermúdez, M.A., Martinod, J., Guyot, J.L., Hérail, G., Riquelme, R., 2018. Review of erosion dynamics along the major N-S climatic gradient in Chile and perspectives. *Geomorphology* 300, 45-68. <https://doi.org/10.1016/j.geomorph.2017.10.016>
- Cerdà, A., Daliakopoulos, I.N., Terol, E., Novara, A., Fatahi, Y., Moradi, E., Salvati, L., Pulido, M., 2021a. Long-term monitoring of soil bulk density and erosion rates in two *Prunus Persica* (L) plantations under flood irrigation and glyphosate herbicide treatment in La Ribera district, Spain. *Journal of Environmental Management* 282, 111965. <https://doi.org/10.1016/j.jenvman.2021.111965>
- Cerdà, A., Terol, E., Daliakopoulos, I.N., 2021b. Weed cover controls soil and water losses in rainfed olive groves in Sierra de Enguera, eastern Iberian Peninsula. *Journal of Environmental Management* 290, 112516. <https://doi.org/10.1016/j.jenvman.2021.112516>
- Chen, J., Xiao, H., Li, Z., Liu, C., Wang, D., Wang, L., Tang, C., 2019. Threshold effects of vegetation coverage on soil erosion control in small watersheds of the red soil hilly region in China. *Ecological Engineering* 132, 109-114. <https://doi.org/10.1016/j.ecoleng.2019.04.010>
- Clar, A.J., 2017. Gota fría y depresión atmosférica: claves de la lluvia fuerte mediterránea. *Mètode: Revista de difusió de la Investigació* 16-23.
- Collins, D.B.G., 2004. Modelling the effects of vegetation-erosion coupling on landscape evolution. *Journal of Geophysical Research* 109. <https://doi.org/10.1029/2003JF000028>
- Cortesi, N., Gonzalez-Hidalgo, J.C., Trigo, R.M., Ramos, A.M., 2014. Weather types and spatial variability of precipitation in the Iberian Peninsula. *International Journal of Climatology* 34, 2661-2677. <https://doi.org/10.1002/joc.3866>
- de Lima, J.L.M.P., Singh, V.P., de Lima, M.I.P., 2003. The influence of storm movement on water erosion: storm direction and velocity effects. *Catena* 52, 39-56. [https://doi.org/10.1016/S0341-8162\(02\)00149-2](https://doi.org/10.1016/S0341-8162(02)00149-2)
- Deshpande, V.V., Telang, M.S., 1950. Pipet Method of Sedimentation Analysis. Rapid Determination of Distribution of particle size. *Anal. Chem.* 22, 840-841. <https://doi.org/10.1021/ac60042a033>
- Di, X., Xiao, B., Dong, H., Wang, S., 2019. Implication of different humic acid fractions in soils under karst rocky desertification. *Catena* 174, 308-315. <https://doi.org/10.1016/j.catena.2018.11.028>
- Dong, C., MacDonald, G., Okin, G.S., Gillespie, T.W., 2019. Quantifying Drought Sensitivity of Mediterranean Climate Vegetation to Recent Warming: A Case Study in Southern California. *Remote Sensing* 11, 2902. <https://doi.org/10.3390/rs11242902>
- Drewry, J.J., Cameron, K.C., Buchan, G.D., 2008. Pasture yield and soil physical property responses to soil compaction from treading and grazing—a review. *Soil Research* 46, 237-256. <https://doi.org/DOI:10.1071/SR07125>
- Egidi, G., Cividino, S., Paris, E., Palma, A., Salvati, L., Cudlin, P., 2021. Assessing the impact of multiple drivers of land sensitivity to desertification in a Mediterranean country. *Environmental Impact Assessment Review* 89, 106594. <https://doi.org/10.1016/j.eiar.2021.106594>
- Fernandez-Anez, N., Krasovskiy, A., Müller, M., Vacik, H., Baetens, J., Hukić, E., Kapovic Solomun, M., Atanassova, I., Glushkova, M., Bogunović, I., Fajković, H., Djuma, H., Boustras, G., Adámek, M., Devetter, M., Hrabalíková, M., Huska, D., Martínez Barroso, P., Vaverková, M.D., Zúmr, D., Jögiste, K., Metslaid, M., Koster, K., Köster, E., Pumpanen, J., Ribeiro-Kumara, C., Di Prima, S., Pastor, A., Rumpel, C., Seeger, M., Daliakopoulos, I., Daskalou, E., Koutroulis, A., Papadopoulou, M.P., Stampoulidis, K., Xanthopoulos, G., Aszalós, R., Balázs, D., Kertész, M., Valkó, O., Finger, D.C., Thorsteinsson, T., Till, J., Bajocco, S., Gelsomino, A., Amodio, A.M., Novara, A., Salvati, L., Telesca, L., Ursino, N., Jansons, A., Kitenberga, M., Stivrins, N., Brazaitis, G., Marozas, V., Cojocar, O., Gumeniuc, I., Sfecla, V., Imeson, A., Veraverbeke, S., Mikalsen, R.F., Koda, E., Osinski, P., Castro, A.C.M., Nunes, J.P., Oom, D., Vieira, D., Rusu, T., Bojović, S., Djordjevic, D., Popovic, Z., Protic, M., Sakan, S., Glasa, J., Kacikova, D., Lichner, L., Majlingova, A., Vido, J., Ferk, M., Tičar, J., Zorn, M., Zupanc, V., Hinojosa, M.B., Knicker, H., Lucas-Borja, M.E., Pausas, J., Prat-Guitart, N., Ubeda, X., Vilar, L., Destouni, G., Ghajarnia, N., Kalantari, Z., Seifollahi-Aghmiuni, S., Dindaroglu, T., Yakupoglu, T., Smith, T., Doerr, S., Cerdà, A., 2021. Current Wildland Fire Patterns and Challenges in Europe: A Synthesis of National Perspectives. *Air, Soil and Water Research* 14, 11786221211028184. <https://doi.org/10.1177/11786221211028184>

- Fernández-González, S., Río, S. del, Castro, A., Penas, A., Fernández-Raga, M., Calvo, A.I., Fraile, R., 2012. Connection between NAO, weather types and precipitation in León, Spain (1948-2008). *International Journal of Climatology* 32, 2181-2196. <https://doi.org/10.1002/joc.2431>
- Fernandez-Raga, M., Castro, A., Marcos, E., Palencia, C., Fraile, R., 2017. Weather types and rainfall microstructure in Leon, Spain. *International Journal of Climatology* 37, 1834-1842. <https://doi.org/10.1002/joc.4816>
- Furl, C., Sharif, H., Zeitler, J.W., Hassan, A.E., Joseph, J., 2018. Hydrometeorology of the catastrophic Blanco River flood in South Texas, May 2015. *Journal of Hydrology: Regional Studies* 15, 90-104. <https://doi.org/10.1016/j.ejrh.2017.12.001>
- Gilabert, J., Llasat, M.C., 2018. Circulation weather types associated with extreme flood events in Northwestern Mediterranean. *International Journal of Climatology* 38, 1864-1876. <https://doi.org/10.1002/joc.5301>
- Guillot, E., Hinsinger, P., Dufour, L., Roy, J., Bertrand, I., 2019. With or without trees: Resistance and resilience of soil microbial communities to drought and heat stress in a Mediterranean agroforestry system. *Soil Biology and Biochemistry* 129, 122-135. <https://doi.org/10.1016/j.soilbio.2018.11.011>
- Hajigholizadeh, M., Melesse, A.M., Fuentes, H.R., 2018. Erosion and sediment transport modelling in shallow waters: A review on approaches, models and applications. *International Journal of Environmental Research and Public Health* 15. <https://doi.org/10.3390/ijerph15030518>
- Hess, P., Brezowsky, H., 2010. *Katalog der Groß wetterlagen Europas (catalog of the European large scale weather types)* (No. 119). Potsdam-Institut für Klimafolgenforschung e.V., Potsdam.
- Hochman, A., Alpert, P., Harpaz, T., Saaroni, H., Messori, G., 2019. A new dynamical systems perspective on atmospheric predictability: Eastern Mediterranean weather regimes as a case study. *Science Advances* 5, eaau0936. <https://doi.org/10.1126/sciadv.aau0936>
- Izquierdo, T., Abad, M., Gómez, Y., Gallardo, D., Rodríguez-Vidal, J., 2021. The March 2015 catastrophic flood event and its impacts in the city of Copiapó (southern Atacama Desert). An integrated analysis to mitigate future mudflow derived damages. *Journal of South American Earth Sciences* 105, 102975. <https://doi.org/10.1016/j.jsames.2020.102975>
- Johnson, J.C., Williams, C.J., Guertin, D.P., Archer, S.R., Heilman, P., Pierson, F.B., Wei, H., 2021. Restoration of a shrub-encroached semi-arid grassland: Implications for structural, hydrologic, and sediment connectivity. *Ecohydrology* 14, e2281. <https://doi.org/10.1002/eco.2281>
- Jones, P.D., Harpham, C., Briffa, K.R., 2013. Lamb weather types derived from reanalysis products. *International Journal of Climatology* 33, 1129-1139. <https://doi.org/10.1002/joc.3498>
- Jónsson, J.Ö.G., Davíðsdóttir, B., 2016. Classification and valuation of soil ecosystem services. *Agricultural Systems* 145, 24-38.
- Kairis, O., Karavitis, C., Salvati, L., Kounalaki, A., Kosmas, K., 2015. Exploring the Impact of Overgrazing on Soil Erosion and Land Degradation in a Dry Mediterranean Agro-Forest Landscape (Crete, Greece). *Arid Land Research and Management* 29, 360-374. <https://doi.org/10.1080/15324982.2014.968691>
- Kassawmar, T., Gessesse, G.D., Zeleke, G., Subhatu, A., 2018. Assessing the soil erosion control efficiency of land management practices implemented through free community labor mobilization in Ethiopia. *International Soil and Water Conservation Research* 6, 87-98. <https://doi.org/10.1016/j.iswcr.2018.02.001>
- Keesstra, S., Mol, G., De Leeuw, J., Okx, J., Molenaar, C., De Cleen, M., Visser, S., 2018a. Soil-Related Sustainable Development Goals: Four Concepts to Make Land Degradation Neutrality and Restoration Work. *Land* 7, 133. <https://doi.org/10.3390/land7040133>
- Keesstra, S., Nunes, J.P., Saco, P., Parsons, T., Poepl, R., Masselink, R., Cerdà, A., 2018b. The way forward: Can connectivity be useful to design better measuring and modelling schemes for water and sediment dynamics? *Science of the Total Environment* 644, 1557-1572. <https://doi.org/10.1016/j.scitotenv.2018.06.342>
- Kidson, J.W., 2000. An analysis of New Zealand synoptic types and their use in defining weather regimes. *International Journal of Climatology* 20, 299-316. [https://doi.org/10.1002/\(SICI\)1097-0088\(20000315\)20:3<299::AID-JOC474>3.0.CO;2-B](https://doi.org/10.1002/(SICI)1097-0088(20000315)20:3<299::AID-JOC474>3.0.CO;2-B)

- Klik, A., Rosner, J., 2020. Long-term experience with conservation tillage practices in Austria: Impacts on soil erosion processes. *Soil and Tillage Research* 203, 104669. <https://doi.org/10.1016/j.still.2020.104669>
- Köppen, W., Geiger, R., 1930. *Handbuch der klimatologie*. Gebrüder Borntraeger Berlin.
- Kottek, M., Grieser, J., Beck, C., Rudolf, B., Rubel, F., 2006. World map of the Köppen-Geiger climate classification updated. *Meteorologische Zeitschrift* 15, 259-263.
- Krasa, J., Dostal, T., Jachymova, B., Bauer, M., Devaty, J., 2019. Soil erosion as a source of sediment and phosphorus in rivers and reservoirs-Watershed analyses using WaTEM/SEDEM. *Environmental Research* 171, 470-483. <https://doi.org/10.1016/j.envres.2019.01.044>
- Lamb, H.H., 1972. *British Isles Weather Types and a Register of the Daily Sequence of Circulation Patterns, 1861-1971*. Stationery Office Books, London.
- Larsen, J.I., MacDonald, L.H., Brown, E., Rough, D., Welsh, M.J., Pietraszek, J.H., Libohova, Z., Benavides-Solorio, J. de D., Schaffrath, K., 2009. Causes of post-fire runoff and erosion: water repellency, cover, or soil sealing? *Soil Science Society of America Journal* 73, 1393-1407.
- Littmann, T., 2000. An empirical classification of weather types in the Mediterranean Basin and their interrelation with rainfall. *Theor Appl Climatol* 66, 161-171. <https://doi.org/10.1007/s007040070022>
- Lopes, A.R., Girona-García, A., Corticeiro, S., Martins, R., Keizer, J.J., Vieira, D.C.S., 2021. What is wrong with post-fire soil erosion modelling? A meta-analysis on current approaches, research gaps, and future directions. *Earth Surface Processes and Landforms* 46, 205-219. <https://doi.org/10.1002/esp.5020>
- López-Vicente, M., Kramer, H., Keesstra, S., 2021. Effectiveness of soil erosion barriers to reduce sediment connectivity at small basin scale in a fire-affected forest. *Journal of Environmental Management* 278, 111510. <https://doi.org/10.1016/j.jenvman.2020.111510>
- Madarász, B., Jakab, G., Szalai, Z., Juhos, K., Kotroczó, Z., Tóth, A., Ladányi, M., 2021. Long-term effects of conservation tillage on soil erosion in Central Europe: A random forest-based approach. *Soil and Tillage Research* 209, 104959. <https://doi.org/10.1016/j.still.2021.104959>
- Martínez-Casasnovas, J.A., Ramos, M.C., García-Hernández, D., 2009. Effects of land-use changes in vegetation cover and sidewall erosion in a gully head of the Penedès region (northeast Spain). *Earth Surface Processes and Landforms* 34, 1927-1937. <https://doi.org/10.1002/esp.1870>
- Martínez-Valderrama, J., Ibáñez, J., Del Barrio, G., Sanjuán, M.E., Alcalá, F.J., Martínez-Vicente, S., Ruiz, A., Puigdefábregas, J., 2016. Present and future of desertification in Spain: Implementation of a surveillance system to prevent land degradation. *Science Total Environment*. 563-564, 169-178. <https://doi.org/10.1016/j.scitotenv.2016.04.065>
- Minea, G., Ioana-Toroimac, G., Moro, G., 2019. The dominant runoff processes on grassland versus bare soil hillslopes in a temperate environment - An experimental study. *Journal of Hydrology and Hydromechanics* 67, 8. <https://doi.org/10.2478/johh-2019-0018>
- Mohammed, S., Alsafadi, K., Talukdar, S., Kiwan, S., Hennawi, S., Alshihabi, O., Sharaf, M., Harsanyie, E., 2020. Estimation of soil erosion risk in southern part of Syria by using RUSLE integrating geo informatics approach. *Remote Sensing Applications: Society and Environment* 20, 100375. <https://doi.org/10.1016/j.rsase.2020.100375>
- Munafò, M., Salvati, L., Zitti, M., 2013. Estimating soil sealing rate at national level-Italy as a case study. *Ecological Indicators* 26, 137-140. <https://doi.org/10.1016/j.ecolind.2012.11.001>
- Nadal-Romero, E., Cortesi, N., González-Hidalgo, J.C., 2014. Weather types, runoff and sediment yield in a Mediterranean mountain landscape. *Earth Surface Processes and Landforms* 39, 427-437. <https://doi.org/10.1002/esp.3451>
- Nadal-Romero, E., González-Hidalgo, J.C., Cortesi, N., Desir, G., Gómez, J.A., Lasanta, T., Lucía, A., Marín, C., Martínez-Murillo, J.F., Pacheco, E., Rodríguez-Blanco, M.L., Romero Díaz, A., Ruiz-Sinoga, J.D., Taguas, E.V., Taboada-Castro, M.M., Taboada-Castro, M.T., Úbeda, X., Zabaleta, A., 2015. Relationship of runoff, erosion and sediment yield to weather types in the Iberian Peninsula. *Geomorphology* 228, 372-381. <https://doi.org/10.1016/j.geomorph.2014.09.011>

- Nearing, M.A., Pruski, F.F., O'Neal, M.R., 2004. Expected climate change impacts on soil erosion rates: A review. *Journal of Soil and Water Conservation* 59, 43-50.
- Negese, A., Fekadu, E., Getnet, H., 2021. Potential Soil Loss Estimation and Erosion-Prone Area Prioritization Using RUSLE, GIS, and Remote Sensing in Chereti Watershed, Northeastern Ethiopia. *Air, Soil and Water Research* 14, 1178622120985814. <https://doi.org/10.1177/1178622120985814>
- Neville, A., 2007. *Mountains of Silver and Rivers of Gold: The Phoenicians in Iberia*. Oxbow Books.
- Norman, L.M., 2020. Ecosystem Services of Riparian Restoration: A Review of Rock Detention Structures in the Madrean Archipelago Ecoregion. *Air, Soil and Water Research* 13, 1178622120946337. <https://doi.org/10.1177/1178622120946337>
- Novara, A., Stallone, G., Cerdà, A., Gristina, L., 2019. The Effect of Shallow Tillage on Soil Erosion in a Semi-Arid Vineyard. *Agronomy* 9, 257. <https://doi.org/10.3390/agronomy9050257>
- Nuñez Mora, J.A., 2007. La riada de octubre de 1957 en Jávea. Análisis meteorológico y climático. AEMET Estudios. <http://hdl.handle.net/20.500.11765/7873>
- Orgiazzi, A., Panagos, P., 2018. Soil biodiversity and soil erosion: It is time to get married: Adding an earthworm factor to soil erosion modelling. *Global Ecology and Biogeography* 27, 1155-1167. <https://doi.org/10.1111/geb.12782>
- Panagos, P., Ballabio, C., Poesen, J., Lugato, E., Scarpa, S., Montanarella, L., Borrelli, P., 2020. A Soil Erosion Indicator for Supporting Agricultural, Environmental and Climate Policies in the European Union. *Remote Sensing* 12, 1365. <https://doi.org/10.3390/rs12091365>
- Panagos, P., Borrelli, P., Poesen, J., Ballabio, C., Lugato, E., Meusburger, K., Montanarella, L., Alewell, C., 2015. The new assessment of soil loss by water erosion in Europe. *Environmental Science and Policy* 54, 438-447. <https://doi.org/10.1016/j.envsci.2015.08.012>
- Pattison, I., Lane, S.N., 2012. The relationship between Lamb weather types and long-term changes in flood frequency, River Eden, UK. *International Journal of Climatology* 32, 1971-1989. <https://doi.org/10.1002/joc.2415>
- Peña-Angulo, D., Estrany, J., García-Comendador, J., Fortesa, J., Tomàs-Burguera, M., Company, J., Alorda, B., Nadal-Romero, E., 2021. Influence of weather types on the hydrosedimentary response in three small catchments on the Island of Mallorca, Spain. *Environmental Research* 192, 110324. <https://doi.org/10.1016/j.envres.2020.110324>
- Peña-Angulo, D., Nadal-Romero, E., González-Hidalgo, J.C., Albaladejo, J., Andreu, V., Bagarello, V., Barhi, H., Batalla, R.J., Bernal, S., Bienes, R., Campo, J., Campo-Bescós, M.A., Canatario-Duarte, A., Cantón, Y., Casali, J., Castillo, V., Cerdà, A., Cheggour, A., Cid, P., Cortesi, N., Desir, G., Díaz-Pereira, E., Espigares, T., Estrany, J., Fernández-Raga, M., Ferreira, C.S.S., Ferro, V., Gallart, F., Giménez, R., Gimeno, E., Gómez, J.A., Gómez-Gutiérrez, A., Gómez-Macpherson, H., González-Pelayo, O., Hueso-González, P., Kairis, O., Karatzas, G.P., Klotz, S., Kosmas, C., Lana-Renault, N., Lasanta, T., Latron, J., Lázaro, R., Le Bissonnais, Y., Le Bouteiller, C., Licciardello, F., López-Tarazón, J.A., Lucía, A., Marín, C., Marqués, M.J., Martínez-Fernández, J., Martínez-Mena, M., Martínez-Murillo, J.F., Mateos, L., Mathys, N., Merino-Martín, L., Moreno-de las Heras, M., Moustakas, N., Nicolau, J.M., Novara, A., Pampalona, V., Raclot, D., Rodríguez-Blanco, M.L., Rodrigo-Comino, J., Romero-Díaz, A., Roose, E., Rubio, J.L., Ruiz-Sinoga, J.D., Schnabel, S., Senciales-González, J.M., Simonneaux, V., Solé-Benet, A., Taguas, E.V., Taboada-Castro, M.M., Taboada-Castro, M.T., Todisco, F., Úbeda, X., Varouchakis, E.A., Vericat, D., Wittenberg, L., Zabaleta, A., Zorn, M., 2019. Spatial variability of the relationships of runoff and sediment yield with weather types throughout the Mediterranean basin. *Journal of Hydrology* 571, 390-405. <https://doi.org/10.1016/j.jhydrol.2019.01.059>
- Peña-Angulo, D., Nadal-Romero, E., González-Hidalgo, J.C., Albaladejo, J., Andreu, V., Barhi, H., Bernal, S., Biddoccu, M., Bienes, R., Campo, J., Campo-Bescós, M.A., Canatario-Duarte, A., Cantón, Y., Casali, J., Castillo, V., Cavallo, E., Cerdà, A., Cid, P., Cortesi, N., Desir, G., Díaz-Pereira, E., Espigares, T., Estrany, J., Farguella, J., Fernández-Raga, M., Ferreira, C.S., Ferro, V., Gallart, F., Giménez, R., Gimeno, E., Gómez, J.A., Gómez-Gutiérrez, A., Gómez-Macpherson, H., González-Pelayo, O., Kairis, O., Karatzas, G.P., Keesstra, S., Klotz, S., Kosmas, C., Lana-Renault, N., Lasanta, T., Latron, J., Lázaro, R., Le Bissonnais, Y., Le Bouteiller, C., Licciardello, F., López-Tarazón, J.A., Lucía, A., Marín-Moreno, V.M.,

- Marín, C., Marqués, M.J., Martínez-Fernández, J., Martínez-Mena, M., Mateos, L., Mathys, N., Merino-Martín, L., Moreno-de las Heras, M., Moustakas, N., Nicolau, J.M., Pampalona, V., Raclot, D., Rodríguez-Blanco, M.L., Rodrigo-Comino, J., Romero-Díaz, A., Ruiz-Sinoga, J.D., Rubio, J.L., Schnabel, S., Senciales-González, J.M., Solé-Benet, A., Taguas, E.V., Taboada-Castro, M.T., Taboada-Castro, M.M., Todisco, F., Úbeda, X., Varouchakis, E.A., Wittenberg, L., Zabaleta, A., Zorn, M., 2020. Relationship of Weather Types on the Seasonal and Spatial Variability of Rainfall, Runoff, and Sediment Yield in the Western Mediterranean Basin. *Atmosphere* 11, 609. <https://doi.org/10.3390/atmos11060609>
- Piñol, J., Terradas, J., Lloret, F., 1998. Climate Warming, Wildfire Hazard, and Wildfire Occurrence in Coastal Eastern Spain. *Climatic Change* 38, 345-357. <https://doi.org/10.1023/A:1005316632105>
- Portugués-Mollá, I., Bonache-Felici, X., Mateu-Bellés, J.F., Marco-Segura, J.B., 2016. A GIS-Based Model for the analysis of an urban flash flood and its hydro-geomorphic response. The Valencia event of 1957. *Journal of Hydrology, Flash floods, hydro-geomorphic response and risk management* 541, 582-596. <https://doi.org/10.1016/j.jhydrol.2016.05.048>
- Prasuhn, V., 2020. Twenty years of soil erosion on-farm measurement: Annual variation, spatial distribution and the impact of conservation programmes for soil loss rates in Switzerland. *Earth Surface Processes and Landforms* 45, 1539-1554. <https://doi.org/10.1002/esp.4829>
- Raclot, D., Le Bissonnais, Y., Louchart, X., Andrieux, P., Moussa, R., Voltz, M., 2009. Soil tillage and scale effects on erosion from fields to catchment in a Mediterranean vineyard area. *Agriculture, Ecosystems & Environment* 134, 201-210. <https://doi.org/10.1016/j.agee.2009.06.019>
- Radziemska, M., Beś, A., Gusiatin, Z.M., Cerdà, A., Mazur, Z., Jeznach, J., Kowal, P., Brtnický, M., 2019. The combined effect of phytostabilization and different amendments on remediation of soils from post-military areas. *Science of The Total Environment* 688, 37-45. <https://doi.org/10.1016/j.scitotenv.2019.06.190>
- Ramos, A.M., Barriopedro, D., Dutra, E., 2015. Circulation weather types as a tool in atmospheric, climate, and environmental research. *Frontiers in Environmental Science* 3. <https://doi.org/10.3389/fenvs.2015.00044>
- Rodrigo-Comino, J., Salvia, R., Egidi, G., Salvati, L., Giménez-Morera, A., Quaranta, G., 2021. Desertification and Degradation Risks vs Poverty: A Key Topic in Mediterranean Europe. *Cuadernos de Investigación Geográfica* 48(1), 23-40. <https://doi.org/10.18172/cig.4850>
- Rodrigo-Comino, J., Senciales, J.M., Sillero-Medina, J.A., Gyasi-Agyei, Y., Ruiz-Sinoga, J.D., Ries, J.B., 2019. Analysis of Weather-Type-Induced Soil Erosion in Cultivated and Poorly Managed Abandoned Sloping Vineyards in the Axarquía Region (Málaga, Spain). *Air, Soil and Water Research* 12, 1178622119839403. <https://doi.org/10.1177/1178622119839403>
- Rodrigo-Comino, J., Senciales-González, J.M., Terol, E., Mora-Navarro, G., Gyasi-Agyei, Y., Cerdà, A., 2020a. Impacts of Weather Types on Soil Erosion Rates in Vineyards at “Celler del Roure” Experimental Research in Eastern Spain. *Atmosphere* 11, 551. <https://doi.org/10.3390/atmos11060551>
- Rodrigo-Comino, J., Terol, E., Mora, G., Giménez-Morera, A., Cerdà, A., 2020b. Vicia sativa Roth. Can Reduce Soil and Water Losses in Recently Planted Vineyards (*Vitis vinifera* L.). *Earth Syst Environ* 4, 827-842. <https://doi.org/10.1007/s41748-020-00191-5>
- Rodríguez-Seijo, A., Santos, B., Silva, E.F. da, Cachada, A., Pereira, R., 2018. Low-density polyethylene microplastics as a source and carriers of agrochemicals to soil and earthworms. *Environmental Chemistry* 16, 8-17. <https://doi.org/10.1071/EN18162>
- Rutebuka, J., Munyeshuli Uwimanzu, A., Nkundwakazi, O., Mbarushimana Kagabo, D., Mbonigaba, J.J.M., Vermeir, P., Verdoodt, A., 2021. Effectiveness of terracing techniques for controlling soil erosion by water in Rwanda. *Journal of Environmental Management* 277, 111369. <https://doi.org/10.1016/j.jenvman.2020.111369>
- Schroeder, M.J., Glovinsky, M., Henricks, V.F., Hood, F.C., Hull, M.K., 1964. *Synoptic weather types associated with critical fire weather*. Pacific Southwest Forest and Range Experiment Station, Berkeley CA.
- Senciales-González, J.M., Ruiz-Sinoga, J.D., 2020. Features of weather types involving heavy rainfall along the southern Spanish Mediterranean. *Cuadernos de Investigación Geográfica* 47 (1), 221-242. <https://doi.org/10.18172/cig.4765>

- Smith, J.A., Baeck, M.L., Steiner, M., Miller, A.J., 1996. Catastrophic rainfall from an upslope thunderstorm in the central Appalachians: The Rapidan Storm of June 27, 1995. *Water Resources Research* 32, 3099-3113. <https://doi.org/10.1029/96WR02107>
- Sobral, A.C., Peixoto, A.S.P., Nascimento, V.F., Rodgers, J., da Silva, A.M., 2015. Natural and anthropogenic influence on soil erosion in a rural watershed in the Brazilian southeastern region. *Regional Environmental Change* 15, 709-720. <https://doi.org/10.1007/s10113-014-0667-z>
- Soil Survey Staff, 2014. *Keys to Soil Taxonomy, 12th ed.* USDA-Natural Resources Conservation Service, Washington, DC, USA.
- Sun, L., Fang, H., Qi, D., Li, J., Cai, Q., 2013. A review on rill erosion process and its influencing factors. *Chinese Geographical Science* 23, 389-402. <https://doi.org/10.1007/s11769-013-0612-y>
- Telak, L.J., Dugan, I., Bogunovic, I., 2021. Soil Management and Slope Impacts on Soil Properties, Hydrological Response, and Erosion in Hazelnut Orchard. *Soil Systems* 5, 5. <https://doi.org/10.3390/soilsystems5010005>
- Trigo, R.M., DaCamara, C.C., 2000. Circulation weather types and their influence on the precipitation regime in Portugal. *International Journal of Climatology* 20, 1559-1581. [https://doi.org/10.1002/1097-0088\(20001115\)20:13<1559::AID-JOC555>3.0.CO;2-5](https://doi.org/10.1002/1097-0088(20001115)20:13<1559::AID-JOC555>3.0.CO;2-5)
- Vanwalleghe, T., Amate, J.I., de Molina, M.G., Fernández, D.S., Gómez, J.A., 2011. Quantifying the effect of historical soil management on soil erosion rates in Mediterranean olive orchards. *Agriculture, Ecosystems & Environment* 142, 341-351. <https://doi.org/10.1016/j.agee.2011.06.003>
- Vautard, R., Yiou, P., D'Andrea, F., Noblet, N., Viovy, N., Cassou, C., Polcher, J., Ciais, P., Kageyama, M., Fan, Y., 2007. Summertime European heat and drought waves induced by wintertime Mediterranean rainfall deficit. *Geophysical Research Letters* 34, 1-5. <https://doi.org/10.1029/2006GL028001>
- Vicente-Serrano, S.M., González-Hidalgo, J.C., Luis, M. de, Raventós, J., 2004. Drought patterns in the Mediterranean area: the Valencia region (eastern Spain). *Climate Research* 26, 5-15. <https://doi.org/10.3354/cr026005>
- Walkley, A., Black, I.A., 1934. An examination of the Degtjareff method for determining soil organic matter, and a proposed modification of the chromic acid titration method. *Soil Science* 37, 29-38.
- Xie, J., Xue, W., Li, C., Yan, Z., Li, D., Li, G., Chen, X., Chen, D., 2019. Water-soluble phosphorus contributes significantly to shaping the community structure of rhizospheric bacteria in rocky desertification areas. *Scientific Report* 9, 18408. <https://doi.org/10.1038/s41598-019-54943-z>
- Zhao, Z., Shen, Y., Wang, Q., Jiang, R., 2020. The temporal stability of soil moisture spatial pattern and its influencing factors in rocky environments. *Catena* 187, 104418. <https://doi.org/10.1016/j.catena.2019.104418>





## EFFECT OF TILLAGE SYSTEMS COMBINED WITH PLASTIC FILM MULCHES AND FERTILIZERS ON SOIL PHYSICAL PROPERTIES IN A WHEAT-AGRICULTURAL SITE IN SOUTHERN IRAQ

AHMED ABED GATEA AL-SHAMMARY<sup>1</sup>, NABIL RAHEEM LAHMOD<sup>2</sup>,  
JESÚS FERNÁNDEZ-GÁLVEZ<sup>3</sup>, ANDRÉS CABALLERO-CALVO<sup>3\*</sup>

<sup>1</sup>*Soil Science and Water Resources Departments, College of Agriculture, University of Wasit, Kut, Iraq.*

<sup>2</sup>*Field crops department, College of Agriculture, University of Wasit, Kut, Iraq.*

<sup>3</sup>*Department of Regional Geographical Analysis and Physical Geography, University of Granada, Spain.*

**ABSTRACT.** This study researches the influence of the three tillage systems (conventional, economical and mulch tillage) when combined with different soil plastic mulching and fertilizer applications on key selected soil physical properties (SPP) at 0-20 cm soil depth in a wheat agricultural site, during summer (from 1<sup>st</sup> June to 31<sup>st</sup> July 2015). SPP include soil porosity ( $\Phi$ ), volumetric soil water content 60 days after irrigation to field capacity ( $\theta_{60}$ ), and mean weight diameter of aggregates (MWD). The term mulch tillage refers here to a soil conservation practice where the soil surface is disturbed by tillage whereby crop residues are mixed with the soil and a certain amount of residues remain on the soil surface, while mulching refers to the placement of inorganic material over the top of a soil surface to protect it. Soil treatments included tillage system: conventional tillage using a combination of a mouldboard plough and a disc harrow (MP+DH), economical tillage using a rotary cultivator (RC), and mulch tillage using a chisel plough (MT+CP); soil plastic mulching: transparent mulching (TM), black mulching (BM) of 200 cm wide with 0.05 cm thick, and without mulching (WM); and fertilisers: composed organic fertiliser (CoF), no-composed organic fertiliser (NoF), and chemical fertiliser (ChF). The split-split-plot design under the randomized complete block design (RCBD) was established in 27 treatments with 3 replicated, to map  $\Phi$ ,  $\theta_{60}$ , and MWD based on 81 soil samples from all treatments. Results showed that the different soil treatments have diverse impacts on SPP. MP+DH resulted in the higher  $\theta_{60}$  ( $0.22 \text{ cm}^3 \text{ cm}^{-3}$ ), MWD (0.85 mm), and  $\Phi$  (56.87%). Our findings showed that MT+CP obtained a higher MWD of 0.98 mm and lower  $\Phi$  of 49% compared to other tillage systems. Soil mulching had significantly modified SPP, with BM resulting in the highest  $\Phi$  (55.65%),  $\theta_{60}$  ( $0.35 \text{ cm}^3 \text{ cm}^{-3}$ ), and MWD (1.06 mm). Results indicated no significant differences between fertiliser types on SPP. The CoF had a significant effect on MWD and related soil characteristics studied. These findings can help us to understand the individual and combined effects of the tillage system, mulching, and fertilization application on some soil characteristics in wheat agriculture. A further study with more focus on the influence of tillage depths and mulching types (plastic vs organic mulch for different crops) under a variety of soils and climatic conditions, as well as on soil thermal properties needs further investigation.

### *Efecto de la combinación de sistemas de cultivo, cubiertas plásticas y fertilizantes sobre las propiedades físicas del suelo de un trigo del sur de Iraq*

**RESUMEN.** Este estudio investiga la influencia de tres sistemas de labranza (convencional, económico y con mantillo) cuando se combinan con diferentes aplicaciones de fertilizantes y cobertura plástica del suelo en propiedades físicas del suelo (SPP), a 0-20 cm de profundidad, en un área agrícola de trigo, durante el verano (del 1 de junio al 31 de julio de 2015). Los SPP incluyen la porosidad del suelo ( $\Phi$ ), el contenido volumétrico de agua del suelo 60 días después del riego a capacidad de campo ( $\theta_{60}$ ) y el diámetro medio ponderado de los agregados

(MWD). El término cultivo con mantillo se refiere aquí a una práctica de conservación en la que la superficie del suelo es alterada por la labranza, de modo que los residuos del cultivo se mezclan con el suelo y una cierta cantidad de estos residuos permanece en la superficie del suelo. El *mulching* se refiere a la colocación de material inorgánico sobre la superficie del suelo para protegerlo. Los tratamientos del suelo incluyeron el sistema de labranza convencional que utiliza una combinación de arado de vertedera y grada de discos (MP+DH), labranza económica que usa un cultivador rotativo (RC) y labranza de cobertura que utiliza un arado de cincel (MT+CP); *mulching* plástico del suelo: *mulching* transparente (TM), *mulching* negro (BM) de 200 cm de ancho con 0,05 cm de espesor, y sin *mulching* (WM); y fertilizantes: fertilizante orgánico compuesto (CoF), fertilizante orgánico no compuesto (NoF) y fertilizante químico (ChF). El diseño de parcelas subdivididas bajo el diseño de bloques completos al azar (RCBD) se estableció en 27 tratamientos con 3 repeticiones, para cartografiar  $\Phi$ ,  $\theta_{60}$  y MWD en base a 81 muestras de suelo con todos los tratamientos. Los resultados mostraron que los diferentes tratamientos del suelo tienen diversos impactos en SPP. MP+DH alcanzó el mayor  $\theta_{60}$  ( $0,22 \text{ cm}^3 \text{ cm}^{-3}$ ), MWD (0,85 mm) y  $\Phi$  (56,87%). Por otro lado, MT+CP obtuvo un MWD mayor de 0,98 mm y un  $\Phi$  menor de 49% en comparación con otros sistemas de labranza. El mantillo del suelo modificó significativamente el SPP, con BM alcanzando el mayor  $\Phi$  (55,65%),  $\theta_{60}$  ( $0,35 \text{ cm}^3 \text{ cm}^{-3}$ ) y MWD (1,06 mm). Los resultados no indicaron diferencias significativas entre los tipos de fertilizantes en SPP. El CoF tuvo un efecto significativo en MWD y se relacionó con las características del suelo estudiadas. Estos hallazgos pueden ayudarnos a comprender los efectos individuales y combinados del sistema de labranza, el *mulching* y la aplicación de fertilizantes en algunas características del suelo en el cultivo del trigo. Un estudio más centrado en la influencia de las profundidades de labranza y los tipos de *mulchings* (*mulching* de plástico versus *mulching* orgánico para diferentes cultivos) en una variedad de suelos y condiciones climáticas, así como en las propiedades térmicas del suelo, necesitaría una investigación más profunda.

**Keywords:** Conventional tillage, soil porosity, soil water content, soil aggregate stability, land management.

**Palabras clave:** labranza convencional, porosidad del suelo, contenido de agua del suelo, estabilidad de agregados del suelo, gestión del suelo.

Received: 11 September 2022

Accepted: 22 March 2023

**\*Corresponding author:** Andrés Caballero Calvo, Department of Regional Geographical Analysis and Physical Geography, University of Granada, Spain. Email address: andrescaballero@ugr.es

## 1. Introduction

The implementations of appropriate tillage systems, mulching, and fertilizers play a key role in improving soil properties as well as increasing crop productivity (Li *et al.*, 2022; Naveen *et al.*, 2021; Rodrigo-Comino *et al.*, 2020). Tillage is the mechanical manipulation of soil for managing crop production. It also has a substantial impact on soil properties such as porosity, water content conservation, and stability of aggregates (Al-Shammary and Al-Sadoon, 2014; Liebhard *et al.*, 2022; Ndzelu *et al.*, 2021; Silva *et al.*, 2021). It is based on the utilization of mechanical applications to overturn soil layers with its crop and weed residues, leading to an increase in soil organic content due to the mixture. There is a wide range of tillage systems: conventional tillage (Mirzaei *et al.*, 2023; Torppa and Taylor, 2022), reduced tillage (Deng *et al.*, 2022), shallow tillage (Arvidsson *et al.*, 2014), optimum tillage (Gorucu *et al.*, 2006), minimum tillage (Githongo *et al.*, 2021), economical tillage (Chen *et al.*, 2020), conservational tillage (Zheng *et al.*, 2022), mulch tillage (Jiang *et al.*, 2022), no/zero tillage (Mirzaei *et al.*, 2022; Zhao *et al.*, 2022), or tillage-plant systems (Li *et al.*, 2019).

Soil mulching is one of the most soil management applications used as the addition of any organic or inorganic material over the top of the soil surface to protect it (Al-Shammary *et al.*, 2020). Some of the benefits include reduced soil erosion (Parlak *et al.*, 2022; Wang *et al.*, 2021), less

compaction (Adekalu *et al.*, 2006), water conservation (Yang *et al.*, 2023), increased control of soil temperature (Yin *et al.*, 2023), and a reduction in weed growth (Agarwal *et al.*, 2022). Soil mulching is also a practical way of increasing soil temperature to levels that are lethal to microorganisms that cause disease in agricultural production (Bu *et al.*, 2013; Rodrigo-Comino, 2018; Steinmetz *et al.*, 2016; Zhao *et al.*, 2023). It is developed and used in different geographical areas with different purposes, for example, in the Middle East and Israel, to reduce soil heating. Still nowadays a great amount of soil mulching investigations is still being undertaken worldwide (Kahlon *et al.*, 2013; Nzeyimana *et al.*, 2017). However, the effect of mulching combined with mechanical and chemical treatments on soil properties has received less attention. Even less in arid and semi-arid areas where water scarcity and land degradation processes are a consequence of human impacts (Rodrigo-Comino *et al.*, 2022) and the imminent climate change such as Iraq (Qader *et al.*, 2023).

Soil porosity ( $\Phi$ ), volumetric soil water content conservation 60 days after irrigation to field capacity ( $\theta_{60}$ ), and mean weight diameter of aggregates (MWD) are some significant soil physical properties (SPP) affecting crop growth and development (Mondal and Chakraborty, 2022). They influence plant growth directly but are also affected by mulching, tillage, and fertilizer application (Zhao *et al.*, 2012). A considerable amount of literature has been published on determining the performance of soil mulching under different conditions. The use of plastic mulches in agricultural fields can influence soil's physical, chemical, and biological properties (Braunack *et al.*, 2015; Jiang *et al.*, 2017; Maul *et al.*, 2014; Rodrigo-Comino *et al.*, 2018; Scarascia-Mugnozza *et al.*, 2012). Furthermore, the plastic cover can reduce the consumption of water use in irrigation, and lead to conserving water (Anikwe *et al.*, 2007; Bhardwaj and Sarolia, 2013; Jiang *et al.*, 2017), decrease soil compaction (Mahadeen, 2014), and improve the heating conditions in the soil (Li *et al.*, 2016). The recent scientific literature is full of examples of countries where the use of these types of mulches are used. For example, Nzeyimana *et al.* (2017) investigated the effect of mulching type on SPP conditions in Rwanda, concluding that soil mulching has a significant influence on bulk density ( $\rho_b$ ). Furthermore, the results revealed that improving SPP depends on the study location and the type of mulching used. Kahlon *et al.* (2013) and Figueiredo *et al.* (2017) also showed that the soil tillage system had a strong influence on SPP in Central Ohio. In addition, Crittenden and de Goede (2016) showed that a tillage system, directly and indirectly, influenced soil water content regimes. Zhang *et al.* (2017) investigated the effect of organic and chemical fertilizers on SPP, showing that organic fertilizer strongly led to a decrease in  $\rho_b$ . Xin (2016) argued that organic and mineral fertilizers can influence SPP in North China, showing a significant decrease in  $\rho_b$ . Although several studies have reported on individual influences of tillage practices, mulching and fertiliser application on SPP, the integrated effect has rarely been studied, particularly under dry soil conditions. Therefore, the main objective of this work is to study the influence of the individual and combined effects of a different combination of tillage, mulching, and fertilizers on SPP.

## **2. Materials and methods**

### *2.1. Experimental site, soil sampling and measurements*

This study was carried out during the summer season of 2015 at Al Qataniyah village experiment, Aziziyah city, Wasit, Iraq (32.9° N, 44.9° E at 36 m a.s.l.). The soil site was categorized under the Typic Torrifluent group texture (Soil Survey Staff, 2014), it is located within arid and semi-arid areas, where the annual average temperature is 45 °C. The rainfall is mostly during the Dec to Feb with rainfall 145 mm, with site slope from (northeast to southwest and eastern outlines to the centre). Soil physical and chemical properties were measured using laboratory standard methods. This was done by collecting soil samples, 7 cm height and 5 cm diameter soil cylinders, at three depths (0-10, 10-20, and 20-30 cm) at randomly selected spots. Disturbed soil samples at each depth were mixed to obtain a representative sample of the corresponding depth. Samples were placed in plastic bags and transfer to the laboratory for drying under ambient conditions and grinding, then samples were passed through a 2 mm sieve. The physical and chemical analyses of the general soil characteristics are shown in Table 1.

Soil bulk density ( $\rho_b$ ) was measured by the ring method (with a volume of 125 cm<sup>3</sup>) for undisturbed cores (Zheng *et al.*, 2021). Particle density ( $D_p$ ) was measured by the pycnometer method (Ruehlmann and Korschens, 2020). Porosity was calculated from measured values of  $\rho_b$  and  $D_p$ . Particle size distribution was measured according to (Soil Survey Staff, 2014). Soil pH and electric conductivity (EC) were measured using an electrical conductivity meter, while soil organic matter (SOM) was determined by the loss on ignition method according to (Jackson, 2005).  $\text{CO}_3^{2-}$ ,  $\text{HCO}_3^{-}$ ,  $\text{Cl}^{-}$ ,  $\text{SO}_4$ ,  $\text{Ca}^{2+}$ ,  $\text{Mg}^{2+}$ ,  $\text{Na}^{+}$ ,  $\text{K}^{+}$  were detected by saturated paste extract, according to (Rhoades, 1983).

The MWD was measured by several steps. Soil samples were taken from each soil treatment and transported to the laboratory to maintain soil structure from distortion or damage and then manually disaggregated at a certain water content suitable to maintain the natural order of the assemblies. Briefly, soil samples were sieved using two sieves: first with a mesh size of 9 mm, and then with a mesh size of 4 mm. Then, the soil aggregates between 4-9 mm were left to dry under laboratory conditions, 50 g from aggregates for each soil treatment was taken and placed on over a group of sieves with mesh sizes 4.75, 2.36, 1.00, 0.50, and 0.25 mm from top to bottom. Then, samples were moistened from the bottom by capillary using distilled water for 6 min and sieved again for 6 min. The contents of each sieve were separated and dried at 105 °C for 24 h. The MWD was computed as  $MWD = \sum_{i=1}^N \bar{x} \omega_i$  (Besalatpour *et al.*, 2013), where:  $\bar{x}$  is the average diameters of each mesh size (mm),  $\omega_i$  is the rate of dry-weight aggregate to total dry-weight of soil expressed as a percentage.

Before tillage practices, the soil at the experimental site has a clay loam surface texture (Soil Survey Staff, 2014) with an average of 35% clay, 41 silt, and 24 sand.  $D_p$  at 0–30 cm depth has an average of 2.63 Mg m<sup>-3</sup>. Soil EC decreased with increased soil depths. SOM was high with values of 6.0 g kg<sup>-1</sup> at 0-10 cm soil depth and 4.0 g kg<sup>-1</sup> at 20-30 cm depth. Main chemicals measured at the three depths include  $\text{CO}_3^{2-}$ ,  $\text{HCO}_3^{-}$ ,  $\text{Cl}^{-}$ ,  $\text{SO}_4^{2-}$ ,  $\text{Ca}^{+2}$ ,  $\text{Mg}^{+2}$ ,  $\text{Na}^{+}$ , and  $\text{K}^{+}$ , are reported in Table 1.

Table 1. Main characteristics of the studied soil.

Soil depth (cm)	EC dsm <sup>-1</sup>	pH	SOM g kg <sup>-1</sup>	C mole c/L in saturated paste extract								$\rho_b$ Mg m <sup>-3</sup>	$D_p$ Mg m <sup>-3</sup>	MWD mm	Particle size distribution %			Texture
				$\text{CO}_3^{2-}$	$\text{HCO}_3^{-}$	$\text{Cl}^{-}$	$\text{SO}_4$	$\text{Ca}^{2+}$	$\text{Mg}^{2+}$	$\text{Na}^{+}$	$\text{K}^{+}$				Clay	Silt	Sand	
0-10	2.06	7.0	6.0	0	7	13	1.4	14.4	4	3.8	0.717	1.21	2.61	0.60	39	40	21	Clay loam
10-20	1.70	7.3	4.8	0	9	8	1.1	7.2	8	2.9	0.651	1.24	2.64	0.56	33	44	23	
20-30	1.34	7.3	4.0	0	10	3	1.0	8.3	2	2.6	0.648	1.29	2.65	0.48	34	40	26	

## 2.2. Experimental design

The field site includes the following experimental design:

- Tillage systems: 1) Conventional tillage: a combination of mouldboard plough followed by a disk harrow (MP+DH), plough to 25 cm depth; 2) Economical tillage: rotary cultivator (RC); and 3) Mulch tillage: chisel plough (CP) to a depth of 30 cm and leaving the remains of the straw crop to cover the soil surface after ploughing.
- Mulching: transparent mulch (TM), black mulch (BM), and without mulch (WM).
- Fertilisers: composted organic fertiliser (CoF), no-composted organic fertiliser (NoF) at an amount of 0.40 kg m<sup>-2</sup> of cattle dune, and chemical fertiliser (ChF) of diammonium phosphate (DAP) at an amount 0.06 kg m<sup>-2</sup>. The CoF was prepared by aerobic decomposition before being used by leaving it for a period of 10 weeks until an appropriate degree of decomposition was reached and, then, mixed with the soil surface manually.

These three individual treatments combined resulted in 27 treatments (3 tillage systems \* 3 mulching \* 3 fertilizers). Each combined treatment was implemented in 4 m<sup>2</sup> plots, leaving 1 m between

each of the experimental units, 1 m between ploughing treatments, and 1 m between replicates to prevent interferences among experimental units. Each of the 27 combined treatments was replicated three times, making a total of 81 experimental plots over the entire area of 585 m<sup>2</sup>, as shown in Figure 1.

The study used a tractor (New Holland T8.320), mouldboard plough (MP) with four boards, rotary plough (RC; mini-1200), chisel plough (CP), and disk harrow (DH). The specifications for the tractor and equipment used are shown in Appendices 1-2. The DH was used to mix fertilisers with the soil. In addition, irrigation to field capacity was made by surface irrigation. After the implementation of the three different tillage systems and the incorporation of the three different fertiliser types, the experimental plots were covered with plastic sheets (mulching) 200 cm wide and 0.05 cm thick for the transparent mulching (TM) and the black mulching (BM). Polyethylene film was used for soil mulching perfectly attached to the soil surface, which is essential to reduce water losses. Finally, the polyethylene sheets from all plots were removed after 60 days and the soil samples were collected to measure  $\Phi$ ,  $\theta_{60}$ , and MWD for each soil treatment.

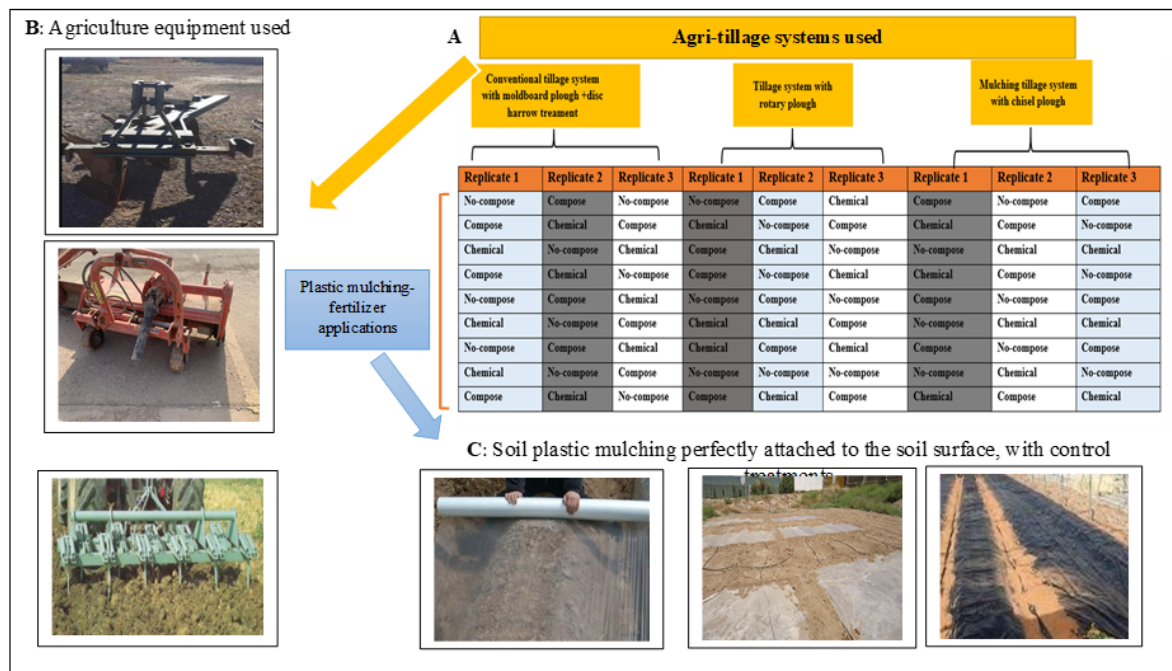


Figure 1. Schematic diagram of the experimental field.

### 2.3. Statistical analysis

The split-split-plot design under the randomized complete block design (RCBD) was used to design and analyze the experimental data.  $\Phi$ ,  $\theta_{60}$ , and MWD were calculated for each soil treatment at 0-20 cm soil depth, and the influence of tillage, mulching, and fertilizer on  $\Phi$ ,  $\theta_{60}$ , and MWD was tested by the two-way ANOVA analysis using SAS 9.4v (SAS, 2013). The results were statistically tested by the least significant difference (LSD) method at the 0.05 probability level.

## 3. Results and discussion

### 3.1. Soil Porosity

The effect of tillage, mulching, and fertilizer on  $\Phi$  are presented in Figure 2. A significant variation between tillage on  $\Phi$  was found, where the CP gave the lowest  $\Phi$  at 49.00%, while the MP+DH gave the

highest  $\Phi$  at 56.87% (Fig. 2a). The reason for this result is the rise of  $\rho_b$  in CP treatment compared with RC and MP+DH treatments, as shown in Figure 2a. Mulching shows significant differences in  $\Phi$  between BM treatment (55.65%) and WM (52.98%). However, the differences between BM and TM treatment and between TM and WM, were non-significant (Fig. 2b). These results are due to decreasing soil  $\rho_b$  with BM compared with TM and WM. The findings show no significant differences between fertiliser applications on  $\Phi$  (Fig. 2c). The interaction between tillage and mulching showed significant differences in  $\Phi$ , with the highest value for MP+DH and BM (58.34%) and the lowest  $\Phi$  for CP+WM (51.29%) (Fig. 2d). Also,  $\Phi$  values were higher for MP+DH than for CP, RC as a result of decreasing SD values in plots ploughed by MP+DH compared with RC ploughing. The general trend in  $\Phi$  values with the three types of tillage from highest to lowest was BM > TM > WM for the majority of soil treatments.

A significant positive correlation was indicated between tillage and fertilizers in  $\Phi$  values (Fig. 2d), with the highest  $\Phi$  value showing for MP+DH and CF (58.60%) and the lowest  $\Phi$  value at CP and CF (49.40%). The interaction between mulching and fertilizer found significant differences in  $\Phi$ , with the highest value for BM and CF (56.77%), and the lowest value for WM (52.14%) (Fig. 2e).

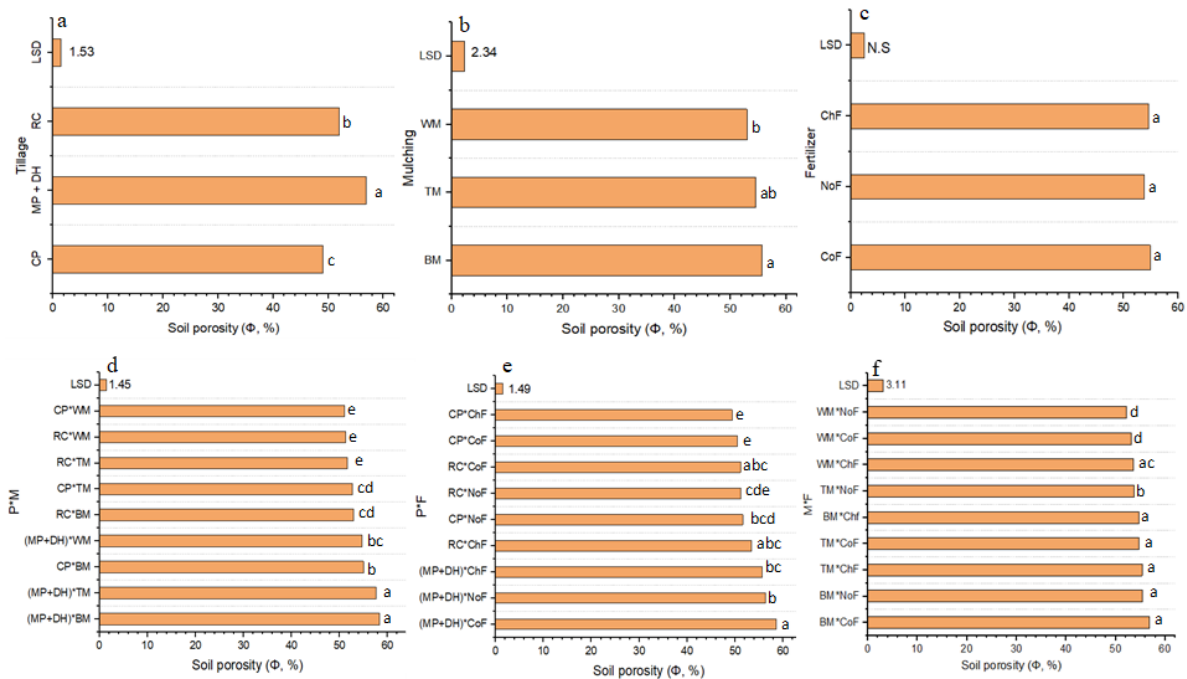


Figure 2. Individual and combined effects of tillage, mulching, and fertilization practices on soil porosity ( $\Phi$ ).  
 LSD: least significant difference (method at the 0.05 probability level, RC: Rotary cultivator, MP+DH: Ploughing mouldboard plough followed by a disk harrow, CP: Chisel plough, TM: Transparent mulch, BM: black mulch, WM: without mulch, CoF: composed organic fertilizer, NoF: no-composed organic fertilizer, ChF: chemical fertilizer, \*: Interaction effect of the treatments.

### 3.2. Soil water conservation

Results in Figure 3 represent the effect of tillage, mulching, and fertilizers on soil water conservation measured as the volumetric soil water content 60 days after irrigation to field capacity ( $\theta_{60}$ ). Results show a significant difference between the tillage system on  $\theta_{60}$  values. The RC gave the highest average  $\theta_{60}$  with  $0.30 \text{ cm}^3 \text{ cm}^{-3}$ , whereas the CP gave the lowest average  $\theta_{60}$  with  $0.15 \text{ cm}^3 \text{ cm}^{-3}$  (Fig. 3a). This is expected due to the increase of  $\rho_b$  with CP treatments. Soil mulching also provides significant differences in  $\theta_{60}$ , with the highest value of  $\theta_{60}$  using BM,  $0.35 \text{ cm}^3 \text{ cm}^{-3}$ , and the lowest value using WM,  $0.17 \text{ cm}^3 \text{ cm}^{-3}$ . The general trend in  $\theta_{60}$  from highest to lowest, is BM > TM > WM, caused by the fact that BM has a stronger effect on reducing evaporation (Anikwe *et al.*, 2007; Bhardwaj

and Sarolia, 2013; Jiang *et al.*, 2017; Mahadeen, 2014). On the other hand, no significant differences between fertilizers on  $\theta_{60}$  values were found. The interaction between tillage and mulching in  $\theta_{60}$  (significance at the p level of 0.05) had the highest value for RC+TM (0.33  $\text{cm}^3 \text{cm}^{-3}$ ), whereas the lowest  $\theta_{60}$  (0.13  $\text{cm}^3 \text{cm}^{-3}$ ) was obtained for CP \* WM (Figure 3d). Also,  $\theta_{60}$  values were higher in BM plots for the three tillage systems compared with TM and WM. Plots ploughed by RC using BM had significantly higher  $\theta_{60}$  values than plots using TM and WM, with values 37% and 43% higher respectively, while  $\theta_{60}$  values in the RC and BM plots were significantly higher than in TM and WM plots with values 30% and 180%, respectively. Furthermore, the interaction between the tillage system and fertilizer type showed non-significant differences between most treatments except for RC and CoF, NCF, and ChF with MP+DH and CoF. The highest  $\theta_{60}$  value was obtained for RC and CoF (0.32  $\text{cm}^3 \text{cm}^{-3}$ ), and the lowest value for MP+DH and CoF (0.18  $\text{cm}^3 \text{cm}^{-3}$ ). The interaction between soil mulching and fertilizer type showed significant differences between most treatments, presenting the highest  $\theta_{60}$  value (0.388  $\text{cm}^3 \text{cm}^{-3}$ ) for BM and ChF, while the lowest value (0.09  $\text{cm}^3 \text{cm}^{-3}$ ) appeared for WM and CoF (Figure 3f). The general trend in  $\theta_{60}$  values considering interactions between mulching and fertilizer type, from highest to lowest, was BM and all fertiliser types > TM and all fertiliser types > WM and all fertiliser types. The reason for this is the influence of soil mulching on soil water consumption by controlling evaporation from the soil surface, which leads to water conservation (Jiang *et al.*, 2017; Mankagh, 2009; Testa *et al.*, 2015; Wang *et al.*, 2009).

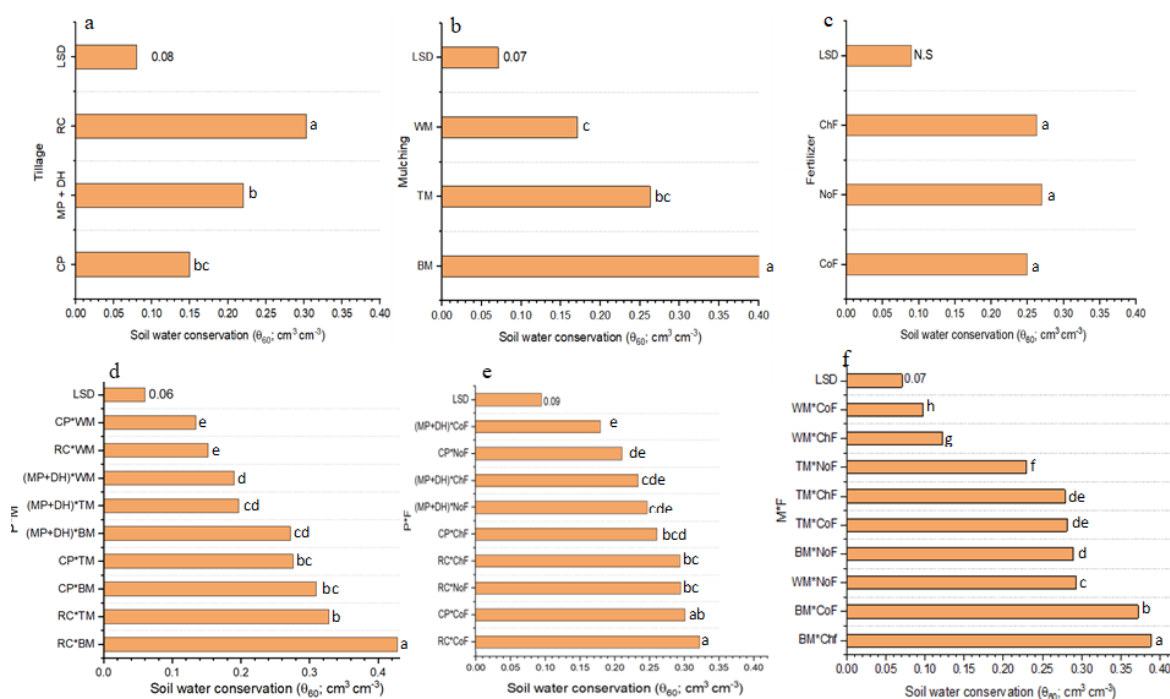


Figure 3. Individual and combined effects of tillage, mulching, and fertilizer practices on soil water conservation ( $\theta_{60}$ ). LSD: least significant difference method at the 0.05 probability level, RC: Rotary cultivator, MP+DH: Ploughing mouldboard plough followed by a disk harrow, CP: Chisel plough, TM: Transparent mulch, BM: black mulch, WM: without mulch, CoF: composed organic fertilizer, NoF: no-composed organic fertilizer, ChF: chemical fertilizer, \*: Interaction effect of the treatments.

### 3.3. Mean weight diameter of aggregates

The effect of tillage, mulching, and fertilizers, as well as their interactions on the mean weight diameter of aggregates (MWD) is shown in Figure 4. Significant differences were found between the tillage system on MWD. The CP showed the highest MWD value of 0.98 mm, whereas the RC showed

the lowest MWD of 0.73 mm (Fig. 4a). This is because ploughing with CP leads to the destruction of soil structure as a result of turning the subsoil to the top by CP, as well as with MP+DH. The mulching type also had a significant effect on MWD, showing higher MWD for BM and TM (1.06 and 0.84 mm, respectively) compared to WM with MWD of 0.66 mm. MWD increased using mulching (Fig. 4b), which could be explained by the increased soil water content with mulching leading to higher stability of the soil aggregates (Ma *et al.*, 2014). As expected, fertilizer type significantly affects MWD. The highest MWD occurred for CoF with 1.02 mm, and lowest for ChF with 0.75 mm (Fig. 4c). Soil structural stability increase with rising the decomposition of organic content (Ye *et al.*, 2017).

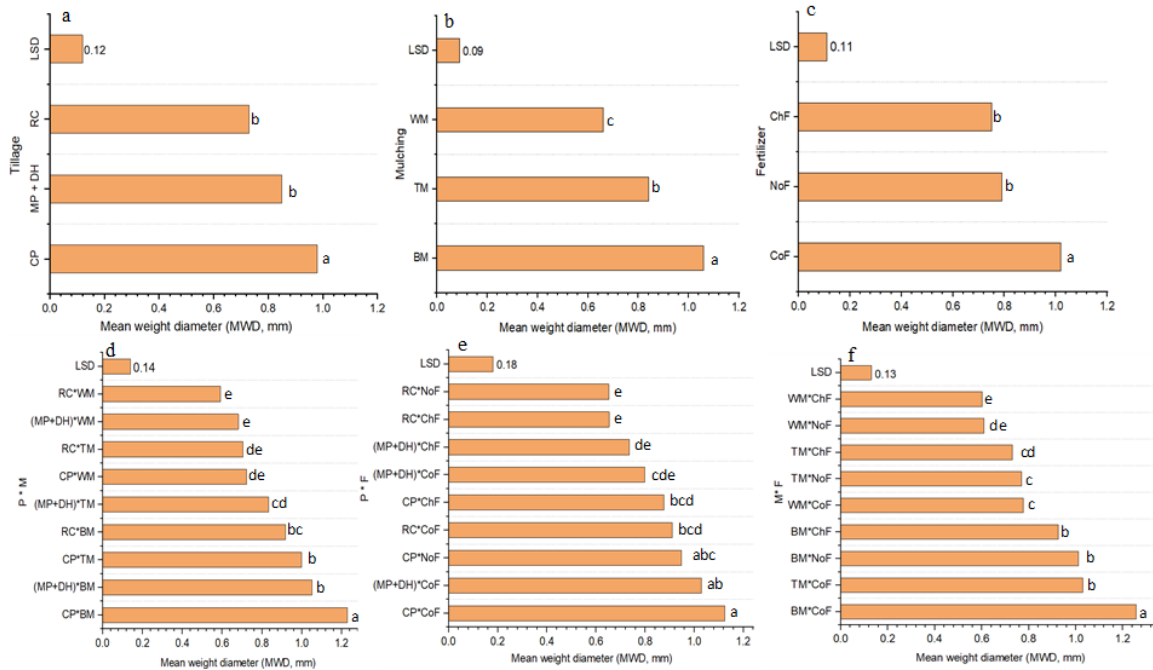


Figure 4. Individual and combined effects of tillage, mulching, and fertilizer practices on mean weight diameter of aggregates (MWD). LSD: least significant difference method at the 0.05 probability level, RC: Rotary cultivator, MP+DH: Ploughing mouldboard plough followed by a disk harrow, CP: Chisel plough, TM: Transparent mulch, BM: black mulch, WM: without mulch, CoF: composed organic fertilizer, NoF: no-composed organic fertilizer, ChF: chemical fertilizer, \*: Interaction effect of the treatments.

The combination of the tillage system and mulching showed significant differences in MWD (Fig. 4d), with the highest MWD value for CP+BM (1.22 mm) and the lowest MWD for RC+WM (0.59 mm). Moreover, the results showed that the interaction between MP+DH and BM had a higher MWD value (1.05 mm) compared to MP+DH, and WM showed a lower value (0.68 mm). A likely explanation is that the lower destruction of soil aggregated by CP compared to turning ploughs, and mulching reduces evaporation allowing the soil to maintain high water content.

Figure 4e shows a significant effect of the combined tillage system and fertilizer type on MWD. The highest value was 1.12 mm for CP+CoF, while the lowest value was 0.65 mm, for RC+NoF and RC+ChF. The stability of soil aggregates is increased by CP, which breaks up and loosens the soil without turning it. As expected, MWD increased as soil organic content increased. Another important finding was that mulching + fertilizer application had a significant influence on MWD, obtaining the highest value (1.25 mm) at BM \* CoF, whereas the lowest (0.60 mm) at WM \* ChF. Thus, the MWD is indirectly influenced by tillage, mulching, and fertilizer treatments.

#### 4. Challenges of the current study

The soil physical properties (SPP) were studied with the impact of the individual and combined effects of soil management practices within arid and semi-arid areas in southern Iraq. The conventional, economical, and mulch tillage system; transparent, black plastic mulch; organic and chemical fertilizers were effect on the SPP in clay loam texture for the wheat-agricultural sites. These results might be applicable to clay loam and clay texture properties. On the other hand, despite these recent limitations, Further investigation about long-term studies based on the influence of tillage and mulching under a variety of soils and climatic conditions of Iraq, as well as on soil thermal properties are strongly recommended. Furthermore, the Long-term no-tillage system effect on soil thermal-physical attributes in wheat /barley cultivation needs to be further studied.

#### 5. Conclusions

The present study was designed to study the individual and combined effects of tillage, mulching, and fertilizer on  $\Phi$ ,  $\theta_{60}$ , and MWD in agricultural land. The main results indicate that tillage systems were significantly positively correlated with  $\Phi$ , and MWD ( $p < 0.05$ ). MP+DH showed higher  $\Phi$ , whereas CH showed higher MWD (0.98 mm) compared to MP+DH, RC (0.85 and 0.73 mm, respectively). The highest values of  $\Phi$ ,  $\theta_{60}$ , and MWD were obtained when BM was used. This was attributed to the influence of BM on reducing water losses, thus, allowing the soil to retain more water. On the other hand, no significant differences between fertilizer types on  $\Phi$  and  $\theta_{60}$  were found. However, fertilizer type was significantly correlated to MWD, with the highest MWD for CoF and the lowest for ChF due to the increasing decomposition of organic content in the CoF. The interaction between MP+DH and BM showed the highest  $\Phi$ , while CP+BM showed the highest MWD.

#### References

- Adekalu, K.O., Okunade, D.A., Osunbitan, J.A., 2006. Compaction and mulching effects on soil loss and runoff from two southwestern Nigeria agricultural soils. *Geoderma* 137(1), 226-230. <https://doi.org/10.1016/j.geoderma.2006.08.012>
- Agarwal, A., Prakash, O., Sahay, D., Bala, M., 2022. Effect of organic and inorganic mulching on weed density and productivity of tomato (*Solanum lycopersicum* L.). *Journal of Agriculture and Food Research* 7, 100274. <https://doi.org/10.1016/j.jafr.2022.100274>
- Al-Shammary, A., Al-Sadoon, J., 2014. Influence of tillage depth, soil mulching systems and fertilizers on some thermal properties of silty clay soil. *GJAR* 2, 18-32.
- Al-Shammary, A., Kouzani, A., Gyasi-Agyei, Y., Gates, W., Rodrigo-Comino, J., 2020. Effects of solarisation on soil thermal-physical properties under different soil treatments: A review. *Geoderma* 363, 114137. <https://doi.org/10.1016/j.geoderma.2019.114137>
- Anikwe, M., Mbah, C., Ezeaku, P., Onyia, V., 2007. Tillage and plastic mulch effects on soil properties and growth and yield of cocoyam (*Colocasia esculenta*) on an ultisol in southeastern Nigeria. *Soil and Tillage Research* 93(2), 264-272. <https://doi.org/10.1016/j.still.2006.04.007>
- Arvidsson, J., Etana, A., Rydberg, T., 2014. Crop yield in Swedish experiments with shallow tillage and no-tillage 1983–2012. *European Journal of Agronomy* 52, 307-315. <https://doi.org/10.1016/j.eja.2013.08.002>
- Besalatpour, A.A., Ayoubi, S., Hajabbasi, M.A., Mosaddeghi, M.R., Schulin, R., 2013. Estimating wet soil aggregate stability from easily available properties in a highly mountainous watershed. *Catena* 111, 72-79. <https://doi.org/10.1016/j.catena.2013.07.001>
- Bhardwaj, R.L., Sarolia, D., 2013. Effect of mulching on crop production under rainfed condition-A review. *Agricultural Reviews* 34(3), 188-197. <https://doi.org/10.5958/j.0976-0741.34.3.003>

- Braunack, M., Johnston, D., Price, J., Gauthier, E., 2015. Soil temperature and soil water potential under thin oxodegradable plastic film impact on cotton crop establishment and yield. *Field Crops Research* 184, 91-103. <https://doi.org/10.1016/j.fcr.2015.09.009>
- Bu, L.-D., Liu, J.-l., Zhu, L., Luo, S.-s., Chen, X.-p., Li, S.-q., Hill, R.L., Zhao, Y., 2013. The effects of mulching on maize growth, yield and water use in a semi-arid region. *Agricultural Water Management* 123, 71-78. <https://doi.org/10.1016/j.agwat.2013.03.015>
- Chen, J., Pang, D.-w., Jin, M., Luo, Y.-l., Li, H.-y., Li, Y., Wang, Z.-l., 2020. Improved soil characteristics in the deeper plough layer can increase grain yield of winter wheat. *Journal of Integrative Agriculture* 19(5), 1215-1226. [https://doi.org/10.1016/S2095-3119\(19\)62679-1](https://doi.org/10.1016/S2095-3119(19)62679-1)
- Crittenden, S., de Goede, R., 2016. Integrating soil physical and biological properties in contrasting tillage systems in organic and conventional farming. *European Journal of Soil Biology* 77, 26-33. <https://doi.org/10.1016/j.ejsobi.2016.09.003>
- Deng, J., Deng, Y., Sun, Z., Wang, G., Cao, L., Yuan, H., Huang, D., Jia, H., 2022. Tillage and residue management affect growing-season soil respiration in paddy fields. *Soil and Tillage Research* 218, 105315. <https://doi.org/10.1016/j.still.2022.105315>
- Figueiredo, P.G., Bicudo, S.J., Chen, S., Fernandes, A.M., Tanamati, F.Y., Djabou-Fondjo, A.S.M., 2017. Effects of tillage options on soil physical properties and cassava-dry-matter partitioning. *Field Crops Research* 204, 191-198. <https://doi.org/10.1016/j.fcr.2016.11.012>
- Githongo, M.W., Kiboi, M.N., Ngetich, F.K., Musafiri, C.M., Muriuki, A., Fliessbach, A., 2021. The effect of minimum tillage and animal manure on maize yields and soil organic carbon in sub-Saharan Africa: A meta-analysis. *Environmental Challenges* 5, 100340. <https://doi.org/10.1016/j.envc.2021.100340>
- Gorucu, S., Khalilian, A., Han, Y.J., Dodd, R.B., Smith, B.R., 2006. An algorithm to determine the optimum tillage depth from soil penetrometer data in coastal plain soils. *Applied Engineering in Agriculture* 22(5), 625-631. <https://doi.org/10.13031/2013.21993>
- Jackson, M.L., 2005. *Soil chemical analysis: Advanced course*. UW-Madison Libraries parallel press.
- Jiang, Q., Madramootoo, C.A., Qi, Z., 2022. Soil carbon and nitrous oxide dynamics in corn (*Zea mays* L.) production under different nitrogen, tillage and residue management practices. *Field Crops Research* 277, 108421. <https://doi.org/10.1016/j.fcr.2021.108421>
- Jiang, X.J., Liu, W., Wang, E., Zhou, T., Xin, P., 2017. Residual plastic mulch fragments effects on soil physical properties and water flow behavior in the Minqin Oasis, northwestern China. *Soil and Tillage Research* 166, 100-107. <https://doi.org/10.1016/j.still.2016.10.011>
- Kahlon, M.S., Lal, R., Ann-Varughese, M., 2013. Twenty two years of tillage and mulching impacts on soil physical characteristics and carbon sequestration in Central Ohio. *Soil and Tillage Research* 126, 151-158. <https://doi.org/10.1016/j.still.2012.08.001>
- Li, P., Gong, Y., Komatsuzaki, M., 2019. Temporal dynamics of <sup>137</sup>Cs distribution in soil and soil-to-crop transfer factor under different tillage systems after the Fukushima Daiichi Nuclear Power Plant accident in Japan. *Science of The Total Environment* 697, 134060. <https://doi.org/10.1016/j.scitotenv.2019.134060>
- Li, Y.-Y., Pang, H.-C., Han, X.-F., Yan, S.-W., Zhao, Y.-G., Jing, W., Zhen, Z., Zhang, J.-L., 2016. Buried straw layer and plastic mulching increase microflora diversity in salinized soil. *Journal of Integrative Agriculture* 15(7), 1602-1611. [https://doi.org/10.1016/S2095-3119\(15\)61242-4](https://doi.org/10.1016/S2095-3119(15)61242-4)
- Li, Z., Zhang, Q., Qiao, Y., Du, K., Li, Z., Tian, C., Zhu, N., Leng, P., Yue, Z., Cheng, H., Li, F., 2022. Influence of straw mulch and no-tillage on soil respiration, its components and economic benefit in a Chinese wheat–maize cropping system. *Global Ecology and Conservation* 34, e02013. <https://doi.org/10.1016/j.gecco.2022.e02013>
- Liebhart, G., Klik, A., Neugschwandtner, R.W., Nolz, R., 2022. Effects of tillage systems on soil water distribution, crop development, and evaporation and transpiration rates of soybean. *Agricultural Water Management* 269, 107719. <https://doi.org/10.1016/j.agwat.2022.107719>

- Ma, R., Cai, C., Wang, J.-Y., Feng, J., Wu, X., Zhu, H., 2014. Effect of antecedent soil moisture on aggregate stability and splash erosion of krasnozem. *Nongye Gongcheng Xuebao. Transactions of the Chinese Society of Agricultural Engineering* 30, 95-103.
- Mahadeen, A.Y., 2014. Effect of polyethylene black plastic mulch on growth and yield of two summer vegetable crops under rain-fed conditions under semi-arid region conditions. *American Journal of Agricultural and Biological Sciences* 9(2), 202. <https://doi.org/10.3844/ajabssp.2014.202.207>
- Mamkagh, A.M.-A., 2009. Effect of tillage time and plastic mulch on growth and yield of okra (*Abelmoschus esculentus*) grown under rainfed conditions. *International J. Agric. Biol.* 11, 453-457.
- Maul, J.E., Buyer, J.S., Lehman, R.M., Culman, S., Blackwood, C.B., Roberts, D.P., Zasada, I.A., Teasdale, J.R., 2014. Microbial community structure and abundance in the rhizosphere and bulk soil of a tomato cropping system that includes cover crops. *Applied Soil Ecology* 77, 42-50. <https://doi.org/10.1016/j.apsoil.2014.01.002>
- Mirzaei, M., Gorji Anari, M., Taghizadeh-Toosi, A., Zaman, M., Saronjic, N., Mohammed, S., Saronjic, N., Mohammed, S., Szabo, S., Caballero-Calvo, A., 2022. Soil nitrous oxide emissions following crop residues management in corn-wheat rotation under conventional and no-tillage systems. *Air, Soil and Water Research* 15, <https://doi.org/10.1177/11786221221128789>
- Mirzaei, M., Gorji Anari, M., Saronjic, N., Sarkar, S., Kral, I., Gronauer, A., Mohammed, S., Caballero-Calvo, A., 2023. Environmental impacts of corn silage production: influence of wheat residues under contrasting tillage management types. *Environmental Monitoring and Assessment* 195(1), 171. <https://doi.org/10.1007/s10661-022-10675-8>
- Mondal, S., Chakraborty, D., 2022. Global meta-analysis suggests that no-tillage favourably changes soil structure and porosity. *Geoderma* 405, 115443. <https://doi.org/10.1016/j.geoderma.2021.115443>
- Naveen, G., Humphreys, E., Eberbach, P.L., Balwinder, S., Sudhir, Y., Kukal, S.S., 2021. Effects of tillage and mulch on soil evaporation in a dry seeded rice-wheat cropping system. *Soil and Tillage Research* 209, 104976. <https://doi.org/10.1016/j.still.2021.104976>
- Ndzelu, B.S., Dou, S., Zhang, X., Zhang, Y., Ma, R., Liu, X., 2021. Tillage effects on humus composition and humic acid structural characteristics in soil aggregate-size fractions. *Soil and Tillage Research* 213, 105090. <https://doi.org/10.1016/j.still.2021.105090>
- Nzeyimana, I., Hartemink, A.E., Ritsema, C., Stroosnijder, L., Lwanga, E.H., Geissen, V., 2017. Mulching as a strategy to improve soil properties and reduce soil erodibility in coffee farming systems of Rwanda. *Catena* 149, 43-51. <https://doi.org/10.1016/j.catena.2016.08.034>
- Parlak, M., Everest, T., Tunçay, T., Caballero-Calvo, A., Rodrigo-Comino, J., 2022. Soil losses due to leek and groundnut root crop harvesting: An unstudied regional problem in Turkey. *Land Degradation & Development* 33(11), 1799-1809. <https://doi.org/10.1002/ldr.4262>
- Qader, S.H., Utazi, C.E., Priyatikanto, R., Najmaddin, P., Hama-Ali, E.O., Khwarahm, N.R., Tatem, A.J., Dash, J., 2023. Exploring the use of Sentinel-2 datasets and environmental variables to model wheat crop yield in smallholder arid and semi-arid farming systems. *Science of The Total Environment* 869, 161716. <https://doi.org/10.1016/j.scitotenv.2023.161716>
- Rhoades, J.D., 1983. Soluble Salts. In A.L. Page (Ed.). *Methods of Soil Analysis*, Part 2., pp. 167-179. American Society of Agronomy <https://doi.org/10.2134/agronmonogr9.2.2ed.c10>
- Rodrigo-Comino, J., 2018. Five decades of soil erosion research in “terroir”. The State-of-the-Art. *Earth-Science Reviews*, 179, 436-447. <https://doi.org/10.1016/j.earscirev.2018.02.014>
- Rodrigo-Comino, J., Senciales, J. M., Cerdà, A., Brevik, E. C., 2018. The multidisciplinary origin of soil geography: A review. *Earth-Science Reviews*, 177, 114-123. <https://doi.org/10.1016/j.earscirev.2017.11.008>
- Rodrigo-Comino, J., López-Vicente, M., Kumar, V., Rodríguez-Seijo, A., Valkó, O., Rojas, C., Pourghasemi, H.R., Salvati, L., Bakr, N., Vaudour, E., Brevik, E.C., Radziemska, M., Pulido, M., Di Prima, S., Dondini, M., de Vries, W., Santos, E.S., Mendonça-Santos, M.L., Yu, Y., Panagos, 2020. Soil science challenges in a new era: a transdisciplinary overview of relevant topics. *Air, Soil and Water Research* 13, 1178622120977491. <https://doi.org/10.1177/1178622120977491>

- Rodrigo-Comino, J., Caballero-Calvo, A., Salvati, L., Senciales-González, J. M., 2022. Sostenibilidad de los cultivos subtropicales: Claves para el manejo del suelo, el uso agrícola y la Ordenación del Territorio. *Cuadernos Geográficos* 61(1), 150-167. <https://doi.org/10.30827/cuadgeo.v61i1.22284>
- Ruehlmann, J., Körschens, M., 2020. Soil particle density as affected by soil texture and soil organic matter: 2. Predicting the effect of the mineral composition of particle-size fractions. *Geoderma* 375, 114543. <https://doi.org/10.1016/j.geoderma.2020.114543>
- SAS, I., 2013. *Base SAS 9.4 procedures guide: statistical procedures*. Cary, NC, USA: SAS Institute Inc.
- Scarascia-Mugnozza, G., Sica, C., Russo, G., 2012. Plastic materials in European agriculture: actual use and perspectives. *Journal of Agricultural Engineering* 42(3), 15-28. <https://doi.org/10.4081/jae.2011.3.15>
- Silva, M.F.d., Fernandes, M.M.H., Fernandes, C., Silva, A.M.R.d., Ferraudo, A.S., Coelho, A.P., 2021. Contribution of tillage systems and crop succession to soil structuring. *Soil and Tillage Research* 209, 104924. <https://doi.org/10.1016/j.still.2020.104924>
- Staff, S.S., 2014. *Keys to soil taxonomy*. United States Department of Agriculture: Washington, DC, USA.
- Steinmetz, Z., Wollmann, C., Schaefer, M., Buchmann, C., David, J., Tröger, J., Muñoz, K., Frör, O., Schaumann, G.E., 2016. Plastic mulching in agriculture. Trading short-term agronomic benefits for long-term soil degradation? *Science of the Total Environment* 550, 690-705. <https://doi.org/10.1016/j.scitotenv.2016.01.153>
- Testa, R., Foderà, M., Di Trapani, A.M., Tudisca, S., Sgroi, F., 2015. Choice between alternative investments in agriculture: The role of organic farming to avoid the abandonment of rural areas. *Ecological Engineering* 83, 227-232. <https://doi.org/10.1016/j.ecoleng.2015.06.021>
- Torppa, K.A., Taylor, A.R., 2022. Alternative combinations of tillage practices and crop rotations can foster earthworm density and bioturbation. *Applied Soil Ecology* 175, 104460. <https://doi.org/10.1016/j.apsoil.2022.104460>
- Wang, J., Shi, X., Li, Z., Zhang, Y., Liu, Y., Peng, Y., 2021. Responses of runoff and soil erosion to planting pattern, row direction, and straw mulching on sloped farmland in the corn belt of northeast China. *Agricultural Water Management* 253, 106935. <https://doi.org/10.1016/j.agwat.2021.106935>
- Wang, Y., Xie, Z., Malhi, S.S., Vera, C.L., Zhang, Y., Wang, J., 2009. Effects of rainfall harvesting and mulching technologies on water use efficiency and crop yield in the semi-arid Loess Plateau, China. *Agricultural Water Management* 96(3), 374-382. <https://doi.org/10.1016/j.agwat.2008.09.012>
- Xin, X., Zhang, J., Zhu, A., Zhang, C., 2016. Effects of long-term (23 years) mineral fertilizer and compost application on physical properties of fluvo-aquic soil in the North China Plain. *Soil and Tillage Research* 156, 166-172. <https://doi.org/10.1016/j.still.2015.10.012>
- Yang, H., Li, J., Wu, G., Huang, X., Fan, G., 2023. Maize straw mulching with no-tillage increases fertile spike and grain yield of dryland wheat by regulating root-soil interaction and nitrogen nutrition. *Soil and Tillage Research* 228, 105652. <https://doi.org/10.1016/j.still.2023.105652>
- Ye, C., Guo, Z., Cai, C., Wang, J., Deng, J., 2017. Effect of water content, bulk density, and aggregate size on mechanical characteristics of Aquults soil blocks and aggregates from subtropical China. *Journal of Soils and Sediments* 17(1), 210-219. <https://doi.org/10.1007/s11368-016-1480-8>
- Yin, W., Fan, Z., Hu, F., Fan, H., He, W., Zhao, C., Yu, A., Chai, Q., 2023. No-tillage with straw mulching promotes wheat production via regulating soil drying-wetting status and reducing soil-air temperature variation at arid regions. *European Journal of Agronomy* 145, 126778. <https://doi.org/10.1016/j.eja.2023.126778>
- Zhang, T., Cai, G., Liu, S., Puppala, A.J., 2017. Investigation on thermal characteristics and prediction models of soils. *International Journal of Heat and Mass Transfer* 106, 1074-1086. <https://doi.org/10.1016/j.ijheatmasstransfer.2016.10.084>
- Zhao, H., Xiong, Y.-C., Li, F.-M., Wang, R.-Y., Qiang, S.-C., Yao, T.-F., Mo, F., 2012. Plastic film mulch for half growing-season maximized WUE and yield of potato via moisture-temperature improvement in a semi-arid agroecosystem. *Agricultural Water Management* 104, 68-78. <https://doi.org/10.1016/j.agwat.2011.11.016>

- Zhao, J., Liu, Z., Lai, H., Yang, D., Li, X., 2022. Optimizing residue and tillage management practices to improve soil carbon sequestration in a wheat–peanut rotation system. *Journal of Environmental Management* 306, 114468. <https://doi.org/10.1016/j.jenvman.2022.114468>
- Zhao, X.-d., Qin, X.-r., Li, T.-l., Cao, H.-b., Xie, Y.-h., 2023. Effects of planting patterns plastic film mulching on soil temperature, moisture, functional bacteria and yield of winter wheat in the Loess Plateau of China. *Journal of Integrative Agriculture*. <https://doi.org/10.1016/j.jia.2023.02.026>
- Zheng, F., Wu, X., Zhang, M., Liu, X., Song, X., Lu, J., Wang, B., Jan van Groenigen, K., Li, S., 2022. Linking soil microbial community traits and organic carbon accumulation rate under long-term conservation tillage practices. *Soil and Tillage Research* 220, 105360. <https://doi.org/10.1016/j.still.2022.105360>
- Zheng, K., Cheng, J., Xia, J., Liu, G., Xu, L., 2021. Effects of Soil Bulk Density and Moisture Content on the Physico-Mechanical Properties of Paddy Soil in Plough Layer. *Water* 13(16), 2290. <https://doi.org/10.3390/w13162290>

## Appendices. Specifications for the tractor and equipment used

### *Appendix 1. Characteristics of the tractor used.*

Specification	New Holland T8.320
Years of production	2007
Engine model / type	6.75T
Engine displacement (cm <sup>3</sup> )	7474
Number of cylinders	6 T
Engine rated power (hp)	125
Type of drive transmission	Mech
Front wheel size	23.1R26
Rear wheel size	13/65-18
Weight	11200 kg

### *Appendix 2. Specification for the agriculture equipment used.*

Specification	Mouldboard plough with four mould-board	Rotary plough, mini 1200 with 7 discs loaded blade	Chisel plough with 7 Blade	Disk harrow/ Double unit /8 Disc of each unit
Working width (cm)	105	128	170	155
Maximum soil tillage depths (cm)	33	20	40	20
Length (cm)	220	-	-	-
Weight (Kg)	300	232	390	-





## ASSESSMENT OF LAND DEGRADATION AND DROUGHTS IN AN ARID AREA USING DROUGHT INDICES, MODIFIED SOIL-ADJUSTED VEGETATION INDEX, AND LANDSAT REMOTE SENSING DATA

ABDESSAMED DERDOUR<sup>1</sup>, ANTONIO JODAR-ABELLAN<sup>2,3\*</sup>,  
AMPARO MELIAN-NAVARRO<sup>4</sup>, RYAN BAILEY<sup>5</sup>

<sup>1</sup>*University Center Salhi Ahmed Naama (Ctr Univ Naama), Department of Natural and Life Sciences, Laboratory for the Sustainable Management of Natural Resources in Arid and Semiarid Zones, Algeria.*

<sup>2</sup>*Spanish Research Council, Centro de Edafología y Biología Aplicada del Segura (CEBAS-CSIC), Soil and Water Conservation Group, Murcia, Spain.*

<sup>3</sup>*University Institute of Water and Environmental Sciences. University of Alicante, Spain.*

<sup>4</sup>*Cartography Engineering and Graphic Expression in Engineering Department, Agro-Environmental Economics, Miguel Hernández University of Elche, 03312 Orihuela, Spain.*

<sup>5</sup>*Department of Civil and Environmental Engineering, Colorado State University (USA).*

**ABSTRACT.** Ain Sefra is part of the Ksour Mountains and it's situated in southwestern Algeria, where the climate is arid. The study area is progressively facing regression and degradation exacerbated by climate change. These trends point to a significant acceleration of desertification and drought and the loss of production systems that play a critical social, ecological, and economic role in the region. To better understand the natural hazard of dryness in Ain Sefra and the impact of climate change, we used various drought indices and remote sensing data. Hence, analyzing precipitation records from 1965 to 2021, through several drought indices, droughts were identified as a recurring phenomenon. Moreover, the frequency of successive dry years is relatively high. There were three most extended continuous dry periods. The first phase lasted seven years from 1980 to 1987, the second twelve years from 1994 to 2006, and the third nine years from 2012 to 2021. Calculation of the Modified Soil-Adjusted Vegetation Index (MSAVI) for five multirate satellite images allowed us to follow the evolution of land use elements in this region from 1977 to 2017. Indeed, the study of these multi-temporal images reveals a considerable growth of sands, moving towards the north and northeast of the zone during the last decades. The combination of drought indices and remote sensing seems to be most promising; whose results are valuable tools for guidance and decision support to local and regional authorities.

***Evaluación de la degradación del suelo y sequías en una región árida utilizando índices de sequía, índice de vegetación ajustado al suelo modificado y datos de sensores remotos Landsat***

**RESUMEN.** Ain Sefra, en las montañas Ksour, está situada en el suroeste de Argelia, donde el clima es árido. El área de estudio se enfrenta progresivamente a la regresión y degradación exacerbada por el cambio climático. Estas tendencias apuntan a una aceleración significativa de la desertificación y la sequía y a la pérdida de sistemas de producción que desempeñan un papel social, ecológico y económico crítico en la región. Para comprender mejor el peligro natural de la sequía en Ain Sefra y el impacto del cambio climático, se usaron varios índices de sequía y datos de

teledetección. Al analizar los registros de precipitación desde 1965 hasta 2021, a través de varios índices de sequía, se identificaron las sequías como un fenómeno recurrente. Además, la frecuencia de años secos sucesivos es relativamente alta. Hubo tres períodos secos continuos más prolongados. La primera fase duró siete años, de 1980 a 1987, la segunda doce años, de 1994 a 2006, y la tercera nueve años, de 2012 a 2021. El cálculo del Índice de Vegetación Ajustado al Suelo Modificado (MSAVI) para cinco imágenes satelitales multifecha nos permitió seguir la evolución de los elementos de uso del suelo en esta región desde 1977 hasta 2017. De hecho, el estudio de estas imágenes multitemporales revela un crecimiento considerable de arenas, moviéndose hacia el norte y noreste de la zona durante las últimas décadas. La combinación de índices de sequía y sensores remotos parece ser muy prometedores, pues sus resultados son valiosas herramientas de orientación y apoyo a la decisión de los entes locales y regionales.

**Keywords:** Ain Sefra, MSAVI, Dry climate, Drought, Sustainability.

**Palabras clave:** Ain Sefra, MSAVI, Clima seco, Sequía, Sostenibilidad.

Received: 28 July 2022

Accepted: 14 January 2023

**\*Corresponding author:** Antonio Jodar-Abellán. Spanish Research Council, Centro de Edafología y Biología Aplicada del Segura (CEBAS-CSIC), Soil and Water Conservation Group, Murcia, Spain. E-mail address: [ajodar@cebas.csic.es](mailto:ajodar@cebas.csic.es)

## 1. Introduction

Climate change has been reported worldwide in recent years (e.g., Ripple *et al.*, 2021; Tahir *et al.*, 2021; UN, 2022). Because of the increased intensity and frequency of severe events such as droughts, heatwaves, sandstorms, forest fires, and floods, scientists are now focusing on the effects of climate change (e.g., Corwin, 2021; Malhi *et al.*, 2021; Niñerola *et al.*, 2020; Camarasa-Belmonte, 2021; Rodrigo-Comino *et al.*, 2022; Eekhout *et al.*, 2021). Droughts are one of the most complicated extreme climatic situations, affecting more people than any other hazard or natural disaster (Wilhite, 2000; Oliveira-Santos *et al.*, 2022; Mendoza-Uribe, 2022). The impacts of droughts have generally been referred to as direct impacts, such as reducing vegetation cover and decreasing soil and vegetation water content (Van Leeuwen *et al.*, 2019; Valdes-Abellan *et al.*, 2020; Palacios-Cabrera *et al.*, 2022; Silva *et al.*, 2022). Therefore, lower crop productivity, less water reservoirs, deterioration in the number of herds, increases in the risk of fires are identified (Fadhil, 2011). If the current year is succeeded by one or more dry years, the drought's severity is felt. In addition, a series of consecutive dry years is more severe than a singular drought (Spinoni *et al.*, 2014; Jodar-Abellan *et al.*, 2019). Drought is a lack of precipitation for an extended period, usually a season or more, resulting in water scarcity affecting agricultural or environmental activities (Mishra and Singh, 2010; Cámara-Artigas *et al.*, 2022; Juárez *et al.*, 2022). Thus, drought is a progressive process that begins with a lack of rainfall, expressed as meteorological drought. It can be classified into four categories: meteorological, agricultural, hydrological, and socioeconomic (Eklund and Seaquist, 2015). Meteorological droughts are also the source of hydrological droughts (Spinoni *et al.*, 2014; Jodar-Abellan *et al.*, 2018). Agricultural droughts depict severe decrease in soil water that results in crop failure. Drought can worsen, resulting in a so-called socioeconomic drought. Its prevalence is linked to natural water reserves, and reservoirs constructed by human when storage cannot meet the demand for water (Guo *et al.*, 2019; Boix-Fayos *et al.*, 2020; Eekhout *et al.*, 2020). As a result, if appropriate safeguards are not taken, it will severely impact economies of the affected regions. Drought features must be accurately estimated to plan for optimal water resource usage and agricultural productivity (Kogan and Guo, 2016).

More than 100 drought indices are used to determine drought globally (Jain *et al.*, 2015). Among all the standardized drought indices, McKee *et al.* (1993) presented the Standardized Precipitation Index (SPI), which is widely used to identify drought in various regions throughout the world (Li *et al.*, 2020; Sobral *et al.*, 2019; Stagge *et al.*, 2015; Tsakiris and Vangelis, 2004). SPI is recommended because it only uses precipitation and is straightforward to calculate at various periods. It also characterizes short- and long-term meteorological and agricultural droughts (Golian *et al.*, 2015). The SPI is directly tied to soil water on short durations, but it can also be related to groundwater and reservoir storage on longer timelines (Keyantash, 2018). According to IPCC assessments, the Mediterranean basin, particularly North Africa, is one of the most vulnerable regions to climate change (Wang, 2005). However, there is a scarcity of data on the North African region (UN, 2022; Derdour *et al.*, 2020). Analysis of remote sensing data can support continuity meteorological data and indices by filling gaps that can occur in long time series, as well as providing a wealth of information about vegetation, soil status, and land use, which is frequently used in drought studies to quantify the growth and degradation of various land use items in response to climatic factors (dry and wet periods) and human activities. Therefore, remote sensing became an alternative to collect information that is challenging to obtain by other means. Over the last decade, data from various satellite-based platforms have figured prominently in drought research (e.g., AghaKouchak *et al.*, 2015; West *et al.*, 2019). Furthermore, advancements in algorithm improvement as well as cloud-based processing and storage capacity have significantly expanded the potential application of remote sensing for drought research. In addition to providing an autonomous experimental capability, remote recognizing data can be used to minimize doubts and constrain modeling efforts aimed at drought estimates. During last years, numerous studies have been published on drought monitoring and its ramifications such as desertification, soil loss, sand dune mobility (e.g., AghaKouchak *et al.*, 2015; Bouarfa *et al.*, 2022a; Wardlow *et al.*, 2012; West *et al.*, 2019; Rahdari and Rodríguez-Seijo, 2021; Zhang and Jia, 2013; Ibañez *et al.*, 2022; Cimusa-Kulimushi *et al.*, 2023).

Drought is one of the most concerning manifestations of climate change in Algeria. Several droughts had previously occurred before the start of the twentieth century, in the 1940s, and the 1970s resulting in low harvests, animal losses, and increased food prices (Seltzer, 1946). Droughts in recent years have been even more notable for their geographic scope and ferocity. They were characterized by rainfall shortages that significantly reduced monthly mean flows (Bouabdelli *et al.*, 2020; Habibi *et al.*, 2018; Lazri *et al.*, 2015). In this work, drought episodes in the region of Ain Sefra, which is located in southwest Algeria, were studied using drought indices such as the previously mentioned SPI, the precipitation mean deviation index (MDX), the rainfall index (RI), the Frequency analyses (FI), and the standard deviations Indicator (SDI). These indices were used at various time scales (1, 3, 6, 9, and 12 months) from a database of the only rainfall station situated in the city, over 56 years (1965-2021), summarizing 672 monthly precipitation series. On the other hand, a diachronic study using remote sensing was conducted to reconstruct the evolution of the sand mobility and vegetation cover in Ain Sefra between 1977 and 2017 using the Modified Soil-Adjusted Vegetation Index (MSAVI). This research aims to understand better the impact of climate change and management methods on these vulnerable areas, detect dry and wet periods in Naâma (Argelia), and then assess their trends over time.

## 2. Materials and Methods

### 2.1. Study area

This study was conducted in southwestern Argelia in the Ain Sefra region (Fig. 1: 32°30'00"N / 33°00'0"N and 0°50'0"W / 0°20'0"W), covering an area of 13,409 km<sup>2</sup>, in the high plains of southern Oran. The case study area is located in western Algeria, between the Tell and Saharan Atlases, in the "Ksour Mountains" region, highly affected by droughts (Haddouche *et al.*, 2008). The study area is composed by sets of massifs with complex structures that are elongated and stretched along the general axis of the southwest/north- east fold (Derdour *et al.*, 2020). These structures are generally related to tectonics, lithology, and erosion. They are made up of hard rocks (limestone, dolomitic limestone and

sandstone) of Jurassic age, whose slopes are generally steep (Derdour *et al.*, 2020). Among these folded formations, the Jurassic anticline culminates at 2236 m a.s.l. in a southwest/northeast direction (Derdour *et al.*, 2017a). The study area is situated in the Wilaya of Naâma, mainly occupied by a flat plain. The altitude increases significantly towards the South (1000 to 1330 m a.s.l.). It is riddled with many small basins of different sizes and origin (Sebkha, Dayas, hydro-wind basins locally called Mekmene, Oglat or Haoud). We distinguish between the salty pits (Chott Chergui, Chott El Gharbi, Sebkh de Nâama) and the Dayas and the Mekmenes, where unsalted surface water accumulates (Bouarfa *et al.*, 2022b). Dayas soils are generally deeper compared to encrusted glaciais. The Chotts and the Sebkhas are salty depressions resulting in a steppe with halophytes. Throughout the Algerian steppe and the pre-Saharan region, multiple traces of wind activity increasingly underline the arid facies of the landscape. Therefore, wind is the fundamental element in shaping semi-arid, infertile, and desert landscapes. The hydrographic network in the study area is endorheic (Derdour and Bouanani, 2019). It is poorly developed and often emerges in areas of evaporation such as Dayas or Sebkhas. The valleys are however quite short, not very sinuous, showing a flat bottom and badly drawn banks. This explains the low slope of the river and the presence of endorheic basins (dayas). Hydrologically, the valleys are not perennial and only flow episodically during rainy periods (Derdour *et al.*, 2017a).

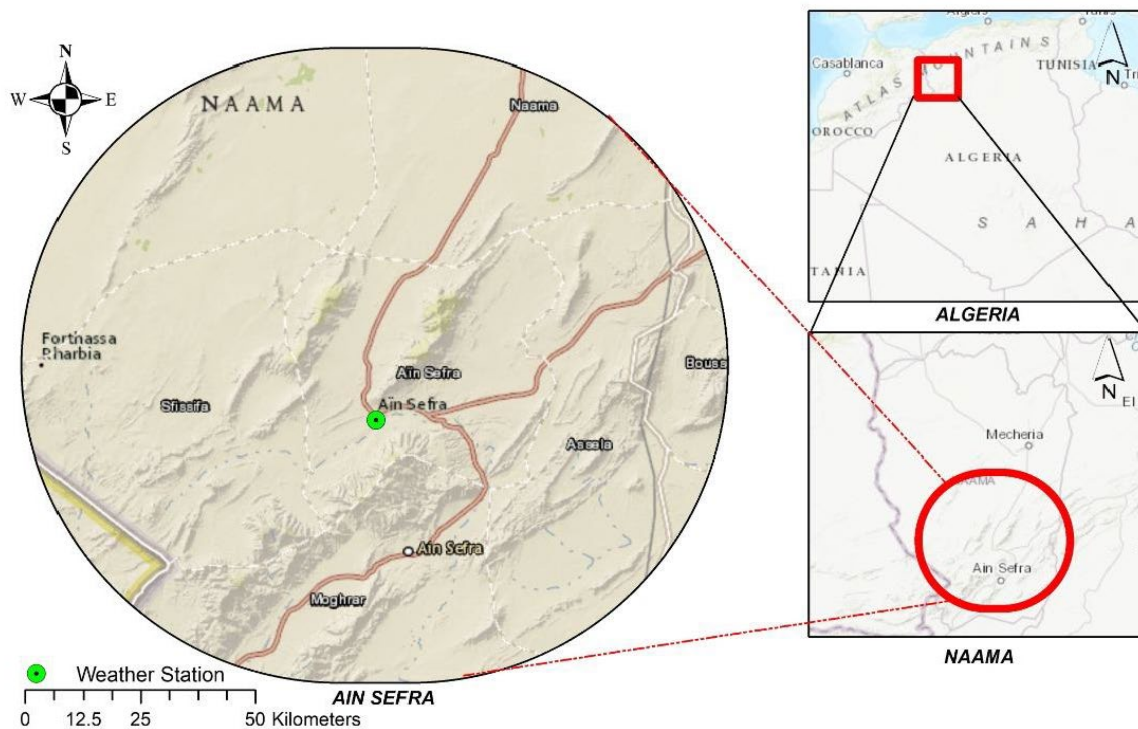


Figure 1. Study area.

## 2.2. Data collection

The precipitation dataset from 1965 to 2021 at Ain Sefra, run by the National Office of Meteorology of Algeria, was used. The climatic data was processed, and the homogeneity of the climatic series was verified. It should be noted that missing data were downloaded from the IOWA State University website (IOWA, 2022). The considered weather station is located at 722729.00 UTMx and 3627490.00 UTM<sub>y</sub> and depicts a mean altitude of 1084 m a.s.l.

Five satellite images type Landsat 2 Multispectral Scanner System were used to get images of the year 1977, Landsat 3 Multispectral Scanner System, and Thematic Mapper (TM) to get images of

the year 1987, Landsat 5 Multispectral Scanner System and Thematic Mapper to get images of the year 1997, Landsat 7 Enhanced Thematic Mapper Plus Instrument to get images of the year 2007, and Landsat 8 Operational Land Imager and Thermal Infrared Sensor to get images of the year 2017 of the study area, downloaded from the US Geological Survey website (USGS, 2022). They allowed for diachronic research in the study area and the detection of changes using remote sensing, a technique for identifying the various states of an object or phenomena when monitored over time. These satellite images from different years (1977, 1987, 1997, 2007, and 2017) were chosen to conduct this comparison study. The selected satellite images were taken in March of every year, around the same time. A post-classification technique performed change detection analysis of multirate satellite images. The Landsat TM data pre-processing in this work contains multiple correction techniques that are carried out in several steps, including radiometric correction, FLAASH atmospheric correction, supervised classification, post-classification, and geometric corrections.

### 2.3. Drought indices

#### 2.3.1. Standardized Precipitation Index (SPI)

The SPI is a multi-scalar stochastic predictor that assesses precipitation deficit during wet and dry spells and allows for drought monitoring on multiple time scales (McKee *et al.*, 1993). This indicator was proposed by the World Meteorological Organization as a jumping-off place for rainfalls monitoring. It has been utilized in numerous prior researches due to its simplicity, and widespread acceptance. The computation is carried out with the help of monthly rainfall data which has been adapted to a probability density function such as gamma over a lengthy period. Any percentile from the chosen distribution model is handled as a percentile on a Gaussian distribution function, and the appropriate Z value is recorded as the SPI value.

The SPI is calculated by fitting a probability density function to the frequency distribution of precipitation accumulated across the time scale of interest. This is done for each month (or any other temporal basis of the raw precipitation time-series as required) and each place in space individually. The normalized normal distribution is then applied to each probability density function. The probability density function of the gamma distribution is as follows (Eq.1):

$$g(x) = \frac{1}{\beta^{\alpha} \Gamma(\alpha)} x^{\alpha-1} e^{-x/\beta} \text{ for } x > 0 \quad (1)$$

where  $x$  is precipitation,  $\alpha > 0$  is the shape  $e$  parameter, and  $\beta > 0$  is the scale parameter.

The gamma probability density function parameters are estimated at the data location for each time scale and observation. To estimate  $\alpha$  and  $\beta$  parameters, maximum likelihood solutions are utilized (Edwards, 1997; Thom, 1966). The SPI is defined as (Eq.2):

$$SPI = \frac{P_i - P_m}{\sigma} \quad (2)$$

where:  $P_i$  is the annual rainfall for a given year (mm),  $P_m$  the mean rainfall (mm), and  $\sigma$  the standard deviation. The data are then used to calculate drought characteristics such as duration, intensity, and severity. Moderate, severe, and extreme drought situations are indicated by ranges of -1.49 to -1.0, -1.5 to -1.99, and  $\leq -2.0$ . Various classifications of drought intensity based on SPI thresholds are available (McKee *et al.*, 1993).

#### 2.3.2. Precipitation Mean Deviation Index (MDX)

The MDX (Eq.3) is the variation between both the annual precipitation level ( $P_i$ ) and the average rainfall level ( $P_m$ ).

$$MDX = P_i - P_m \quad (3)$$

The yearly distribution of precipitation offers immediate information on the variability of rainfall rates. It is easy to distinguish the wet and dry years by comparing it to the series average. It also makes it possible to estimate the precipitation shortage at the year's level and picture and establish the number of shortfall periods and their sequence. A deficit year is one in which the precipitation is less than the mean, and a surplus year is when the standard is exceeded.

### 2.3.3. Rainfall Index (RI)

The RI reflects how much precipitation is collected in comparison to the long-duration mean designed for a certain place and timeframe. The rainfall index  $RI$  is defined as (Eq.4):

$$RI = P_i / P_m \quad (4)$$

In particular, if this ratio is more than one, the year is characterized as wet, and as dry if it is less than one. We have used the difference relative to the norm ( $R_{IM}$ ), to identify rainfall in a lengthy set of rainfall records (Eq.5).

$$R_{IM} = RI - 1 \quad (5)$$

The cumulative of the indices ( $R_{IM}$ ) of successive years makes it possible to identify the main trends by disregarding the slight fluctuations from one year to the next. It is a wet trend when the total of the indexes rises and a dry trend for the opposite scenario (Bergaoui and Alouini, 2002).

### 2.3.4. Frequency analyses (FI)

Frequency analyses are commonly used based on the characteristics of a phenomenon such as droughts. Annual rain is classified in increasing order based on their chance of not surpassing ( $F$ ), which is calculated as follows (Eq.6):

$$F = \left( \frac{r}{N+1} \right) \cdot 100 \quad (6)$$

where  $r$  is the ranking of the year based on an increasing categorization of rainfall quantities;  $N$  is the number of years of monitoring. Years are categorized into five groups of likelihoods of non-exceedance, as shown in Table 1.

Table 1. Classification of frequency.

Class	Frequency
Very dry	$F < 15\%$
Dry	$15\% \leq F < 35\%$
Normal	$35\% \leq F < 65\%$
Wet	$65\% \leq F < 85\%$
Very wet	$85\% \leq F$

### 2.3.5. Standard deviations Indicator (SDI)

This index is measured by considering the annual rainfall mean readings ( $P_m$ ) in relation to the value of standard deviations ( $\sigma$ ) whose formulation is as follows (Eq.7, Bergaoui and Alouini, 2002):

$$\sigma = \left[ \frac{1}{(N-1)} \right] \sum (P_i - P_m)^{1/2} \quad (7)$$

when  $P_i$  is less than  $P_m - \sigma$ , serious droughts are identified. However, if  $P_i$  is a smaller amount than  $P_m - 2\sigma$  the drought is severe, as depicted in Table 2.

Table 2. Drought severity classes.

Type of drought	Comparison criterion
Moderate	$P_m - \sigma < P_i < P_m$
Strong	$P_m - 2\sigma < P_i < P_m - \sigma$
Very strong	$P_i < P_m - 2\sigma$

#### 2.4. Diachronic analysis using Remote Sensing

In this study, we used Landsat satellite images to understand the change observed in sand and vegetation cover. Hence, we tested statistically the "change detection" technique over 40 years (between 1977 and 2017) by using an index that considers soil influence called the Modified Soil-Adjusted Vegetation Index (MSAVI). This index, proposed by Qi et al. (1994), suggests an enhancement to the original soil-adjusted vegetation index (SAVI). In particular, the L-shaped adjustment parameter that characterizes the soil and its vegetation cover rate in the MSAVI is no longer a constant, but it is automatically adjusted to local conditions. This index has been widely used in the low vegetation zone, as in the case of our study area. MSAVI is determined as a ratio of the R (red) and NIR (near infra-red) wavelengths values with an inductive L function utilized to amplify the lessening of soil influences on the flora signal.

Likewise, MSAVI values range from -1 to 1, where i) -1 to 0.2 indicate bare soil; ii) 0.2 to 0.4 is the seed germination stage; and iii) 0.4 to 0.6 is the leaf development stage.

### 3. Results and Discussion

#### 3.1. Drought indices

##### 3.1.1. Standardized Precipitation Index (SPI)

The rainfall index was calculated to characterize precipitation deficiencies at various time periods in a specific location. This analysis, which considers the futility of time, mainly reflects drought's influence on the availability of numerous water supplies. Droughts receive a negative rating, whereas floods receive a positive value. The SPI of the study area was calculated by fitting rainfall series collected over 56 years from 1965 to 2021 (McKee *et al.*, 1993). The chronological variation of the SPI index relative to the station of Ain Sefra shows that the SPI goes through a global deficit trend with the existence of many distinct wet and dry periods (Fig. 2). The values of SPI of the study area ranged from -2.608 to 1.986, where the drought years represent 14.28 % of the series ( $SPI \leq -1.00$ ), the wet years represent 7.14% ( $SPI > 1.00$ ), and the near-normal years ( $-0.99 < SPI < 0.99$ ) represent 78.57%. In addition, three wet periods were identified, 1967 to 1980, 1987 to 1994, and 2006 to 2012, the year 2008 being highly wet ( $SPI = 1.99$ ). In contrast, there were three dry periods, 1980 to 1986, 1994 to 2005, and 2012 to 2021, the year 2016 being arid ( $SPI = -2.61$ ). The most crucial peak for Ain Sefra is negative ( $SPI = -2.61$ ). Throughout Ain Sefra's chronology, floods have frequently been produced by rainy periods after extended periods of dryness, such as the floods of 1990 ( $SPI = 1.71$ ) and floods of 2008 ( $SPI = 1.99$ ). The main statistical parameters of SPI in the study area are: a value of 1.99 to the max positive, -2.61 to the max negative, 0.58 to the mean positive and -0.76 to the mean negative.

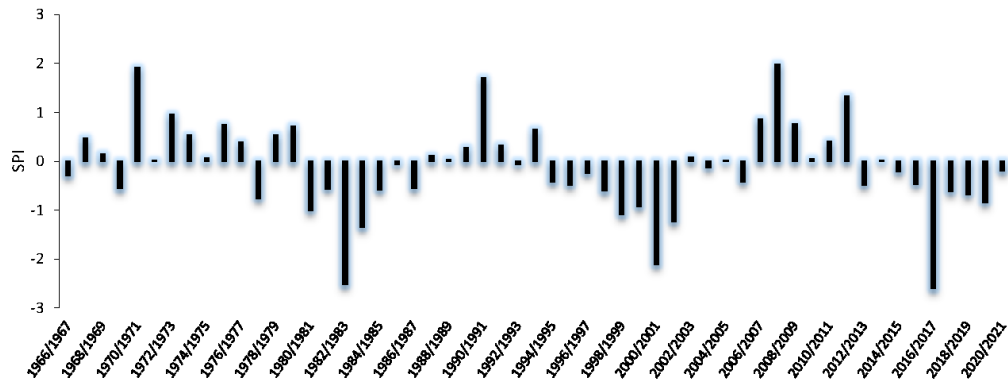


Figure 2. Annual SPI evolution at the study area.

### 3.1.2. Precipitation Mean Deviation Index (MDX)

The computation of the index of the divergence from the average of the rainfall series at the study area (Fig. 3) makes it possible to show that during this long observation period of 56 years (1966-2021), there were 48.2% of surplus years and 51.8 % of deficit years. An essential deficit retained from this rainfall series is  $-146.66$  mm recorded in 2020-2021. It is worth remarking here that there are four sequences of a single isolated dry year (1973, 1977, 1992, 2013), one sequence of two successive dry years (2019 to 2021), and three sequences of more than two subsequent dry years (1980 to 1984, 1986 to 1990, 1995 to 2007). The most extended drought sequence was between 1995 and 2007, with 12 consecutive dry years. During 1980-2001, the overall trend is drought, but this is interspersed with a short period with a wet tendency.

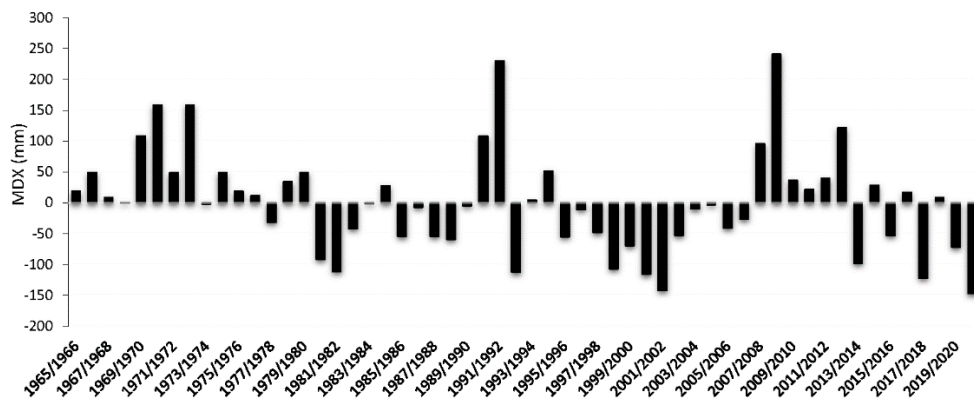


Figure 3. Precipitation Mean Deviation Index at the study area during the monitoring period.

### 3.1.3. Rainfall Index (RI)

The analysis of drought by the RI and cumulative deviations shows an alternation of sequences with a generally dry trend and arrangements with a naturally wet trend (Fig. 4). The RI values at the study area ranged from  $-146.66$  to  $240.33$ , and the values of varied from  $-0.72$  to  $1.19$ . From 1980 to 1990 and from 1992 to 2007, the overall trend is represented by drought. But it is interspersed with short periods with a wet movement, the most important of which extend over consecutive years (1990 to 1992, 1993 to 1995, and 2008 to 2013). This confirms the findings based on the SPI results.

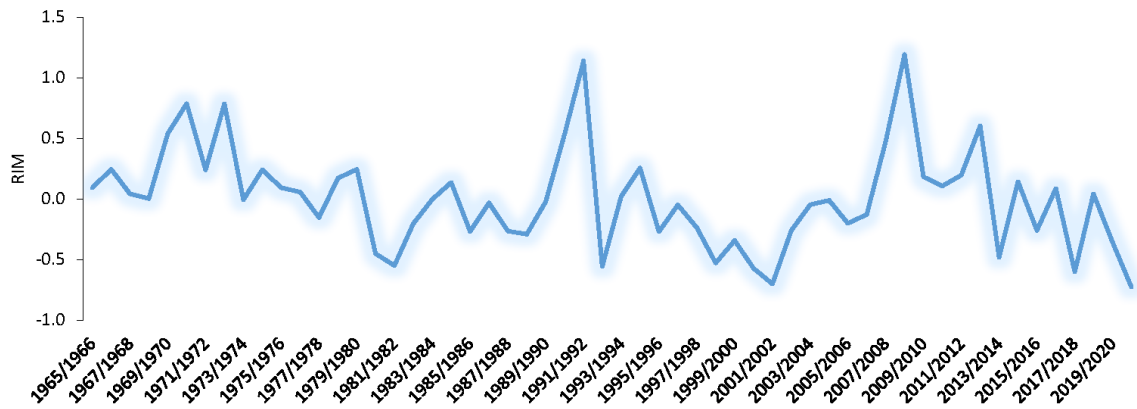


Figure 4. Rainfall Index at the study area during the monitoring period.

### 3.1.4. Standard deviations Indicator (SDI)

The calculation of the deviation indicator from the average of the rainfall series of the station of Ain Sefra (Fig. 5) makes it possible to show rainfall evolution during this long observation period (56 years from 1966 to 2021). Thus, the graphic allows us to distinguish, among the deficit years, 62.50% of years of moderate drought, 10.71% of years of severe drought, and 26.78% of years of very severe drought.

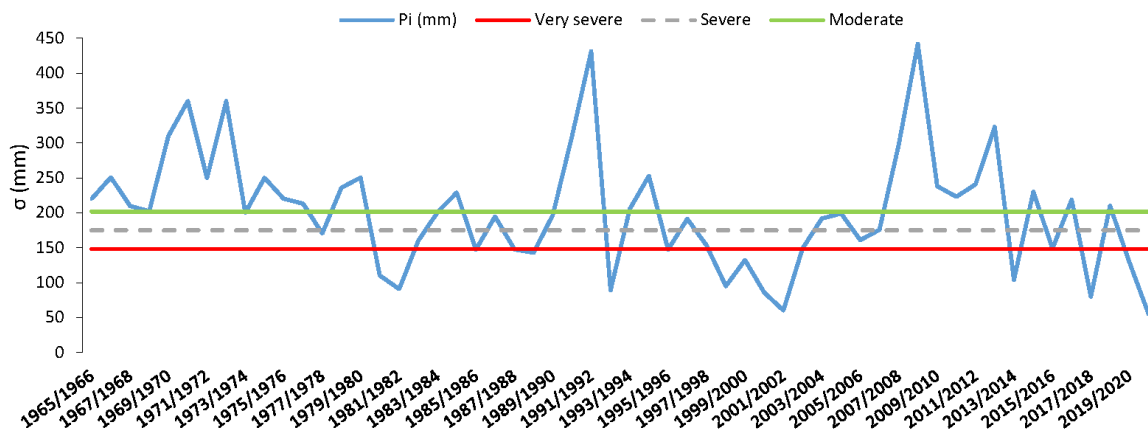


Figure 5. Precipitation Standard Deviation Index at the study area.

### 3.1.5. Frequency analyses

In this study, dry and wet years have been identified with the MDX and the RI. To better specify the degree of drought recorded, we have used other indices such as the frequency analysis. The application of frequency analysis to the rainfall series of the weather station gave us a higher accuracy for standard years than years with deficit and surplus. Thus, Figure 6 represents variations in annual rainfall in the function of the hydrological years by comparison with the different classes of frequencies. For the station of Ain Sefra, over the 56 years of observation: 7 were very dry, 11 were dry, representing a 32.14% of the series, 15 standard years represented a rate of 26.78%, 11 wet years, and 12 were very wet, representing a 41.07% of the series. We conclude that SPI and the frequency analysis indices have nearly the same results and descriptions based on these results. However, the frequency analysis has more detailed explanations, particularly regarding the standard years concerning SPI and MDX indices. Nevertheless, the frequency analysis does not make it possible to identify the overall trends in rainfall at the level of the station studied.

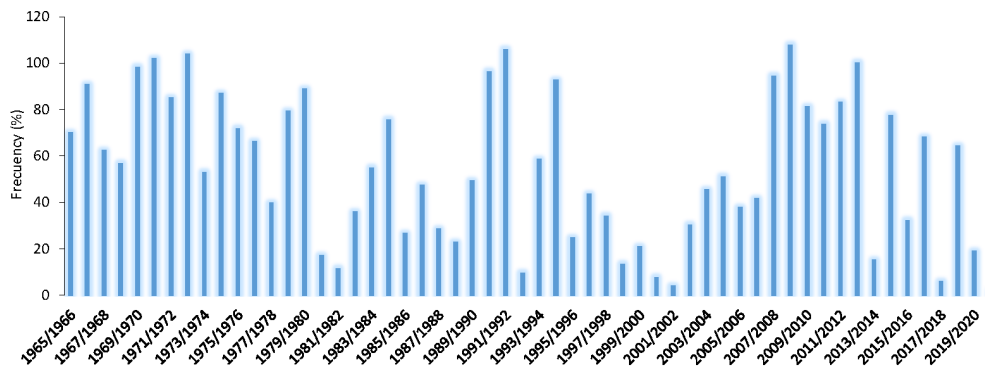


Figure 6. Frequency analysis for the rainfall series at the study area.

### 3.1.6. Persistence of drought

The drought is perceived more intensively if the year in question follows one or more dry years. A series of consecutive dry years is more severe than a single drought. For the station of Ain Sefra, drought, as determined by the SDI, occurred during three sequence periods and represented by 50% of the entire series, one of 12 years (from 1994 to 2006), the other of 7 years (1980 to 1987), and the third of 9 years (from 2012 to 2021). Following the analysis of the dry years determined by the frequency analysis method at the Ain Sefra station, it was found that there were 18 dry years, where six sequences of a single isolated dry year (1985, 1992, 1995, 2013, 2015, 2017), three sequences of two successive dry years (1980 to 1982, 1987 to 1989, 2019 to 2021) and one sequence of six subsequent dry years (1997 to 2003). For the region, the percentage of an isolated dry year is 10.71%. Sequences of consecutive dry years (two or more) represent 21.43%, according to the analysis of rainfall data from the Ain Sefra station, which characterizes the most representative example of the whole area. Through several drought indices, we can conclude that drought is a recurring phenomenon. A summary of different indices used in this study is given in Table 3.

Table 3. Summary indexes for evaluating droughts at the study area from 1965 to 2021.

	Dry years		Isolated dry years		Successive dry years	
	Value	%	Value	%	Value	%
MDX	29	51.78	6	10.71	4	41.07
SPI	8	14.28	3	7.14	1	1.78
RI	29	51.78	6	10.71	4	41.07
FI	18	32.14	6	10.71	4	41.07
SDI	15	26.78	5	8.92	3	26.78

### 3.2. Diachronic analysis using Remote Sensing

Results of the accomplished diachronic analysis are showed with maps plotting the changes obtained from multi-temporal Landsat images (between 1977 and 2017). The calculation of the MSAVI of the satellite images covering the study area for March 1977, 1987, 1997, 2007, and 2017 allowed us to visualize the impact of drought over time (Fig. 7). The confusion matrix was used to evaluate the categorization and plotted in Figures 7 and 8. Thus, the kappa coefficient was employed to measure the classification quality. This matrix indicates the trust level and the main confusion during an image classification (some class pixels can be confused by others). When the kappa coefficient exceeds 0.8 (80%), the classification is considered conventional and relevant. In our study, the kappa value exceeded this threshold of 80% in all the cases (1977: 92.2%; 1987: 96.4%; 1997: 89%; 2007: 83.2%; 2017: 88%). Thus, this statement allowed us to verify our findings. After rigorous examination, it was discovered

that the dynamism of sands in the study area has gone through numerous phases over the five sequences studied (1977, 1987, 1997, 2007, and 2017), ranging from regression to progression. This trend is primarily due to the drought, but other aspects such as wind speed, extensive labor, and overgrazing could also be considered. In general, the sand invasion has increased. This upward trend of sand encroachment has maintained to the present day and represents a serious hazard. Likewise, according to our map examinations, we conclude that the area's sandy accumulations have evolved and become unsteady through time. Maps of the diachronic study have clearly shown that there has been a very significant evolution of sands in terms of area, showing a transition towards the north and the north-east of the study area during the last 56 years (1965-2021), being droughts the main cause from the author's knowledge. In 2017, the sand encroachment massively increased by 286.61% compared with 1977, as in Figure 8, while the vegetation cover category was affected by the type of year, dry or wet. Vegetation cover represented 20.64% of the study area in 2007 in the wet year, where the SPI value was 1.99, and represented only 0.78% of the study area in 1977, where the SPI value was -0.76. The vegetation density decreased considerably in 1997 compared to 1987, owing to consecutive dry years. Table 4 summarizes the evolution of land use components of the study area (1977-2017).

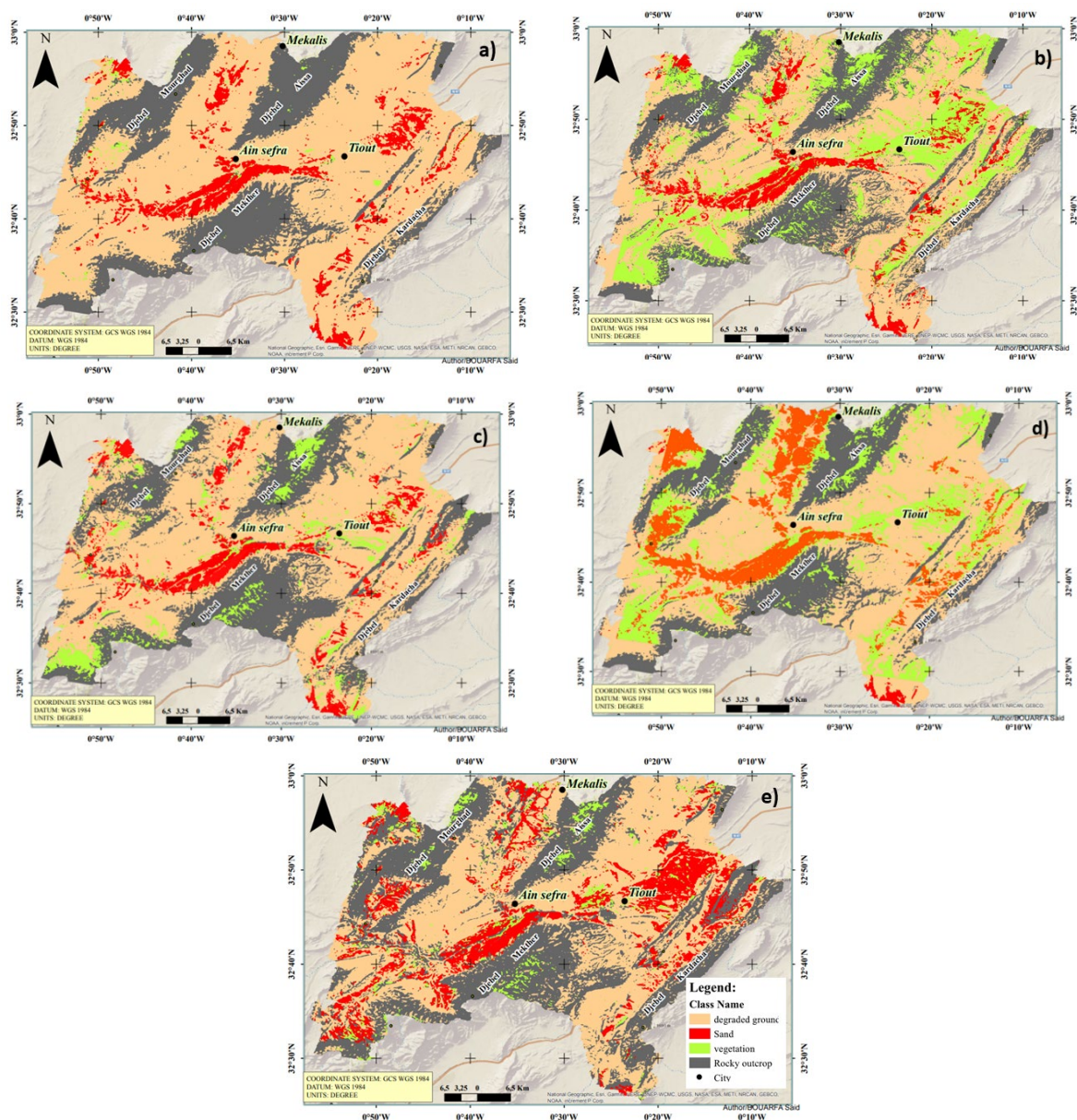


Figure 7. Diachronic Study (a: 1977; b: 1987; c: 1997; d: 2007; e: 2017).

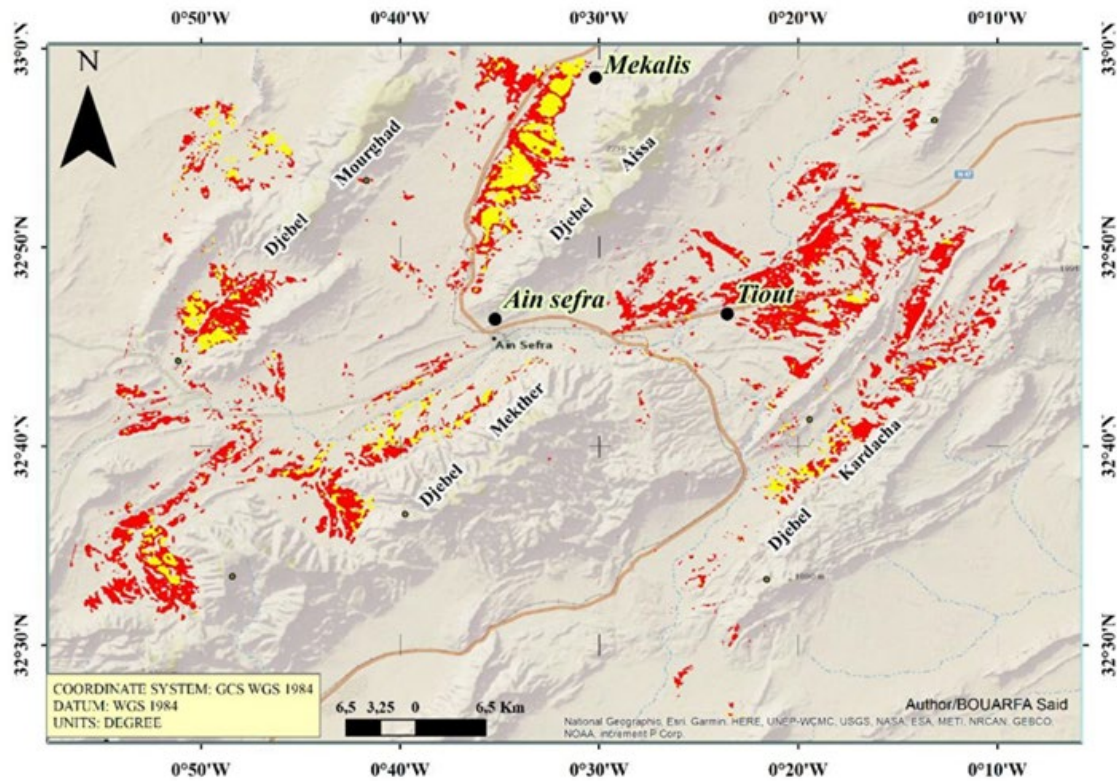


Figure 8. Evolution of sands between 1977 and 2017. Yellow color: new accumulation of sands. Red color: latest dunes higher than 2m.

Table 4. Evolution of land use components of the study area (1977-2017).

Year	Class (%)			
	Sands	Degraded Soils	Outcrops	Vegetation
1977	8.29	63.92	27.01	0.78
1987	11.86	40.71	30.72	16.71
1998	12.2	42.03	39.16	6.61
2007	15.66	25.03	38.67	20.64
2017	23.76	40.47	30.41	5.36

#### 4. Conclusions

This paper assessed the potential change in the Ain Sefra region's climate from 1965 to 2021 using, among others, drought indices and remote sensing. The study area is affected by extreme weather events, from droughts to floods. The drought indices used in this study present suitable pictures and perceptions of drought in the research area. The chronological variation of the SPI index relative to the station of Ain Sefra shows that the SPI goes through a global deficit trend with the existence of many distinct wet and dry periods. The values of SPI in the study area range from -2.608 to 1.986, where the most significant peak is negative. Three consecutive dry periods were identified in the first of 7 years (1980 to 1987), the second of 12 years (from 1994 to 2006), and the third of 9 years (from 2012 to 2021), where the year 2016 is arid with an SPI value of -2.61. Contrariwise, three wet periods were distinguished from 1967 to 1980, 1987 to 1994, and 2006 to 2012, where 2008 was highly more wet (SPI=1.99). Floods are often caused by wet periods after long consecutive dry periods throughout the history of Ain Sefra, such as the floods of 1990 (SPI=1.71) and floods of 2008 (SPI=1.99). The MDX showed that during this long observation period of 56 years (1965-2021) in Ain Sefra, we had recorded 48.2% surplus years and 51.8% deficit years. The rainfall index showed that the overall trend is represented by drought from 1980 to 1990 and 1992 to 2007. Still, it is interspersed with short periods

with a wet movement, the most important of which extend over consecutive years (1990 to 1992, 1993 to 1995, and 2008 to 2013). According to frequency analyses, over the 56 years of observation: 7 were very dry, 11 were dry, representing 32.14% of the series, 15 standard years represented 26.78%, 11 wet years, and 12 were very wet, representing a 41.07% of the series. The results obtained in this study showed that drought is a recurring phenomenon.

A diachronic assessment was used in the study area to monitor droughts between 1977 and 2017. The MSAVI index of the satellite images covering the study area for March of 1977, 1987, 1997, 2007, and 2017 allowed us to visualize the impact of droughts over time. Following our results plotted as maps, key findings emerge that the area of sandy accumulations has increased in extent and becomes unsteady through time. The maps of the diachronic study have clearly shown that there has been a very significant evolution of sands in terms of area with a transition of it towards the north and the north-east. These issues are mainly related with droughts according to the author's knowledge. This upward trend of sand encroachment has continued to the present day and represents a severe hazard. In 2017, the sand encroachment massively increased by 286.61% compared to 1977. The combination of drought indices and remote sensing seems to be most promising, their findings being valuable tools for supervision and assessment supporting decisions of local and regional authorities.

## Acknowledgements

Financial support to perform this study was provided partially by the University Center Salhi Ahmed Naama (Algolia). Antonio Jodar-Abellan acknowledges financial support received from the XTREME Spanish National Project (Ref: PID2019-109381RB-I00/AEI/10.13039/501100011033). In the same way, the authors acknowledge the reviewers and editor of this manuscript whose comments contributed greatly to improve this paper.

## References

- AghaKouchak, A., Farahmand, A., Melton, F., Teixeira, J., Anderson, M., Wardlow, B. D., Hain, C., 2015. Remote sensing of drought: Progress, challenges and opportunities. *Reviews of Geophysics* 53(2), 452-480. <https://doi.org/10.1002/2014rg000456>
- Bergaoui, M., Alouini, A., 2002. Caractérisation de la sécheresse météorologique et hydrologique: cas du bassin versant de Siliana en Tunisie. *Science et changements planétaires/Sécheresse* 12(4), 205-213.
- Boix-Fayos, C., Boerboom, L.G.J, Janssen, R., Martínez-Mena, M., Almagro, M., Pérez-Cutillas, P., Eekhout, J.P.C., Castillo, V., de Vente, J., 2020. Mountain ecosystem services affected by land use changes and hydrological control works in Mediterranean catchments. *Ecosystem Services* 44, 101136. <https://doi.org/10.1016/j.ecoser.2020.101136>
- Bouabdelli, S., Meddi, M., Zeroual, A., Alkama, R., 2020. Hydrological drought risk recurrence under climate change in the karst area of Northwestern Algeria. *Journal of Water Climate Change* 11(S1), 164-188. <https://doi.org/10.2166/wcc.2020.207>
- Bouarfa, S., Abdessamed, D., Okkacha, Y., Almaliki, A.H., Jodar-Abellan, A., Hussein, E.E., 2022a. Sedimentological investigation of the potential origin and provenance of sand deposits in an arid area: a case study of the Ksour Mountains Region in Algeria. *Arabian Journal of Geosciences* 15, 1460. <https://doi.org/10.1007/s12517-022-10697-z>
- Bouarfa, S., Youb, O., Khaouani, B., Berrabah, D., Djoudi, W., 2022b. Assessing Aeolian Sand Potential in Ain Sefra Region-Southwestern of Algeria. *Technium Social Sciences Journal* 30(1), 710-726. <https://doi.org/10.47577/tssj.v30i1.6169>
- Cámara-Artigas, R., de Souza, B.I., de Lima, R.P., 2022. Climatic changes and distribution of plant formations in the state of Paraíba, Brazil. *Cuadernos de Investigación Geográfica* 48, 157-174. <https://doi.org/10.18172/cig.5044>

- Camarasa-Belmonte, A.M., 2021. Flash-flooding of Ephemeral Streams in the Context of Climate Change. *Cuadernos de Investigación Geográfica* 47, 121-142. <https://doi.org/10.18172/cig.4838>
- Corwin, D.L., 2021. Climate change impacts on soil salinity in agricultural areas. *European Journal of Soil Science* 72(2), 842-862. <https://doi.org/10.1111/ejss.13010>
- Cimusa-Kulimushi, L., Bigabwa-Bashagaluke, J., Prasad, P., Heri-Kazi, A.B., Lal Kushwaha, N., Masroor, M.D., Choudhari, P., Elbeltagi, A., Sajjad, H., Mohammed, S., 2023. Soil erosion susceptibility mapping using ensemble machine learning models: A case study of upper Congo River sub-basin. *Catena* 222, 106858. <https://doi.org/10.1016/j.catena.2022.106858>
- Derdour, A., Bouanani, A. 2019. Coupling HEC-RAS and HEC-HMS in rainfall–runoff modeling and evaluating floodplain inundation maps in arid environments: case study of Ain Sefra city, Ksour Mountain. SW of Algeria. *Environmental Earth Sciences* 78(19), 1-17. <https://doi.org/10.1007/s12665-019-8604-6>
- Derdour, A., Bouanani, A., Babahamed, K., 2017a. Floods typology in semiarid environment: Case of Ain Sefra watershed (Ksour mountains, Saharian atlas, SW of Algeria). *Journal of Fundamental and Applied Sciences* (29), 283-299. <https://doi.org/10.4314/JFAS.V10I3.29>
- Derdour, A., Bouanani, A., Babahamed, K., 2017b. Hydrological modeling in semi-arid region using hec-hms model. Case study in Ain Sefra watershed, Ksour mountains (sw-Algeria). *Journal of Fundamental and Applied Sciences* 9(2), 1027-1049. <http://dx.doi.org/10.4314/jfas.v9i2.27>
- Derdour, A., Mahamat Ali, M. M., Chabane Sari, S. M. 2020. Evaluation of the quality of groundwater for its appropriateness for drinking purposes in the watershed of Naama, SW of Algeria, by using water quality index (WQI). *SN Applied Sciences* 2(12), 1-14. <https://doi.org/10.1007/s42452-020-03768-x>
- Edwards, D.C., Thomas, M.B., 1997. *Characteristics of 20th century drought in the United States at multiple time scales*. Report. Colorado State University, Fort Collins, USA. Available at: <https://mountainscholar.org/handle/10217/170176>
- Eekhout, J.P.C., Boix-Fayos, C., Pérez-Cutillas, P., de Vente, J., 2020. The impact of reservoir construction and changes in land use and climate on ecosystem services in a large Mediterranean catchment. *Journal of Hydrology* 590, 125208. <https://doi.org/10.1016/j.jhydrol.2020.125208>
- Eekhout, J.P.C., Millares-Valenzuela, A., Martínez-Salvador, A., García-Lorenzo, R., Pérez-Cutillas, P., Conesa-García, C., de Vente, J., 2021. A process-based soil erosion model ensemble to assess model uncertainty in climate-change impact assessments. *Land Degradation and Development* 32, 2409-2422. <https://doi.org/10.1002/ldr.3920>
- Eklund, L., Seaquist, J. 2015. Meteorological, agricultural and socioeconomic drought in the Duhok Governorate, Iraqi Kurdistan. *Natural Hazards* 76(1), 421-441. <https://doi.org/10.1007/s11069-014-1504-x>
- Fadhil, A.M., 2011. Drought mapping using Geoinformation technology for some sites in the Iraqi Kurdistan region. *International Journal of Digital Earth* 4(3), 239-257. <https://doi.org/10.1080/17538947.2010.489971>
- Golian, S., Mazdiyasi, O., AghaKouchak, A., 2015. Trends in meteorological and agricultural droughts in Iran. *Theoretical Applied Climatology* 119(3), 679-688. <https://doi.org/10.1007/s00704-014-1139-6>
- Guo, Y., Huang, S., Huang, Q., Wang, H., Fang, W., Yang, Y., Wang, L., 2019. Assessing socioeconomic drought based on an improved Multivariate Standardized Reliability and Resilience Index. *Journal of Hydrology* 568, 904-918. <https://doi.org/10.1016/j.jhydrol.2018.11.055>
- Habibi, B., Meddi, M., Torfs, P. J., Remaoun, M., Van Lanen, H. A., 2018. Characterisation and prediction of meteorological drought using stochastic models in the semi-arid Chélif–Zahrez basin (Algeria). *Journal of Hydrology: Regional Studies* 16, 15-31. <https://doi.org/10.1016/j.ejrh.2018.02.005>
- Haddouche, I., Toutain, B., Saidi, S., Mederbal, K., 2008. How to reconcile the development of steppe populations and the fight against desertification? Case of the wilaya of Nâama (Algeria). *Food and Agricultural Organization of the United Nations* 7 (3): 25-31. <https://agris.fao.org/agris-search/search.do?recordID=QC2013000069>

- Ibañez, J., Gartzia, R., Alcalá, F.J., Martínez-Valderrama, J., 2022. The Importance of Prevention in Tackling Desertification: An Approach to Anticipate Risks of Degradation in Coastal Aquifers. *Land* 11, 1626. <https://doi.org/10.3390/land11101626>
- IOWA, 2022. IOWA State University, IOWA Environmental Mesonet: ASOS-AWOS-METAR Data Download. Retrieved from [https://mesonet.agron.iastate.edu/request/download.phtml?network=DZASOS&fbclid=IwAR2kyKYKq2gy98a2tBKVSHzIKwHSXgdjovmDHQOdSl\\_8wmgbkwcmKmmr9YA](https://mesonet.agron.iastate.edu/request/download.phtml?network=DZASOS&fbclid=IwAR2kyKYKq2gy98a2tBKVSHzIKwHSXgdjovmDHQOdSl_8wmgbkwcmKmmr9YA)
- Jain, V.K., Pandey, R.P., Jain, M.K., Byun, H.R., 2015. Comparison of drought indices for appraisal of drought characteristics in the Ken River Basin. *Weather Climate Extremes* 8, 1-11 <https://doi.org/10.1016/j.wace.2015.05.002>
- Jodar-Abellan, A., Ruiz, M., Melgarejo, J., 2018. Climate change impact assessment on a hydrologic basin under natural regime (SE, Spain) using a SWAT model. *Revista Mexicana de Ciencias Geológicas* 35 (3), 240-253. <http://dx.doi.org/10.22201/cgeo.20072902e.2018.3.564>
- Jodar-Abellan, A., Fernández-Aracil, P., Melgarejo-Moreno, J., 2019. Assessing Water Shortage through a Balance Model among Transfers, Groundwater, Desalination, Wastewater Reuse, and Water Demands (SE Spain). *Water* 11 (5): 1009-1027. <https://doi.org/10.3390/w11051009>
- Juárez, O., Corbat, M.C., Fucks, E., 2022. Evolución y dinámica geomorfológica de la cuenca del río Amarillo, en el Sistema del Famatina (La Rioja, Argentina). *Revista Mexicana de Ciencias Geológicas* 39, 1. 54-70. <http://dx.doi.org/10.22201/cgeo.20072902e.2022.1.1637>
- Keyantash, J., 2018. *The Climate Data Guide: Standardized Precipitation Index (SPI)*. Retrieved from <https://climatedataguide.ucar.edu/climate-data/standardized-precipitation-index-spi>
- Kogan, F., Guo, W., 2016. Early twenty-first-century droughts during the warmest climate. *Geomatics, Natural Hazards Risk* 7(1), 127-137. <https://doi.org/10.1080/19475705.2013.878399>
- Lazri, M., Ameer, S., Brucker, J. M., Lahdir, M., Schad, M., 2015. Analysis of drought areas in northern Algeria using Markov chains. *Journal of Earth System Science* 124(1), 61-70. <https://doi.org/10.1007/s12040-014-0500-6>
- Li, L., She, D., Zheng, H., Lin, P., Yang, Z.L., 2020. Elucidating diverse drought characteristics from two meteorological drought indices (SPI and SPEI) in China. *Journal of Hydrometeorology* 21(7), 1513-1530. <https://doi.org/10.1175/jhm-d-19-0290.1>
- Malhi, G.S., Kaur, M., Kaushik, P., 2021. Impact of climate change on agriculture and its mitigation strategies: A review. *Sustainability* 13(3), 1318. <https://doi.org/10.3390/su13031318>
- McKee, T.B., Doesken, N.J., Kleist, J., 1993. The relationship of drought frequency and duration to time scales. *Eighth Conference on Applied Climatology*. 17-22. California. Available at: [https://www.droughtmanagement.info/literature/AMS\\_Relationship\\_Drought\\_Frequency\\_Duration\\_Time\\_Scales\\_1993.pdf](https://www.droughtmanagement.info/literature/AMS_Relationship_Drought_Frequency_Duration_Time_Scales_1993.pdf)
- Mendoza-Uribe, I., 2022. Identification of changes in the rainfall regime in Chihuahua's state (México). *Cuadernos de Investigación Geográfica* 48, 111-132. <https://doi.org/10.18172/cig.5049>
- Mishra, A.K., Singh, V.P. 2010. A review of drought concepts. *Journal of Hydrology* 391(1-2), 202- 216. <https://doi.org/10.1016/j.jhydrol.2010.07.012>
- Niñerola, A., Ferrer-Rullan, R., Vidal-Suñé, A., 2020. Climate change mitigation: Application of management production philosophies for energy saving in industrial processes. *Sustainability* 12(2), 717. <https://doi.org/10.3390/su12020717>
- Oliveira-Santos, N., Souza-Machado, R.A., Lois-González, R.C., 2022. Identification of levels of anthropization and its implications in the process of desertification in the Caatinga biome (Jeremoabo, Bahia-Brazil). *Cuadernos de Investigación Geográfica*, 48. 41-57. <https://doi.org/10.18172/cig.5212>
- Palacios-Cabrera, T.A., Valdés-Abellán, J., Jódar-Abellán, A., Rodrigo-Comino, J., 2022. Land-use changes and precipitation cycles to understand hydrodynamic responses in semiarid Mediterranean karstic

- watersheds. *Science of the Total Environment* 819 (153182), 1-12. <https://doi.org/10.1016/j.scitotenv.2022.153182>
- Qi, J., Chehbouni, A., Huete, A.R., Kerr, Y.H., Sorooshian, S., 1994. A modified soil adjusted vegetation index. *Remote Sensing of Environment* 48(2), 119-126. [https://doi.org/10.1016/0034-4257\(94\)90134-1](https://doi.org/10.1016/0034-4257(94)90134-1)
- Rahdari, M.R., Rodríguez-Seijo, A., 2021. Monitoring Sand Drift Potential and Sand Dune Mobility over the Last Three Decades (Khartouran Erg, Sabzevar, NE Iran). *Sustainability* 13, 9050. <https://doi.org/10.3390/su13169050>
- Ripple, W.J., Wolf, C., Newsome, T.M., Gregg, J.W., Lenton, T.M., Palomo, I., Duffy, P.B., 2021. World scientists's warning of a climate emergency 2021. *BioScience* 71(9), 894-898. <https://doi.org/10.1093/biosci/biz088>
- Rodrigo-Comino, J., Salvia, R., Egidi, G., Salvati, L., Giménez-Morera, A., Quaranta, G., 2022. Desertification and Degradation Risks vs Poverty: A Key Topic in Mediterranean Europe. *Cuadernos de Investigación Geográfica* 48 (1), 23-40. <https://doi.org/10.18172/cig.4850>
- Seltzer, P., 1946. *Le climat de l'Algérie*. Inst. Météor. et de phys-du globe. Univ. Alger. 219 pag. Available at: [https://www.scirp.org/\(S\(czeh2tfqyw2orz553k1w0r45\)\)/reference/ReferencesPapers.aspx?ReferenceID=1268152](https://www.scirp.org/(S(czeh2tfqyw2orz553k1w0r45))/reference/ReferencesPapers.aspx?ReferenceID=1268152).
- Silva, L.F., de Souza, B.I., Cámara, A.R., 2022. Identification of desertified and preserved areas in a conservation unit in the state of Paraíba-Brazil. *Cuadernos de Investigación Geográfica* 48(1), 59-78. <https://doi.org/10.18172/cig.5098>
- Sobral, B.S., de Oliveira-Junior, J.F., de Gois, G., Pereira-Júnior, E.R., de Bodas Terassi, P.M., Muniz-Júnior, J.G.R., Zeri, M., 2019. Drought characterization for the state of Rio de Janeiro based on the annual SPI index: trends, statistical tests and its relation with ENSO. *Atmospheric Research*, 220, 141-154. <https://doi.org/10.1016/j.atmosres.2019.01.003>
- Spinoni, J., Naumann, G., Carrao, H., Barbosa, P., Vogt, J., 2014. World drought frequency, duration, and severity for 1951–2010. *International Journal of Climatology*, 34(8), 2792-2804. <https://doi.org/10.1002/joc.3875>
- Stagge, J.H., Tallaksen, L.M., Gudmundsson, L., Van Loon, A.F., Stahl, K., 2015. Candidate distributions for climatological drought indices (SPI and SPEI). *International Journal of Climatology*, 35(13), 4027-4040. <https://doi.org/10.1002/joc.4267>
- Tahir, F., Ajjur, S.B., Serdar, M.Z., Al-Humaiqani, M., Kim, D., Al-Thani, S.K., Al-Ghamdi, S.G., 2021. *Qatar Climate Change Conference 2021: A Platform for addressing key climate change topics facing Qatar and the world*. Report available at: [https://www.academia.edu/66926850/Qatar\\_Climate\\_Change\\_Conference\\_2021\\_A\\_Platform\\_for\\_addressing\\_key\\_climate\\_change\\_topics\\_facing\\_Qatar\\_and\\_the\\_world](https://www.academia.edu/66926850/Qatar_Climate_Change_Conference_2021_A_Platform_for_addressing_key_climate_change_topics_facing_Qatar_and_the_world)
- Thom, H.C.S., 1966. Some methods of climatological analysis. World Meteorological Organization. *Technical Note* n° 81, 69 pages. Available at: [https://library.wmo.int/doc\\_num.php?explnum\\_id=1961](https://library.wmo.int/doc_num.php?explnum_id=1961)
- Tsakiris, G., Vangelis, H., 2004. Towards a drought watch system based on spatial SPI. *Water Resources Management* 18(1), 1-12. <https://doi.org/10.1023/b:warm.0000015410.47014.a4>
- UN, 2022. *Provisional State of the Global Climate 2022*. United Nations (UN). 60 pages. Report available at: <https://www.un.org/en/climatechange/reports>
- USGS, 2022. The USGS *Global Visualization Viewer (GloVis)*, *Landsat Data*. Retrieved from <https://glovis.usgs.gov/>
- Valdes-Abellán, J., Pardo, M.A., Jodar-Abellan, A., Pla, C., Fernandez-Mejuto., M. 2020. Climate change impact on karstic aquifer hydrodynamics in southern Europe semi-arid region using the KAGIS model. *Science of the Total Environment* 723 (138110), 1-9. <https://doi.org/10.1016/j.scitotenv.2020.138110>
- Van Leeuwen, C.C.E., Cammeraat, E.L.H., de Vente, J., Boix-Fayos, C., 2019. The evolution of soil conservation policies targeting land abandonment and soil erosion in Spain: A review. *Land Use Policy* 83, 174-186. <https://doi.org/10.1016/j.landusepol.2019.01.018>

- Wang, G., 2005. Agricultural drought in a future climate: results from 15 global climate models participating in the IPCC. 4<sup>th</sup> Assessment. *Climate dynamics* 25(7), 739-753. <https://doi.org/10.1007/s00382-005-0057-9>
- Wardlow, B.D., Anderson, M.C., Verdin, J.P., 2012. *Remote sensing of drought: Innovative monitoring approaches*. Publisher CRC Press. 484 pages. Available at: <https://www.routledge.com/Remote-Sensing-of-Drought-Innovative-Monitoring-Approaches/Wardlow-Anderson-Verdin/p/book/9781138075207#>
- West, H., Quinn, N., Horswell, M., 2019. Remote sensing for drought monitoring & impact assessment: Progress, past challenges and future opportunities. *Remote Sensing of Environment* 232, 111291. <https://doi.org/10.1016/j.rse.2019.111291>
- Wilhite, D.A., 2000. Drought as a natural hazard: concepts and definitions. In Donald A. Wilhite (Ed.), *Drought: A Global Assessment*, pp. 3–18. Available at: <https://digitalcommons.unl.edu/droughtfacpub/69/>
- Zhang, A., Jia, G., 2013. Monitoring meteorological drought in semiarid regions using multi-sensor microwave remote sensing data. *Remote Sensing of Environment*, 134, 12-23. <https://doi.org/10.1016/j.rse.2013.02.023>





## SOIL EROSION DUE TO RAINFALL AND THE IMPACTS OF CLIMATE CHANGE IN AN ANDEAN HIGHLAND IN COLOMBIA

PEDRO SIMÓN LAMPREA-QUIROGA<sup>1\*</sup>

OMAR JARAMILLO-RODRÍGUEZ<sup>2</sup>

WLADIMIR MEJÍA AYALA<sup>3</sup>

<sup>1</sup>*Forestry engineer, PhD in Geography; Independent investigator; Postal address: 111321000, Bogota, Colombia.*

<sup>2</sup>*Geographer, MSc in Geography; Independent investigator; Postal address: 111211, Bogotá, Colombia.*

<sup>3</sup>*Agroforestry engineer, PhD in Geography; Pedagogical and Technological University of Colombia (UPTC) in agreement with the Agustín Codazzi Geographic Institute (IGAC). Postal address: 101221, Bogotá, Colombia.*

**ABSTRACT.** Trends and median slope of daily rainfall that can affect rainfall aggressiveness and cause erosion in the Bogotá - Duitama corridor were studied. For this, the daily records of 26 stations (35 years, from 1980 to 2014) were evaluated, using the Sen's statistic and the Mann-Kendall test with confidence levels higher than 90%. The studied area covered about 8,100 km<sup>2</sup>, located between 2,100 and 3,300 m a.s.l. in the Colombian Andes. Four stations with positive trends in median annual rainfall were found (from 6.90 mm/year to 28.80 mm/year) and one station with a decrease in median rainfall of -6.86 mm/year. In order to analyze the pluvial aggressiveness as the main agent of soil erosion, the Modified Fournier Indices (MFI) were generated for periods of 10 days. With the maximum decadal Modified Fournier Indices (MFI<sub>dmax</sub>) of each year, it was possible to establish the median positive trend (Sen) of rainfall aggressiveness in five stations and three stations with negative trends. Through the correlation between the degree of erosion with the square of the decadal average maximum values of each year (MFI<sub>dmax</sub><sup>2</sup>) and the negative annual precipitation, a coefficient of determination (R<sup>2</sup>) greater than 0.50 was found. The validation of MFI<sub>dmax</sub><sup>2</sup> to explain the degree of soil erosion is a new useful methodology for land use planning and monitoring. In this way, developing countries have the possibility of using a tool to face the processes of pluvial erosion, vulnerability and adaptation to climate change.

### *Erosión del suelo por lluvias e impactos del cambio climático en un altiplano andino en Colombia*

**RESUMEN.** Se estudiaron las tendencias y la mediana de la pendiente de las lluvias diarias que pueden afectar la agresividad de las lluvias y causar erosión en el corredor Bogotá - Duitama. Para ello, se evaluaron los registros diarios de 26 estaciones (35 años, de 1980 a 2014), utilizando el estadístico de Sen y la prueba de Mann-Kendall con niveles de confianza superiores al 90%. El área de estudio abarcó alrededor de 8.100 km<sup>2</sup>, ubicada entre los 2.100 y 3.300 m s. n. m. en los Andes colombianos. Se encontraron cuatro estaciones con tendencias positivas en la precipitación media anual (de 6,90 mm/año a 28,80 mm/año) y una estación con una disminución en la precipitación media de -6,86 mm/año. Para analizar la agresividad pluvial como principal agente de erosión del suelo, se generaron los Índices de Fournier Modificado (IFM) para periodos de 10 días. Con los Índices de Fournier

Modificados ( $IFM_{dmax}$ ) máximos decenales de cada año, fue posible establecer la mediana de la tendencia positiva (Sen) de la agresividad de la lluvia en cinco estaciones y tres estaciones con tendencias negativas. Mediante la correlación entre el grado de erosión con el cuadrado de los valores máximos medios decadales de cada año ( $MFI_{dmax}^2$ ) y la precipitación anual negativa, se encontró un coeficiente de determinación ( $R^2$ ) superior a 0,50. La validación de  $IFM_{dmax}^2$  para explicar el grado de erosión del suelo es una nueva metodología útil para la planificación y el seguimiento del uso del suelo. De esta manera, los países en desarrollo tienen la posibilidad de utilizar una herramienta para enfrentar los procesos de erosión pluvial, vulnerabilidad y adaptación al cambio climático.

**Keywords:** Climate trends, rainfall aggressiveness, decadal modified Fournier index, Mann-Kendall.

**Palabras clave:** Tendencias climáticas, agresividad pluvial, índice de Fournier Modificado decadal, Mann-Kendall.

Received: 24 February 2023

Accepted: 28 September 2023

\***Corresponding author:** Pedro Simón Lamprea-Quiroga, Postal address: 111321000, Bogota, Colombia. E-mail address: pslamprea@yahoo.com

## 1. Introduction

With the global predictions projected for the year 2070 by Borrelli *et al.* (2020), based on a semi-empirical modelling approach and the Revised Universal Soil Loss Equation (RUSLE), soil erosion rates of  $43 \cdot 10^9$  (+9.2 to -7) Mg yr<sup>-1</sup> are predicted, with respect to a baseline of 2015. These projections for all global dynamics scenarios indicate a trend towards a more vigorous hydrological cycle (extreme values), which could increase global water erosion from 30% to 66 %. For their part, Arias-Muñoz *et al.* (2023) in the middle-upper basin of the Mira river, in the Andes of Ecuador, on the border with Colombia, estimated an average erosion rate of 32 t/ha/year, which can reach a maximum value of 812 t/ha/year.

Studies carried out by the Institute of Hydrology, Meteorology and Environmental Studies (IDEAM *et al.*, 2015), indicate that 40% of the territory of Colombia presents some degree of erosion. The problem is especially relevant due to the large proportion of affected soils with some degree of erosion in the departments of Cundinamarca (80.3% of 23,984 km<sup>2</sup>) and Boyacá (72.1% of 23,175 km<sup>2</sup>). Severe erosion covers 6.8% of the department of Boyacá, while 5% occurs in the department of Cundinamarca. Due to erosion in the Colombian Andes, this soil degradation has been affecting more than 90% of the territory with agricultural vocation, which leads to the deterioration of the peasant productive base.

Additionally, the impacts of climate change, whose effects could initially be seen in rainfall erosion, may be related to the variations in rainfall patterns and the increase in winds, thus affecting drought. However, although some of the poor moisture conditions can be partially offset by heavy rains, erosion can affect soil and water resources due to increased storms (Basher *et al.*, 2012).

For their part, Almagro *et al.* (2017) argue that due to the variability and changes in rainfall, it is important to consider that the impacts of climate change on the erosivity of rainfall can lead to processes of greater soil degradation. Therefore, it is critical to identify ways and methods of how the country can adapt itself, reduce its vulnerability, and increase its resilience towards this phenomenon. For these reasons, the present study focuses on developing simple and practical methods with available

daily precipitation data, which allow for improving soil conservation measures and adaptation processes to changes in rain erosivity. Likewise, it is worth taking into account that, although other authors (di Lena *et al.*, 2021) studied the trend of the Modified Fournier Index (MFI), no studies were found with the maximum annual values of MFI calculated for 10 days; together with its verification with the degree of soil erosion for the same period studied through regression equations.

However, despite the multiple scenarios evaluated and the numerous methods and models to assess erosion, it is not clear how to quantify the impact of climate change on soil erosion (Xiaofei *et al.*, 2021) and select the most appropriate erosion model for the Andean territory. Therefore, there is little knowledge of the implications of the model's conceptualization on projected soil erosion rates under climate change (Eekhout and de Vente, 2020).

Additionally, it is necessary to take into account that the soil can be affected by different rainfall regimens and intensities, which should be studied through indices developed by the institutions with the available information. Similarly, although from the review of previous studies, it has not been possible to establish any clear association of erosion with climate change, further research should be carried out based on the different ways environmental sustainability is impacted. This situation leads to the need for a better understanding of the benefit of the soils in climate regulation and ecosystem services (Lal *et al.*, 2021).

Based on the above, the objective was to determine the existence or absence of changes or trends in rainfall that may lead to soil erosion; with the hypothesis, in which: there is a relationship of soil erosion with the trend or change in the indices of pluvial aggressiveness.

## **2. Materials and methods**

### *2.1. Study area*

The study area was delimited to the rural corridor between Bogotá (the capital of Colombia in the department of Cundinamarca) and Duitama (the northeast city of the department of Boyacá), a territory that contains the representative customs of the Altiplano Cundiboyacense in terms of their agricultural practices (Lamprea Quiroga and Sanabria Marin, 2020). The shape of the land corresponds to a flat to gently undulating relief of the Colombian Andes, derived from water accumulation processes in lakes and swamps, with subsequent sedimentation processes from its steep edges; along the Bogotá, Suárez and Chicamocha rivers. This plateau also presents the largest population process in Colombia (Instituto Geográfico Agustín Codazzi [IGAC], 2014)

The corridor presents a relative geomorphological homogeneity with a gradual decline (fundamental to studying pluvial erosion and not making the analysis more complex with mass removal), over an altitudinal range of 2,100 to 3,300 meters above sea level. The main crops are potatoes, fruit trees and vegetables. Livestock is pasture-fed.

The land cover is dominated by agricultural activities (58%) and forests (29%). The soils belong to the order Entisols, Inceptisols and Andisols. The minimum temperatures oscillate between 6.5 to 11°C, and the maximum between 12 and 18 °C. (Instituto de Hidrología *et al.*, 2015). In the department of Cundinamarca, there are 28 municipalities (4,252 km<sup>2</sup>) and 32 in Boyacá (3,847 km<sup>2</sup>), covering an area close to 8,100 km<sup>2</sup>, approximately 170 km long by 47 km wide (Fig. 1).

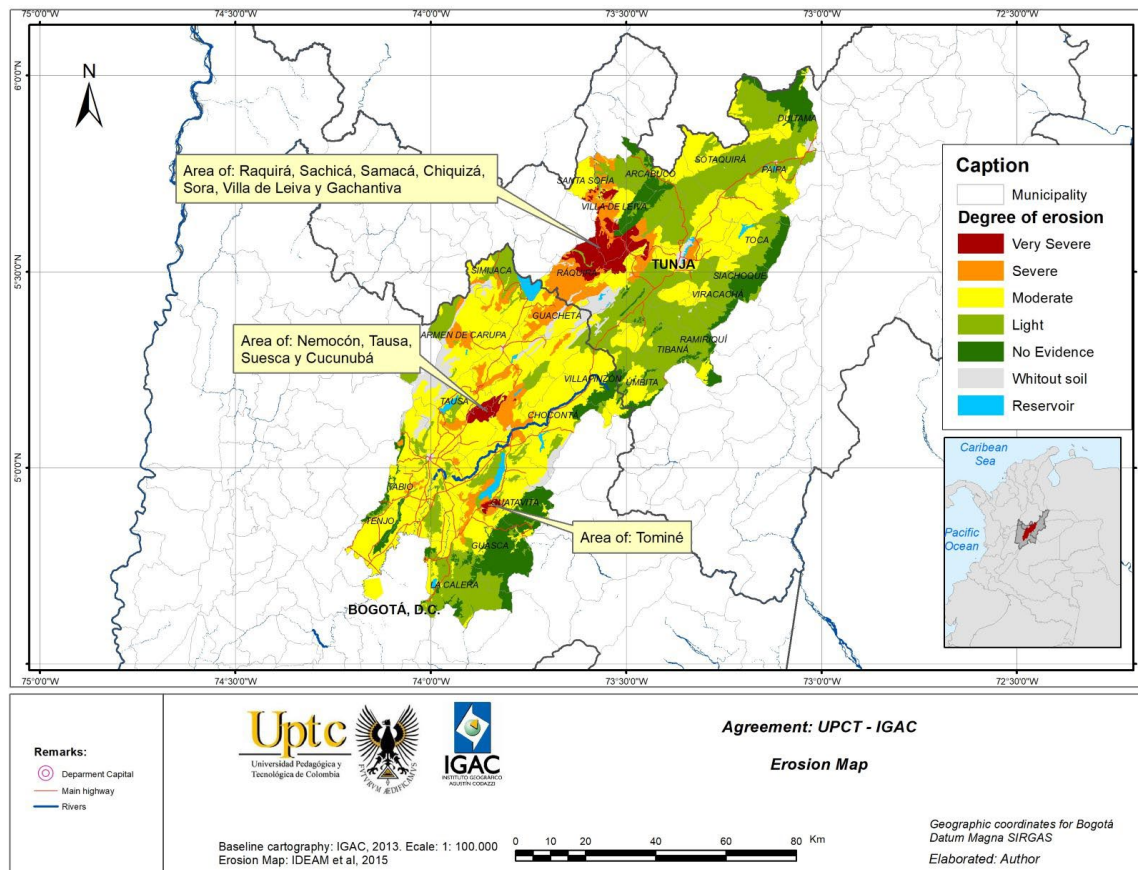


Figure 1. Distribution of the degree of erosion. Source: Own elaboration based on Instituto de Hidrología *et al.* (2015).

## 2.2. Erosion

The national study of soil degradation by erosion in Colombia (Instituto de Hidrología -IDEAM- *et al.*, 2015) provided reference information on the erosive process. In IDEAM *et al.* (2015, pp. 23-43) the methodological development is described. With this, the study area's classification and distribution of eroded surfaces were developed. Figure 1 shows the degree of very severe erosion in red. Very severe erosion, in Cundinamarca, affects the municipalities of Guatavita, Nemocón, Tausa, Suesca, Cucunubá and Guasca (between 240 and 1,080 ha), resulting in a total area close to 5,600 ha (1.3%) of the area study. This surface increases to more than 9% of the department of Cundinamarca, adding the areas with severe erosion (orange colour). In Boyacá, very severe erosion is found (between 400 and 7,120 ha) in the municipalities of Ráquirá, Sáchica, Samacá, Chíquiza, Sora, Villa de Leyva, Gachantivá, Santa Sofía and Cucaita, which together add up to 20,570 ha (5.5 %). If severe erosion is added, it reaches about 12% affectation in the department of Boyacá.

## 2.3. Data source

### 2.3.1. Pluviometry

The climatic stations were selected based on the following: a) the largest number of stations (26 of 54) with records between 1980 and 2014 (35 years); b) Stations with more than 90% of the total daily precipitation records, although the methodology for trend analysis is not sensitive to missing value (Pal, 2009). Table 1 shows the selected stations.

The period from 1980 to 2014 was selected, mainly based on the collection of information from the erosion map (Instituto de Hidrología *et al.*, 2015). In contrast, the randomness of the series was verified with the Turning Point test, according to the methodology exposed by Clarke (1984, p. 26).

Table 1. Information from the weather stations used.

Name Station	Cat.	Elevation m a.s.l.	Latitude			Longitude			Depart.	Municipality
			°	min.	s	°	min.	s		
Arcabuco	PM	2600	5	45	38.1	73	26	38.9	Boy.	Arcabuco
Azulejos Los	PG	2780	5	39	4.9	73	12	3.6	Boy.	Tuta
Casa Amarilla	PM	3200	5	32	1.7	73	9	48.6	Boy.	Toca
Cerezo El	PM	2900	5	41	57.5	73	4	18.3	Boy.	Paipa
Cómbita	PM	2820	5	37	44.1	73	19	26.4	Boy.	Cómbita
Emporio Hacienda El	PM	2120	5	36	5.8	73	32	38.6	Boy.	Villa de Leyva
Nuevo Colón	AM	2438	5	21	13.7	73	27	23.4	Boy.	Nuevo Colón
Ráquira	PM	2290	5	32	19.6	73	37	52.9	Boy.	Ráquira
San Pedro de Iguaque	PG	2985	5	38	24.0	73	27	1.6	Boy.	Chíquiza
Siachoque	PM	2720	5	30	26.4	73	15	1.0	Boy.	Siachoque
Surbatá Bonza	AM	2485	5	48	8.8	73	4	28.1	Boy.	Duitama
Tibaná	PM	2115	5	18	55.0	73	23	45.4	Boy.	Tibaná
Turmequé	PM	2400	5	19	4.1	73	19	46.4	Boy.	Turmequé
U P T C	CP	2690	5	33	12.8	73	21	19.0	Boy.	Tunja
Úmbita	PM	2300	5	13	8.8	73	26	40.4	Boy.	Úmbita
Villa Carmen	CP	2600	5	30	42.1	73	29	44.8	Boy.	Samacá
Villa de Leiva	CP	2215	5	39	21.0	73	32	38.2	Boy.	Villa de Leyva
Amoladero El	PM	2963	4	51	28.7	73	44	43.4	Cundi.	Guatavita
Aepto. El Dorado	SP	2547	4	42	20.1	74	9	2.4	Cundi.	Bogotá
Cucunubá	PM	2620	5	15	3.7	73	46	14.7	Cundi.	Cucunubá
Hato El	PM	2575	4	52	0.0	74	9	13.9	Cundi.	Tenjo
Leticia	PM	2650	5	18	11.5	73	42	35.1	Cundi.	Lenguazaque
Potreros	PM	2802	4	49	43.7	73	46	9.4	Cundi.	Guatavita
Silos	CO	2709	5	7	3.8	73	42	5.1	Cundi.	Chocontá
Simijaca	PG	2590	5	30	40.7	73	51	49.3	Cundi.	Simijaca
Santa Cruz de Siecha	PM	3100	4	47	3.4	73	52	14.9	Cundi.	Guasca

Source: Own elaboration based on information from IDEAM.

Notes: Depart: Department; Cundi.: Cundinamarca; Boy.: Boyacá; Cat: Station category; PM: Pluviometry; PG: Pluviographic; AM: Agrometeorological; CP: Climatic Principal; SP: Synoptic; °: degree; min: minute; s: seconds.

#### 2.4. Precipitation analysis and comparison with the erosion map

The methodology developed with the daily values of precipitation by the station is summarized in the following major steps: a) Analysis of the daily precipitation, complete the series and generate the decadal Modified Fournier Indices ( $MFI_d$ ). Rainfall analyses were carried out over periods of ten days, which is decisive for evaluating the short-term effects of the main erosive and productive agent. b) Obtaining the maximum annual value of the decadal Modified Fournier index ( $MFI_{dmax}$ ). c) Evaluation of trends in annual precipitation and the  $MFI_{dmax}$ . d) Obtaining the multiannual mean value of the maximum values of the indices ( $MFI_{dmax}$ ). e) Calculation of the weighted erosion level of the erosion map (IDEAM *et al.*, 2015) to obtain the correlation and regression with the multiannual average of the  $MFI_{dmax}$  and annual rainfall. Table 2 presents a synthesis of the methodology developed, based on the analysis of the behaviour of rainfall, to determine the existence of changes or trends that may affect the erosivity of rainfall.

The Pearson correlation coefficients between all stations were calculated to complete the daily rainfall. From this process, groups of five stations were formed to carry out the process of completing the daily precipitation data, with a) The Normal Ratio method used by Linsley *et al.*, (1977, p. 64), including the influence of the El Niño Ocean Indices from the National Weather Service Climate

Prediction Center (National Oceanic and Atmospheric Administration [NOAA], 2021) according to (Medina *et al.*, 2008); and b) Based on the least mean square error (RMSE) between the Homogeneous Fields Method of Antelo and Fernández (2014) and the Normal Ratio method, mentioned above, the way to complete the daily rainfall data for each station was chosen.

*Table 2. Methodological synthesis process with its techniques and activities.*

<b>Techniques for daily precipitation analysis and MFI<sub>d</sub></b>	<b>Techniques for trend analysis, compare with the erosion map, correlation and regression.</b>
Rainfall consistency analysis with the Turning Point or Gust Test (Clarke, 1984).	Obtaining the maximum annual value of the decadal Modified Fournier Index (MFI <sub>dmax</sub> ).
Completion of the rainfall series with the Normal Ratio method (Linsley <i>et al.</i> , 1977), including the influence of the ENSO adapted from Medina <i>et al.</i> (2008) or the Homogeneous Fields method (Antelo R. & Fernández, 2014) according to the lower value of the Root Mean Square Error (RMSE).	Evaluation of the trends (Mann-Kendall, 1948) of annual rainfall and MFI <sub>dmax</sub> , with their Median slopes (Sen, 1968).
Generation of decadal Modified Fournier Indices (MFI <sub>d</sub> ) (Gómez, 1999).	Obtaining the multiannual average value of the maximum values of the MFI <sub>dmax</sub> , by rain gauge station.
	Calculation of the weighted erosion level from the erosion map (IDEAM <i>et al.</i> , 2015) to obtain the correlation and regression with the multiannual average of the MFI <sub>dmax</sub> and annual rainfall.

#### 2.4.1. Generation of decadal Modified Fournier Indices

Since pluviographs are scarcer in the developing countries of Latin America, the analysis of the aggressiveness of the rains was based on the availability of the records of the pluviometers, instead of the pluviographs. For this reason, Modified Fournier indices were used.

According to Kirby and Morgan (1984), in Gómez (1999), the analysis carried out by Fournier around the year 1960 with the sedimentary values of more than 140 rivers in Europe, Asia and the United States, obtained a high correlation between the sediment load and an index generated with annual and monthly rainfall. Although Fournier (1960) initially obtained a high correlation of the sediment load versus the relationship between the monthly precipitation of the rainiest month ( $p$ ) and the average annual precipitation ( $P$ ), this index ( $p^2/P$ ) was later modified by Arnoldus (1977) in Renard and Freimund, (1994). With the modified Fournier index, the correlation of  $R^2$  with the R factor (rain erosion factor in the universal soil loss equation -USLE-) increased from 0.55 to 0.91. The modification introduced by Arnoldus (1977) is illustrated in equation 1.

$$MFI = \sum_{i=1}^{12} \frac{p_i^2}{P} \quad (\text{Equation 1})$$

Where MFI is Modified Fournier Index (mm),  $p_i$  is the rainfall for the  $i^{\text{th}}$  month (mm),  $P$  is the annual rainfall (mm), and  $i$  the month.

#### 2.4.2. Obtaining decadal Modified Fournier Indices

Firstly, the rain patterns were divided into periods of ten days. Decade 1, from day 1 to 10; decade 2, from day 11 to 20; and decade 3, from the 21<sup>st</sup> to the 28<sup>th</sup> or 29<sup>th</sup> or 30<sup>th</sup> or 31<sup>st</sup>, depending on the number of days in each month, as proposed by Gómez (1991; 1999). With these decadal Modified Fournier indices (MFI<sub>d</sub>), the monthly Modified Fournier indices (MFI<sub>dm</sub>) and annual (MFI<sub>da</sub>) can be obtained through the corresponding accumulation. The modified MFI<sub>d</sub> at the decadal level (every 10 days) used in the present investigation was:

$$MFI_d = \sum_{i=1}^{10} \frac{p_i^2}{P} \quad (\text{Equation 2})$$

Where  $MFI_d$  is the Decadal Modified Fournier Index ( $\text{mm dec.}^{-1}$ ),  $p_i$  is precipitation of each of the 10 days (mm),  $P$  is the Average precipitation in the corresponding decade (mm), and  $i$  the day.

### 2.5. Obtaining the maximum annual value of $MFI_{dmax}$

Of the 36 decadal Modified Fournier indices of each year ( $MFI_{dmax}$ ), the maximum value of each year by rainfall station was selected. Thus, the aggressiveness trends of the rains were evaluated using the maximum annual value of the  $MFI_d$  of each station, according to the methodology of Chow *et al.* (1994, p. 394) and Suresh (2008, p. 563).

### 2.6. Evaluation of trends in annual precipitation and the $MFI_{dmax}$

With the records of the total annual rainfall for each station, the trends were evaluated with different levels of statistical confidence (90.0%; 95.0%; 97.5%; 99.0% and 99.5%). These statistical confidence levels were applied to all the series analysed, taking into account the sensitivity of the method Mann (1945) and Kendall (1948). The value of the median slope was obtained with the method proposed by Sen (1968).

#### 2.6.1. Trend analysis method with decadal Fournier indices

With this methodology (analysing the maximum annual values) it was intended to measure the potential impact of the acting agent (rain) on soil erosion over time (trend) as an expression of climate change.

#### 2.6.2. Sen's test

Sen (1968) developed a non-parametric estimator to evaluate the magnitude of the data trend, which consists of evaluating the presence of a slope (positive or negative) of the time series (equidistantly distributed data, in days, months, years, etc.). For this, the algorithm proposed by Hirsch and Smith (1982) is used, which is an extension of those suggested by Theil (1950) and Sen. According to Hirsch and Smith (in Gallego, 2003), Sen's test is a robust method to doubtful values, the lack of records and atypical data since it is evaluated through the median for  $N$  pairs of data with the following expression:

$$Q_1 = \frac{X_{i'} - X_i}{i' - i} \quad (\text{Equation 3})$$

Where  $Q_1$  is the slope between the data pairs  $X_{i'}$  and  $X_i$ ;  $X_{i'}$  is the measurement at time  $i'$ ;  $X_i$  is the measurement at the time  $i$ ;  $i'$  is time after time  $i$ ; and  $N'$  is the calculated number of slopes, between the data pairs.

The median of the  $N$  values of  $Q_1$  is the estimator of the slope of Sen. The median slope ( $Q$ ) is obtained with the estimator of the slope of Sen, through:

$$Q' = Q_{\left[\frac{N'+1}{2}\right]}, \text{ if } N' \text{ is odd; } \quad y \quad Q' = \frac{Q_{\left(\frac{N'}{2}\right)} + Q_{\left(\frac{N'+2}{2}\right)}}{2}, \text{ if } N' \text{ is even.} \quad (\text{Equation 4})$$

### 2.6.3. Mann-Kendall (M-K) test

The Mann–Kendall test allows for the detection of the existence of a trend in a time series but does not provide an estimate of its magnitude. The M-K test is a nonparametric test based on a test earlier developed by Kendall (1948).

The null hypothesis ( $H_0$ ) of the M-K test is that the data ( $x_1, x_2 \dots, x_n$ ) are identically and independently distributed random variables, and the alternative hypothesis ( $H_1$ ) is that they are distributed with a decreasing or increasing trend, using the statistic called  $S\tau$  of Kendall, with the following expression:

$$S\tau = \sum_{i=1}^{n-1} = \sum_{j=i+1}^n \text{sgn}(X_i - X_j) \quad (\text{Equation 5})$$

The function  $\text{sgn}(X)$  is the sign function, whose value is -1, 0 or 1; depending on whether the argument is negative, null, or positive, respectively.

The variance of ( $S$ ) of the null hypothesis is obtained with the following equation:

$$\text{Var}(S) = \frac{n(n-1)*(2n+5) - \sum_{p=1}^q t_p(t_p-1)*(2t_p+5)}{18} \quad (\text{Equation 6})$$

In equation 6,  $n$  is the Number of data;  $t_p$  is the number of measurements equal to a particular value; and  $q$  el number of linked values (Number of linked groups). A linked group is a set of data from a sample that have the same value.

The range of levels for a specific confidence interval is carried out when evaluating  $C$ , through the following expression:

$$C_\alpha = Z_{1-\frac{\alpha}{2}} * \sqrt{\text{Var}(S)} \quad (\text{Equation 7})$$

Where  $C_\alpha$  is distributed as a Normal distribution with mean 0 and variance 1. To test for an upward or downward trend, the confidence level is compared to the absolute value of  $Z$ ; which is obtained from the Normal distribution tables. Based on the previous equation, the values, low ( $M_1$ ) and high ( $M_{2+1}$ ), can be found using the confidence limits with the following expressions:

$$M_1 = \frac{N' - C_\alpha}{2}; \quad M_{2+1} = \frac{N' + C_\alpha}{2} \quad (\text{Equation 8})$$

The selection of the slopes corresponds to  $M_1$  and  $M_{2+1}$ , which are the respective Confidence Limits ( $CL_u$  and  $CL_l$ ; upper and lower)

## 2.7. Obtaining the multiannual average value of the maximum values of the $MFI_{dmax}$

With the 35 maximum annual values of the  $MFI_{dmax}$ , the average quantity was obtained, with which the aggressiveness of the rains was characterized within the evaluated period (1980 to 2014).

## 2.8. Correlation between the level of erosion weighted vs. $MFI_{dmax}$ and precipitation

Based on the erosion map in Figure 1, made by Instituto de Hidrología *et al.* (2015), the weighted average of the five degrees of erosion in the surrounding areas within a radius of 1 kilometre was calculated. The assigned weighting values, with the ranges of erosion levels obtained, are shown in Table 3.

Table 3. Weighting values and erosion levels.

Value applied to the degree of erosion in the weighting	Ranges of the levels of erosion generated	Degree of erosion
0.5	$\leq 0.5$	Without evidence of erosion.
1.0	0.6 to 1.0	Light
2.0	1.1 to 2.0	Moderate
4.5	2.1 to 4.5	Severe
5.0	4.6 to 5.0	Very severe

With the level of erosion obtained from the weighting of the areas around one kilometre from each rain measurement station, the correlation and regression process are subsequently carried out with the average value of the  $MFI_{dmax}$  and the annual precipitation.

Additionally, it should be noted that Microsoft Excel was used to calculate the previous equations and the median of the slope of Sen in the M-K test. Regarding the maps with isolines, these are generated through a Geographic Information System (GIS) and the inverse interpolation distance weighted (IDW) method.

### 3. Results and discussions

#### 3.1. Pluviometry and rain trends

Most of the rain measurement stations record two periods, with the highest amounts in April and October, corresponding to the bimodal regime. The stations with a monomodal regime are located towards the southeast side, in the municipality of Guasca, Cundinamarca, concentrating rainfall in June and July. Figure 2 shows the map with the multiannual mean isohyets.

Additionally, Table 4 synthesizes the values obtained from the average annual accumulated daily rainfall and the results obtained with the slope trend tests (M-K and Sen). Positive trends were found in four stations, with more than 95% of the confidence level (CL) statistic. Similarly, the Potreritos station presented a negative trend with 90% CL. This station is located southwest of the corridor at 2,802 m a.s.l. in Guatavita, with high annual rainfall (1,717 mm), yielding a median decrease of about 6.9 mm/year.

Table 4 highlights the significant median increase of more than 28 mm of rain/year at the Tibaná station, followed by the El Dorado airport station (8.5 mm/year) in Bogotá, Silos in Chocontá (6.9 mm/year) and Surbatá Bonza in Duitama (6.4 mm/year). The increases in rainfall are located in stations that register sufficient contribution of annual rainfall for the plants and where severe or very severe erosive processes are not recorded.

The climate change in the rains patterns of the El Dorado airport (Bogotá) is consistent with the studies performed by Rojas *et al.* (2010), who reported a variation of 13.1 mm/year for the period 1985 to 2008. Although these authors found increases for the period 1987 to 2008, in the municipalities of Villa de Leyva (12.2 mm/year) and Tenjo (9.8 mm/year), with CL of 95% and 90%, respectively, in this study, these variations were not found. This lack of trend for the 35 years leads us to suggest that the difference concerning the positive trend could be derived from the relatively short period (22 years) selected in the study by Rojas *et al.* (2010). In other words, the employed tests are sensitive to the length and cut-off year of the period analysed.

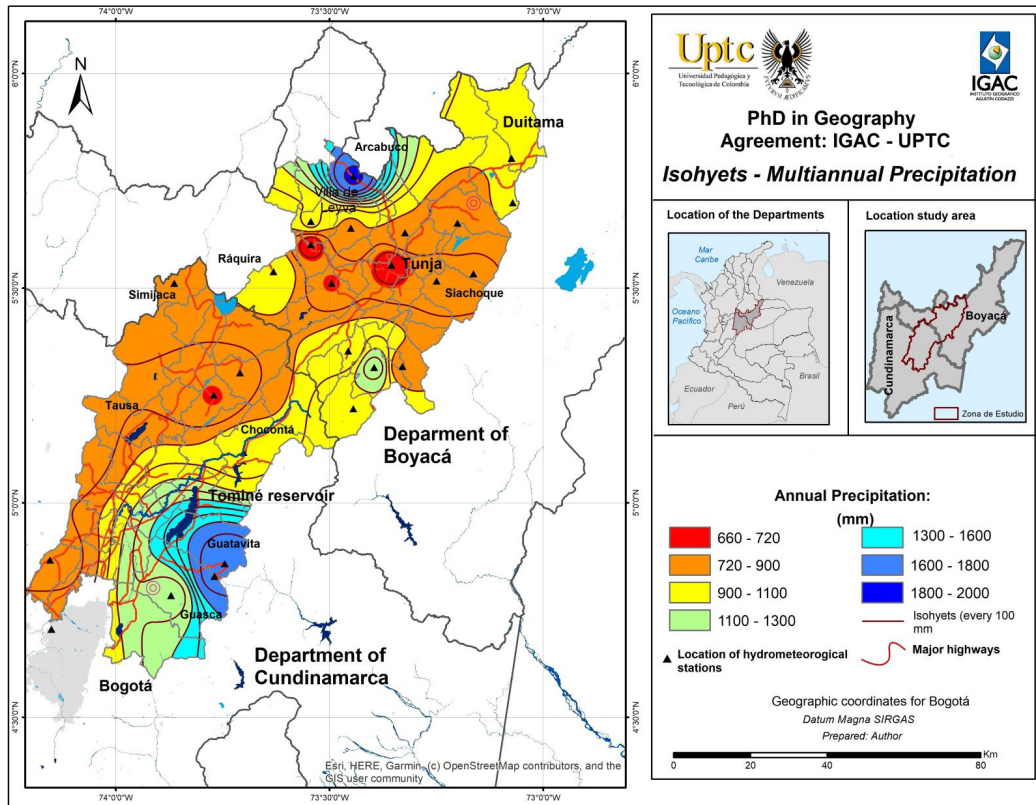


Figure 2 Multiannual mean total precipitation map 1980-2014.

Table 4. Sen and Mann-Kendall (M-K) test with Confidence Levels (CL) for annual rainfall.

Station	Median (Sen) (mm year <sup>-1</sup> )	M-K	Confidence Level (CL) (%)	CL <sub>l</sub> Slope	CL <sub>u</sub> Slope	Multianual rain (mm)
<b>El Dorado</b>	<b>8.504</b>	(+)	<b>99.0</b>	<b>19.475</b>	<b>0.225</b>	<b>860</b>
<b>Silos</b>	<b>6.911</b>	(+)	<b>97.5</b>	<b>12.449</b>	<b>0.135</b>	<b>976</b>
UPTC	2.385			-1.500	5.780	660
<b>Surbatá Bonza</b>	<b>6.392</b>	(+)	<b>95.0</b>	<b>0.205</b>	<b>11.561</b>	<b>904</b>
Villa de Leiva	4.213			-1.150	10.273	1,017
Villa Carmen	1.011			-2.063	5.267	717
Casa Amarilla	-0.668			-4.777	4.129	790
El Emporio	-1.070			-4.800	3.077	665
<b>Potreritos</b>	<b>-6.868</b>	(-)	<b>90.0</b>	<b>-12.494</b>	<b>-1.427</b>	<b>1,717</b>
El Amoladero	7.673			-1.617	15.516	1,769
Úmbita	1.643			-2.171	5.950	1,077
Nuevo Colón	2.118			-0.681	5.318	930
Simijaca	1.851			-3.414	6.112	869
Ráquira	0.979			-6.933	7.675	994
Arcabuco	3.966			-10.820	19.444	1,813
Siachoque	-0.8600			-7.381	4.5027	759
Azulejos	-1.336			-6.839	3.797	826
Cómbita	5.850			-0.653	12.925	896
El Cerezo	-2.194			-7.566	3.841	915
San Pedro de Iguaque	-3.316			-11.378	4.381	890
<b>Tibaná</b>	<b>28.800</b>	(+)	<b>99.5%</b>	<b>11.750</b>	<b>47.465</b>	<b>1,234</b>
Turmequé	-5.565			-11.542	1.974	826
Cucunubá	1.940			-2.275	6.809	717
El Hato	3.795			-0.474	8.691	759
Leticia	3.817			-1.413	8.821	793
Santa Cruz de Siecha	3.154			-3.376	13.011	1,157

Notes: CL<sub>l</sub>: Lower confidence limit; CL<sub>u</sub>: Upper confidence limit; (+): Positive trend (-): Negative trend with the MK test; CL: Confidence level. The records in bold showed a trend.

Additionally, it is necessary to take into account that despite having found negative median slopes (decrease in annual precipitation), several stations did not present a negative trend in precipitation, with a statistical CL greater than 90%. Figure 3 shows in red the stations with median negative slopes less than -1.0 – see. Table 4 for more information.

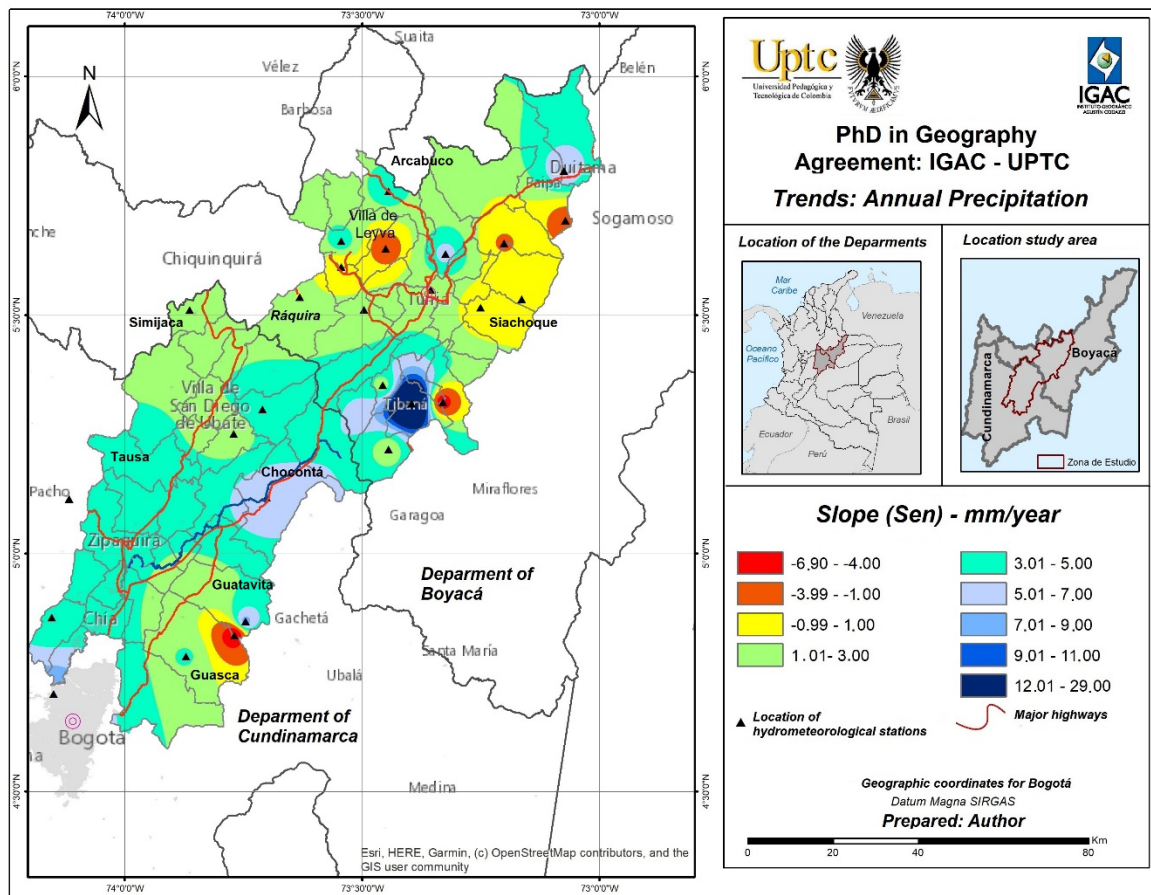


Figure 3. Distribution map of annual precipitation trends.

### 3.2. Rainfall aggressiveness considering the decadal modified Fournier Index ( $MFI_d$ )

For the study of the erosive aggressiveness of the rain, it is necessary to take into account that all the analysis was carried out based on the Modified Fournier index ( $MFI_d$ ) for 10 days (decadal). Thus, to classify the aggressiveness of the rain through the Maximum decadal Modified Fournier Index of each year ( $MFI_{dmax}$ ), the qualification made by Gómez (1975; in Gómez, 1999) is taken as a reference – see Table 5.

Although the classification made in Table 5 by Gómez (1975; in Gómez 1999) was based on studies in the Colombian coffee region (an area with greater amounts and intensities of rain than in the Cundiboyacense highlands), there is a coincidence of the stations classified with the  $MFI_{da}$  greater than 210 mm (medium degree of aggressiveness) with the areas that present degrees of severe and very severe erosion.

Next, the aggressiveness of the areas with the greatest rainfall was characterised by the average maximum annual values per station ( $MFI_{dmax}$ ). The average spatial distribution of the  $MFI_{dmax}$  can be seen in Figure 4, where the map with the isolines with the greatest rainfall aggressiveness is shown in orange, red and purple colours.

Table 5. Rainfall aggressiveness rating with Modified Fournier Index (MFI).

MFI <sub>a</sub> (mm)	MFI <sub>da</sub> (mm)	MFI <sub>dmax</sub> (mm dec year <sup>-1</sup> ) (*)	Degree of erosion	Precipitation characteristics
< 5.0	< 140	< 20.0	Light	Light rains are well distributed.
5.1 - 8.0	140.1 - 210	20.1 - 25.0	Low	Low-intensity, frequent and well-distributed rains.
8.1 - 10.0	210.1 - 280	25.1 - 30.0	Moderate	Rains of medium intensity, frequent, of good to regular distribution.
10.1 - 14.0	280.1 - 350	30.1 - 35.0	Hight	Heavy rains, frequent or not, from good to bad distribution.
> 14.0	> 350	> 35.0	Very high	Heavy to very heavy rains, frequent or not, from good to bad distribution.

Notes: MFI<sub>d</sub>: Decadal Modified Fournier Index; MFI<sub>da</sub>: Annual Decadal Modified Fournier Index; MFI<sub>dmax</sub>: Average annual maximum decadal Modified Fournier index; (\*): Classification adopted with the present investigation. Source: Adapted from Gomez (1975) in Gómez (1999).

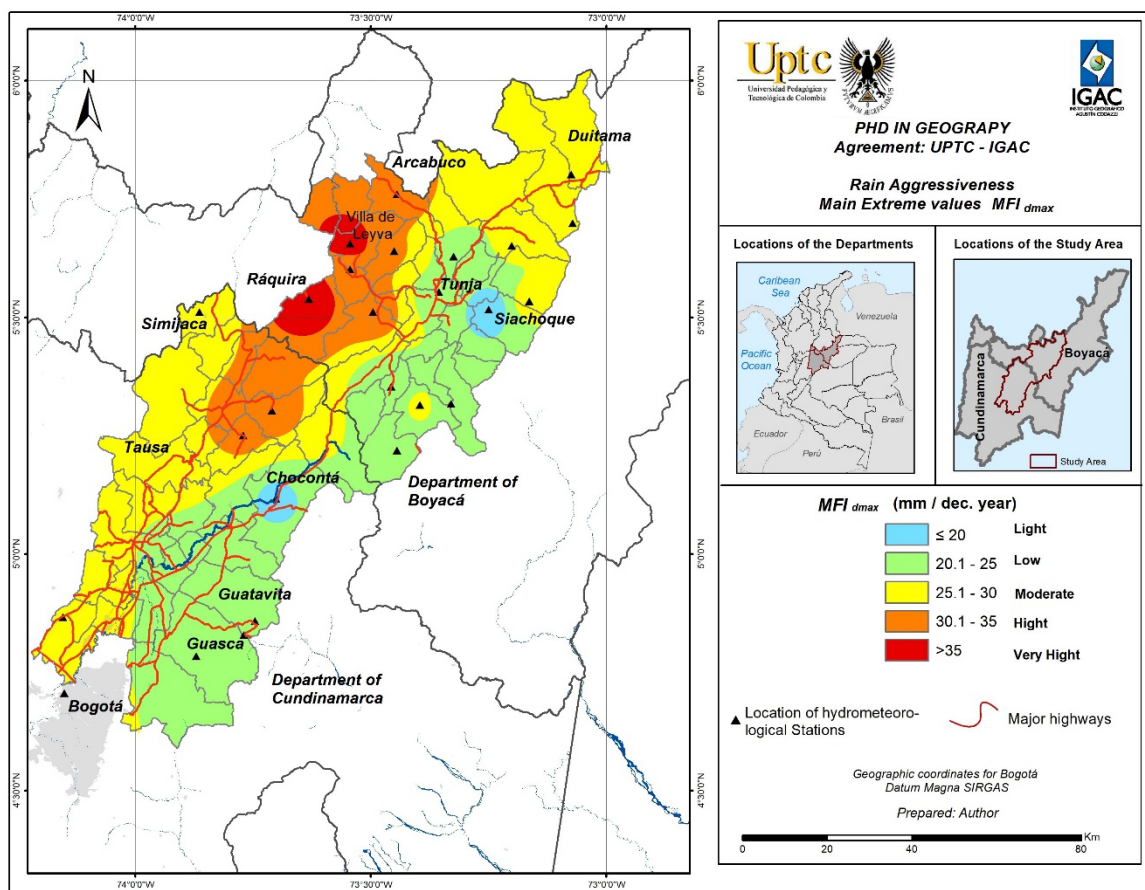


Figure 4. MFI average annual maximum decadal.

Based on the comparison of the map of the average MFI<sub>dmax</sub> and the map of soil degradation (Instituto de Hidrología *et al.*, 2015), there is a high correspondence with the degrees of severe and very severe erosion in the department of Boyacá in the municipalities of Ráquira, Villa de Leyva, SÁCHICA, Samacá, Chíquiza, Sora, Santa Sofía and Cucaita; which are located towards the western side of the middle – upper third, of the corridor studied (see polygons in red and fuchsia colours).

In the department of Cundinamarca, the municipalities of Nemocón, Tausa, Suesca and Cucunubá present very severe and severe degrees of erosion, which is consistent in this study with an

average  $IFM_{dmax}$  greater than 30 mm/decade. In Cundinamarca, possibly due to the lack of rainfall stations in the southeast of the study area, in Guatavita (south of the Tominé reservoir), the aggressive behaviour of the rains was not detected through the  $MFI_{dmax}$ . This situation may correspond to a water shadow on the leeward side of the mountain that blocks the path of moist winds from the eastern plains (see Fig. 4).

### 3.2.1. Trends of annual maximum decadal Modified Fournier indices $MFI_{dmax}$

After obtaining the decadal Modified Fournier indices ( $MFI_d$ ), the maximum values of each year ( $MFI_{dmax}$ ) were selected, to do so, the M–K and Sen tests were employed to evaluate the existence or absence of the trend of the aggressiveness of the rain. The results of the trends of the maximum decadal Modified Fournier Indices of each year by the station are shown in Table 6.

Table 6 includes the “Erosion Level” column, which corresponds to a weighted average of the areas found within a radius of 1 kilometre from each station, based on the degree of erosion in Figure 1 (Instituto de Hidrología *et al.*, 2015). Table 6 is ordered by the level of erosion. Additionally, the following aspects are highlighted.

Table 6. M-K and Sen tests for averages of the decadal annual maximum values of the Modified Fournier Indices ( $MFI_{dmax}$ ) and multiannual Precipitation mean (Pp)

Station	Median (Sen) (mm year <sup>-1</sup> )	CL $MFI_{dmax}$ (%)	CL <sub>l</sub> Slope $MFI_{dmax}$ (mm year <sup>-1</sup> )	CL <sub>u</sub> Slope $MFI_{dmax}$ (mm year <sup>-1</sup> )	Mean $MFI_{dmax}$ (mm dec year <sup>-1</sup> )	Erosion level (weighted average)	Pp (mm year <sup>-1</sup> )
El Amoladero	-0.054		-0.155	0.126	21.72	0.73	1.769
Arcabuco	-0.099		-0.363	0.105	32.00	0.93	1.813
Turmequé	0.088		-0.125	0.282	23.34	1.00	826
<b>Tibaná</b>	<b>0.353</b>	<b>95.0</b>	<b>0.068</b>	<b>0.748</b>	<b>25.38</b>	<b>1.00</b>	<b>1.234</b>
<b>Surbatá Bonza</b>	<b>0.353</b>	<b>90.0</b>	<b>0.041</b>	<b>0.609</b>	<b>25.80</b>	<b>1.00</b>	<b>904</b>
Casa Amarilla	0.140		-0.154	0.388	25.90	1.00	790
<b>El Dorado</b>	<b>0.330</b>	<b>90.0</b>	<b>0.008</b>	<b>0.637</b>	<b>27.33</b>	<b>1.00</b>	<b>860</b>
<b>Úmbita</b>	<b>0.268</b>	<b>99.5</b>	<b>0.003</b>	<b>0.697</b>	<b>23.86</b>	<b>1.04</b>	<b>1.077</b>
<b>San Pedro de Iguaque</b>	<b>-0.462</b>	<b>97.5</b>	<b>-1.018</b>	<b>-0.018</b>	<b>30.20</b>	<b>1.49</b>	<b>890</b>
Potreros	-0.086		-0.264	0.090	23.35	1.56	1.717
Santa Cruz de Siecha	-0.105		-0.360	0.104	22.17	1.60	1.157
El Hato	0.206		-0.189	0.680	28.01	1.74	759
Simijaca	-0.003		-0.293	0.306	27.97	1.84	869
Nuevo Colón	0.036		-0.323	0.410	20.85	1.91	930
<b>Cómbita</b>	<b>-0.344</b>	<b>95.0</b>	<b>-0.742</b>	<b>-0.047</b>	<b>23.96</b>	<b>1.98</b>	<b>896</b>
Siachoque	0.020		-0.161	0.166	17.82	2.00	759
Silos	0.034		-0.169	0.248	19.64	2.00	976
El Cerezo	0.144		-0.197	0.471	27.76	2.00	915
Azulejos	-0.087		-0.294	0.194	25.22	2.00	826
Leticia	0.184		-0.068	0.512	30.92	<b>2.00</b>	793
UPTC	0.109		-0.081	0.285	22.47	2.00	660
Villa Carmen	0.294		-0.044	0.646	31.98	2.45	717
Cucunubá	0.663		-0.901	2.206	30.45	2.63	717
Villa de Leiva	0.128		-0.208	0.567	36.97	4.50	1.017
El Emporio	0.230		-0.027	0.496	31.51	4.70	665
Ráquira	0.319		-0.167	0.926	38.20	4.92	994

Notes: CL: Confidence level of the trend; CL<sub>l</sub>: lower confidence limit; CL<sub>u</sub>: upper confidence limit.

The color of the cells corresponds to the median values in yellow, green to the lowest value of erosive aggressiveness ( $MFI_{dmax}$ ) and greater precipitation, and red where the highest values of  $MFI_{dmax}$  and less precipitation are found.

Although the C6mbita stations (erosion level 1.98; moderate) and San Pedro de Iguaque (erosion level 1.49; moderate) presented a negative trend; The aggressiveness of the rain ( $MFI_{dmax}$ , mm dec yr<sup>-1</sup>) was close to the range of the moderate value (25.1 to 30.0) in the C6mbita (23.96) and San Pedro de Iguaque (30.2) stations.

With a behaviour contrary to the previous situation, positive trends were detected in the  $IMF_{dmax}$  of the Tiban6 (25.38), Surbat6 Bonza (25.80), El Dorado (27.33) and 6mbita (23.86) stations. However, these values of pluvial aggressiveness were located in low (20.1 to 25.0) to moderate (25.1 to 30.0) ranges, in addition to showing slight levels of light erosion ( $\leq 1.04$ ).

The previous results allow us to establish that despite the fact that the aggressiveness of the rain ( $MFI_{dmax}$ ) showed a positive trend in four rain measurement stations, the level of soil erosion was slight ( $< 1.04$ ) in the period 1980 - 2014. In the opposite sense, the two stations that presented moderate levels of erosion (1.1 to 2.0) showed negative trends in the  $MFI_{dmax}$ .

Additionally, the previous results do not show changes in the areas that, until 2014, had severe to very severe levels of erosion. On the one hand, no trends were found and there are averages of high rainfall aggressiveness (30.1 to 35.0) or higher in most of the terrains with degrees of severe (2.10 to 4.50) to very severe (4.51 to 5.00) erosion. Therefore, their degradation conditions due to trends in the aggressiveness of the rains remained in the same adverse conditions.

### 3.2.2. Relationship between erosion and the mean maximum of $MFI_{dmax}$

The best regression model between the erosion level (Y) and the  $MFI_{dmax}$  was obtained by squaring the values of this index, shown in equation 9.

$$\text{Level of Erosion (Y)} = - 0,0070 + 0,0027 (MFI_{dmax})^2 \quad (\text{Equation 9})$$

By including the multiannual mean precipitation (Pp) in a multiple regression model, it was possible to increase the explanatory power with equation 10.

$$\text{Level of Erosion (Y)} = 1,0105 - 0,0010 (Pp) + 0,0026 (MFI_{dmax})^2 \quad (\text{Equation 10})$$

Using Analysis of Variance and the F test, the existence of a relationship between at least one of the independent variables with the level of erosion at 95% confidence in the two previous models was verified. The coefficients of determination ( $R^2$ ) and determination ( $\bar{R}^2$ ) adjusted to explain the level of erosion were: 0.445 and 0.421 for equation 9; and 0.519 and 0.478 for equation 10.

The explanation of the levels of soil erosion in more than 50%, based on rainfall, leaves for the inherent conditions of the soil, and agricultural management measures that facilitate the retention of moisture in the land, the key to avoiding erosion.

### 3.3. *Other aspects of rainfall aggressiveness indices and annual precipitation*

Based on Table 6, it could be expected that severe or greater erosion occurs in 50% of the cases, where the multiannual average precipitation is less than 720 mm/year, and there are no factors that allow water retention in the land. This annual rainfall threshold is close to the value reported by Hudson (1982) regarding the relationship between precipitation and soil erosion (about 750 mm/year), who adds that the factor that most influences soil erosion by water is the average annual rainfall. In regions with little precipitation, water erosion may be small. However, when little precipitation falls, the water is retained by the water-hungry vegetation, with runoff it is almost nil. At the opposite extreme, rainfall greater than 1,000 mm per year often results in dense forest vegetation that protects the soil.

The approach by Hudson (1982) is oriented in a similar direction to the one exposed by (Várallyay, 2010). The latter author expects that, with greater precipitation, especially heavy rains and electrical storms, an increased rate of erosion will result from greater runoff. However, the increase in moisture could be offset by the increasing soil conservation effect of denser and more permanent vegetation due to increased water supply.

Regarding the non-concordance of the threshold of 720 mm year<sup>-1</sup> and the higher degrees of erosion in the south of the Tominé reservoir (Guatavita), it could be explained by the effect of the rain shadow (leeward), which despite the high humidity (with more than 1,700 mm/year) in the upper part (2,960 m a.s.l.) of Guatavita, presents severe erosion in the lower part of the mountain (2630 m a.s.l. without rain gauges). Additionally, it should be noted that there is no clear association of the erosive phenomenon with respect to the increase in precipitation, even more so when the spatial variations of the climatic characteristics can be found in mountain areas (di Lena *et al.*, 2021; Valdés-Pineda *et al.*, 2016).

#### 4. Conclusions

Climate changes between 1980 and 2014 with a statistical confidence level greater than 90% using the Mann-Kendall test, and the trends of the median slope with the Sen statistic, were detected. Increases in annual precipitation at El Dorado Airport (Bogotá), Silos (Chocontá), Surbatá Bonza (Duitama) and Tibaná, and decreases in Potreritos (Guatavita), were observed. Similarly, increases in the aggressiveness of rain (decadal annual maximum Modified Fournier Index -MFI<sub>dmax</sub>) in Úmbita, Tibaná, Surbatá Bonza (Duitama) and El Dorado (Bogotá), with decreases in said index were detected in San Pedro de Iguaque (Chíquiza) and Cómbita.

With the application of methods for calculating the median slope and the detection of trends in rainfall aggressiveness through MFI<sub>dmax</sub>, a new and useful methodology is presented for the planning and monitoring of territorial ordering against soil degradation processes due to rain erosion.

Although changes with statistical confidence levels (>90%) were found in annual precipitation and in pluvial aggressiveness (MFI<sub>dmax</sub>) that can cause soil erosion, it cannot be established that greater soil degradation can be explained solely by the change climate of the above variables.

Finally, the level of soil erosion can be explained ( $R^2$  0.519 and  $\bar{R}^2$  adjusted 0.478) through a regression model based on the square of the average of the maximum annual values of the decadal Modified Fournier Indices, and the negative value of the average annual precipitation.

#### Acknowledgments

The authors wish to thank IDEAM for providing the rainfall data. Likewise, IGAC, and the Pedagogical and Technological University of Colombia, for their support in the research process.

#### References

- Almagro, A., Oliveira, P.T.S., Nearing, M.A., Hagemann, S., 2017. Projected climate change impacts in rainfall erosivity over Brazil. *Scientific Reports*, 7(1). <https://doi.org/10.1038/s41598-017-08298-y>
- Antelo R., Fernández, M., 2014. *Estimación de datos faltantes de precipitación diaria para las distintas ecorregiones de la República Argentina*. 1-13. <https://www.ina.gov.ar/ifrh-2014/Eje3/3.02.pdf>
- Arias-Muñoz, P., Saz, M.A., Escolano, S., 2023. Estimation of soil erosion through the RUSLE model. Case study: upper-middle basin of Mira River in Andean-Ecuador. *Investigaciones Geográficas* 79, 207-230. <https://doi.org/10.14198/INGEO.22390>

- Basher, L., Elliott, S., Hughes, A., Tait, A., Page, M., Rosser, B., McIvor, I., Douglas, G., Jones, H., 2012. *Impacts of climate change on erosion and erosion control methods - A critical review. Final report* (New Zealand Government, Ed.). Ministry for Primary Industries. <https://www.mpi.govt.nz/dmsdocument/4074/direct>
- Borrelli, P., Robinson, D., Panagos, P., Lugato, E., Yang, J., Alewell, C., Wuepper, D., Montanarella, L., Ballabio, C., 2020. Land use and climate change impacts on global soil erosion by water (2015-2070). *Proceedings of the National Academic of Sciences of the USA [PNAS]*, 117(36), 21994-22001. <https://doi.org/10.1073/pnas.2001403117/-/DCSupplemental>
- Chow, V., Maidment, D., Mays, L., 1994. *Hidrología aplicada* (McGraw-Hill, Ed.). McGraw-Hill.
- Clarke, R., 1984. *Mathematical models in hydrology* (FAO, Ed.). Food and Agriculture Organization of the United Nations (FAO).
- di Lena, B., Curci, G., Vergni, L., 2021. Analysis of rainfall erosivity trends 1980–2018 in a complex terrain region (Abruzzo, central Italy) from rain gauges and gridded datasets. *Atmosphere* 12(6). <https://doi.org/10.3390/atmos12060657>
- Eekhout, J., de Vente, J., 2020. How soil erosion model conceptualization affects soil loss projections under climate change. *Progress in Physical Geography: Earth and Environment* 44(2), 212-232. <https://doi.org/10.1177/0309133319871937>
- Fournier, F., 1960. *Climat et érosion: la relation entre l'érosion du sol par l'eau et les précipitations atmosphériques* (Presses universitaires de France, Ed.; 1st ed.). Presses universitaires de France.
- Gallego, M., 2003. *Estudio de la variabilidad climática en la península Ibérica* [Tesis doctoral, Universidad de Extremadura]. <https://dialnet.unirioja.es/descarga/tesis/256.pdf>
- Gómez, E., 1991. El potencial de erosión pluvial por período decadal y su manejo conservacionista. Zona suroccidental departamento de Antioquia (Metodología de Fournier). *Boletín de Ciencias de La Tierra* 10, 1-21. <https://revistas.unal.edu.co/index.php/rbct/article/view/94915>
- Gómez, E., 1999. *Procesos erosivos: Estrategias para su caracterización e implementación de sus prácticas básicas de control y prevención* (Universidad Nacional de Colombia, Ed.). Universidad Nacional de Colombia.
- Hudson, N., 1982. *Conservación del suelo* (Reverté S.A., Ed.). Reverté.
- Instituto de Hidrología, M. y E.A. [IDEAM], Ministerio de Ambiente y Desarrollo Sostenible, Universidad de Ciencias Aplicadas y Ambientales [UDCA], 2015. *Estudio nacional de la degradación de suelos por erosión en Colombia* (IDEAM & UDCA, Eds.). IDEAM y UDCA.
- Instituto Geográfico Agustín Codazzi [IGAC], 2014. Conclusiones - Glosario. In IGAC (Ed.), *Nombres geográficos de Colombia: Región Cundiboyacense, datos pertinentes del proceso de apropiación y socialización del territorio*. Imprenta Nacional de Colombia.
- Kendall, M.G., 1948. *Rank correlation methods* (Charles Griffin & Company Limited, Ed.). <http://125.22.75.155:8080/view/web/viewer.html?file=/bitstream/123456789/11758/1/Rank%20Correlation%20Methods.pdf>
- Lal, R., Monger, C., Nave, L., Smith, P., 2021. The role of soil in regulation of climate. *Royal Society*, B (376), 20210084. <https://doi.org/10.1098/rstb.2021.0084>
- Lamprea Quiroga, P.S., Sanabria Marin, R., 2020. Teoría general de sistemas en el diálogo del conocimiento campesino del altiplano cundiboyacense colombiano con las ciencias edáfica y climática. *Perspectiva Geográfica* 25(2), 34-55. <https://doi.org/10.19053/01233769.9283>
- Linsley, R., Kohler, M., Paulus, J., 1977. *Hidrología para ingenieros* (McGraw-Hill Latinoamericana S.A., Ed.; 2.a). McGraw-Hill.
- Mann, H.B., 1945. Nonparametric Tests Against Trend. *Econometrica* 13(3). <https://doi.org/10.2307/1907187>
- Medina, R., Montoya, C., Jaramillo, A., 2008. Estimación estadística de valores faltantes en series históricas de lluvia. *Cenicafé* 59(3), 260-273.

- National Oceanic and Atmospheric Administration [NOAA], 2021, April 1. *The Oceanic El Niño Index (ONI)*. [http://www.cpc.ncep.noaa.gov/products/analysis\\_monitoring/ensostuff/ensoyears.shtml](http://www.cpc.ncep.noaa.gov/products/analysis_monitoring/ensostuff/ensoyears.shtml)
- Pal, I., 2009. *Rainfall trends in India and their impact on soil erosion and land management*. Thesis Doctor of Philosophy, University of Cambridge. <https://doi.org/10.17863/CAM.13976>
- Renard, K., Freimund, J., 1994. Using monthly precipitation data to estimate the R-factor in the revised USLE. *Journal of Hydrology* 157, 287-306.
- Rojas, E., Arce, B., Peña, A., Boschell, F., Ayarza, M., 2010. Cuantificación e interpolación de tendencias locales de temperaturas y precipitaciones en zonas alto andinas de Cundinamarca y Boyacá (Colombia). *Corpoica. Ciencia y Tecnología Agropecuaria* 11(2), 173-182. <http://www.redalyc.org/articulo.oa?id=449945029009>
- Sen, P.K., 1968. Estimates of regression coefficient base on Kendall's Tau. *Journal of American Statistical Association* 63(324), 1379-1389. <https://www.pacificclimate.org/~werner/zyp/Sen%201968%20JASA.pdf>
- Suresh, R., 2008. *Watershed hydrology. Principles of hydrology*. A. K. Jain & Standard Publishers Distributions.
- Valdés-Pineda, R., Pizarro, R., Valdés, J., Carrasco, P., García-Chevesich, P., Olivares, C., 2016. Spatio-temporal trends of precipitation, its aggressiveness and concentration, along the Pacific coast of South América (36–49°S). *Hydrological Sciences Journal* 61(11), 2110-2132. <https://doi.org/10.1080/02626667.2015.1085989>
- Várallyay, G., 2010. The impact of climate change on soils and on their water management. In *Agronomy Research* (Vol. 8). <http://agronomy.emu.ee/vol08Spec2/p08s214.pdf>
- Xiaofei, M., Chengyi, Z., Jianting Z., 2021. Aggravated risk of soil erosion with global warming. A global meta-analysis. *Catena* 200, 105129. <https://doi.org/10.1016/j.catena.2020.105129>





## SURVEYING THREE-DIMENSIONAL PERSPECTIVES OF THE FLOW STRUCTURE AROUND THE BRIDGE PILE DEPENDING ON THE VEGETATION PATTERN DISTRIBUTION

NAZANIN MOHAMMADZADE MIYAB<sup>1</sup>, RAMIN FAZLOULA<sup>2\*</sup> ,  
MANOUCHEHR HEIDARPOUR<sup>3</sup>, ATAOLLAH KAVIAN<sup>4</sup> ,  
JESÚS RODRIGO-COMINO<sup>5</sup> 

<sup>1</sup>*Ph.D. Graduated, Water Engineering Department, Sari Agricultural Sciences and Natural Resources University, Sari, Iran.*

<sup>2</sup>*Water Engineering Department, Sari Agricultural Sciences and Natural Resources University, Sari, Iran.*

<sup>3</sup>*Water Engineering Department, Faculty of Agriculture, Isfahan University of Technology, Isfahan, Iran.*

<sup>4</sup>*Watershed Management Department, Sari Agricultural Sciences and Natural Resources University, Sari, Iran.*

<sup>5</sup>*Department of Regional Geographic Analysis and Physical Geography, Faculty of Philosophy and Letters, Campus Universitario de Cartuja, University of Granada, 18071 Granada, Spain.*

**ABSTRACT.** Modeling techniques have enabled us to understand how to protect vital infrastructures using nature-based solutions. In this research, we demonstrated that by selecting a specific vegetation pattern distribution upstream of the pile as a nature-based solution, we could reduce the amount of scouring around the bridge piles. This is essential to avoid the negative impacts that occur after landslides, flash floods, or mudflows close to populated areas. This solution can mitigate the global problem of bridge failure. To achieve this goal, an Acoustic Doppler Velocimetry device (ADV) was used to measure the velocity components in an experimental channel with a 90 cm width, 15 meters long, and 60 cm high. Two different widths of vegetation were used: the overall vegetation, with a 90 cm width, and the patched one, with a 10 cm width, positioned upstream of the bridge pile. In the case of using patched vegetation, a 36% reduction was observed in the amount of scouring around the bridge pile compared to the free-vegetation case, showing the positive effect of using vegetation to reduce scouring. In both cases, the amount of negative Reynolds shear stresses decreased when the presence of vegetation was registered. Using octant analysis, the overall vegetation was shown to convert internal events into external ones in front of the pile. However, in the case of using patched vegetation, internal events were also observed in addition to external events. Patchy vegetation changed the transverse direction of outward vortices from internal to external. In the presence of patchy vegetation, the dominance of the inward event decreased sharply. The presence of vegetation in the flow path affected some bursting events and, as a result, reduced scouring. The results showed that each of the used vegetation models has a different effect on bursting events, and these events can affect the amount of scouring hole depth.

***Estudio de las perspectivas tridimensionales de la estructura de flujo alrededor del pilote del puente en función de la distribución del patrón de vegetación***

**RESUMEN.** Las técnicas de modelado nos permiten comprender cómo proteger infraestructuras vitales mediante soluciones basadas en la naturaleza. En esta investigación, demostramos que, al seleccionar una distribución

específica del patrón de vegetación aguas arriba de un pilote, podríamos reducir la cantidad de socavación alrededor de los pilotes de un puente. Esto es clave para evitar los impactos negativos que ocurren después de los deslizamientos de tierra, las inundaciones repentinas o los flujos de lodo cerca de áreas pobladas. Esta solución puede mitigar la desestabilización de infraestructuras como los puentes. Para lograr este objetivo, se utilizó un dispositivo de *Velocimetría Acoustic Doppler* (VAD) para medir los componentes de velocidad en un canal experimental de 90 cm de ancho, 15 metros de longitud y 60 cm de altura. Se utilizaron dos anchos diferentes de vegetación: la vegetación en general, con un ancho de 90 cm, y la parcheada, con un ancho de 10 cm, ubicada aguas arriba del pilote del puente. En el caso de usar vegetación parcheada, se observó una reducción del 36% en la cantidad de socavación alrededor del pilote del puente en comparación con la vegetación libre, mostrando el efecto positivo de utilizar vegetación para reducir la socavación. En ambos casos, la cantidad de tensión negativa de Reynolds disminuyó en presencia de vegetación. Mediante un análisis de octantes, se demostró que la vegetación en general convirtió los eventos internos en externos frente a la estructura. Sin embargo, en el caso de utilizar vegetación parcheada, también se observaron eventos internos además externos. En presencia de vegetación irregular cambió la dirección transversal de los vórtices hacia afuera de internos a externos. En presencia de vegetación irregular, la dominancia del evento interno disminuyó bruscamente. La vegetación en la trayectoria del flujo afectó algunos eventos de fractura y, como resultado, redujo la socavación. Los resultados mostraron que cada uno de los modelos de vegetación utilizados tiene un efecto diferente en los eventos de fractura y estos eventos pueden afectar la profundidad del agujero de socavación.

**Keywords:** Coherent structure, octant analysis, quadrant analysis, vegetation management, nature-based solutions.

**Palabras clave:** Estructura coherente, análisis de octantes, análisis de cuadrantes, gestión de la vegetación, soluciones basadas en la naturaleza.

Received: 20 June 2023

Accepted: 13 November 2023

**\*Corresponding author:** Ramin Fazloulou. Water Engineering Department, Sari Agricultural Sciences and Natural Resources University, Mazandaran province, Iran. E-mail: r.fazloulou@sanru.ac.ir; raminfazl@yahoo.com

## 1. Introduction

Scouring transfers materials from the bed and riverbanks around the bridge piles, abutments, and other hydraulic structures by the water flow (Shahriar *et al.*, 2021). It is important to note that three primary sources of scour contribute to the final results, which are: (i) long-term aggradation and degradation, (ii) contraction scour, and (iii) local scour. Long-term aggradation involves the deposition of material eroded from the upstream of the bridge. In contrast, degradation is scouring that occurs due to a deficit in sediment supply from upstream over relatively long reaches, as appearing in clear-water conditions (Arneson *et al.*, 2012). Several studies in the United States have reported extensive irreparable damages caused by bridge failure due to scour and state that scour around foundation structures is a leading cause of bridge collapse (Briaud *et al.* 2005). The defeat due to erosion and irreparable damages is not only an issue in the United States but globally. Considering the future scenarios where climate change could incorporate a concentration of extreme precipitation events after long periods of droughts, extreme weather conditions, and efficient solutions becoming indispensable (Clarke *et al.*, 2022). The potential economic, financial, and human life lost due to scour-induced failures signifies the importance of identifying the principal causes of scour and taking necessary mitigation actions before damage is incurred (Short *et al.*, 2016).

Many empirical models have been developed to estimate the equilibrium scour depth in bridge piers (Vonkeman and Basson, 2019). The development of these models includes experimental and field

data or both, ultimately leading to the creation of mathematical and numerical models (Shahriar *et al.*, 2021). However, scouring around the piers is a complex process influenced by many factors that are not considered when developing empirical models (Ettema *et al.*, 1998). Also, under the same hydraulic and geometric conditions, different models give significantly different scour estimates. In the design step, using a model that gives non-conservative results may lead to bridge failure, while choosing a very conservative model would lead to an unfavorable economic effect (Beg and Beg, 2013). This issue highlights the necessity of investigating the flow structure around the bridge foundation in different laboratory conditions and understanding and documenting foundation scouring estimation models after a comprehensive understanding of the flow structure.

In general, two approaches have been proposed to prevent the scouring of bridge piers. First, strengthening the bed, and second, changing the flow pattern to reduce the strength of the eddies created around the pile (Zaid *et al.*, 2019). To date, many results have been reported on the interaction between flow and vegetation in channels. For example, the effects of patched vegetation on river morphology, sediment transport, and hydro-environmental sequences have been demonstrated to be very efficient (Caroppi *et al.*, 2019; Afzalimehr *et al.*, 2021). Using vegetation as a nature-based solution would allow protecting rivers, controlling erosion, and trapping sediments (Rossi *et al.*, 2018). Vegetation in rivers and floodplains increases resistance, decreases flow capacity, and changes sediment transport and sedimentation (Mohammadzade *et al.*, 2015). The interaction between flow and vegetation is a complex process, and research in this field has led to essential simplifications in practical applications (Tempest *et al.*, 2015). Investigation of the flow velocity and turbulence intensity distribution around the bridge pile when vegetation is present in the scouring area could provide helpful information. It is well-known that vegetation absorbs significant momentum (Huai *et al.*, 2019), thereby changing the shear stress distribution structure, but this condition has yet to be examined around bridges.

According to past research (Miyab *et al.*, 2022), it can be predicted that the presence of vegetation upstream of the bridge pile can be an effective solution in reducing the amount of scouring. However, investigating the flow structure around the bridge pile is still unknown and has outstanding potential. Supposing the presence of vegetation can be a factor in protecting the bridge piles against the scouring phenomenon. In that case, it will be valuable to analyze its interaction with the flow around the bridge foundations based on studying turbulent flow components. In addition to being simple and cost-effective, the vegetation solution does not add to the construction costs. Although the studies conducted on the scouring of bridge foundations are extensive, they have yet to provide a single solution to reduce scouring for different hydraulic conditions, which indicates a weakness in understanding the structure and behavior of the flow around the bridge foundation. Also, most of the methods used in the studies are not environmentally friendly. Therefore, in the current research, the vegetation cover upstream at different spatial patterns will be evaluated as an effective solution to change the flow structure to reduce the eddies created around the bridge pile. This research desires to recognize the coherent flows formed around the bridge pile in the presence and absence of vegetation through quadrant and octant analysis. Furthermore, the amount of Reynolds shear stress and scour profile formed around the bridge support are investigated when vegetation is located upstream of the bridge pile.

This research aims to investigate the effect of different vegetation patterns upstream of bridge piles on flow structure, coherent flows, Reynolds shear stress, and scour profile. Specifically, it will compare the flow velocity and turbulence intensity distribution around bridge piles with and without vegetation and analyze the effect of different vegetation patterns on bursting events and scour depth. We consider this research significant in terms of multidisciplinary due to its diverse applications within control measures related to physical geography, forestry, civil, and terrain engineering studies. Vegetation cover is a simple, cost-effective, and environmentally friendly solution to reduce the loss of money invested in vital infrastructures. This study allows us to understand the flow structure around bridge piles with vegetation, which could be essential for designing effective protection measures for land management plans from the catchment to the regional scales.

## 2. Methods and Materials

### 2.1. Experimental channel

This study was conducted in a flume with a length of 15 meters, a width of 90 cm, and a height of 60 cm, featuring a maximum flow rate of 50 liters per second, located in the hydraulic laboratory of Isfahan University of Technology. The flume had a plexiglass bottom and sidewalls, presenting a rectangular cross-section. The water level was regulated by a sliding gate downstream of the flume. To mitigate turbulence in the flow, there was a flow-calming chamber in the inlet tank constructed with perforated bricks and honeycomb. A digital flow meter measured the flow rate of the inlet stream. Throughout the channel, excluding one meter at the beginning and end, a Teflon platform was installed, standing 20 cm high. A layer of sediments, composed of bed material, was affixed to the platforms to adjust the roughness coefficient. In each series of experiments, a one-meter distance between two platforms was filled with sifted sand, and its surface was smoothed entirely using a trowel and a leveler. Figure 1a shows the schematic view of the experimental channel.

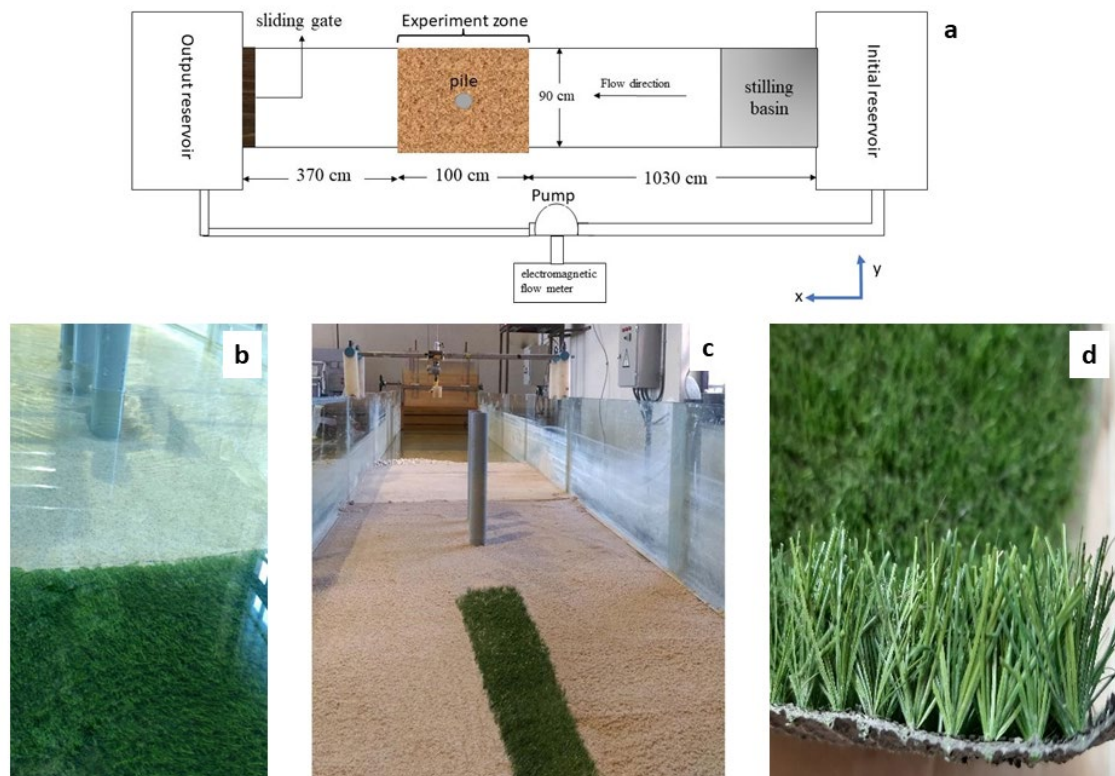


Figure 1. a) The schematic view of the experimental, b) the distribution of overall vegetation upstream of the bridge pile, c) the distribution of patch vegetation upstream of the bridge pile and figure d) the density of used vegetation channel.

### 2.2. Depth and velocity meters

A limnimeter with an accuracy of 1 mm was used to measure the scour hole profile. This limnimeter was placed on a frame with four support points on the upper edge of the channel. Two parallel bars were attached to the frame body for its transverse movement. In this way, the limnimeter could move in two directions perpendicular to each other and easily measure the scour profile (Kabiri *et al.*, 2022). Velocity measurement was conducted at different points using the new generation ADV three-dimensional velocity meter manufactured by Nortek, Norway. Due to the cable structure of this device, it was possible to measure the velocity from different angles. The manufacturer calibrated this device,

and it remains unchanged as long as the device is not physically damaged. This device can assess the characteristics of turbulence. One of the merits of this device is its ability to collect data with high frequency and measure far from the desired surface, minimizing the difference caused by the presence of the measuring device in the flow. Measurements in the ADV device are based on a physical phenomenon called the Doppler effect.

The number of raw data recorded by the device depends on the frequency set for the device and the measurement time. In this project, ADV was set to 200 Hz and 2 minutes, resulting in the average velocity of a point among  $120 \times 200 = 24,000$  points. Additional data collection and filtering software used were Vectrino+, WinADV, and Excel. To filter the data for each point among the 24,000 collected velocities, inappropriate data (correlation  $< 70$  and SNR  $< 15$  or SNR  $< 5$ ) were removed, and based on other data, the average speed was obtained (Nortek, 2004).

### 2.3. The bed material size and pile diameter

In this study, following Chiew and Melville (1987), the diameter of the pile was chosen to be 5 cm (symbol  $D$ ). The distance between the axis of the pile and the wall was suitable because of the channel width. The bridge pile was installed at a distance of 1062 cm from the channel's beginning. According to Raudkivi and Ettema (1983), to achieve the maximum scouring depth, the formation of ripples should be prevented. For this purpose, the average size of sediment particles should be greater than 0.7 mm. Chiew and Melville (1987) acknowledged that when the ratio of the pile diameter to the average size of the particles is greater than 50, the effect of the particle size on the scour depth can be ignored. In this research, sand particles with a diameter greater than 0.7 mm will be selected. The characteristics of the bed material are as follows (Pope, 2000):

$$\sigma_g = \left(\frac{d_{84}}{d_{16}}\right)^{0.5} \tag{1}$$

$$Gr = \frac{1}{2} \left(\frac{d_{84}}{d_{50}} + \frac{d_{50}}{d_{16}}\right) \tag{2}$$

$$D_g = (d_{16} \cdot d_{84})^{0.5} \tag{3}$$

$$Cu = \frac{d_{60}}{d_{10}} \tag{4}$$

Where  $d_{50}$  represents the average size of sediment particles,  $Cu$  is the uniformity coefficient,  $Dg$  means the geometric mean size,  $\sigma_g$  corresponds to the standard geometric deviation and  $Gr$  registers the grading factor. According to the uniformity coefficient of  $Cu$  and  $d_{50}$ , the type of sand bed material was uniform (McGlinchey, 2009). Table 1 shows the geometric characteristics of sediment particles.

Table 1. Geometric characteristics of sediment particles used in this research.

<b>d<sub>50</sub> (mm)</b>	<b>Cu</b>	<b>Dg</b>	<b>σg</b>	<b>Gr</b>
0.77	1.133	0.763	1.075	1.075

The thickness of the bed was determined according to the maximum scour depth. For this purpose, an estimate of the maximum scour depth was first obtained. Laursen (1963) presented the relationship based on the pile diameter to calculate the maximum scour depth.

$$d_{sm} = 1.05D^{0.75} \tag{5}$$

Where  $D$  is the pile diameter in meters and  $d_{sm}$  is the maximum scour depth in meters. Therefore, with the help of the above relationship and the chosen diameter of 5 cm for the pile, the maximum scouring depth of 11 cm was obtained, so the height of the substrate particles chose 20 cm to ensure accuracy.

## 2.4. Experimental setup

Two types of dense artificial grass vegetation with a height of two centimeters (10 % of the flow depth) were located upstream of the bridge pile. The vegetation used width is once 90 cm, i.e., the entire width of the stream ( $V_o$ ), and once 10 cm of the stream width ( $V_p$ ) in the central axis of the channel. The vegetation cover was placed 30 cm above the bridge pile. Figure 1b shows the distribution of overall vegetation upstream of the bridge pile, Figure 1c shows the distribution of patch vegetation upstream of the bridge pile and Figure 1d shows the density of used vegetation. A single pile with a 5 cm diameter was placed perpendicular to the bed in the flow direction to conduct the experiments. The shields diagram was used to determine the appropriate hydraulic conditions for maximum scour (Cao *et al.*, 2006). An average flow rate of 0.036 m<sup>3</sup>/s and a depth of 20 cm were established for the channel's sand bed. At the experiment's end, the scour hole dimensions were measured. Eventually, several velocity profiles were taken using ADV upstream and downstream of the bridge pile.

## 2.5. Reynolds shear stress (RSS)

Reynolds shear stress (RSS) is a measure of the friction between layers of a fluid due to turbulent flow. It is a key factor in sediment transport and other physical processes. RSS is caused by the uneven motion of fluid particles in turbulent flow. When fluid particles collide with each other, they transfer momentum from one particle to another. This transfer of momentum creates friction between the layers of fluid. RSS is important in physical geography and civil and terrain engineering studies because it plays a role in various physical processes, such as sediment transport, erosion, and deposition. For example, RSS can erode riverbanks and transport sediment downstream. It can also cause the deposition of sediment in floodplains and estuaries. RSS is also crucial for understanding river flow and other fluid dynamics. Turbulent currents account for a significant part of river flows. In this flow type, fluid particles deviate from their original path and move irregularly. In this case, in addition to the fluid's inherent viscosity, the dispersed movements of particles also contribute to flow resistance, and a feature called eddy viscosity is introduced to express it (Pickering *et al.*, 2021).

Turbulent flow characteristics play a significant role in the sediment transport process, including diffusion, erosion, sedimentation, and flow resistance. In turbulent flow, the generation and destruction of small and large eddies cause fluctuations in flow parameters. In this flow, instantaneous parameters such as velocity can be expressed as follows:

$$u = \bar{u} + u' \quad (6)$$

$$v = \bar{v} + v' \quad (7)$$

$$w = \bar{w} + w' \quad (8)$$

Where  $\bar{u}$ ,  $\bar{v}$  and  $\bar{w}$  are the time average of the velocity components in x, y and z directions and  $u'$ ,  $v'$  and  $w'$  are the fluctuation values of velocity.

Reynolds shear stress is calculated from the following equation:

$$\tau = -\rho u'w' \quad (9)$$

## 2.6. Quadrant analysis

Turbulent flow in open channels is not a completely random process. However, some continuous temporal and spatial patterns can be identified in them. These patterns are known as coherent structures in turbulent flow. They significantly affect the distribution of shear stress in open channel processes. As a result, coherent structures play an essential role in the erosion and sedimentation of the bed, the phenomena of mixing, nutrient distribution in the river, and aquatic plant implantation. Coherent structure in flow refers to a three-dimensional region of the flow in which at least one of the main

variables of the flow (for example, velocity, temperature, and density components) shows a significant correlation with itself and with another variable in a range of time and space. This temporal and spatial spectrum is much larger than the flow's most minor local temporal and spatial scales (Cellino and Lemmin, 1999).

Turbulence has a significant inherent complexity, leading to various interpretations of its nature. The quadrant analysis method is used to study the presence of coherent structures in flow fields and their contribution to the total shear stress. The quadrant analysis method involves studying the relationship between the velocity fluctuations in the flow direction ( $u'$ ) and perpendicular to the flow ( $w'$ ). For this,  $u'$  and  $w'$  are plotted against each other, forming a quadrant plane in the trigonometric coordinate system, as indicated in Table 2. This plane represents a bursting cycle (Carino and Brodkey, 1969; Lu and Willmarth, 1973; Willmarth and Lu, 1972), including the four events.

Table 2. A quadrant plane in the trigonometric coordinate system.

Bursting name	Quadrant	$u'$	$w'$	Property
Outward	Q1	+	+	High speed fluid away from the bottom
Ejection	Q2	-	+	Low speed fluid away from the bottom
Inward	Q3	-	-	Low speed fluid moving to the bottom
Sweep	Q4	+	-	High speed fluid moving to the bottom

The occurrence probability of event  $k$  is calculated as the normalized occurrence frequency,  $f_k$ , for a particular class of events related to different classes of events (Termini, 2015):

$$f_k = \frac{n_k}{N} \tag{10}$$

$$N = \sum_1^4 n_k \quad k = 1, 2, \dots, 4$$

Primary research to understand the turbulent structure of coherent flows in channel walls and beds dates back to the last 30 years (Corino and Brodkey, 1969; Kline *et al.*, 1967; Kim *et al.*, 1971; Grass 1971; Afzalimehr and Anctil, 2000). Some researchers interpreted this coherent structure as periodically organized events in the time domain that manifest their impact in the Reynolds shear stress time series (Carino and Brodkey, 1969; Lu and Willmarth, 1973). The first event ( $Q_1$ ) involves the occurrence of high-velocity fluid movement from the bed to the water surface, the second event ( $Q_2$ ) is characterized by low-velocity fluid movement to the water surface, the third event ( $Q_3$ ) involves low-velocity fluid movement toward the bed, and the fourth ( $Q_4$ ) event shows high-velocity fluid movement towards the bed. The cycle that includes these four events is referred to as bursting events (Kabiri *et al.*, 2022). It is important to note that ejection and sweep events generate turbulent energy, and outward and inward interactions are associated with energy dissipation. Additionally, ejection and sweep are often linked to the removal and transfer of sediments (Pope, 2000; Vijayasree *et al.*, 2020). Sweep events are associated with the initiation of bed load movement, while ejections are responsible for lifting and carrying the bed load (Sterk *et al.*, 1998). The investigation of the flow downstream of the submerged vegetation patch by Mayaud *et al.* (2016) demonstrated high frequencies of  $Q_2$  (ejection) and  $Q_4$  (sweep) events in the crest of the vegetation patch (Mayaud *et al.*, 2016). In contrast, it is reported that the dominance of outward and inward interactions in the shear layer is induced by the flow passing above the vegetation patch, which is a notable characteristic of the flow in the downstream region of a submerged vegetation patch in a more distant region (Kazem *et al.*, 2021a; Przyborowski *et al.*, 2019; Keshavarzi *et al.*, 2014).

## 2.7. Octant analysis

As mentioned, quadrant analysis is based on the analysis of the probability distribution of the two longitudinal ( $u'$ ) and vertical components ( $v'$ ) of the velocity fluctuation. However, in rivers and natural channels, the flow structure is coherently structured in three dimensions, especially where an obstacle is placed in the flow path. The velocity in the lateral direction cannot be neglected, as it can induce significant secondary circulation (Keshavarzi *et al.*, 2014). Additionally, two-dimensional analysis cannot define sediment entrainment as a three-dimensional phenomenon (Ortiz *et al.*, 2013; Zong and Nepf, 2010). In general, eight burst event classes in 3D octant analysis are defined based on the sign of velocity fluctuations, as outlined in Table 3. The symbols used in this research are inspired by the work of Keshavarzi *et al.* (2014) and Kazem *et al.* (2021b). Keshavarzi (2014) stated that the deviations of group events are towards the internal direction or the central line (internal events), while the deviations of group B events are away from the central line and towards the channel walls (external events) (Keshavarzi *et al.*, 2014). This study considers three categories of results for octant analysis: (1) the probability of occurrence of bursting events ( $Op$ ), (2) the attack angle of bursting events, and (3) the stability of each event ( $S_i$ ). Calculating the probability of occurrence of events is similar to the quadrant analysis approach. It is equal to the frequency of occurrence ( $f_k$ ) for a specific event class relative to different events (Bento *et al.*, 2021).

$$f_k = \frac{n_k}{N} \quad (11)$$

$$N = \sum_{k=1}^8 n_k, k = 1, 2, 3, \dots, 8$$

Table 3. Eight bursting event classes in 3D octant analysis based on the sign of velocity fluctuations.

Group	Classes of Bursting Events	Class name	$u'$	$v'$	$w'$
A (internal)	Outward interaction	PPP	+	+	+
	Ejection	NNP	-	-	+
	Inward interaction	NNN	-	-	-
	Sweep	PPN	+	+	-
B (external)	Outward interaction	PNP	+	-	+
	Ejection	NPP	-	+	+
	Inward interaction	NPN	-	+	-
	Sweep	PNN	+	-	-

Octant analysis is a method for classifying bursts of turbulence in three dimensions, offering more detail than quadrant analysis, which only considers two dimensions. Turbulent bursts are sudden, localized increases in turbulence intensity and play a crucial role in sediment transport and other physical processes. The probability of occurrence of a burst is the fraction of time that the burst occurs at a given point in the flow field. The attack angle of a burst is the angle between the mean flow direction and the direction of the burst. The stability of a burst is a measure of how long the burst lasts. Table 3 displays the eight bursting event classes in 3D octant analysis based on the sign of velocity fluctuations. In this table, the symbol  $N$  is used for velocity fluctuations with a negative value, and  $P$  is used for positive velocity fluctuations in the class name column. The first letter represents  $u'$ , the second letter represents  $v'$ , and the third letter represents  $w'$ . The force applied to sediment particles in the bed strongly depends on the angle of inclination of the three-dimensional flow velocity fluctuations ( $\theta_i$ ). Understanding the attack angle of bursting events helps comprehend the entrainment sediment process (Breusers *et al.*, 1977; Bridge and Bennett 1992; Esfahani and Keshavarzi, 2011; Esfahani and Keshavarzi, 2013; Bernard and Handler, 1990). The attack angle is calculated as follows:

$$\theta_i = \left| \arctan \left( \frac{w'}{\sqrt{u'^2 - v'^2}} \right) \right| \quad (12)$$

Esfahani and Keshavarzi (2013, 2021) and Liu and Bai (2013) employed the aforementioned technique to comprehend the bursting process in a meandering channel (Liu and Bai, 2013; Carnacina *et al.*, 2019; Guan *et al.*, 2019). They recognized that this technique offers greater clarity in understanding coherent flow structures and their impact on sediment entrainment in meanders. Keshavarzi (2014) delved into the coherent structures around the bridge pile (Keshavarzi *et al.*, 2014). Their findings indicated that near the bed, internal ejection and external sweep events play a role in the scouring mechanism around the single bridge pile. Using this technique, Kazem *et al.* (2021b) examined the eddy structures in a channel with patched vegetation (i.e., artificial bars). They observed that in a channel with a small width of vegetation patch, the flow passing through the vegetation (x direction) and the side flow around the vegetation patch significantly influence the formation of flow structures outside the vegetation (Kazem *et al.*, 2021b). MATLAB programming software was employed for quadrant and octant analysis, and subsequent results were analyzed.

### 3. Results and discussion

#### 3.1. Scouring contour map

Figure 2 (2a-2c) displays contour maps of scouring profiles for single piles without vegetation, with overall vegetation, and with patch vegetation, respectively. In all figures, the X-axis represents the distance from the beginning of the channel, and the flow direction is from left to right. Scouring depths are 6.5 cm in the free-vegetation case, 4.7 cm in the overall vegetation case (Vo-case), and 4.1 cm in the patchy vegetation case (Vp-case). According to the results of this research, the highest amount of scouring occurred in the free-vegetation case. Patched vegetation could reduce the scour depth by 36%. Additionally, vegetation decreased the longitudinal and transverse expansion of the scouring hole.

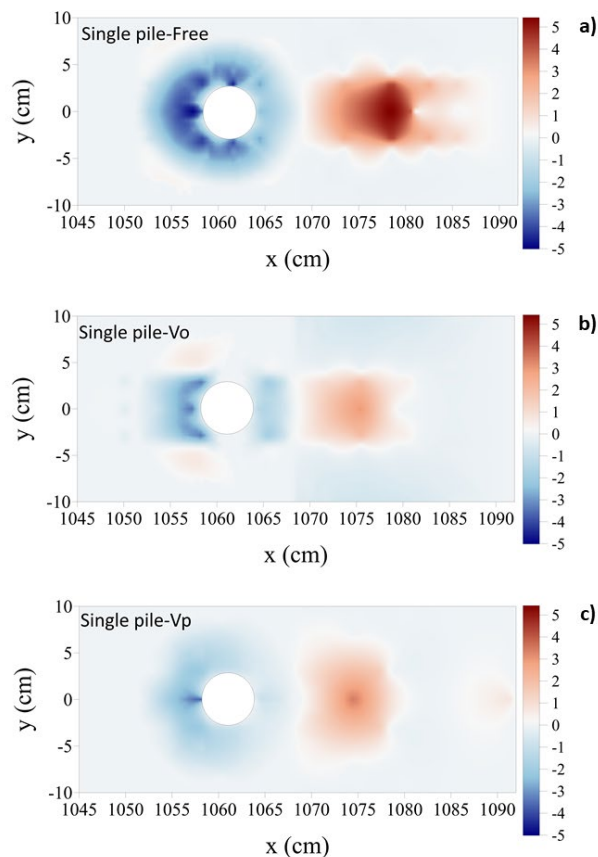


Figure 2. Contour map of scour profile for single pile a) in without vegetation case, b) in the presence of overall vegetation case and c) in the presence of patched vegetation case.

### 3.2. Reynolds shear stress

Figure 3 illustrates the distribution of Reynolds shear stress (RSS). The horizontal axis ( $x$ ) indicates the distance from the beginning of the channel in centimeters, and the vertical axis ( $z$ ) indicates the height from the bed represented in centimeters too. Given that RSS is proportional to the flow's capacity to transport sediments and reflects the exchange of turbulent motion between fluid layers, it is understandable that such capacity increases with the enlargement of the scour hole (Bernard Handler, 1990; Carnacina *et al.*, 2019). In all cases upstream of the pile, the region with the maximum RSS developed upstream of the scour hole. This is where the maximum flow power for scouring (area of large value enlarged) was established, aligning with the findings of Bento *et al.* (2021) and Guan *et al.* (2019). The maximum RSS occurs upstream of the pile where the maximum positive and negative velocity values occur, indicating that the velocity in this region can be highly unstable.

The presence of vegetation decreased the negative values of shear stress and reduced the intensity of RSS upstream of the pile. Downstream of the bridge pile, the negative values of shear stress increased, especially at the point closest to the pile, where these negative values are higher in the Vo-case. In the Vo-case, the highest shear stress values downstream of the pile occurred where the accumulation of sediments was observed.

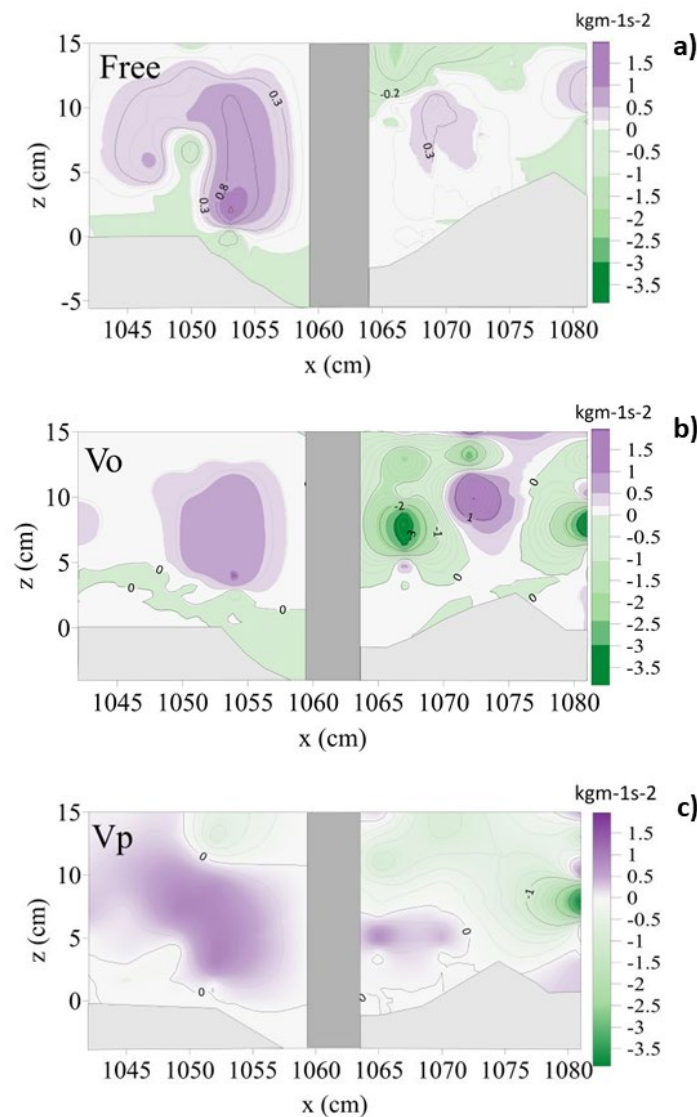


Figure 3. Reynolds shear stress distribution profile for single pile a) in without vegetation case, b) in the presence of overall vegetation case and c) in the presence of patched vegetation case.

### 3.3. Quadrant analysis

Figure 4 depicts the occurrence probability of quadrant classes. The location of the bridge pile is from  $x=1059.5$  cm to  $x=1064.5$  cm. The results demonstrated that in the upstream of the pile in the free-vegetation case, the sweep near the bed and the inward in the middle part of the flow depth were the dominant events, both of which increased as they approached the pile. The presence of vegetation caused a significant increase in the probability of ejection events at points very close to the bed and near the water surface and the sweep events at mid-depth points and near the bed. Kabiri (2022) also observed an increase in the probability of ejection and sweep in the presence of vegetation, which can be caused by a decrease in momentum of the water flow. In the free-vegetation case, the possibility of ejection and outward events is dominant downstream of the pile. In the presence of vegetation, the probability of an outward event increased in the middle flow depth range and was closer to the bed. Also, the ejection increased in the Vo-case near the water surface and in the Vp-case in the mid-depth of flow. In the upstream of the pile, the zone of ejection events in the Vp-case is closer to the water level than Vo-case, which is in accordance with Kazem et al.'s results (2021b). Downstream of the pile in the Vp-case, the ejection and sweep events are closer to the water surface and the outward and inward are closer to the bed. Also, the possibility of outward and inward occurrences has increased. The horizontal axes show  $x$ (cm), and the vertical axes show  $z$ (cm).

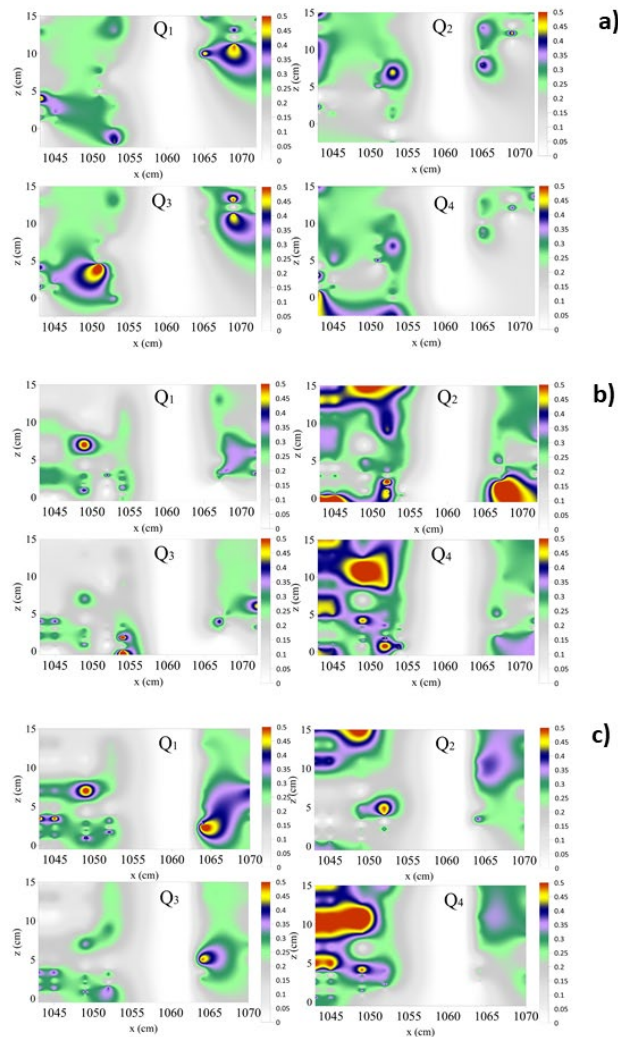


Figure 4. Probability of occurrence of quadrant classes profile for single pile a) in without vegetation case, b) in the presence of overall vegetation case and c) in the presence of patched vegetation case.



In classes A and B of the second zone, the  $O_p$  of events was between 18 and 26 % (26% belonging to internal sweep), showing no dominant event. However, in terms of stability, internal ejection with 46 and internal sweep events with 45.3 was the most stable. In the third zone, the  $O_p$  varied between 15 and 24% (24 % belonging to internal ejection), and the  $S_t$  varied between 30 and 40%. Sediment scoured from the upstream accumulated behind the pile, creating a mound of sediment that caused Zone 1 to be absent. In the second zone downstream of the pile, external ejection is dominant, with a 30%  $O_p$  and  $S_t$  of 58 near the mound of sediments. Also, above that, internal outward is the most dominant event with a 47%  $O_p$  and  $S_t$  of 50. In the third zone near the water surface, internal inward, with a 47%  $O_p$  and  $S_t$  of 50, and external ejection, with a 43%  $O_p$  and  $S_t$  of 47, are the dominant events near the second zone. Angles of attack downstream of the pile are reduced compared to the upstream.

Figure 6 shows the results of the  $O_p$  of octant analysis event sample, and the  $S_t$ 's value of each octant event of Group B in the free-vegetation case. The numbers written inside the graphs show the angle of each event in radians. In the Vo-case at the pile upstream: in  $z > 0$  cm, the dominant events are external ejection with a 60 %  $O_p$  and 57 %  $S_t$  and external inward with a 52 %  $O_p$  and 55 of  $S_t$ , and in  $z < 0$  cm internal outward with 41 %  $O_p$  and  $S_t$  57 is dominant. In the second zone, the  $O_p$  of events varied between 19 and 35 percent. In terms of stability, external outward with an  $O_p$  of 35 % and  $S_t$  of 57, followed by external sweep with an  $O_p$  of 34 % and  $S_t$  of 55, were the most dominant events. In the third zone, the external sweep is with an  $O_p$  of 52 % and  $S_t$  of 61, and in the second place is external ejection with an  $O_p$  of 30 % and  $S_t$  of 41.

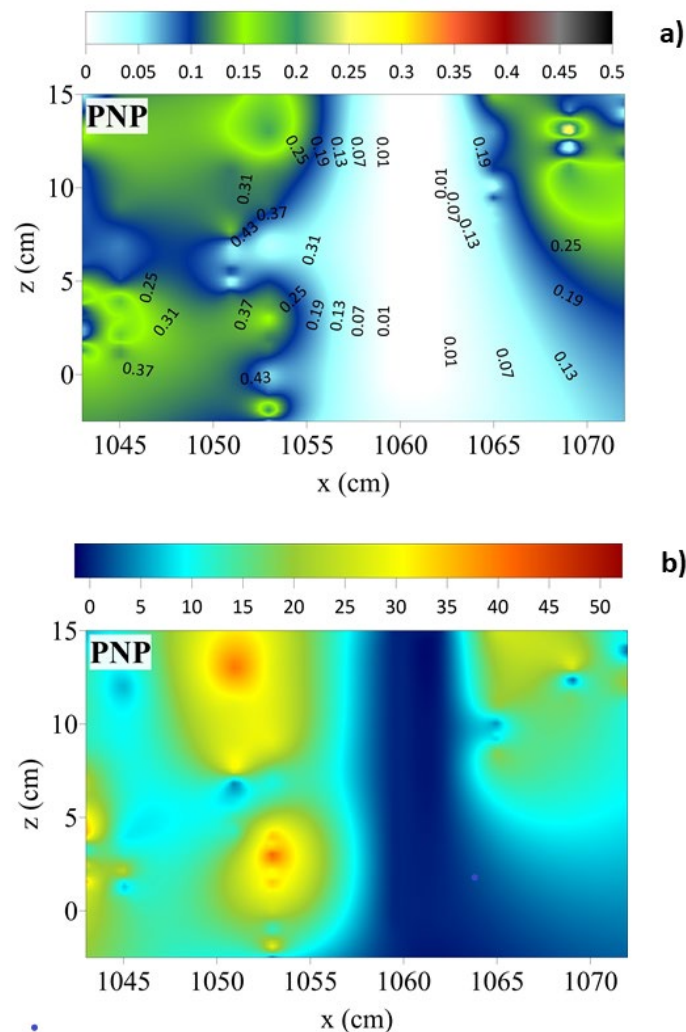


Figure 6. The sample of B group events of octant analysis: a) the  $O_p$  results; b) the  $S_t$  in free vegetation case.

Downstream of the pile in the first zone, external ejection was the most dominant event with  $O_p$  of 63 % and  $S_t$  of 45 %, followed by internal outward with a 33 %  $O_p$  and  $S_t$  of 56 %. In the second zone, internal outward with an  $O_p$  of 31 %,  $S_t$  of 52 % after that, internal ejection with an  $O_p$  of 29 %, and  $S_t$  of 41 % are the dominant events. In the third zone, the range of  $O_p$  was observed between 13 and 20 percent, showing no dominant phenomenon in this zone. In terms of  $S_t$ , external sweep had the highest stability, i.e., 42. Figure 7 shows the events of octant analysis: (a) the  $O_p$  results; (b) the  $S_t$  in Vo-case. Upstream of the bridge pile in the Vp-case: in the first zone, internal outward with a 61%  $O_p$  and 42  $S_t$ , external sweep with a 39%  $O_p$  and 42  $S_t$ , and internal ejection with 36%  $O_p$  and 65  $S_t$  were the most dominant events. In the second zone, external sweep with  $O_p$  of 45% and  $S_t$  of 59, internal ejection with a probability of 36% and stability of 65%, and external outward with an  $O_p$  of 35% and  $S_t$  of 57% were the dominant events. In the third zone, the external sweep was dominant with an  $O_p$  of 52% and  $S_t$  of 62 events.

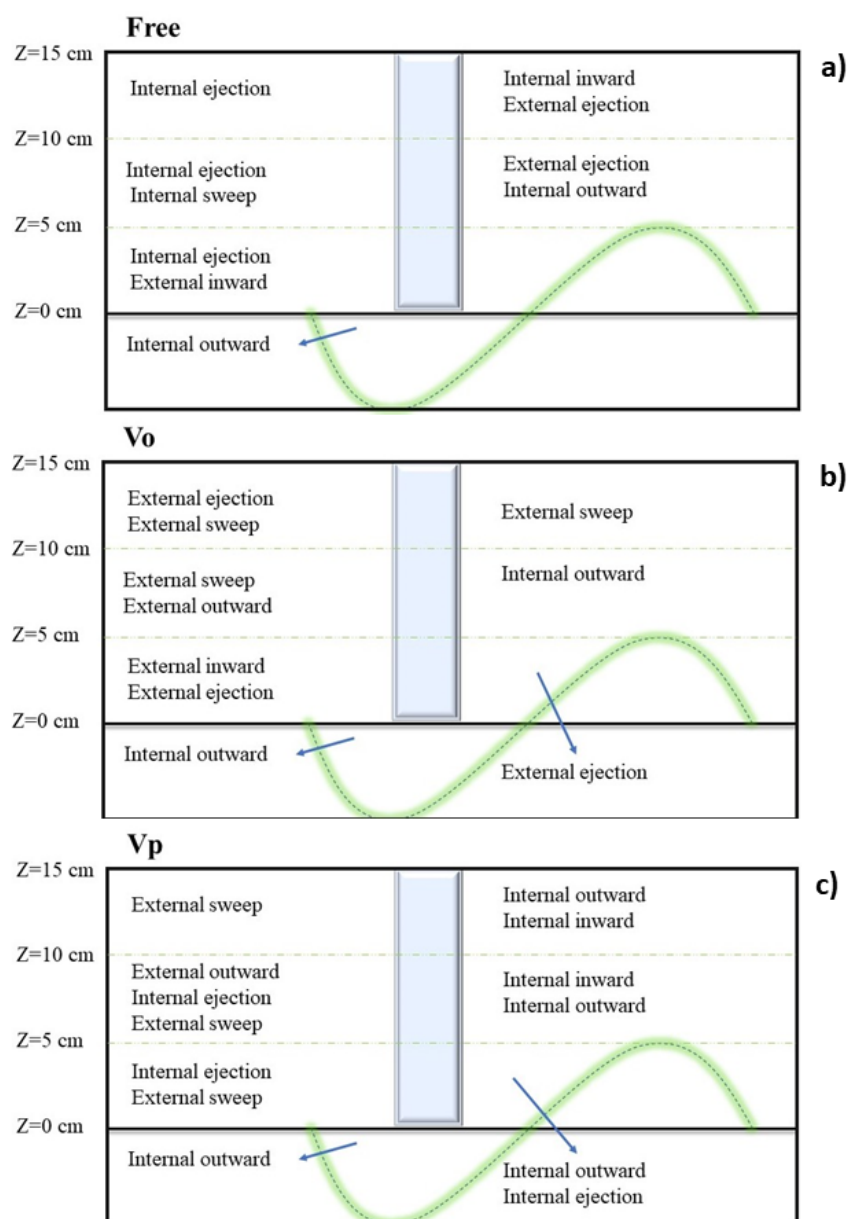


Figure 7. Schematic diagram of dominant phenomena upstream and downstream of the bridge pile a) in without vegetation case, b) in the presence of overall vegetation case and c) in the presence of patched vegetation case.

Downstream of the bridge pile in the Vp-case: in the first zone, internal outward with 47 %  $O_p$  and 52  $S_t$  and internal ejection with 37 %  $O_p$  and 50  $S_t$  were the most dominant events. In the second zone, internal inward with  $O_p$  of 37 % and  $S_t$  of 50 and internal outward with  $O_p$  of 31 % and  $S_t$  of 51 were the dominant phenomena. In the third zone, the  $O_p$  was between 9 and 26 percent, which internal outward having the most dominance with a 26 %  $O_p$  and 61  $S_t$ . In terms of stability, internal inward has a  $S_t$  of 60 with an  $O_p$  of 18. Figure 7 schematically shows the bridge's pile, which phenomenon prevails in each zone.

#### 4. Conclusions

This study highlights the substantial impact of vegetation on scour rate, Reynolds stress, and coherent flow structure around bridge piles. The presence of vegetation results in a remarkable 36% reduction in scour depth and induces changes in the distribution of Reynolds stress. The maximum Reynolds stress region shifts upstream of the pile, leading to a decrease in negative shear stress upstream and an increase downstream. Quadrant analysis illustrates that vegetation promotes the occurrence of ejection and sweep events, while octant analysis indicates the dominance of internal outward events within the scour hole. In the free-vegetation case, near the bed, the eddies move toward the walls, but as one moves away from the bed, the eddies shift toward the central axis. The overall vegetation redirects the flow towards the walls in the base area, reducing scouring. Stability and event probability increase with the presence of vegetation. Overall vegetation transforms internal events into external ones in front of the pile. However, in the case of patched vegetation, both internal and external events are observed. With a potential 36% reduction in scour depth, vegetation can play a crucial role in mitigating flood risk and stabilizing bridge structures. Future research should delve into quantifying the effects of various vegetation patterns and densities on flow characteristics and scour development. The findings hold substantial implications for flood risk management. Vegetation emerges as a key player in reducing flow velocity and scour depth, thereby enhancing flood resilience and decreasing the risk of bridge failure due to erosion. Engineers can leverage this information to inform the design and maintenance of structures in flood-prone areas, considering vegetation management strategies to bolster flood resilience.

#### References

- Afzalimehr, H., Riazi, P., Jahadi, M., Singh, V.P., 2021. Effect of vegetation patches on flow structures and the estimation of friction factor. *ISH Journal of Hydraulic Engineering* 27(sup1), 390-400. <https://doi.org/10.1080/09715010.2019.1660920>
- Afzalimehr, H., Anctil, F., 2000. Accelerating shear velocity in gravel-bed channels. *Hydrological Sciences Journal* 45(1), 113-124. <https://doi.org/10.1080/02626660009492309>
- Arneson, L.A., Zevenbergen, L.W., Lagasse, P.F., Clopper, P.E., 2012. *Evaluating scour at bridges* (No. FHWA-HIF-12-003). National Highway Institute (US).
- Beg, M., Beg, S., 2013. Scour reduction around bridge piers: A review. *International Journal of Engineering Inventions* 2(7), pp.7-15.
- Bento, A.M., Viseu, T., Pêgo, J.P., Couto, L., 2021. Experimental characterization of the flow field around oblong bridge piers. *Fluids* 6(11), 370. <https://doi.org/10.3390/fluids6110370>
- Bernard, P.S., Handler, R.A., 1990. Reynolds stress and the physics of turbulent momentum transport. *Journal of Fluid Mechanics* 220, 99-124. <https://doi.org/10.1017/S0022112090003202>
- Briaud, J.L., Chen, H.C., Li, Y., Nurtjahyo, P., Wang, J., 2005. SRICOS-EFA method for contraction scour in fine-grained soils. *Journal of Geotechnical and Geoenvironmental Engineering* 131(10), 1283-1294. [https://doi.org/10.1061/\(ASCE\)1090-0241\(2005\)131:10\(1283\)](https://doi.org/10.1061/(ASCE)1090-0241(2005)131:10(1283))
- Breusers, H.N.C., Nicollet, G., Shen, H.W., 1977. Local scour around cylindrical piers. *Journal of Hydraulic Research* 15(3), 211-252. <https://doi.org/10.1080/00221687709499645>

- Bridge, J.S., Bennett, S.J., 1992. A model for the entrainment and transport of sediment grains of mixed sizes, shapes, and densities. *Water Resources Research* 28(2), 337-363. <https://doi.org/10.1029/91WR02570>
- Carnacina, I., Leonardi, N., Pagliara, S., 2019. Characteristics of flow structure around cylindrical bridge piers in pressure-flow conditions. *Water* 11(11), 2240. <https://doi.org/10.3390/w11112240>
- Cao, Z., Pender, G., Meng, J., 2006. Explicit formulation of the Shields diagram for incipient motion of sediment. *Journal of Hydraulic Engineering* 132(10), 1097-1099. [https://doi.org/10.1061/\(ASCE\)0733-9429\(2006\)132:10\(1097\)](https://doi.org/10.1061/(ASCE)0733-9429(2006)132:10(1097))
- Caroppi, G., Västilä, K., Järvelä, J., Rowiński, P.M., Giugni, M., 2019. Turbulence at water-vegetation interface in open channel flow: Experiments with natural-like plants. *Advances in Water Resources* 127, 180-191. <https://doi.org/10.1016/j.advwatres.2019.03.013>
- Cellino, M., Lemmin, U., 1999. Coherent flow structure analysis in suspension flows. *Proc. (CD-ROM) 28th IAHR Congr.*
- Clarke, B., Otto, F., Stuart-Smith, R., Harrington, L., 2022. Extreme weather impacts of climate change: an attribution perspective. *Environmental Research: Climate*, 1(1), p.012001.
- Chiew, Y.M., Melville, B.W., 1987. Local scour around bridge piers. *Journal of Hydraulic Research*, 25(1), 15-26. <https://doi.org/10.1080/00221688709499285>
- Corino, E.R., Brodkey, R.S., 1969. A visual investigation of the wall region in turbulent flow. *Journal of Fluid Mechanics* 37(1), 1-30. <https://doi.org/10.1017/S0022112069000395>
- Esfahani, F.S., Keshavarzi, A., 2011. Effect of different meander curvatures on spatial variation of coherent turbulent flow structure inside ingoing multi-bend river meanders. *Stochastic environmental research and risk assessment* 25(7), 913-928. <https://doi.org/10.1007/s00477-011-0506-4>
- Esfahani, F.S., Keshavarzi, A., 2013. Dynamic mechanism of turbulent flow in meandering channels: considerations for deflection angle. *Stochastic Environmental Research and Risk Assessment* 27(5), 1093-1114. <https://doi.org/10.1007/s00477-012-0647-0>
- Ettema, R., Melville, B.W., Barkdoll, B., 1998. Scale effect in pier-scour experiments. *Journal of Hydraulic Engineering* 124(6), pp.639-642.
- Grass, A.J. 1971. Structural features of turbulent flow over smooth and rough boundaries. *Journal of Fluid Mechanics* 50(2), 233-255. <https://doi.org/10.1017/S0022112071002556>
- Guan, D., Chiew, Y.M., Wei, M., Hsieh, S. C. 2019. Characterization of horseshoe vortex in a developing scour hole at a cylindrical bridge pier. *International Journal of Sediment Research* 34(2), 118-124. <https://doi.org/10.1016/j.ijsrc.2018.07.001>
- Huai, W.X., Zhang, J., Wang, W.J., Katul, G.G., 2019. Turbulence structure in open channel flow with partially covered artificial emergent vegetation. *Journal of Hydrology* 573, pp.180-193. <https://doi.org/10.1016/j.jhydrol.2019.03.071>
- Kabiri, F., Tabatabai, M.R.M., Shayannejad, M., 2022. Effect of vegetative bed on flow structure through a pool-riffle morphology. *Flow Measurement and Instrumentation*, 102197. <https://doi.org/10.1016/j.flowmeasinst.2022.102197>
- Kazem, M., Afzalimehr, H., Sui, J., 2021a. Characteristics of turbulence in the downstream region of a vegetation patch. *Water* 13(23), 3468. <https://doi.org/10.3390/w13233468>
- Kazem, M., Afzalimehr, H., Sui, J., 2021b. Formation of coherent flow structures beyond vegetation patches in channel. *Water* 13(20), 2812. <https://doi.org/10.3390/w13202812>
- Keshavarzi, A., Melville, B., Ball, J., 2014. Three-dimensional analysis of coherent turbulent flow structure around a single circular bridge pier. *Environmental Fluid Mechanics* 14(4), 821-847. <https://doi.org/10.1007/s10652-013-9332-1>
- Kline, S.J., Reynolds, W.C., Schraub, F.A., Runstadler, P.W., 1967. The structure of turbulent boundary layers. *Journal of Fluid Mechanics* 30(4), 741-773. <https://doi.org/10.1017/S0022112067001740>

- Kim, H., Kline, S.J., Reynolds, W.C., 1971. The production of turbulence near a smooth wall in a turbulent boundary layer. *Journal of Fluid Mechanics* 50(1), 133-160. <https://doi.org/10.1017/S0022112071002490>
- Laursen, E.M., 1963. An analysis of relief bridge scour. *Journal of the Hydraulics Division* 89(3), 93-118. <https://doi.org/10.1061/JYCEAJ.0000896>
- Liu, X., Bai, Y., 2013. Three-dimensional bursting phenomena in meander channel. *Transactions of Tianjin University* 19(1), 17-24. <https://doi.org/10.1007/s12209-013-2073-x>
- Lu, S.S., Willmarth, W.W., 1973. Measurements of the structure of the Reynolds stress in a turbulent boundary layer. *Journal of Fluid Mechanics* 60(3), 481-511. <https://doi.org/10.1017/S0022112073000315>
- Mayaud, J.R., Wiggs, G.F., Bailey, R.M., 2016. Dynamics of skimming flow in the wake of a vegetation patch. *Aeolian Research* 22, 141-151. <https://doi.org/10.1016/j.aeolia.2016.08.001>
- McGlinchey, D., 2009. *Characterisation of bulk solids*. John Wiley and Sons.
- Miyab, N.M., Fazloulou, R., Heidarpour, M., Kavian, A., Rodrigo-Comino, J., 2022. Experimental design of nature-based-solution considering the interactions between submerged vegetation and pile group on the structure of the river flow on sand beds. *Water* 14(15), 2382. <https://doi.org/10.3390/w14152382>
- Mohammadzade, N., Afzalimehr, H., Singh, V.P., 2015. Experimental investigation of influence of vegetation on flow turbulence. *International Journal of Hydraulic Engineering* 4(3), 54-69. <https://doi.org/10.5923/j.ijhe.20150403.02>
- Nortek, A.S., 2004. VECTRINO velocimeter user guide (Rev. C). *AS Nortek: Carlsbad, CA, USA*.
- Ortiz, A.C., Ashton, A., Nepf, H., 2013. Mean and turbulent velocity fields near rigid and flexible plants and the implications for deposition. *Journal of Geophysical Research: Earth Surface* 118(4), 2585-2599. <https://doi.org/10.1002/2013JF002858>
- Pickering, E., Rigas, G., Schmidt, O.T., Sipp, D., Colonius, T., 2021. Optimal eddy viscosity for resolvent-based models of coherent structures in turbulent jets. *Journal of Fluid Mechanics* 917. <https://doi.org/10.1017/jfm.2021.232>
- Pope, S.B., 2000. *Turbulent flows*. Cambridge University Press.
- Przyborowski, Ł., Łoboda, A.M., Bialik, R.J., 2019. Effect of two distinct patches of Myriophyllum species on downstream turbulence in a natural river. *Acta Geophysica* 67(3), 987-997. <https://doi.org/10.1007/s11600-019-00292-4>
- Raudkivi, A.J., Ettema, R. 1983. Clear-water scour at cylindrical piers. *Journal of Hydraulic Engineering* 109(3), 338-350. [https://doi.org/10.1061/\(ASCE\)0733-9429\(1983\)109:3\(338\)](https://doi.org/10.1061/(ASCE)0733-9429(1983)109:3(338))
- Rossi, M.J., Ares, J.O., Jobbágy, E.G., Vivoni, E.R., Vervoort, R.W., Schreiner-McGraw, A.P., Saco, P.M., 2018. Vegetation and terrain drivers of infiltration depth along a semiarid hillslope. *Science of the Total Environment* 644, 1399-1408. <https://doi.org/10.1016/j.scitotenv.2018.07.052>
- Short, F.T., Kosten, S., Morgan, P.A., Malone, S., Moore, G E., 2016. Impacts of climate change on submerged and emergent wetland plants. *Aquatic Botany* 135, 3-17. <https://doi.org/10.1016/j.aquabot.2016.06.006>
- Shahriar, A.R., Ortiz, A.C., Montoya, B.M., Gabr, M.A., 2021. Bridge Pier Scour: An overview of factors affecting the phenomenon and comparative evaluation of selected models. *Transportation Geotechnics* 28, 100549. <https://doi.org/10.1016/j.trgeo.2021.100549>
- Sterk, G., Jacobs, A. F .G., Van Boxel, J.H., 1998. The effect of turbulent flow structures on saltation sand transport in the atmospheric boundary layer. *Earth Surface Processes and Landforms: The Journal of the British Geomorphological Group* 23(10), 877-887. [https://doi.org/10.1002/\(SICI\)1096-9837\(199810\)23:10%3C877::AID-ESP905%3E3.0.CO;2-R](https://doi.org/10.1002/(SICI)1096-9837(199810)23:10%3C877::AID-ESP905%3E3.0.CO;2-R)
- Termini, D., 2015. Experimental analysis of horizontal turbulence of flow over flat and deformed beds. *Archives of Hydro-Engineering and Environmental Mechanics* 62(3-4), 77-99. <https://doi.org/10.1515/heem-2015-0021>

- Tempest, J.A., Möller, I., Spencer, T., 2015. A review of plant-flow interactions on salt marshes: The importance of vegetation structure and plant mechanical characteristics. *Wiley Interdisciplinary Reviews: Water* 2(6), 669-681.
- Vijayasree, B.A., Eldho, T.I., Mazumder, B.S., 2020. Turbulence statistics of flow causing scour around circular and oblong piers. *Journal of Hydraulic Research*, 58(4), 673-686. <https://doi.org/10.1080/00221686.2019.1661292>
- Vonkeman, J.K., Basson, G.R., 2019. Evaluation of empirical equations to predict bridge pier scour in a non-cohesive bed under clear-water conditions. *Journal of the South African Institution of Civil Engineering* 61(2), 2-20.
- Zaid, M., Yazdanfar, Z., Chowdhury, H., Alam, F., 2019. A review on the methods used to reduce the scouring effect of bridge pier. *Energy Procedia* 160, 45-50.
- Zong, L., Nepf, H. 2010. Flow and deposition in and around a finite patch of vegetation. *Geomorphology* 116(3-4), 363-372. <https://doi.org/10.1016/j.geomorph.2009.11.020>



## ASSESSMENT OF ECOLOGICAL CAPACITY FOR URBAN PLANNING AND IMPROVING RESILIENCE IN THE EUROPEAN FRAMEWORK: AN APPROACH BASED ON THE SPANISH CASE

RAFAEL CÓRDOBA HERNÁNDEZ<sup>1\*</sup>, FEDERICO CAMERIN<sup>2</sup>

<sup>1</sup> *Departamento de Urbanística y Ordenación del Territorio, Escuela Técnica Superior de Arquitectura, Universidad Politécnica de Madrid, Spain.*

<sup>2</sup> *Departamento de Urbanismo y Representación de la Arquitectura, Escuela Técnica Superior de Arquitectura, Universidad de Valladolid, Spain.*

**ABSTRACT:** The basic idea underlying this research is that urban planning is one of the main causes of environmental degradation. Despite its relevance in impacting ecosystems, the current methodological assessments across Europe still fail to include spatial planning as a relevant factor. This paper aims to formulate an innovative methodology for the evaluation of ecosystems for protecting land at risk of degradation. This methodology is exemplified by the case of Spanish spatial planning applied in the Community of Madrid, being also capable to be employed in other European State Members after a cartographic adaptation. The proposed methodology specifically implements a European approach to the scale of regional and local spatial planning based on the “Mapping and Assessment of Ecosystems and their Services” (MAES) project. Among the main results, four outcomes stand out. The first is the novelty to provide a methodology capable of dealing with natural values at regional and municipal levels based on a spatial-planning-based scale (1:20,000). The second result regards the incorporation of new attributes tied to existing ecosystems during the drafting of spatial plans, thus improving the quality of the information to make better decisions in terms of environmental protection. The third result is the more accurate environment assessment due to the inclusion of a new element of direct pressure on ecosystems, while the fourth outcome is that the proposed methodology detects the impacts of the drivers of change in the Community of Madrid. Although the cartographic information is defined at the regional scale, the results obtained can be linked to the municipal planning scale. The proposed methodology can be a much more useful tool for regional spatial planning for three main reasons: it works at the same scale as regional planning (1:20,000), it incorporates the environmental information necessary for the correct identification of natural values and impacts at the municipal level, and it works with geographic information systems. These reasons allow an easier and quicker incorporation of ecosystems in spatial planning tools by simultaneously interpreting and comparing different land protection issues such as ecosystem loss and ecosystem services.

### ***Evaluación de la capacidad ecológica para la planificación urbana y la mejora de la resiliencia en el contexto europeo: un enfoque basado en el caso español***

**RESUMEN:** La principal idea que subyace en esta investigación es que la planificación urbana es una de las principales causas de la degradación medioambiental. Sin embargo, pese a la importancia de su impacto en el medio natural y en los ecosistemas, las evaluaciones metodológicas actuales en toda Europa siguen sin incluir la ordenación del territorio como un factor relevante. Por ello, el documento pretende formular una metodología innovadora de evaluación de los ecosistemas para la protección del territorio en riesgo de degradación. Esta

metodología se ejemplifica con el caso de la planificación territorial española aplicada en el caso concreto de la Comunidad de Madrid, siendo también susceptible de ser empleada en otros Estados Miembros europeos tras una adaptación cartográfica. En concreto, la metodología propuesta implementa un enfoque europeo a escala de planificación territorial regional y local basado en el proyecto “Mapping and Assessment of Ecosystems and their Services” (MAES). Entre los principales resultados ligados a esta propuesta, cabe destacar cuatro resultados. El primero es la novedad en el tratamiento de los valores naturales a escala regional y municipal a partir de una escala basada en la planificación urbana y territorial (1:20.000). Como segunda cuestión destaca la incorporación de nuevos atributos ligados a los ecosistemas existentes en la elaboración de los planes de ordenación del territorio, mejorando así la calidad de la información para tomar mejores decisiones en materia de protección del medio ambiente por el planificador. El tercer resultado es una evaluación más precisa del medio ambiente debido a la inclusión del concepto de presión directa sobre los ecosistemas, mientras que la cuarta consecuencia sería que la metodología propuesta detecta los impactos de los motores del cambio en la Comunidad de Madrid. Además, aunque la información cartográfica viene definida a escala regional, los resultados obtenidos pueden vincularse a la escala de planificación municipal. La metodología propuesta puede ser una herramienta mucho más útil para la ordenación del territorio municipal por tres razones principales: trabaja a la misma escala que el planeamiento general (1:20.000), incorpora la información ambiental necesaria para la correcta identificación de los valores e impactos naturales a escala municipal, y trabaja con sistemas de información geográfica. Estas razones permiten abordar con mayor facilidad y rapidez la inclusión de los ecosistemas en la formalización de la ordenación del territorio, interpretando y comparando simultáneamente diferentes aspectos de la protección del territorio como la pérdida de ecosistemas y los servicios ecosistémicos.

**Keywords:** Sustainable development, Ecosystem Services, environmental impact, regional planning, resilience.

**Palabras clave:** Desarrollo sostenible, ecosistema, impacto ambiental, planeamiento territorial, resiliencia.

Received: 15 January 2023

Accepted: 26 May 2023

\* **Corresponding author:** Rafael Córdoba Hernández, Departamento de Urbanística y Ordenación del Territorio, Escuela Técnica Superior de Arquitectura, Universidad Politécnica de Madrid, Spain. E-mail address: rafael.cordoba@upm.es

## 1. Introduction

The increasing pace of massive global urbanization is generating a variety of socio-environmental pressures and impacts that are clearly going beyond the physical boundaries of cities and are consequently having negative impacts even beyond their administrative boundaries. These dynamics include changes in land-use and land-cover (Baveye *et al.*, 2016; Keesstra *et al.*, 2016), which affect ecosystem functions and services, such as water regulation and retention (Stürck *et al.*, 2014), climate regulation (Ghaley *et al.*, 2014), and biomass production (Larondelle and Haase, 2012). Whereas the importance of ecosystems and the associated benefits are attested by the European Union (EU), national, and regional policies and the different tools for their assessment and mapping, the integration of environmental aspects into spatial planning is a major challenge for planners (Hurlimann and March, 2012).

As advocated by the United Nations (United Nations Habitat, 2015), the integration of ecosystem service (ES) knowledge into spatial and land-use planning – especially if promoted from the early stages of the planning processes – could support decision-making in formulating more sustainable economic, social, cultural, and environmental goals and decisions (Longato *et al.*, 2021). The integration of ES assessment and monitoring tools in spatial planning processes could help to address the serious issues affecting our territories such as sprawling urbanization (Córdoba Hernández, 2021; Maruna *et al.*,

2019; Ronchi *et al.*, 2019; Thoidou, 2021) or flood risks (McGranahan *et al.*, 2007) by promoting policies and actions aimed at protecting, enhancing, and restoring ecosystems.

Scholars have identified the following main benefits of integrating ES knowledge into spatial planning management processes: i) a broader inclusion of relevant issues to address during the management process (Masoudi *et al.*, 2023; Veidemanė *et al.*, 2017), ii) a synthesizing perspective to interpret multiple data and information (Arkema *et al.*, 2015; Verutes *et al.*, 2017), and iii) effective stakeholder involvement with a higher degree of participation (Adem Esmail and Geneletti, 2017; Spyra *et al.*, 2019). Overall, these benefits can make a contribution to legitimate decisions on more sustainable spatial allocation of uses and management options (Longato *et al.*, 2021).

### *1.1. The role of ecosystem preservation in territorial resilience*

The starting point of this research is the concept of ‘territorial resilience’, that is, the capacity of positive adaptation shown by some cities or regions to face crises stemming from external events or processes and to emerge stronger after a process of internal transformation (Méndez, 2012). As highlighted by Hamilton (2009) and Pickett *et al.* (2004), this definition shows the contradictions and complexity of the urban and territorial land system. A good quality of biological, physical, and chemical characteristics of ecosystems is fundamental to mitigate shocks and increase resilience. These three factors are the pillars of the capacity of the ecosystems to generate ES. However, these qualities are often under threat from a variety of sources.

The Millennium Ecosystem Assessment (2003) identified five main pressures on ecosystems: land cover change; climate change; overexploitation of resources (e.g., through irrigation and harvesting); the introduction of alien invasive species; and the use of fertilizers, and air and water pollution. These processes affect the integrity of ecosystems and, consequently, disrupt their contributions to society and the environment (Büttner *et al.*, 2017; Kramer and Verkaar, 1998), contributing thus to a decrease in territorial resilience.

The frequency of events that put pressure on ecosystems can have low or high impacts on them. Low-impact events are integrated into ecosystems, e.g., through interactions between natural hazards and ecosystem characteristics, leaving existing biodiversity and ES functioning largely intact. However, when these changes are more significant, such as those associated with climate change, an ecosystem may lose its capacity to recover and may even disappear, favoring the substitution with a new ecosystem. Fragmentation is also a significant factor affecting the vulnerability of ecosystems: a small disturbance may have the same or even a greater impact on fragmented ecosystems than a larger disturbance on well-connected ecosystems (Urban *et al.*, 1987).

Therefore, the design and implementation of biodiversity strategies and action plans, and the use of evidence-based planning tools to design networks of protected areas, ecosystem connectivity and biodiversity conservation are fundamental tasks for achieving an integrated ecosystem management. Fulfilling these tasks would increase the resilience of cities and territories in dealing with climate change, natural disasters, and disturbances.

Reducing or at least not increasing the existing vulnerability of the ecosystems and the environment in general is a primary goal of various ES assessment frameworks such as ‘TEEB - The Economics of Ecosystems and Biodiversity’ (Kumar, 2012) or ‘CICES – Common International Classification of Ecosystem Services’ (United Nations, 2017). These assessment frameworks sometimes lack providing arguments to promote land conservation against urban development. Ecosystem assessment, in turn, can lead to the identification of the most important ecosystem goods and services and thus to appropriate land-use regulations.

International scholars recognize that mapping these issues makes it possible to reflect on how spatial planning and land-use management can incorporate and integrate these aspects into practical

experience (Burkhard and Maes, 2017; Verhagen *et al.*, 2015). However, these frameworks fall short without a regulatory framework that should help technicians evaluate land protection and conservation. The Spanish legislation has begun to address this issue with the approval of the Law 7/2021 on Climate Change and Energy Transition. This Law integrates the existing Law 7/2015 on Land-Use and Urban Regeneration – “Ley de Suelo y Rehabilitación Urbana” in Spanish – by establishing that climate change-related risks must be taken into account in land-use planning, in particular the “risks associated with the loss of ecosystems and biodiversity and the deterioration or loss of essential ecosystem goods, functions, and services” (Jefatura del Estado, 2021a, Disposición final cuarta).

### *1.2. The contextualization of the ecosystems preservation in the Spanish and EU policy system*

At the European level, the loss of ecosystems and their goods and services has been recognized by the “EU 2030 Strategy on Biodiversity”(European Commission, 2020). This strategy aims to halt biodiversity loss and degradation of ES and to restore them as far as possible, being closely related to the European Environment Agency’s (EEA) recommendation to integrate the results of the ES assessment into spatial planning. This recommendation is essential as it can identify areas with high and very high capacity to provide ES (European Environment Agency, 2014).

In line with the EU strategy and recommendation, the Spanish government approved the “National Strategy for Green Infrastructure and Ecological Connectivity and Restoration” in 2021. This document establishes the future provision of a specific cartographic planning-support tool that will allow the spatially explicit mapping of national ecosystems based on elements defined as “green infrastructure” (Jefatura del Estado, 2021b). These elements refer to the list provided by the Law 33/2015 on Natural Heritage and Biodiversity (Article 15.3): “Protected areas; endangered habitats and species; mountain areas; river courses; wetlands; livestock trails; ocean currents; submarine canyons; migratory routes that facilitate connectivity; systems of high natural value created as a result of good practices applied by different economic sectors; priority habitats to be restored; areas affected by nature conservation banks; and the instruments used by administrations in the application of the European Landscape Convention signed in Florence on 20 October 2000” (Jefatura del Estado, 2015). The release of this new tool is expected in three years after the approval of the Law 7/2021, i.e., in 2024.

One year before, the EU Biodiversity Strategy to 2020 proposed to the Member States to develop a mapping and assessment of ecosystems and their services. To do so, an EU-wide ecosystem assessment has been introduced to provide harmonized information on the state of ecosystems and biodiversity, and their capacity to provide ES. The European Commission supports Member States by providing useful data and guidelines for the mapping (e.g., a report with a list of possible indicators to assess and map ES), along with the release of new and updated data (e.g., through the Copernicus service portfolios and the habitat classification of the European Nature Information System EUNIS). This work formed the basis for the mapping and assessment of ecosystems and their services at EU level following the MAES (Mapping and Assessment of Ecosystems and their Services) analytical framework (European Environment Agency, 2018).

The European Commission is developing MAES to identify ecosystems in collaboration with many entities, such as the Member States and the EEA based on thematic pilot projects focusing on nature, agriculture, forests, freshwater, marine, and urban and terrestrial ecosystems. The first reports resulting from MAES consist of an analytical framework that provides common typologies of European ecosystems to be mapped and a typology of ES to be considered (Maes *et al.*, 2013). This typological classification takes into account regular cartographic aspects by using data from the CORINE Land Cover (CLC) project for its design, and allows the comparison of different sectors of the European territory and the maintenance of a pan-European scale (Büttner *et al.*, 2021; Heymann *et al.*, 1994).

Recognizing what services – and to what extent –the ecosystems of a territory provide to society requires an understanding of the number of ecosystems in a given territory that are affected by spatial

planning. This information can be obtained through an updated map of vegetation or habitat, with a resolution appropriate to the scale of the spatial plan (regional or municipal).

The quality requirements for cartography are limited by the availability of resources and the risk of decisions based on them. On the one hand, the upper limit of the requirements is set by the philosophical-logical principle known as Ockham's razor – i.e., of two competing theories, the simpler explanation of an entity is to be preferred. This approach emphasizes the need to use as few resources as possible to solve a problem. The methodology proposed by this paper does not require a new cartography, but starts from an existing one that has the necessary standard for this purpose. On the other hand, the lower limit of the requirements is determined by the social impact of map-based decisions. Uncertainty or lack of social impact can lead to a social risk of adverse outcomes if decisions are based on incorrect data.

The Driver-Pressure-State-Impact-Response (DPSIR) framework used by the proposed methodology stems from DPSIR's first report. DPSIR is a theoretical framework used to systematically classify the information needed to analyse environmental problems and to identify actions to solve them. (Turner *et al.*, 2010) Drivers of change (D) exert pressures (P) on the state of ecosystems (S) at any given time, affecting habitats and biodiversity (I) across Europe at all combinations of intensities and, consequently, affecting the number of services they can provide. If these impacts are not eliminated, policy makers should implement appropriate responses (R) by taking measures to address the negative impacts. These drivers are referred as pressures to adapt the terminology to the DPSIR framework applicable to European policy framework.

### *1.3. Goals and hypothesis*

This work aims to propose a methodological assessment for ecosystems and their services that can be used to support spatial planning at the regional level. The specific objectives are: i) to propose a high-resolution mapping method to assess and map ecosystems and their services, as well as their vulnerability to degradation or loss of essential ecosystem goods, functions, and services at the local level; and ii) to analyze/compare the extent to which the results of the assessment are or not aligned with current regulations establishing ecosystem protection regimes, and how they can support the development of better protection regulations.

The research hypothesis is that the European Ecosystem Assessment Methodology provides important keys to understand the main stressors acting on ecosystems but, by not considering spatial planning, it neglects one of the main causes of environmental degradation. The methodology aims to overcome this situation by making a comparison between the protection derived from spatial planning and the ecosystems.

## **2. Methods and materials**

The European Environment Agency's (EEA) methodology still does not consider spatial planning as a complementary tool capable to address the pressures on ecosystems and their services, although EEA claims that spatial planning can support policy decisions for the environmental conservation and protection (European Environment Agency, 2015b, 2015a). Implementing the methodology and integrating spatial planning into the Strategic Environmental Assessment (SEA) requires working at a scale where spatial planning and SEA can work together and with accessible information. Although this task is quite complex at the European or national level, the regional land legislation in Spain – the case study chooses is the Community of Madrid – may be the appropriate level to implement the methodology.

To achieve the aforementioned objectives, the proposed methodology is based on four levels of work – or steps. Thus, Steps 1 and 2 are performed to obtain a high-resolution cartographic method for

assessing and mapping ecosystems and their services, as well as their vulnerability to degradation or loss of essential ecosystem goods, functions, and services at the local scale (Fig. 1 left):

- **Step 1. Homologation of the initial information with the necessary scale adaptation.** For this purpose, the case study uses the information available from the Spanish National Geographic Institute (IGN) and the Madrid Spatial Data Infrastructure Server (IDEE-Madrid). Both IGN and IDEE-Madrid provide open information that can be processed using Geographic Information Systems (GIS) applications.
- **Step 2. Identification of the main direct drivers of change.** Once the main ecosystems have been detected using the European Nature Information System (EUNIS), they are grouped for characterization according to the main impacts identified by the Millennium Ecosystem Assessment. This step is performed through the Mapping and Assessment of Ecosystems and their Services (MAES), which identifies the impacts of habitat change, climate change, overexploitation of resources, introduction of invasive species, and pollution and nutrient enrichment.

Steps 3 and 4 are devoted to analyze/compare the extent to which the results of the assessment do or do not match existing spatial planning regulations and how they can support the development of better protection regulations (Fig. 1 right):

- **Step 3. Identification, assessment, and relevance of ecosystem services.** Based on the general classification of ecosystem inputs used by the Common International Classification of Ecosystem Services (CICES), the main ecosystems identified are characterized according to the MAES grouping. A total of 5 provisioning, 13 regulating, and 7 cultural ESs are identified. These ESs are valued independently and considering the interactions between each of the inputs to obtain a more complex qualification of these inputs.
- **Step 4. Introduction of spatial planning as a factor in the ecosystem assessment.** Once the plan for the provision of services has been drawn up, it is possible to compare it with the existing land-use plan or to identify the areas that could suffer a major ecosystem transformation as a result of the land-use plan proposals. Based on the previous considerations, there is the need to distinguish transformations associated with the loss of ecosystems and those related to biodiversity loss. This distinction is performed by considering the direct drivers of change associated with the degradation or loss of essential ecosystem goods, functions, and services, as described below. This comparison requires to overlay and/or cross-reference the studies carried out in the four steps with the land-use plan.

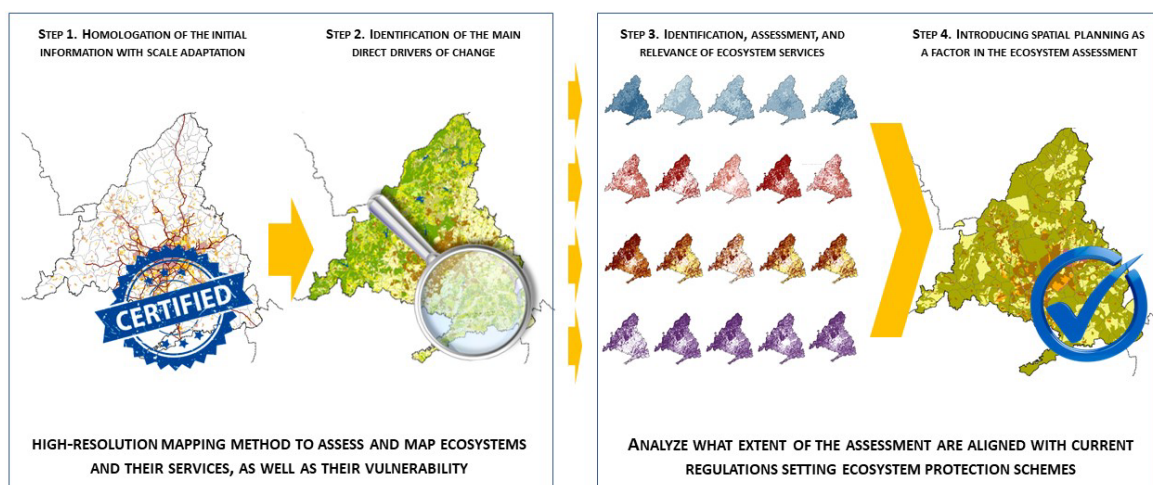


Figure 1. Diagram of the main research phases and objectives.

The implementation of this methodology, especially between steps 2 and 4, relies on the increasing use of remote sensing tools and Geographic Information Systems (GIS), together with the improved accessibility of satellite images and open classification methods from multiple sources. The cartographic management carried out on the different thematic aspects has been essential for their analysis, evaluation, and presentation. Free access to land use information was performed on the basis of the European Inspire Directive. The latter establishes the general guidelines for the proper functioning and service of the European Community's spatial information infrastructure and makes the information provided by the different Member States compatible. The use of regional sources is necessary to cross-reference the results of the assessment of the direct drivers of change and the loss of ecosystem services to modify the existing spatial planning tools.

The main functions performed by GIS enable to detect the different issues either by assessing the different ecosystems according to MAES's conceptual framework for assessment (Step 2) or by the SEEA Ecosystem Accounting assessment (Step 3). A series of maps are then used to create new thematic maps as developed in sections 2.2 and 2.3. These new maps are then processed to derive hazard zones which are overlaid on the spatial planning information to identify areas where specific problems overlap and to define the risks in these areas.

### *2.1. Step 1. Homologation of the initial information with the necessary scale adaptation*

As suggested by MAES framework, the mapping and assessment of ecosystems and their services proposed in this study is mainly based on land cover data (i.e., CLC data). CLC-based maps can be produced repeatedly by the territorial administration at relatively low cost in terms of time and money, being sufficiently suitable for most purposes and with a higher level of detail than necessary. However, maps with more reliable data (e.g., at a scale greater than 1:20,000) can be produced at excessive cost or with complex assumptions. Depending on the time required to produce them, maps would not be commensurate with the urgency of the objective. Therefore, the proposed mapping method is in line with the MAES method promoted at the European level, mainly by refining it and adapting it to the scope and scale of the work.

The CLC data supporting ecosystem assessment in spatial planning can be summarized in the following five conflicts, which the proposed mapping method aims to overcome:

- Reference scale. Due to its European dimension, the CLC provides consistent land and land use and land cover information at a detailed scale (1:100,000), which is however not accurate for a more regional scale (Fig. 2). This element creates a conflict with the Royal Decree 2159/1978 on "Planning Regulations for the development and application of the Law on Land Regime and Spatial Planning". This Decree only establishes the minimum scales at which "urban land" and "land for development" must be represented (respectively 1:2,000 and 1:5,000). Instead, the Decree leaves the Autonomous Communities (i.e., the Spanish Regions) free to interpret the regional scale. In fact, Article 39.2 states that the regional spatial plans "shall affect the entire territory included in their scope at an appropriate scale" (Jefatura del Estado, 1978).
- Minimum mapping unit. CLC updates (1990, 2000, 2006, 2012, and 2018) record land, land use, and land cover information using 5 ha as the minimum mapping unit for change. However, the minimum unit of the CLC is 25 ha, which is more appropriate to the territorial scale of other Spanish national documentary sources, such as the Information System on Land Occupation (*Sistema de Información sobre Ocupación del Suelo de España – SIOSE*).
- Hierarchical simplification. The CLC is the basis for ecosystem coverage at the European level, but there is a serious knowledge gap at the regional level. CLC provides information and, according to its third level of hierarchical aggregation, generates a classification of up to 44

ecosystem types. However, this classification cannot be useful at the regional scale where certain types are more relevant for the EU inventory.

- The CLC does not include certain types of natural information that are instead provided by the Spanish Autonomous Communities and the General State Administration, such as the forest map. Many Spanish Regions provide these maps at a scale of 1:10,000, including information on the type of vegetation, type of use, and classification. Such maps can provide more detailed information in relation to CLC.
- Raster representation of freely available information. The open-access MAES documentation on the European Nature Information System website is in raster format. This is a problem because the raster format makes the adaptation to the local vectorial cartography unfeasible in different regions or areas where the resolution of the cell size is not suitable for the analysis with spatial planning tools.

These conflicts may require adaptation of the data source to achieve greater precision regarding CLC in terms of mapping resolution and ecosystem type's information.

The resolution of these conflicts implied the decision to reclassify the categories of the SIOSE database to integrate it into the Spanish National Plan for Territory Observation (*Plan Nacional de Observación del Territorio – PNOT*). The output has a larger scale of definition (1:25,000) than the CLC (1:100,000) for the classification of ecosystem types and meets the European requirements established by the INSPIRE Directive (Infrastructure for Spatial Information in the European Community).

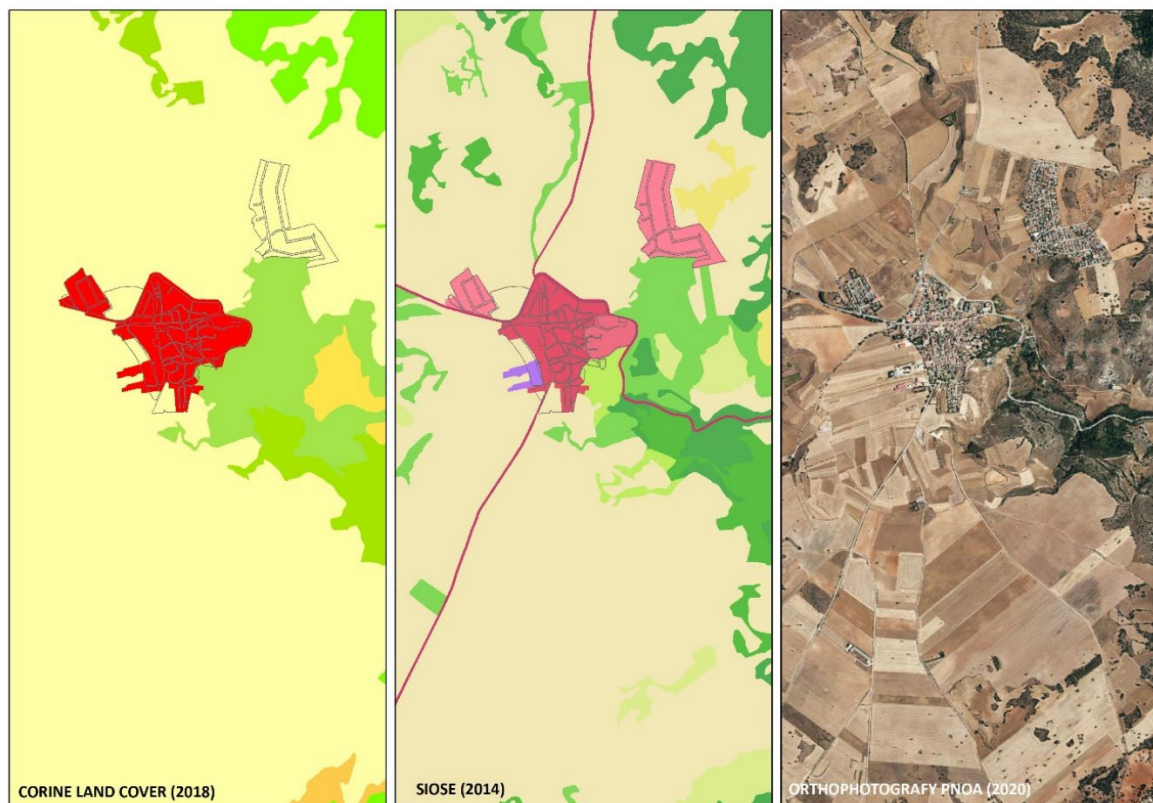
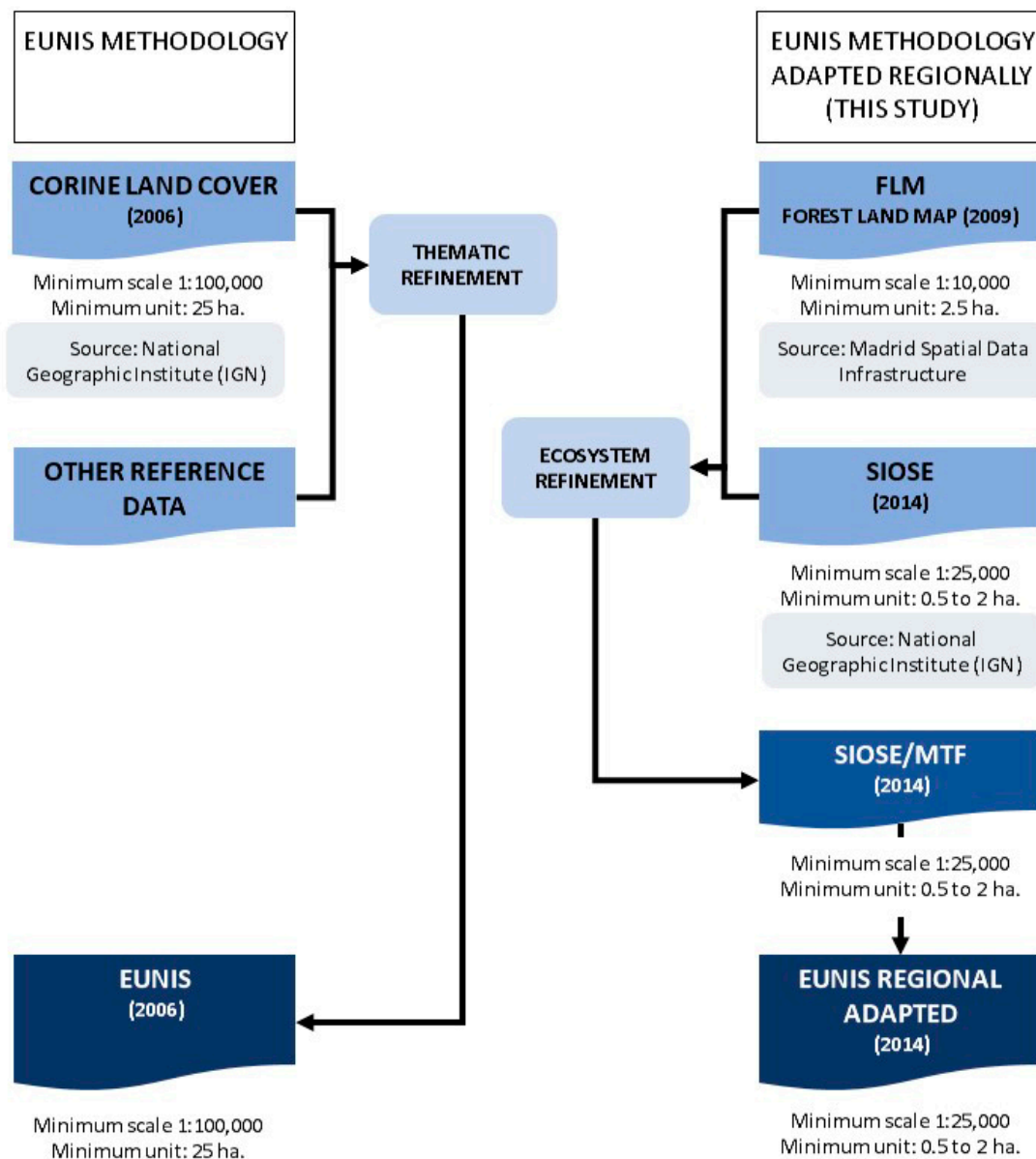


Figure 2. Degree of definition of the minimum mappable unit in the Pezuela de las Torres area (Madrid).  
Source: Authors' elaboration based on CLC 2012, SIOSE 2014 and orthophotography 2018.

The better definition of SIOSE is achieved through the incorporation of data produced by the Autonomous Communities at 1:10,000 and 1:5,000. The result is the definition of a series of surface coverages with a minimum surface of representation area of 0.5 ha for water, crops, wetlands, beaches, riparian vegetation, and sea cliffs, 1 ha for urban areas, and up to 2 ha in agricultural, forestry and natural areas. In the case of CLC, instead, the minimum representation area was 25 ha by default. This greater precision not only results in a more accurate delineation of ecosystems, but also incorporates with greater approximation the elements that divide habitats, such as communication or energy infrastructure.

This adapted information is approached with the methodological proposal of this study (Fig. 3) and compared it with the similar process followed by the identification and grouping of ecosystems by the EUNIS. The result is a map with the same information as it would have been obtained by using the EUNIS methodology, but with greater definition and updated to the latest monitoring date of the SIOSE national project. The resulting map – which can be called an “adapted EUNIS regional map” – could be continuously upgraded in the future by following the same steps to integrate updated data.



*Figure 3. Comparison of EUNIS methodology with EUNIS methodology adapted regionally (this study).*

Identifying the ES of a particular territory is the next step: the resulting information needs to be adapted to the regional scale. Although EUNIS is based on information provided by the CLC, the information supplied by the Spanish SIOSE is used as the basis for this study for the abovementioned reasons.

In this way, the ecosystems identified in the European Nature Information System (EUNIS) habitat groupings (Davies *et al.*, 2004) can be unambiguously recognized in the study area. These ecosystems are divided into marine and/or coastal habitats; surface water areas; wetlands; grasslands, herbs, mosses or lichens; heathlands, scrub and tundra; forests, woodlands and wooded areas; habitats with very little or no vegetation; agricultural, horticultural and domestic habitats; and artificial habitats.

The application of this method to the Community of Madrid (Fig. 4) shows that the main ecosystem is “forests, woods and other wooded land” (28.81%). Deciduous, coniferous, mixed, and transitional woodland cover slightly more than half of this ecosystem, being located in between northern and southern Sierra. The ecosystem “regularly or recently cultivated agricultural, horticultural, and domestic habitats” occupies a slightly smaller area (27.79%), being mainly located on the *meseta*, in the southern and eastern sectors of the region: it includes rainfed arable land, permanent irrigated land, and agroforestry systems.

“Built-up, industrial, and other human-made habitats” (15.07%) is the fourth largest ecosystem after “heathland, scrub and tundra” (17.34%), but its territorial distribution significantly fragments the regional territory, creating a central strip that clashes head-on with attempts to create ecological corridors or other nature-based solutions. Finally, the ecosystem “lodazales, peat bogs, and fens” occupies a small area within the Community, with only 61.77 ha (0.01%).

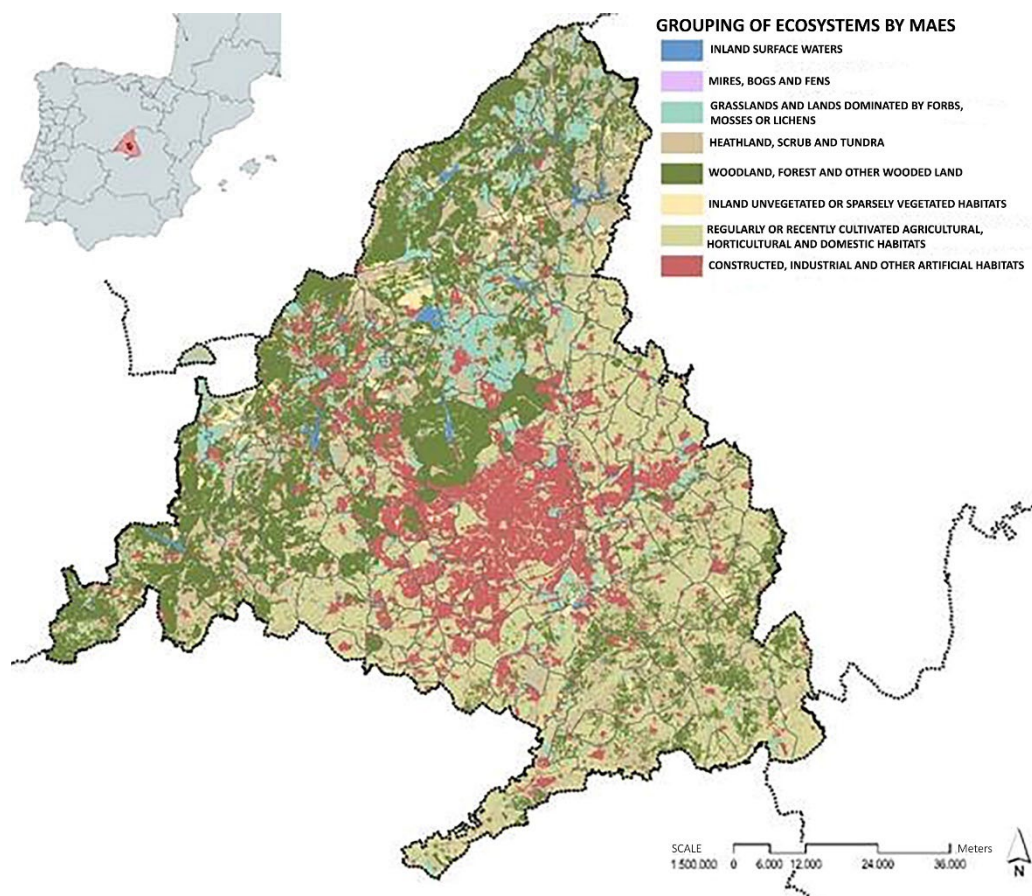


Figure 4. Identification of the Community of Madrid within Spain and its main ecosystems. Source: Authors' elaboration based on data from CORINE and EUNIS projects.

## 2.2. Step 2. Identification of the main impacts on ecosystems

Once the ecosystems have been grouped, the next step of the methodology is assessing the human impacts on ecosystems and their effects on the capacity to provide services. This assessment takes into account the difficulties in assessing the different pressures, trends, and impacts corresponding to each ecosystem due to the lack of specific data. Therefore, the five main drivers of change identified by the Millennium Ecosystem Assessment (2003) (i.e., land cover change, climate change, overexploitation of resources, introduction of alien invasive species, and use of fertilizers and air and water pollution) are linked to the ecosystems for their assessment. These drivers create environmental pressures that can alter the condition of habitats and the species composition of ecosystems, thereby reducing their resilience and affecting their ability to provide services (European Environment Agency, 2016). Based on these results, it is possible to identify the ecosystems that could undergo high pressure in the future.

Pressures, trends, and impacts on the ecosystems are challenging to assess. However, the combined effect of all the pressures over time results in the severity and extent of changes affecting an ecosystem and its ability to provide its services to natural and human systems. Therefore, the second step of the methodology is to assess these ecosystems using the MAES's conceptual framework for assessment. This approach consists of describing the different ecosystems from a qualitative assessment and establishing different relative scales according to the major pressures of the Millennium Ecosystem Assessment (2003). These scales are relative in the sense that all ES must be assessed at a specific geographical scale. In this case, the assessment provides the different levels of risk in reducing ES in an area by classifying potential future impacts as “very high” (VH), “high” (H), “moderate” (M) and “low” (L) based on the main direct drivers of change identified by the Millennium Ecosystem Assessment (Table 1).

Table 1. Intensity of the impact of direct drivers of change on ecosystems at the territorial level. Source: Mapping and assessing the condition of Europe's ecosystems: progress and challenges (European Environment Agency, 2016). Urban -URB; cropland -CR; grassland -GR; forest -FR; heathland and shrubland -H&S; sparsely vegetated land -S&V; wetlands -WET; freshwater (rivers and lakes -R&L) and marine -MAR. very high (VH), high (H), moderate (M) and low (L).

Main direct drivers of change	MAES's conceptual framework for assessments								
	URB	CR	GR	FR	H&S	S&V	WET	R&L	MAR
Habitat transformation	VH	VH	M	H	M	H	VH	VH	VH
Climate change	M	M	M	L	M	L	M	M	M
Overexploitation of resources	L	H	L	M	L	M	H	H	H
Introduction of invasive species	H	M	M	M	M	L	M	M	H
Pollution and nutrient enrichment	VH	VH	L	M	L	L	VH	VH	H

This second step develops an analytical assessment methodology based on the DPSIR framework (drivers, pressures, state, impact, and response model of intervention) which aims to establish a cause-effect relationship between human actions on the ecosystem. This methodology groups habitats into 12 ecosystem types, being divided into terrestrial (urban -U; cropland -CR; grassland -GR; forest -FR; heathland and shrubland -H&S; sparsely vegetated land -S&V; and wetlands -WET), freshwater (rivers and lakes -R&L) and marine (marine estuaries and transitional waters; coastal, continental shelves; and open ocean -MAR) ecosystems.

These ecosystems are not the same everywhere but adapt themselves to the climatic conditions of each location, so not all stressors affect similar ecosystems in the same way. As a result, similar

ecosystems in different bioclimatic zones of Europe may respond differently to climate change and ecosystem responses to natural hazards are specific to each bioclimatic zone. Neither the application of the proposed methodology at regional scale nor the MAES allow for a precise assessment of pressures and future trends for all ecosystems taking into account the abovementioned specificities. Despite these limitations, a territorial diagnosis based on ES can identify their goods and services and assess their relevance with the aim of analyzing future urban pressures and the ways they affect the provision of ES.

The identification of the ecosystems is performed through the CLC grouping based on the categories developed by MAES and adapted territorially through SIOSE. In this way, the risk assessments of ecosystem loss and the ecosystem goods and services can be assigned to each of the polygons that make up each ecosystem (Fig. 5).

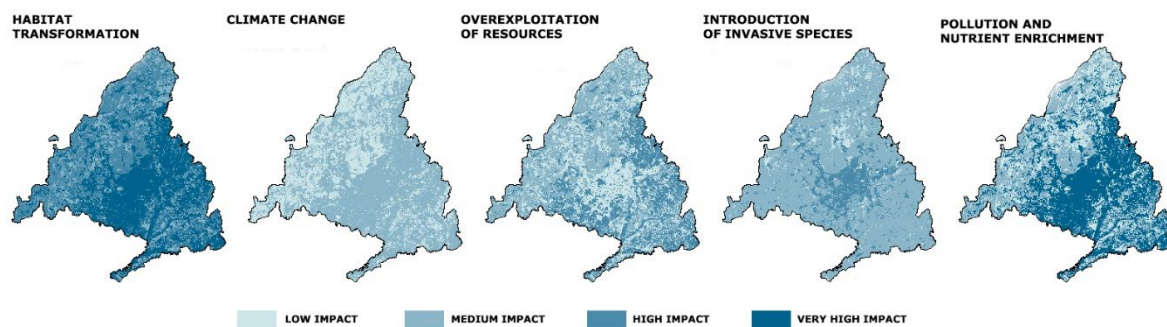


Figure 5. Assessment of the main drivers of ecosystem change. Source: Authors' elaboration based on SIOSE14 data.

The identification of effects is based on observing the effects of each driver on the different ecosystems. The effects can be observed in isolation – when considering only the effects of habitat transformation – or jointly – in the case of simultaneous analysis of the synergistic effects of the five actions. For instance, half of the Community of Madrid's surface is currently at very high risk due to cumulative impacts. The areas most affected by habitat transformation are urban ecosystem types, crops, wetlands, and rivers.

On the contrary, the effects of climate change would be moderate or low in the Community of Madrid, with urban areas, croplands, wetlands, and rivers suffering most from changes in temperature and precipitation, and rural areas from extreme events and fires.

The areas where overexploitation of resources could be most pronounced are croplands, wetlands, lakes, and rivers, i.e., where intensive agriculture through the overexploitation of crops and groundwater are already having their primary effects.

In terms of the potential risks associated with the introduction of exotic plant and animal species, the greatest risk lies in urban areas, i.e., where invasive species are being introduced into public and private gardens and parks. The mitigation of impacts in the rest of the regional territory shows a great homogeneity, except for the abovementioned areas. Only grassland ecosystems would have low impacts.

The effects of pollution and nutrient enrichment would particularly affect urban ecosystems, cultivated ecosystems, wetlands, lakes, and rivers. Soil contamination by heavy metals from industrial activities, air pollution, and critical ozone levels, and water pollution from poor management of sewage, sludge, and waste are particularly noticeable.

### *2.3. Step 3. Identification, assessment, and relevance of ecosystem services*

The *Common International Classification of Ecosystem Services* (CICES) considers ES to arise from living organisms (biota) or from the interaction of biotic and abiotic processes. The classification identifies three families of ES: provisioning, regulating, and cultural.

The values of the three families of ES are obtained using a variety of economic valuation techniques. These techniques do not assign a price on nature, but simply estimate the economic value of a limited number of services at a time. Despite limitations in certain contexts, an economic assessment can help to put nature conservation on an equal footing with urban development, and thus help decision-makers to better understand their trade-offs. Conducting this assessment is controversial as it raises a number of significant ethical and cultural considerations (Brand, 2009; Saner and Bordt, 2016).

The proposed grouping of Step 3 is the same that the work carried out in Step 2 on the cartographic basis of the MAES ecosystem groupings. Therefore, the most sensitive ecosystems are identified to subsequently outline the “ecosystem vulnerability associated with the degradation or loss of essential ecosystem goods, functions, and services”. The aim is to detect ecosystems with high or very high values in their contribution of goods and services that make them worthy of special protection to prevent their disappearance or degradation.

The SEEA Ecosystem Accounting (SEEA EA) offers a territorial approach to the problem of measuring the flows of ES and calculating their condition in terms of capacity to provide services. SEEA EA adopts a spatial approach because of the benefits that the society receives from ecosystems depend on the relationship between ecosystems and the location of the beneficiaries (United Nations, 2017).

The territorialization of these aspects involves the identification of ecosystems, but also the recognition and assessment of the ES and the interactions between them (Ruhl *et al.* 2008; Bagstad *et al.* 2013). These assessments come from various academic papers that, while presenting different degrees of territorialization, are carried out on a European-continental basis (Córdoba Hernández and Martí Guitera, 2022; Fernández de Manuel *et al.*, 2020; Henderson, 2015; Jacobs *et al.*, 2013). For instance, a negative interaction between the services provided by an ecosystem occurs when trade-offs arise. Such a dynamic may occur when a grassland ecosystem has a high input of food, but a low input of raw materials. These two ESs are mutually exclusive in a trade-off, so as the ecosystem provides both ESs independently, when combined they cancel each other out.

The biophysical assessment of ESs requires an assessment of both the capacity of ecosystems to provide relevant services and the estimation of their demand. The resulting cartography paves the way for understanding the distribution and importance of each contribution in the territory, as ecosystems take values for each contribution. The relationship with the capacity of ecosystems to provide services is presented in three areas to facilitate the understanding of the spatial distribution of each service.

As it happened in Step 2, a qualitative assessment is performed by introducing a new relative scale. The new scale ranges are established taking into account the assessments provided by different sources at international (Henderson, 2015; Longcore and Rich, 2004) and national levels (Fernández de Manuel *et al.*, 2020). The different inputs on ecosystems are identified as “low” (L), “medium” (M) or “high” (H) regardless of the documentary sources used.

This identification should be carried out for each of the 25 ESs grouped according to the CICES methodology. In this way, the ES can be mapped independently to obtain results at other levels such as the groupings of ESs by families of contribution (supply, regulation, and cultural) or by their overall territorial relevance. According to the European Environment Agency, regulation is the most remarkable contribution of ESs. Up to 13 different ESs can be distinguished and assessed differently depending on the ecosystem that produces them. (Table 2).

Table 2. Biophysical assessment of the different contributions of each service family. Green area – GA; cropland –CR; grassland -GR; forest -FR; heathland and shrubland -H&S; sparsely vegetated land -S&V; wetlands -WET; freshwater (rivers and lakes -R&L) and marine -MAR.

Ecosystem services	MAES's conceptual framework for assessments									
	GA	CR	GR	FR	H&S	S&V	WET	R&L	MAR	
Habitat maintenance	M	M	H	H	H	H	H	H	H	
Climate	M	L	M	H	M	L	M	M	M	
Noise reduction	H	-	-	H	L	-	-	-	-	
Thermal buffering	H	L	M	H	M	L	A	A	L	
Air quality	H	L	M	H	M	L	A	A	L	
REGULATION Hydrological cycle	M	-	H	H	H	L	A	A	M	
Erosion control	-	-	H	H	H	M	-	-	H	
Soil fertility	-	-	H	H	H	L	-	-	M	
Natural disturbances	-	-	H	H	H	-	H	H	H	
Biological control	H	M	H	H	H	H	H	H	M	
Pollination	M	H	H	L	H	M	-	-	-	
Endemic species conservation	-	M	H	H	H	H	H	H	H	
Soil production	-	-	M	H	M	L	-	-	-	

The methodological assessment has considered the approximate biodiversity of each ecosystem, assuming that the greater the number of species, the higher the number of conserved habitats. Cultivated fields show high values where large natural grasslands are scarce and, especially when they are well managed, they constitute a remarkable habitat for a multitude of bird species, from birds of prey to partridges and even bustards. In addition, if properly managed, the boundaries between agricultural parcels can become real biodiversity corridors, as they were in the past. These parcels were home to a wide variety of plant species in their bordering vegetation, which provided shelter for rodents and birds. In this case, the territorial importance of certain ESs, such as the conservation of endemic species, soil fertilization or the buffering of high temperatures, can be assessed (Fig. 6).

The assessment applied to the Community of Madrid divides the regional territory in two major zones (Fig. 6). The first is made up of the sierras, the plateau, and the so-called “western tension zone”, which includes numerous municipalities between the two sierras, such as Guadarrama, Galapagar, Santa María de la Alameda, and San Lorenzo de El Escorial. Despite the high altitude, this zone is provided with wooded ecosystems, scrub, and grassland ecosystems, being a typical example of the Mediterranean flora, among which holm oaks, junipers, and cork oaks stand out in the slopes of the Sierra de Hoyo de Manzanares. Here, extensive cattle population feeds on its fawn's pasture, producing meat of excellent quality, certified as *Ternera de Guadarrama* (Guadarrama Beef). The second major zone comprises the metropolitan concentric circles. On the one hand, the northern and western ones, which are also important for their regulatory contributions. These metropolitan concentric circles clearly divide this major zone into an area with very high contributions and an area with very low or no contributions. On the other hand, the eastern (made up of municipalities such as Alcalá de Henares, Coslada or Rivas-Vaciamadrid) and southern (made up of municipalities such as Getafe, Alcorcón, and Leganés) circles present little or no contributions in respectively 72% and 85% of their territory.

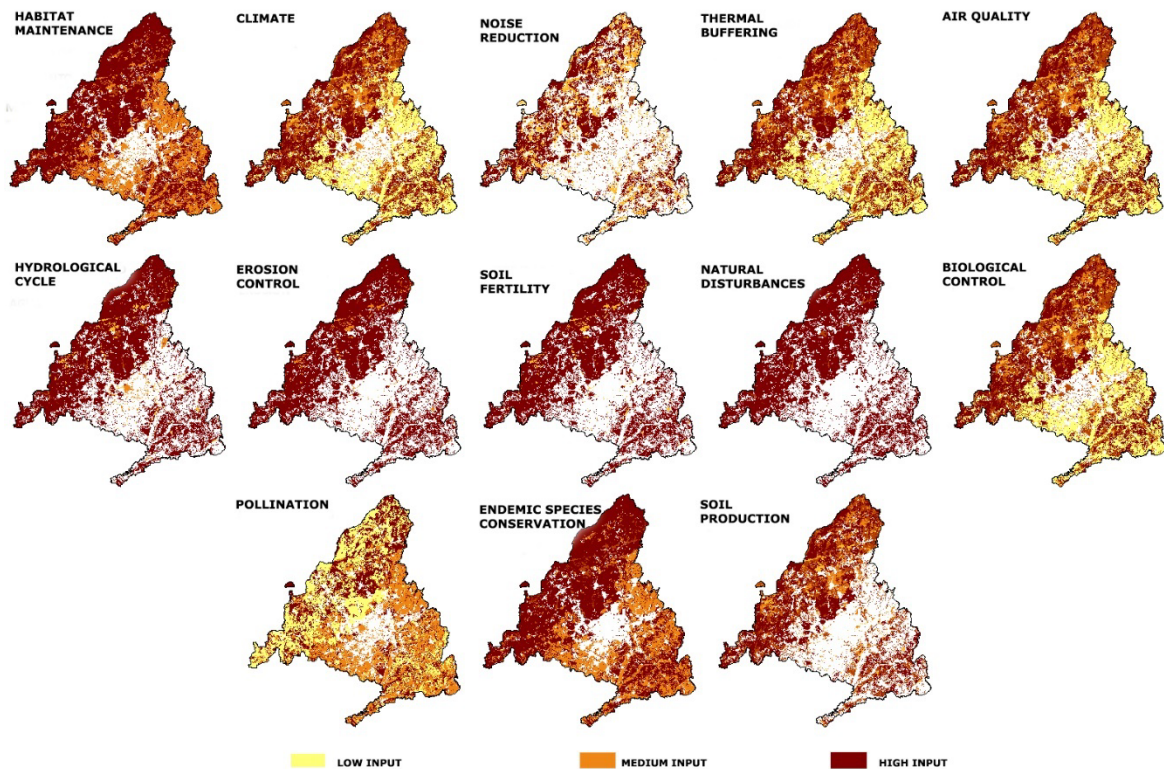


Figure 6. Territorialization of biophysical inputs of the regulating good service by ecosystem. Source: Authors' elaboration based on SIOSE14 data.

#### 2.4. Step 4. Introduction of spatial planning as a factor in the ecosystem assessment

At the same time, it is necessary to analyze the spatial planning of the area where ecosystem vulnerability is to be assessed. Municipal spatial planning should be as up-to-date as possible with the physical reality: this is what can be called “effective planning”. Effective planning aims to introduce the existing situation of the reality to analyze according to the current spatial planning and the names of classes and categories updated according to the regional land legislation.

Therefore, the territory to assess as vulnerable includes areas that are not affected by any sectoral legislation preventing urban development and areas comprising the ecosystems most vulnerable to impacts. These two types of areas should be assessed for future protection when it comes to modify the municipal spatial plan or to introduce a new one. Step 4 proposes two categories of protection in accordance with the criteria introduced by the fourth final provision of “Law 7/2021, of 20 May, on Climate Change and Energy Transition in the Royal Legislative Decree 7/2015, of 30 October, approving the revised text of the Law on Land and Urban Rehabilitation”:

- Ecosystem vulnerability through spatial planning in relation to the ecosystem and biodiversity loss due to the direct drivers of change identified by the Millennium Ecosystem Assessment. This vulnerability regards areas with high or very high biodiversity transformation based on the combined effects of habitat transformation, climate change, introduction of invasive species, and pollution and nutrient enrichment identified in section 2.2.
- Ecosystem vulnerability to spatial planning in relation to the degradation or loss of essential ecosystem goods, functions, and services. This vulnerability concerns ecosystems with high or very high values in their contribution of goods-services. Their values make them worthy of special protection to prevent their disappearance or depletion.

The result of this step provides a new dimension of environmental problems affecting the Community of Madrid's territory, whose southern metropolitan concentric circle and the southern and eastern regional sectors have been identified as the most sensitive.

Bringing together the ecosystem vulnerability associated with the risks from ecosystem loss and the ecosystem vulnerability associated with the loss of services can help to change the perception of the real estate developments that the Community of Madrid should be promoting today. If none of the current development plans were implemented, the existing ES would not be reduced, nor would new sensitive areas be created by the drivers of change. On the contrary, the situation would be the opposite. The creation of a new classification of land – which could be called “resilient” – could introduce new reasons for protecting the Community of Madrid's territory. Table 3 shows the result of the new classification.

*Table 3. Reclassification of Land for Development due to Ecosystem Vulnerability. associated with planning. NM: North Mountain; SM: South Mountain; ME: Meseta; WT: Western tension area; ST: South tension area; ET: East tension area; NT: North tension area; WC: Western Metropolitan Crown; SC: South Metropolitan Crown; EC: Eastern Metropolitan Crown; NC: Northern Metropolitan Crown; MD: Madrid municipality; CM: Madrid Community.*

Z	S (Ha)	SURB ECOSYSTEMICALLY VULNERABLE		SURB WITH HIGH RISK OF ECOSYSTEM LOSS		SURB FOR LOSS OF ECOSYSTEM INPUTS	
		S (Ha)	%	S (Ha)	%	S (Ha)	%
NM	17,083	11,910	69.7%	3,633	30.5%	8,277	69.5%
SM	4,572	4,128	90.3%	2,149	52.1%	1,979	47.9%
ME	43,147	41,939	97.2%	22,566	53.8%	19,373	46.2%
TW	6,909	4,825	69.8%	1,882	39.0%	2,943	61.0%
ST	14,853	13,607	91.6%	10,960	80.5%	2,647	19.5%
ET	16,956	16,036	94.6%	13,014	81.2%	3,022	18.8%
NT	8,216	7,036	85.6%	5,173	73.5%	1,863	26.5%
WC	7,044	6,356	90.2%	4,802	75.6%	1,554	24.4%
SC	7,690	7,370	95.8%	7,062	95.8%	308	4.2%
EC	5,020	4,416	88.0%	4,092	92.7%	324	7.3%
NC	8,143	4,313	53.0%	2,913	67.5%	1,400	32.5%
MD	6,196	5,847	94.4%	4,831	82.6%	1,016	17.4%
CM	145,828	127,783	87.7%	83,077	65.0%	44,706	35.0%

### 3. Results

#### 3.1. Step 1. Homologation of the initial information with the necessary scale adaptation

The potentialities identified in the two international territorializations of ecosystems will be adapted to the specificities and scale of the national territory to provide a systematization adaptable to the different Member States. These cartographies are the European Nature Information System (EUNIS) project, which carries out an initial identification and grouping of ecosystems, and the Mapping and Assessment of Ecosystems and their Services (MAES) project, which regroups them according to the main impacts identified by the Millennium Ecosystem Assessment.

This identification is crucial as it may enable the European Commission to take joint decisions and policies in order to address biodiversity issues and ecosystem loss. However, the decisions are poorly effective at the national level due to their territorial scope and scale of work. For this reason, the first contribution of the research is to adapt the scale of the information provided by the national

databases to facilitate the reinterpretation of the issues at scales closer to spatial planning. This achievement relied on the information provided by the Spanish Land Occupancy System (SIOSE), which has solved the various problems posed by the previous methodologies for their adaptation to spatial planning. These issues are the scale of the project, the minimum unit to map, the hierarchical simplification, the lack of integration of other types of natural information made available by the Autonomous Communities and the General State Administration, and the raster representation of freely accessible information.

This new identification of ecosystems is a much more useful tool as it begins to work at the scale used in spatial planning (1:20,000) and incorporates the environmental information necessary for the correct identification of natural values at the municipal level, as well as their main impacts.

The possibility of working with a vectorial tool, despite its territorial scale, allows including in the analysis the delimitations of the various territorial and sectoral planning, their zoning and, above all, the current spatial planning itself.

### *3.2. Step 2. Identification of the main impacts on ecosystems*

A vantage point offered by this methodology is the mapping of ESs and their synergies, i.e., when the provisioning of two services increase or decrease simultaneously. CICES identifies different ecosystem inputs but does not territorialize them. In this second step, one of the issues to address is precisely territorialization. Based on the EUNIS ecosystems identification, the methodology assigned a specific value for each of the different contributions the ecosystems may provide. This step in turn provides the opportunity to incorporate this information into the early stages of the spatial planning process, thereby improving the quality of information and the outcome.

This new information on ecosystems can be compared with the spatial plan proposal at the various stages of its formulation. Highlighting the impact of new land for development on the natural environment and ecosystems can thus lead to elaborate alternatives that better fit with environmental goals. In this way, a national or regional database containing this information would enable better and systematized reasons for land protection, or even to redefine current regional and sectoral spatial planning tools according to the identified risks or the ecosystemic contributions bordering on the current perimeters.

### *3.3. Step 3. Identification, assessment, and relevance of ecosystem services*

The introduction of spatial planning as a factor in the ecosystem assessment allows the incorporation of a new element of direct pressure on ecosystems. While this is a novelty, it would not be useful to incorporate it into the international methodologies identified in this paper due to the significant differences between planning systems at the European level.

Despite this controversy, it is worth recalling that among the direct drivers of change, habitat transformation is labelled as a pressure so it should undoubtedly be linked to spatial planning activities. The issue here is that at the European level only the direct degradation of habitat elements or functions, or the loss of a habitat and its replacement, are analyzed in terms of their impact on biodiversity. In other words, the analysis is on ex-post effects.

The consideration of spatial planning as a factor is essential because it identifies the pieces of land that are susceptible to transformation and incorporation into the urban project. The consequence of approaching spatial planning as a remarkable temporal element for ecosystem assessment led to two main results. The first is the identification of the future impact of spatial plans on ecosystems and, the second, is the modification of the existing spatial planning tools according to the impact and to the reduction in resilience that they cause.

### 3.4. Step 4. Introduction of spatial planning as a factor in the ecosystem assessment

Comparing current spatial planning protection with the assessments of both the main direct drivers of change and ecosystem inputs led to a remarkable result. This outcome is the identification of land whose capacity for positive adaptation to change would be most severely compromised by urbanization, being thus unable to reinforce endogenous weaknesses and to remove much of the response capacity. According to this identification, Table 4 spots ecosystems that, regardless of current spatial planning's contents, should be protected or preserved to maintain existing resilience, whether high or low.

Table 4. Assessment of ecosystems for their protection. Urban -URB; cropland -CR; grassland -GR; forest -FR; heathland and shrubland -H&S; sparsely vegetated land -S&V; wetlands -WET; freshwater (rivers and lakes -R&L) and marine -MAR

		MAES's conceptual framework for assessments								
		URB	CR	GR	FR	H&S	S&V	WET	R&L	MAR
MAIN DIRECT DRIVERS OF CHANGE	Habitat transformation	VH	VH	M	H	M	H	VH	VH	VH
	Climate change	M	M	M	L	M	L	M	M	M
	Overexploitation of resources	L	H	L	M	L	M	H	H	H
	Introduction of invasive species	H	M	M	M	M	L	M	M	H
	Pollution and nutrient enrichment	VH	VH	L	M	L	L	VH	VH	H
ECOSYSTEM INPUTS	Supply	L	M	M	H	M	L	L	L	L
	Regulation	L	H	H	H	H	L	L	L	L
	Cultural	L	H	H	H	H	L	H	H	H

Table 4 shows that the drivers of change have the greatest impact on arable, wetland, coastal, river, and lake ecosystems, while forests, heathlands, and shrublands provide the greatest services to society. All of them should be protected for different reasons to maintain or increase the current resilience of a specific area.

The less-protected ecosystems would be those belonging to grasslands and sparsely vegetated areas, as they would have low values in either of the two approaches analyzed. However, the proposed methodology for determining these values does not exclude a certain degree of flexibility that could guarantee an increase in the level of protection for ecosystems with high or medium values whether considered necessary or unique in the area.

Prior to Law 7/2021 on Climate Change and Energy Transition, the definition of the basic criteria for land use did not specifically mention the assessment of risks related to the loss of ecosystems and biodiversity and the degradation or loss of essential ecosystem goods, functions, and services. It would be a mistake to ignore these risks and not protect land, as land is fundamental to building adequate resilience.

This research views lack of protection as a vulnerability for the future and therefore seeks its identification in order to address the problem before it arises. Once the vulnerability is identified, the lack of protection for either of the previous two considerations should be addressed through land protection and a clear statement of compatible uses and reasons for protection.

## **4. Discussion**

### *4.1. Ecosystem protection as a reclassification argument*

The Spanish Autonomous Communities hold exclusive competence in matters of “land-use planning, town planning, and housing” – “Ordenación del Territorio, Urbanismo y Vivienda” in Spanish. This fact means that the regulations in these matters may vary from Region to Region and follow general principles set by the State. The State, in turn, limits itself to regulating the basic conditions for exercising the right to property, the general guarantees of compulsory expropriation and the land assessment system, the patrimonial responsibilities of the administration, and various aspects related to the cadaster. Most municipalities rely on a model that divides land into three classes (urban, for development, and undevelopable). The main differences between the three classes depend on the definitions and reasons given by the Autonomous Communities, which may lead them to consider land in one way or another.

Several Regions made a clear effort to specify the criteria according to which certain areas must be excluded from development, by classifying them as “undevelopable land”, while the General Municipal Master Plans (*Plan General de Ordenación Urbana*, PGOU, in Spanish) may establish different categories within the “undevelopable land”. It is worth noting that the regional legislation specifies the reasons why certain areas must be protected from urbanization. Most of these reasons are based on natural, environmental, and landscape values, which may already be recognized in sectoral legislation or may be progressively granted by the municipal authority itself. The classification of certain land as “undevelopable” may also be based on other criteria related to the principles of sustainability, such as the rational and orderly growth of the city or the structural characteristics of the municipality. Nevertheless, sectoral legislation or spatial planning does not regulate these criteria, so it is up to the decision makers to recognize these values and determine the land-use.

An essential step for promoting territorial resilience and land protection and conservation is the correct identification of the most vulnerable areas to the loss of ecosystems and the services they provide. The identification of such land corresponds to the “land for development” and can be carried out in two ways. On the one hand, the identification of “land to develop” that has not yet been transformed and, on the other hand, the verification of the existence of ES.

### *4.2. The challenges of spatial planning towards a real land protection*

Article 128.1 of the Spanish Constitution lays down a compelling principle: “The entire wealth of the country in its different forms, irrespective of ownership, shall be subordinated to the general interest”. Public administrations should therefore guarantee reliable land classification and take effective measures against speculation, but this seems a complex issue. By adopting this principle in whatever form or ownership, land classification should also be subordinated to the general interest. Doing so through spatial planning would result in the harmonization of two constitutional rights: spatial planning – aimed at economic and social development – and environmental protection. A general social consensus on the need to protect and preserve biodiversity due to its fragility seems to be quite clear in Spanish society (Brand, 2009; European Commission, 2020; Hurlimann and March, 2012). However, a large extent of the Community of Madrid would experience higher ecosystem values or significant risks of being affected by the pressures identified by the Millennium Ecosystem Assessment as this regional territory is expected to be heavily urbanized (Córdoba Hernández and Morcillo Álvarez, 2020; Valenzuela Rubio, 2010). The economic values and the relevant risks occur usually simultaneously as the most sensitive ecosystems tend to produce the largest inputs, but this methodology proposes to study them separately to enable elaborating adequate reasons for land protection.

Today, the design of spatial planning instruments must not only address the traditional problems of the rural-urban imbalance. Planning has to deal with less controllable vectors, such as the recent displacement of people due to environmental problems or risk situations caused by climate change

(Maes *et al.*, 2013). These vectors increase the resilience factors in need of assessment, making land conservation more relevant. The design and implementation of strategies and action plans for ecosystem conservation and the use of evidence-based planning tools to design networks of protected areas and their connectivity are pillars for a better integrated management of the natural environment and increased resilience (European Commission, 2020; Pickett *et al.*, 2004). A fundamental role pertains to national and regional land-use legislation as both of them should regulate spatial planning and uphold protected areas from urbanization process and incompatible activities according to spatial planning, sectoral legislation, and ecosystem values.

The resilience of an area strongly depends on the reduction of its vulnerability, or at least preventing it from increasing. As a consequence, vulnerability should be considered in the environmental assessment procedures required by the land-use legislation. Today, these procedures focus on fulfilling the required formalities but lack in-depth analyses. On the one hand, the environmental assessment focuses on the protection of certain nationally and internationally agreed elements such as the Natura 2000 Network or on compliance with sectoral legislation – e.g., cattle routes, water, and public utility forests. On the other hand, these tasks do not consider the qualities and services the ecosystems provide. Having complete and reliable information on the state of ecosystems – and the services they provide – and monitoring the changes that may occur would help to answer the following question: Are urban development processes meeting the objectives of the Strategic Environmental Assessment and conserving the natural environment?

As argued by several authors (Adem Esmail and Geneletti, 2017; Longato *et al.*, 2021; Spyra *et al.*, 2019; Veidemanė *et al.*, 2017), the development of new information on ecosystems and their goods and services can help support the implementation of environmental legislation, the integration of environmental objectives into urban policies, and the changes needed to achieve these objectives.

## 5. Conclusion

Urban ecological restoration often focuses on everything but nature, intervening in elements such as public transportation, renewable energy production, and energy-efficient building systems. While these are major aspects of reinventing urban life, they are not enough. Any vision of a sustainable urban future must focus directly on nature and on the presence and preservation of existing green features and natural ways of living.

In this paper, we proposed a new methodology for the evaluation of ecosystems for protecting land at risk of degradation. The proposed methodology can become a useful tool for land use planning for three main reasons: it works at the same scale as regional planning (1:20,000), it incorporates the environmental information necessary for the correct identification of natural values and impacts at the municipal level, and it works with geographic information systems. These reasons are the right basis for a simpler and faster integration of ecosystems in the drafting and approval process of land use planning, while at the same time they led to an interpretation and comparison of different aspects of land protection, such as ecosystem loss and ES.

The methodology also introduces two innovations. The first is the possibility of working with a vector tool. Despite its territorial scale, the vector tool integrates three factors into the municipal plan – i.e., the delimitations of the different territorial and sectoral planning, their zoning, and the current municipal planning. The second is the possibility of mapping ESs that are not mapped in international cartography. By doing so, the methodology adds a new set of attributes to the existing ecosystems based on the interactions between ecosystems and their own services. The direct consequence of such novelties may be the incorporation of this information in the municipal plan from the early stages of its drafting, improving the quality of the information provided and the outcome.

Finally, the new information on ecosystems can be compared with land-use planning proposals to identify alternative ways of managing the natural environment and conserving terrestrial ecosystems. Firstly, by organizing the range of the reasons for land protection and, secondly, by redefining the zoning of the spatial plans according to the identified risks or ecosystem services. At the national level, the introduction of spatial planning in the ecosystem assessment led to the inclusion of a new element of direct pressure on ecosystems based on the Law 7/2021 on Climate Change and Energy Transition. At the international level, the incorporation of this methodology in the drafting of international planning is perfectly compatible due to the use of free information and the adequate scales it uses.

## **Acknowledgements**

Rafael Córdoba Hernández collected and reelaborated the results of his doctoral thesis “*La estructura territorial resiliente: Análisis y formalización a través del Planeamiento Urbanístico*” (Córdoba Hernández, 2021) carried out in the PhD “Sostenibilidad y Regeneración Urbana” (Universidad Politécnica de Madrid). Federico Camerin has participated as co-author within the research project “*La Regeneración Urbana como una nueva versión de los Programas de Renovación Urbana. Logros y fracasos*”. This project is co-funded by the Spanish Ministry of Universities in the framework of the Recovery, Transformation and Resilience Plan, by the European Union – NextGenerationEU and by the Universidad de Valladolid. This collaboration was performed at the Grupo de Investigación en Arquitectura, Urbanismo y Sostenibilidad (GIAU+S) of Departamento de Urbanística y Ordenación del Territorio, Escuela Técnica Superior de Arquitectura, Universidad Politécnica de Madrid.

## **References**

- Adem Esmail, B., Geneletti, D. 2017. Design and impact assessment of watershed investments: An approach based on ecosystem services and boundary work. *Environmental Impact Assessment Review* 62, 1-13. <https://doi.org/10.1016/j.eiar.2016.08.001>
- Arkema, K. K., Verutes, G. M., Wood, S. A., Clarke-Samuels, C., Rosado, S., Canto, M., Rosenthal, A., Ruckelshaus, M., Guannel, G., Toft, J., Faries, J., Silver, J. M., Griffin, R., Guerry, A. D. 2015. Embedding ecosystem services in coastal planning leads to better outcomes for people and nature. *Proceedings of the National Academy of Sciences* 112(24), 7390-7395. <https://doi.org/10.1073/pnas.1406483112>
- Bagstad, K. J., Johnson, G. W., Voigt, B., Villa, F. 2013. Spatial dynamics of ecosystem service flows: A comprehensive approach to quantifying actual services. *Ecosystem Services* 4, 117-125. <https://doi.org/10.1016/j.ecoser.2012.07.012>
- Baveye, P. C., Baveye, J., Gowdy, J. 2016. Soil «ecosystem» services and natural capital: Critical appraisal of research on uncertain ground. *Frontiers in Environmental Science* 4, <https://doi.org/10.3389/fenvs.2016.00041>
- Brand, F. 2009. Critical natural capital revisited: Ecological resilience and sustainable development. *Ecological Economics* 68(3), 605-612. <https://doi.org/10.1016/j.ecolecon.2008.09.013>
- Burkhard, B., Maes, J. 2017. Mapping Ecosystem Services. In: B. Burkhard and J. Maes (Eds.), *Mapping Ecosystem Services*. Pensoft Publishers. <https://doi.org/10.3897/ab.e12837>
- Büttner, G., Kostztra, B., Soukup, T., Sousa, A., Langanke, T. 2017. CLC2018 *Technical Guidelines*. European Environment Agency, 60 p. [https://land.copernicus.eu/user-corner/technical-library/clc2018technicalguidelines\\_final.pdf](https://land.copernicus.eu/user-corner/technical-library/clc2018technicalguidelines_final.pdf)
- Büttner, G., Kosztra, B., Maucha, G., Pataki, R., Kleeschulte, S., Hazeu, G., Vittek, M., Schröder, C., Littkopf, A. 2021. *CORINE Land Cover, User Manual*. <https://land.copernicus.eu/> [Accessed 07-June-2021]
- Córdoba Hernández, R. 2021. *Estructura territorial resiliente: análisis y formalización a través del planeamiento urbanístico*. Tesis Doctoral inédita. Universidad Politécnica de Madrid. <https://doi.org/10.20868/UPM.thesis.69364>

- Córdoba Hernández, R., Morcillo Álvarez, D. 2020. Marco territorial de la producción de espacio en la región funcional de Madrid. *Ciudades* 23, 71-93. <https://doi.org/10.24197/CIUDADES.23.2020.71-93>
- Córdoba Hernández, R., Martí Guitera, L. 2022. Ecosystem vulnerability due to urban growth policies. The role of regulatory ecosystem contributions in the land use planning. *SUPTM 2022: 1st Conference on Future Challenges in Sustainable Urban Planning & Territorial Management*, 4. <https://doi.org/10.31428/10317/10599>
- Davies, C. E., Moss, D., Hill, M. O. 2004. *EUNIS Habitat Classification Revised 2004*. *Technology*, October, 310 p. <https://www.eea.europa.eu/data-and-maps/data/eunis-habitat-classification>
- European Commission. 2020. *EU Biodiversity Strategy for 2030. Bringing nature back into our lives*. COM(2020), 23. [https://eur-lex.europa.eu/resource.html?uri=cellar:a3c806a6-9ab3-11ea-9d2d-01aa75ed71a1.0001.02/DOC\\_1&format=PDF](https://eur-lex.europa.eu/resource.html?uri=cellar:a3c806a6-9ab3-11ea-9d2d-01aa75ed71a1.0001.02/DOC_1&format=PDF)
- European Environment Agency. 2014. *Spatial analysis of green infrastructure in Europe*. EEA Technical Report 2/2014. <http://www.eea.europa.eu/publications/spatial-analysis-of-green-infrastructure>
- European Environment Agency. 2015a. *EU 2010 Biodiversity Baseline — Adapted to the MAES Typology (2015)*. EEA Technical Report 9/2015. <http://www.eea.europa.eu/publications/eu-2010-biodiversity-baseline-revision>
- European Environment Agency. 2015b. *European Ecosystem Assessment - Concept, Data and Implementation*. EEA Technical report 6/2015. <https://www.eea.europa.eu/publications/european-ecosystem-assessment>
- European Environment Agency. 2016. *Mapping and assessing the condition of Europe's ecosystems: progress and challenges*. EEA Report 3/2016. <https://www.eea.europa.eu/publications/mapping-europes-ecosystems>
- European Environment Agency. 2018. *European waters Assessment of status and pressures 2018*. EEA Report 7/2018. <https://www.eea.europa.eu/publications/state-of-water>
- Fernández de Manuel, B., Peña, L., Ametzaga, I., Onaindia, M. 2020. *Guía práctica para la integración de los servicios de los ecosistemas en la formulación de planes y programas territoriales y urbanísticos*. Universidad del País Vasco. [http://web-argitalpena.adm.ehu.es/pasa\\_pdfFin.asp](http://web-argitalpena.adm.ehu.es/pasa_pdfFin.asp)
- Ghaley, B. B., Vesterdal, L., Porter, J. R. 2014. Quantification and valuation of ecosystem services in diverse production systems for informed decision-making. *Environmental Science and Policy* 39, 139-149. <https://doi.org/10.1016/j.envsci.2013.08.004>
- Hamilton, W. A. H. 2009. Resilience and the city: the water sector. *Proceedings of the Institution of Civil Engineers - Urban Design and Planning* 162(3), 109-121. <https://doi.org/10.1680/udap.2009.162.3.109>
- Henderson, J. 2015. Avian Urban Ecology: Behavioural and Physiological Adaptations. *Biodiversity* 16(1), 51-52. <https://doi.org/10.1080/14888386.2015.1009944>
- Heymann, Y., Steenmans, C., Croisille, G., Bossard, M., Lenco, M., Wyatt, B., Weber, J.-L., O'Brian, C., Cornaert, M.-H., Sifakis, N. 1994. *CORINE land cover. Technical guide*. Environment, nuclear safety and civil protection series. European Commission, Directorate-General, Environment, Nuclear Safety and Civil Protection.
- Hurlimann, A. C., March, A. P. 2012. The role of spatial planning in adapting to climate change. *Wiley Interdisciplinary Reviews: Climate Change* 3(5), pp. 477-488. <https://doi.org/10.1002/wcc.183>
- Jacobs, S., Stevens, M., Reeth, W. Van, Daele, T. Van, Schneiders, A., Demolder, H., Thoonen, M., Gossum, P. Van, Peymen, J. 2013. *Capacity for delivery of ecosystem services - Interim evaluation of a method based on agriculture and expert knowledge in Flanders*.
- Jefatura del Estado. 1978. *Real Decreto 2159/1978, de 23 de junio, por el que se establece el Reglamento del Planeamiento Urbanístico*. Boletín Oficial del Estado, 221, de 15 de septiembre, 21592-21606. <https://www.boe.es/eli/es/rd/1978/06/23/2159>
- Jefatura del Estado. 2015. *Ley 33/2015, de 21 de septiembre, por la que se modifica la Ley 42/2007, de 13 de diciembre, del Patrimonio Natural y de la Biodiversidad*. Boletín Oficial del Estado, 227, de 22 de septiembre, 83588-83632.
- Jefatura del Estado. 2021a. *Ley 7/2021, de 20 de mayo, de cambio climático y transición energética*. Boletín Oficial del Estado, 121, de 21 de mayo, 62009 a 62052.

- Jefatura del Estado. 2021b. Orden PCM/735/2021, de 9 de julio, por la que se aprueba la Estrategia Nacional de Infraestructura Verde y de la Conectividad y Restauración Ecológicas. Boletín Oficial del Estado, 166, de 13 de julio, 83217-83470. <https://www.boe.es/eli/es/o/2021/07/09/pcm735>
- Keesstra, S. D., Bouma, J., Wallinga, J., Tittonell, P., Smith, P., Cerdà, A., Montanarella, L., Quinton, J. N., Pachepsky, Y., Van Der Putten, W. H., Bardgett, R. D., Moolenaar, S., Mol, G., Jansen, B., and Fresco, L. O. 2016. The significance of soils and soil science towards realization of the United Nations sustainable development goals. *SOIL* 2(2), 111-128. <https://doi.org/10.5194/soil-2-111-2016>
- Kramer, K., Verkaar, H. J. 1998. Disturbed disturbances: The complicated management of sustainable forest ecosystems. In: M. Nabuurs, G.J. Nuutinen, T. Bartelink, H.Korhonen (Eds.), *Forest scenario modelling for ecosystem management at landscape level Proceedings 19*, pp. 47-62. ISBN: 952-9844-40-9.
- Kumar, P. 2012. *The Economics of Ecosystems and Biodiversity: Ecological and Economic Foundations*. Routledge. 456 p. <https://doi.org/10.4324/9781849775489>
- Larondelle, N., Haase, D. 2012. Valuing post-mining landscapes using an ecosystem services approach - An example from Germany. *Ecological Indicators* 18, 567-574. <https://doi.org/10.1016/j.ecolind.2012.01.008>
- Longcore, T., Rich, C. 2004. Ecological light pollution. *Frontiers in Ecology and the Environment* 2(4), 191-198. [https://doi.org/10.1890/1540-9295\(2004\)002\[0191:ELP\]2.0.CO;2](https://doi.org/10.1890/1540-9295(2004)002[0191:ELP]2.0.CO;2)
- Longato, D., Cortinovis, C., Albert, C., Geneletti, D. 2021. Practical applications of ecosystem services in spatial planning: Lessons learned from a systematic literature review. *Environmental Science & Policy* 119, 72-84. <https://doi.org/10.1016/j.envsci.2021.02.001>
- Maes, J., Teller, A., Erhard, M., Liqueste, C., Braat, L., Berry, P., Egoh, B., Puydarrieux, P., Fiorina, C., Santos-Martín, F., Paracchini, M. L., Keune, H., Wittmer, H., Hauck, J., Fiala, I., Verburg, P. H., Condé, S., Schägner, J. P., Miguel, J. S., ... Bidoglio, G. (2013). *Mapping and Assessment of Ecosystems and their Services. An analytical framework for ecosystem assessments under Action 5 of the EU Biodiversity Strategy to 2020*. [https://ec.europa.eu/environment/nature/knowledge/ecosystem\\_assessment/pdf/MAESWorkingPaper2013.pdf](https://ec.europa.eu/environment/nature/knowledge/ecosystem_assessment/pdf/MAESWorkingPaper2013.pdf)
- Maruna, M., Crnčević, T., Milojević, M. P. 2019. The institutional structure of land use planning for urban forest protection in the post-socialist transition environment: Serbian experiences. *Forests* 10(7). <https://doi.org/10.3390/f10070560>
- Masoudi, M., Asrari, E., Razaghi, S., Karimi, F., Cerdà, A. (2023). A new proposed model of EMOLUP for assessing of ecological capability of different utilizations and land use planning in Sepidan Township, Iran. *Cuadernos de Investigación Geográfica- Geographical Reserach Letters*. <https://doi.org/10.18172/cig.5443>
- McGranahan, G., Balk, D., Anderson, B. 2007. The rising tide: Assessing the risks of climate change and human settlements in low elevation coastal zones. *Environment and Urbanization* 19(1), 17-37. <https://doi.org/10.1177/0956247807076960>
- Méndez, R. 2012. Ciudades y metáforas: sobre el concepto de resiliencia urbana. *Ciudad y Territorio. Estudios territoriales* XLIV(172), 215-232. <http://www.fomento.gob.es/NR/rdonlyres/FF63AECF-CF4B-4A59-968B-D9B701ACA03B/113205/CyTET172.pdf>
- Millennium Ecosystem Assessment. 2003. *Ecosystems and human well-being: a framework for assessment*. Island Press. [http://pdf.wri.org/ecosystems\\_human\\_wellbeing.pdf](http://pdf.wri.org/ecosystems_human_wellbeing.pdf)
- Pickett, S. T. A., Cadenasso, M. L., Grove, J. M. 2004. Resilient cities: meaning, models, and metaphor for integrating the ecological, socio-economic, and planning realms. *Landscape and Urban Planning* 69(4), 369-384. <https://doi.org/10.1016/j.landurbplan.2003.10.035>
- Ronchi, S., Salata, S., Arcidiacono, A., Piroli, E., Montanarella, L. 2019. Policy instruments for soil protection among the EU member states: A comparative analysis. *Land Use Policy* 82, 763-780. <https://doi.org/10.1016/j.landusepol.2019.01.017>
- Ruhl, J. B., Kraft, S. E., Lant, C. L. 2008. *The Law and Policy of Ecosystem Services*. Island Press, Washington, DC. 350 p.
- Saner, M. A., Bordt, M. 2016. Building the consensus: The moral space of earth measurement. *Ecological Economics* 130, 74-81. <https://doi.org/10.1016/j.ecolecon.2016.06.019>

- Spyra, M., Kleemann, J., Cetin, N. I., Vázquez Navarrete, C. J., Albert, C., Palacios-Agundez, I., Ametzaga-Arregi, I., La Rosa, D., Rozas-Vásquez, D., Adem Esmail, B., Picchi, P., Geneletti, D., König, H. J., Koo, H., Kopperoinen, L., Fürst, C. 2019. The ecosystem services concept: a new Esperanto to facilitate participatory planning processes? *Landscape Ecology* 34(7), 1715-1735. <https://doi.org/10.1007/s10980-018-0745-6>
- Stürck, J., Poortinga, A., Verburg, P. H. 2014. Mapping ecosystem services: The supply and demand of flood regulation services in Europe. *Ecological Indicators* 38, 198-211. <https://doi.org/10.1016/j.ecolind.2013.11.010>
- Thoidou, E. 2021. Spatial planning and climate adaptation: Challenges of land protection in a peri-urban area of the mediterranean city of thessaloniki. *Sustainability* 13(8). <https://doi.org/10.3390/su13084456>
- Turner, R. K., Morse-Jones, S., Fisher, B. 2010. Ecosystem valuation: A sequential decision support system and quality assessment issues. *Annals of the New York Academy of Sciences* 1185, 79-101. <https://doi.org/10.1111/j.1749-6632.2009.05280.x>
- United Nations. 2017. *System of Environmental-Economic Accounting 2012*. United Nations. <https://doi.org/10.5089/9789211615630.069>
- United Nations Habitat. 2015. International Guidelines on Urban and Territorial Planning. <https://unhabitat.org/international-guidelines-on-urban-and-territorial-planning>
- Urban, D. L., O'Neill, R. V., Shugart, H. H. J. 1987. Landscape Ecology: A hierarchical perspective can help scientists understand spatial patterns. *BioScience* 37(2), 119-127.
- Valenzuela Rubio, M. 2010. La planificación territorial de la región metropolitana de Madrid. Una asignatura pendiente. *Cuadernos Geográficos* 47, 95-129. <https://doi.org/10.30827/cuadgeo.v47i0.603>
- Veidemane, K., Ruskule, A., Strake, S., Purina, I., Aigars, J., Sprukta, S., Ustups, D., Putnis, I., Klepers, A. 2017. Application of the marine ecosystem services approach in the development of the maritime spatial plan of Latvia. *International Journal of Biodiversity Science, Ecosystem Services & Management* 13(1), 398-411. <https://doi.org/10.1080/21513732.2017.1398185>
- Verhagen, W., Verburg, P. H., Schulp, N., Störck, J. 2015. Mapping ecosystem services. In: J.A. Bouma, P.J.H. van Beukering (Eds.), *Ecosystem Services: From Concept to Practice*. Cambridge University Press. pp. 65-86. <https://doi.org/10.1017/CBO9781107477612.006>
- Verutes, G. M., Arkema, K. K., Clarke-Samuels, C., Wood, S. A., Rosenthal, A., Rosado, S., Canto, M., Bood, N., Ruckelshaus, M. 2017. Integrated planning that safeguards ecosystems and balances multiple objectives in coastal Belize. *International Journal of Biodiversity Science, Ecosystem Services & Management* 13(3), 1-17. <https://doi.org/10.1080/21513732.2017.1345979>



## REMOTE SENSING AND SPATIAL DATABASES FOR INVESTIGATING LATENT URBAN-RURAL DYNAMICS IN RURAL, INLAND DISTRICTS OF SOUTHERN ITALY

VITO IMBRENDA<sup>1,2</sup> , CASANDRA MUÑOZ GOMEZ<sup>3\*</sup> ,  
MARIAGRAZIA D'EMILIO<sup>1</sup>, CATERINA SAMELA<sup>1</sup> ,  
LUCA SALVATI<sup>4</sup>, NADIA MATARAZZO<sup>5</sup> ,  
MARIA LANFREDI<sup>1,2</sup> , ROSA COLUZZI<sup>1,2</sup> 

<sup>1</sup>*Institute of Methodologies for Environmental Analysis, Italian National Research Council (IMAA-CNR),  
c.da Santa Loja snc, 85050 Tito, PZ, Italy.*

<sup>2</sup>*NBFC, National Biodiversity Future Center, 90133 Palermo, PA, Italy.*

<sup>3</sup>*National School of Earth Sciences (ENCiT) of National Autonomous University of Mexico (UNAM).  
Av. Antonio Delfín Madrigal 300, C.U., Coyoacán, 04510 Ciudad de México, CDMX, México.*

<sup>4</sup>*Department of Methods and Models for Economics, Territory and Finance (MEMOTEF), Faculty of  
Economics, Sapienza University of Rome, Via del Castro Laurenziano 9, 00161 Rome, RM, Italy.*

<sup>5</sup>*Department of Economic and Statistical Sciences, University "Federico II", Naples, Italy.*

**ABSTRACT.** It is well-known that rural-urban patterns help to capture socioeconomic interactions between different settlement forms. The sustainability challenge requires to consider the evolution of these patterns as a reliable indicator of the dynamics of land use change and potential land degradation processes occurred in a time frame. In this research, by using multisource data (Corine Land Cover, Keyhole KH-9 and Landsat satellite images), we trace the diachronic evolution (1990-2018) of the rural-urban pattern in the provinces of Avellino and Benevento (Campania region, Southern Italy) with a specific focus on the key municipality of Ariano Irpino (1975-2018). The analysis confirms the considerable urban growth occurred in the study area, mostly in the form of urban sprawl phenomena decoupled from population growth. This happens concurrently with a transformation of the agricultural sector projected toward a greater specialization favouring agritourism activities and valuable crops (e.g., vineyards). These findings can support policy makers in future planning activities by mixing conservation, mitigation, and restoration actions.

### ***Sensores remotos y bases de datos espaciales para la investigación de la dinámica urbana-rural latente en distritos rurales del interior de Italia meridional***

**RESUMEN.** El uso de patrones rurales-urbanos es una herramienta bien conocida que nos ayuda para capturar interacciones socioeconómicas entre distintas formas de asentamientos. El desafío de la sostenibilidad requiere considerar la evolución de estos patrones como un indicador fiable de la dinámica del cambio de uso de suelo y los posibles procesos de degradación ocurridos en un marco de tiempo. En esta investigación, utilizando datos de múltiples fuentes (imágenes de satélite Corine Land Cover, Keyhole KH-9 y Landsat), se trazó la evolución diacrónica (1990-2018) del patrón rural-urbano en las provincias de Avellino y Benevento (región de Campania, Sur de Italia) con un enfoque específico en el municipio clave de Ariano Irpino (1975-2018). El análisis confirma el considerable crecimiento urbano ocurrido en el área de estudio, principalmente en forma de fenómenos de

expansión desacoplados del crecimiento demográfico. Esto ocurre simultáneamente con la transformación del sector agrícola proyectada hacia una mayor especialización favoreciendo actividades de agroturismo y cultivos valiosos (p. ej., viñedos). Estos hallazgos pueden ayudar a los formuladores de políticas en futuras actividades de planificación al combinar acciones de conservación, mitigación y restauración.

**Keywords:** Rural-urban pattern, urban sprawl, inner areas, remote sensing, Corine Land Cover.

**Palabras clave:** Patrones urbano-rurales, expansión urbana, áreas internas, sensores remotos, Corine Land Cover.

Received: 24 July 2023

Accepted: 21 November 2023

**\*Corresponding author:** Casandra Muñoz Gomez. National School of Earth Sciences (ENCiT) of National Autonomous University of Mexico (UNAM). Av. Antonio Delfín Madrigal 300, C.U., Coyoacán, 04510 Ciudad de México, CDMX, México. E-mail address: casandragomez@encit.unam.mx

## 1. Introduction

Rural-urban is a lexical dichotomy traditionally used to indicate the complex relationships among rural and urban areas, considered as two different models of territorial organization and socio-economic context. Therefore, understanding both rural and urban areas is pivotal towards sustainable land use development (Van Vliet *et al.* 2020). Dynamics involving rural and urban areas have resulted in deep transformations of landscapes over time with significant side effects from a socio-economic and cultural point of view. Van Noorloos *et al.* (2018) point out that we need to identify in more detail the indirect and long-term effects that urban land investments have on livelihoods as well as the differentiation and complexity of these effects for different actors. The initial, striking dualism, conceiving urban and rural areas as two opposing socio-economic realities with different functional and spatial configurations, has then been replaced by an approach looking at their complementarity and subsidiarity in pursuing a sustainable development of territories. It is important that the ideas that inform rural-urban understanding today capture the abstract yet experientially recognizable spatialities that reflect human's interactions with the physical land (Dymitrow and Stenseke, 2016).

In particular, nowadays, the challenge of sustainability suggests looking at the evolution of the rural-urban pattern as an effective indicator of land cover dynamics, useful for highlighting inequalities and vulnerabilities of various geographical contexts and for indicating the most appropriate actions to preserve soil surface against sealing and contamination and its numerous environmental and socio-economic functions (Blum, 2005; EC, 2006; Carlucci *et al.*, 2018). As a matter of fact, the rural-urban migration, the expansion of urbanized areas and the simultaneous exacerbation of climate change (Wang *et al.*, 2020; Nickayin *et al.*, 2021; Zasada *et al.*, 2013; Coluzzi *et al.*, 2020; Lanfredi *et al.*, 2020; Zambon *et al.*, 2018) can cause changes on a local and global scale in several ways (Tas and Lightfoot, 2005; Sailor, 2014; Telesca *et al.*, 2009; Biasi *et al.*, 2015). Among them, they can influence the disaster risk and the vulnerability or exposure of the population to them, including escalation of environmental degradation (D'Emilio *et al.*, 2018; Barakat *et al.*, 2019; Horion *et al.*, 2019; Yu *et al.*, 2021; Samela *et al.*, 2022a; Kosmas *et al.*, 2016), change of hydrological processes with consequent rise in flood risk (Samela *et al.*, 2020; Samela *et al.*, 2022b), risk of extreme weather and geological events due to increased population vulnerability and concentration and, at times, reduced resilience (Lankao and Qin, 2011).

In this scenario, in the last decades, the international community and the European Union have repeatedly stressed the importance of protecting soil, environmental heritage and landscape by issuing specific directives (e.g., Habitats Directive, Water Framework Directive, European Landscape

Convention, etc.) and have also set strategic goals to reach within specific time frames: a state of land degradation neutrality (LDN) on a global scale by 2030 (UN, 2015) and the reduction to zero of net land take by 2050 (EC, 2016). Every nation joining the Conventions is required to meet these objectives. In this context, especially for the second target, also Italy should promote a considerable effort since it must reverse a long-standing trend of continuous and significant growth in land consumption from the 1950s to today (about 180%, see e.g., Romano and Zullo, 2014; Bimonte and Stabile, 2017; Munafò, 2019; Bianchini *et al.*, 2021) which currently places the nation in the list of European countries with the highest percentage of land consumption in relation to the surface area (Marchetti *et al.*, 2017). In addition, a tendential contraction of agricultural areas has been recorded since the 1960s (Congedo *et al.*, 2017) which testifies how the natural capital of Italy is progressively decreasing, with consequent negative impacts on the quality of environment and landscape (e.g., land degradation, see Salvati *et al.*, 2012; Recanatesi *et al.*, 2016; Imbrenda *et al.*, 2022; Lanfredi *et al.*, 2022; Rodrigo-Comino *et al.* 2022; Nickayin *et al.*, 2022) and in terms of socio-economic disparities (Salvati and Zitti, 2007; Salvati and Zitti, 2009). These impacts generally affect the urban-rural fringe in the world, which is among the most ecologically vulnerable areas due to its peculiarities of transition space (Goodarzi *et al.*, 2019; Zhou *et al.*, 2020; Coluzzi *et al.*, 2022; Zambon *et al.*, 2017).

Paying attention to the wide debate on land consumption in Italy, the analysis of the phenomenon of urban sprawl is recently conquering a primary role (Bencardino, 2015; Cecchini *et al.*, 2019). Urban sprawl, fuelled by economic growth (Di Felicianantonio *et al.*, 2018), is notoriously characterized as a highly dispersed settlement model with low or very low density, implying a considerable loss of soil (Bruegmann, 2005; Marquard *et al.*, 2020; Ciommi *et al.*, 2018; Ciommi *et al.*, 2019) with detrimental implications on water and soil management (Chelleri *et al.*, 2019; Duvernoy *et al.*, 2018; Perrin *et al.*, 2018; Salvati *et al.*, 2008). The concept of urban sprawl was born in the second half of the twentieth century in the U.S.A., where cities had predominantly assumed suburban forms as opposed to the European ones which tended to be dense and compact (Barattucci, 2004; Salvati, 2014; Salvati *et al.*, 2019; Salvati *et al.*, 2013). In recent years, the American model has influenced also Europe and Italy, first affecting large cities and gradually involving the urban forms of small towns so much that, currently, these show land consumption rates per new inhabitant higher than those of large cities (Bonora, 2013).

Small towns in Italy, especially those of Southern regions, are mostly characterized by a demographic decline and economic marginalisation, falling into the so-called "inner areas" for which Territorial Cohesion Agency has recently launched a specific Strategy (National Strategy for Inner Areas 2014-2020 and 2021-2027). This is aimed at mobilizing the huge potential of these areas by breaking isolation constraints to make them economically attractive (Carlucci and Lucatelli, 2013) and rebalance in a polycentric direction the development of marginal areas. Therefore, we conducted a research focused on two provinces (NUTS-3 - Nomenclature of territorial units for statistics - Level 3) of Southern Italy: Avellino and Benevento belonging to the Campania Region (NUTS-2) including a large number of municipalities falling in the "inner areas". Territorial databases and satellite images were used for the multitemporal reconstruction (1990-2018) of the rural-urban pattern in both regions. A specific focus has been dedicated on some emblematic municipalities, such as the case of Ariano Irpino (province of Avellino) for which the diachronic analysis was extended to the period 1975-2018. The opportunity offered by remote sensing products and derivatives to look back in time and follow the evolution of specific environmental or anthropogenic phenomena, allowed us to highlight some issues common to the two provinces. We expect to be able to provide decision-makers with relevant information useful for preparing more effective territorial planning and to identify the best mitigation/recovery solutions against the challenge "urban sprawl".

## 2. Methodology

### 2.1. Study area

The study area are the provinces of Avellino and Benevento (Campania region, Southern Italy), characterized by the presence of many municipalities belonging to the inner areas, with a low infrastructural level and a rugged topography (Table 1 and Fig. 1).

Table 1. Main demographic features of the investigated areas

Name of the administrative unit	Surface area (km <sup>2</sup> )	Inhabitants (01/01/2019)	Population density (in./ km <sup>2</sup> )	Number of Municipalities
Province of Avellino	2 806,07	418 306	149,07	118
Province of Benevento	2 080,44	277 018	133,15	78
Municipality of Ariano Irpino	186,70	21 756	116,53	-

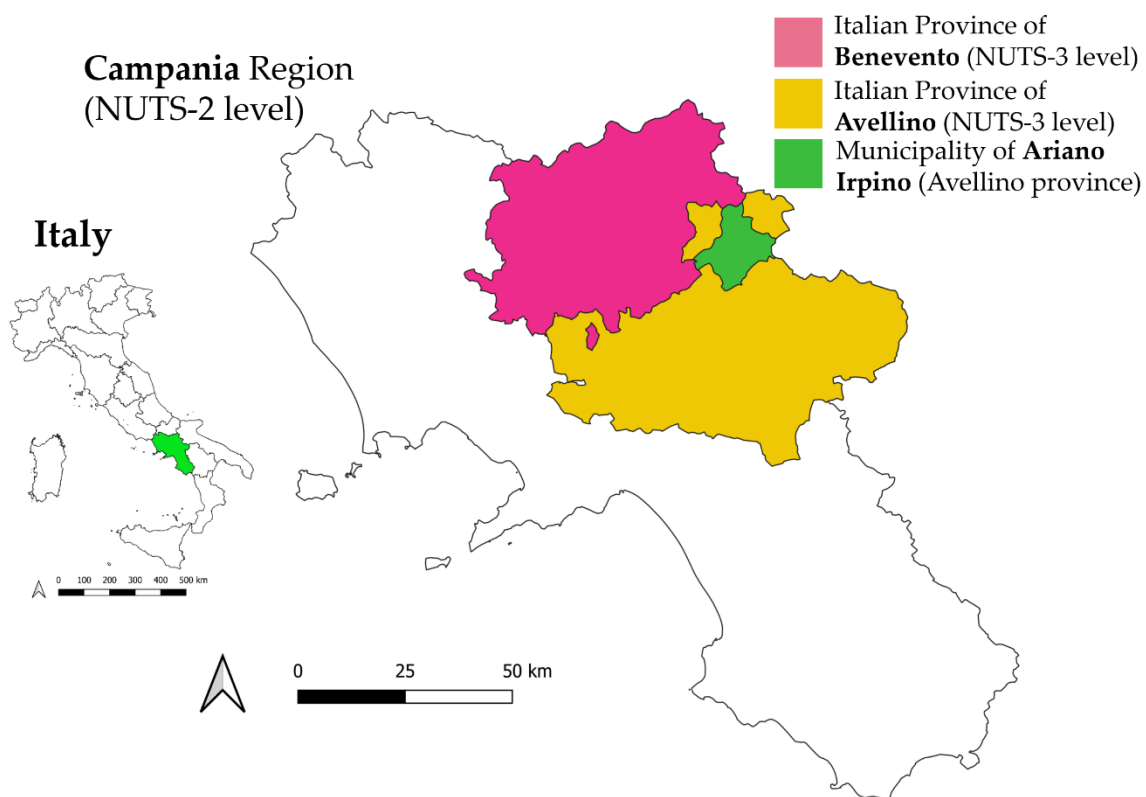


Figure 1. Study area. Italian Provinces of Benevento and Avellino corresponding to the NUTS-3 and the municipality of Ariano Irpino (Avellino) belonging to the Campania region (NUTS-2).

### 2.2. Data

The availability of multitemporal satellite data derived from different sensors represents a valuable tool for the characterization of landscape changes (Bajocco *et al.*, 2015). In this study, a satellite image acquired by the Keyhole KH-9 (belonging to the CORONA program providing imagery deployed by USA for espionage purposes) and NASA (National Aeronautics and Space Administration) Landsat images were processed for the analysis of land cover changes (following the methods explained by Song *et al.*, 2015; Fekete, 2020; Simoniello *et al.*, 2015; Bajocco *et al.*, 2016). The CORONA program, designed and used between the 60s and 70s of the last century, has recently been declassified allowing access for non-military purposes and users. It provides high resolution data (with a pixel size resolution up to 1.80 meters) with a wide spatial coverage (some missions have frames covering strips up to 250 km

long), which can be purchased at low cost with respect to other similar products (Stratoulis, 2020). Landsat data, on the other hand, are among the first sources of medium-resolution multispectral images with global coverage: the first satellite of the Landsat mission was launched into orbit in 1972 and carried the Multispectral Scanner-MSS sensor with 80m of spatial resolution (see e.g., Irons *et al.*, 2012; Quaranta *et al.*, 2020). Since 2013, Landsat 8 data are available with a 30-m spatial resolution, and they are distributed free of charge (Fig. 2). Finally, high-resolution satellite images available in Google Earth have been used for the analysis of the current land cover conditions in the study area.

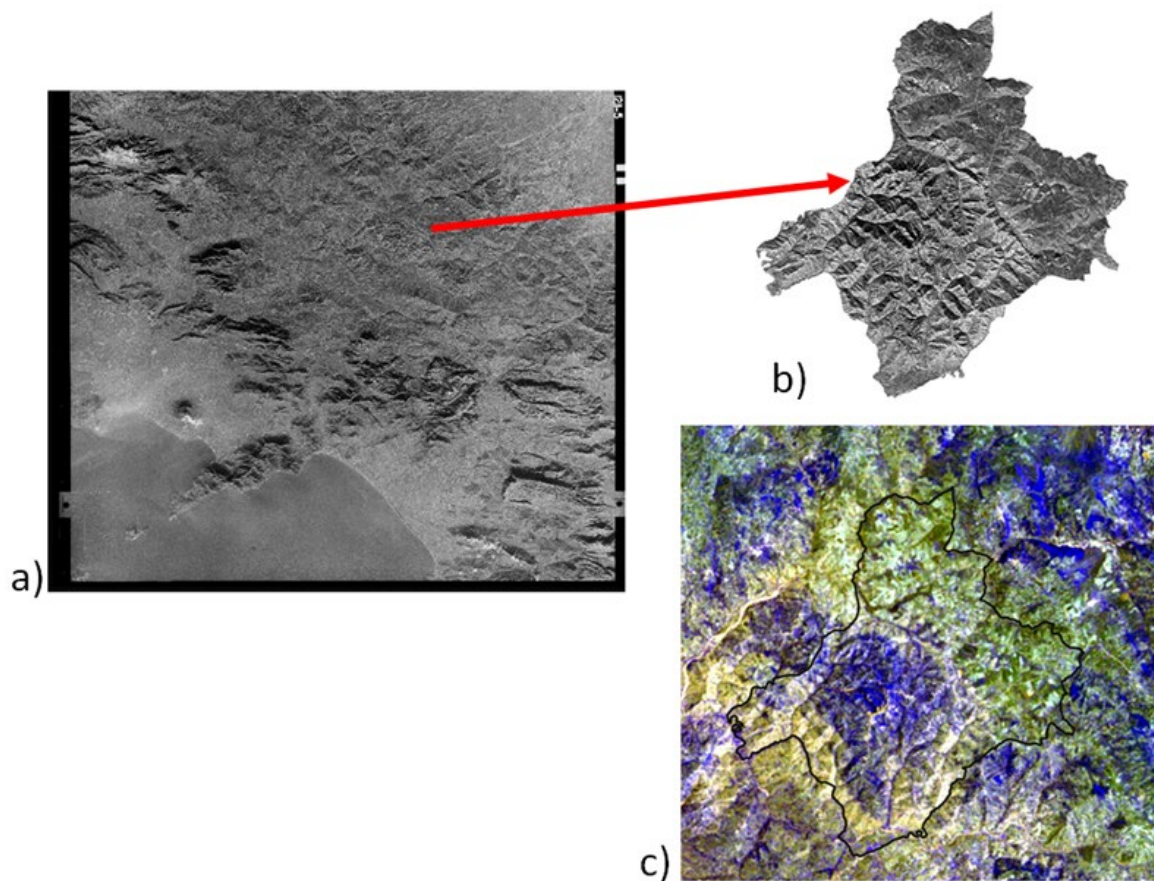


Figure 2. (a) Satellite image acquired by Keyhole KH-9 on 29/12/1975 including areas of the provinces of Benevento and Avellino; (b) municipal area of Ariano Irpino cropped from the Keyhole KH-9 image; (c) Landsat MSS satellite image acquired on 16/07/1975 including the municipality of Ariano Irpino, false-colour composition (black lines represent the municipal boundaries).

The database of Corine Land Cover (CLC) project has also been used in this study (Büttner *et al.*, 2002). The CLC inventory was born at a European level mainly to detect and monitor land cover/land use features and changes, with the aim of supporting the nations involved in many applications (environmental, agricultural, ecological, planning, etc.). The first structuring of the CLC project dates to 1985 when the Council of the European Community through Decision 85/338/EEC launched the so-called CORINE (COoRdination of INformation on the Environment) program to provide Member States with homogeneous territorial information on the state of the environment. The first CLC was issued in 1990, while updates have been released in 2000, 2006, 2012, and 2018. The National Reference Centers Land Cover (NRC/LC) group of the Eionet (European Environment Information and Observation Network) belonging to the European Environment Agency (EEA) took care of the elaboration. The 2012 version was the first to include CLC time series into the Copernicus program, thus ensuring sustainable funding for the future. Finally, the 2018 version was produced using Sentinel-2 satellite data (10-m spatial resolution). In this research, the 1990 and 2018 CLC maps were used at the third level, which includes a

total of 44 classes (see next Figures) with a minimum cartographic unit (MCU) of 25 ha and an accuracy of approximately 85% (Diaz-Pacheco and Gutiérrez, 2014; Ahrens and Lyons, 2019; Cieślak *et al.*, 2020).

### 2.3 Methods

For the study of the rural-urban pattern, all the different information layers (indices or maps obtained from the analysis of satellite data and territorial databases) have been organized in a GIS (Geographic Information System) environment. Specifically, CLC layers have been analysed using zonal statistics tools included in the free and open-source software QGIS. As regards remote sensing data, a Keyhole KH-9 image acquired on 29/12/1975 and a Landsat MSS2 image acquired on 16/7/1975 were used. On the first, after a pre-processing for geo-referencing the image, the urban areas have been identified through photointerpretation. Through the analysis of multispectral Landsat image, the vegetation cover areas have been identified by estimating the Normalized Difference Vegetation Index (NDVI), defined as follows:

$$NDVI = \frac{\rho_{nir} - \rho_{red}}{\rho_{nir} + \rho_{red}}$$

where  $\rho_{nir}$  e  $\rho_{red}$  stand for the spectral reflectance measurements acquired in the near-infrared (NIR) and RED (visible) regions respectively, corresponding to different segments of the electromagnetic spectrum. This index is a proxy of the vegetation vigor, density and overall health of the examined covers (Rouse, 1973; Bonfiglio *et al.*, 2002). To capture land cover changes that took place between 1975 and 2018 in the municipality of Ariano Irpino, the 1975 land cover map and 1990 and 2018 CLC maps have been compared. The 1975 land cover map has been produced by using the Keyhole KH-9 and Landsat satellite images, while the 1990 and 2018 CLC maps have been used in a simplified version by merging the Level-3 classes into the following macro-categories: vegetation, agricultural areas/bare soil and urban areas.

## 3. Results

### 3.1. Province of Benevento

The multitemporal analysis of the CLC (1990-2018) for the Province of Benevento (Fig. 3) shows a considerable increase of urbanized areas of 2,428 hectares, which corresponds to a percentage growth of over 45%. This amplifies the weight of impermeable surfaces with respect to the entire provincial extent (from 2.59 % in 1990 to 3.76% in 2018, see Figs. 3 and 4).

Indeed, the most alarming fact is the increase in the contribution of the discontinuous urban fabric on the overall sealed surfaces, which goes from about 68% in 1990 to about 86% in 2018, confirming the expansion of low-density settlements (Bencardino and Valanzano, 2015). Concurrent to the phenomenon of land consumption, a demographic contraction of about 4.5% (population goes from 292,175 in 1990 to 279,127 in 2018) is recorded in the period considered accompanied by no changes in the extent of the main agricultural covers (surface variations for each crop type are below 1%).

In particular, this last phenomenon is also characterized by a tendency towards a lower specialization evidenced by the reduction of non-irrigated arable land (class 211), orchards (class 222) and olive groves (class 223) and an increase in the CLC classes defined as "heterogeneous agricultural areas", such as *complex cultivation patterns* (Class 242) and *land principally occupied by agriculture, with significant areas of natural vegetation* (Class 243). Given the endemic crisis that has hit the primary sector in recent years, these findings also reveal a transition phase of local agricultural entrepreneurship. It seems that farming entrepreneurs were more interested in differentiating the nature of investments on different types of crops in order to lower the risk threshold of the economic enterprise (Figs. 3 and 4). As an example of the dynamics observed, we report the case of San Bartolomeo in Galdo, a municipality

of 4,644 inhabitants in 2018, whose land use trend at the municipal scale shows the same tendency seen at the provincial scale. The strong demographic decrease (about -27% in the period 1990-2018) is coupled with a considerable urban growth (+55 hectares corresponding to an increase of over 85%) with the contribution of the discontinuous urban fabric on the total urban coverage that rises from 65% in 1990 to 76.6% in 2018 (Fig. 5).

The agricultural component also follows the trend observed at the provincial scale. There is a substantial conservation of the overall agricultural areas, which are mainly destined to mixed crops including, in addition to traditional arable land, also perennial crops (especially olive groves) and stable meadows.

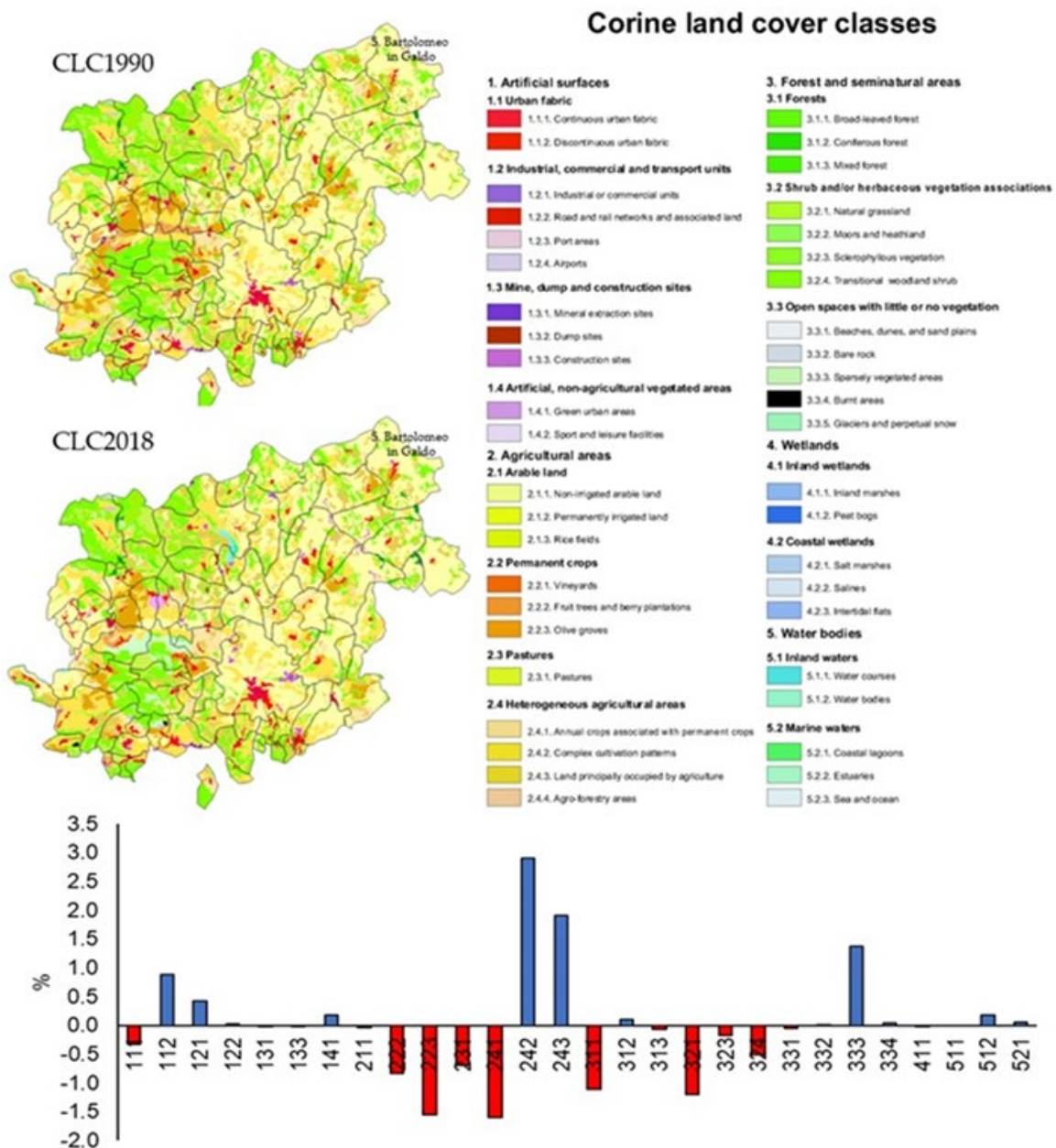


Figure 3. 1990 and 2018 CLC maps of the Province of Benevento (the legend is extracted from Copernicus site, <https://land.copernicus.eu/Corinelandcoverclasses.eps.75dpi.png/view>) and percentage variations for CLC classes (level 3) observed in the period 1990-2018 for the Province of Benevento.

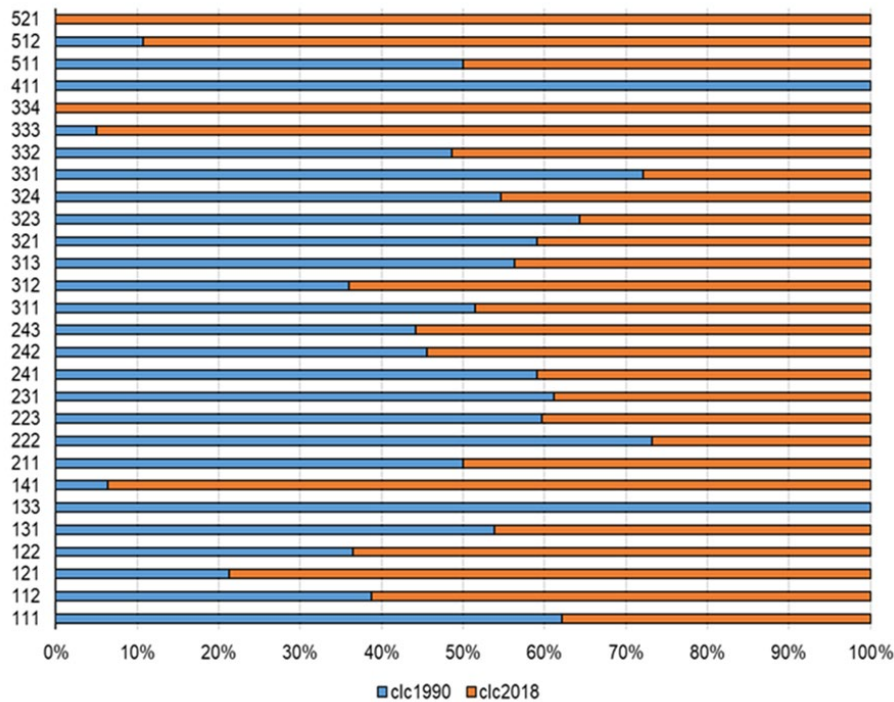


Figure 4. Proportion of CLC classes (level 3) identified between 1990 (in blue) and 2018 (in orange) in the province of Benevento. See the legend of figure 3 to know the correct code.

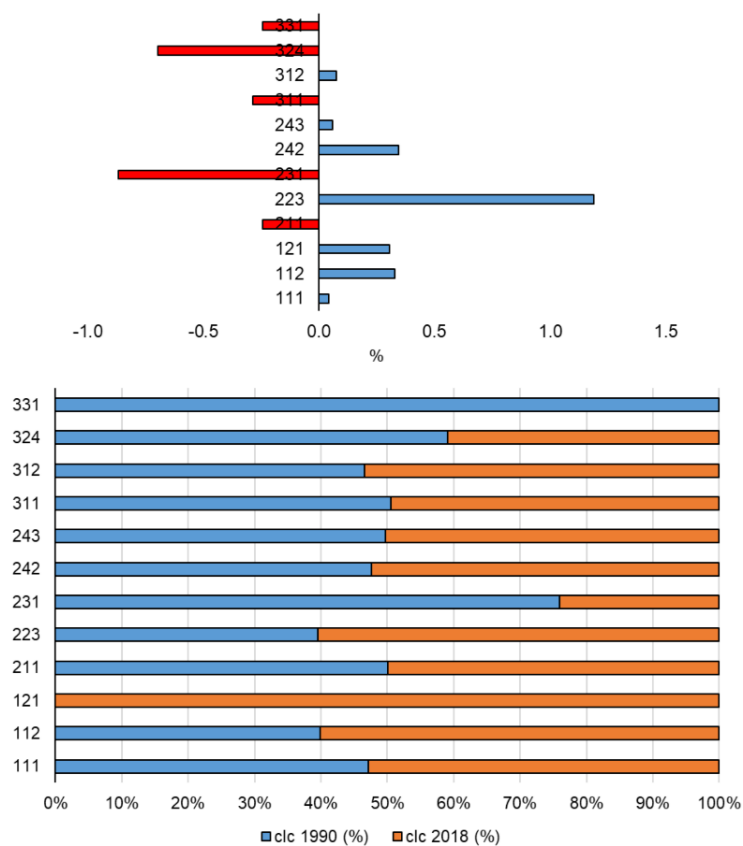


Figure 5. Percentage differences for CLC classes (level 3) observed in the period 1990-2018 for the municipality of San Bartolomeo in Galdo and proportion of CLC classes (level 3) between 1990 (blue) and 2018 (orange) in the municipality of San Bartolomeo in Galdo. See the legend of figure 3 to know the correct code.

### 3.2. Province of Avellino

The multitemporal analysis of the CLC (1990-2018) for the Province of Avellino (Fig. 6) highlights an increase in urbanized areas of 3,896 ha, corresponding to a percentage growth of over 31%. The overall weight of the sealed areas with respect to the overall surface of the Avellino Province goes from 3.1% in 1990 to 4.5% in 2018. Also in this case, the already prevalent contribution of the discontinuous urban fabric on the total urban surface (75.3% in 1990) increases further (80.8%) in 2018 (Figs. 6 and 7). This accounts for a territorial structure that had a dispersive configuration since the 90s, which further consolidated in the last thirty years. In parallel with this phenomenon of land consumption, there is a demographic contraction of about 4.4% in the period considered (population goes from 437,131 in 1990 to 418,306 in 2018) and a sort of agricultural stasis with a modest increase in areas devoted to agriculture (+ 2.1% in the period considered) with a very limited variations in the surfaces of the individual

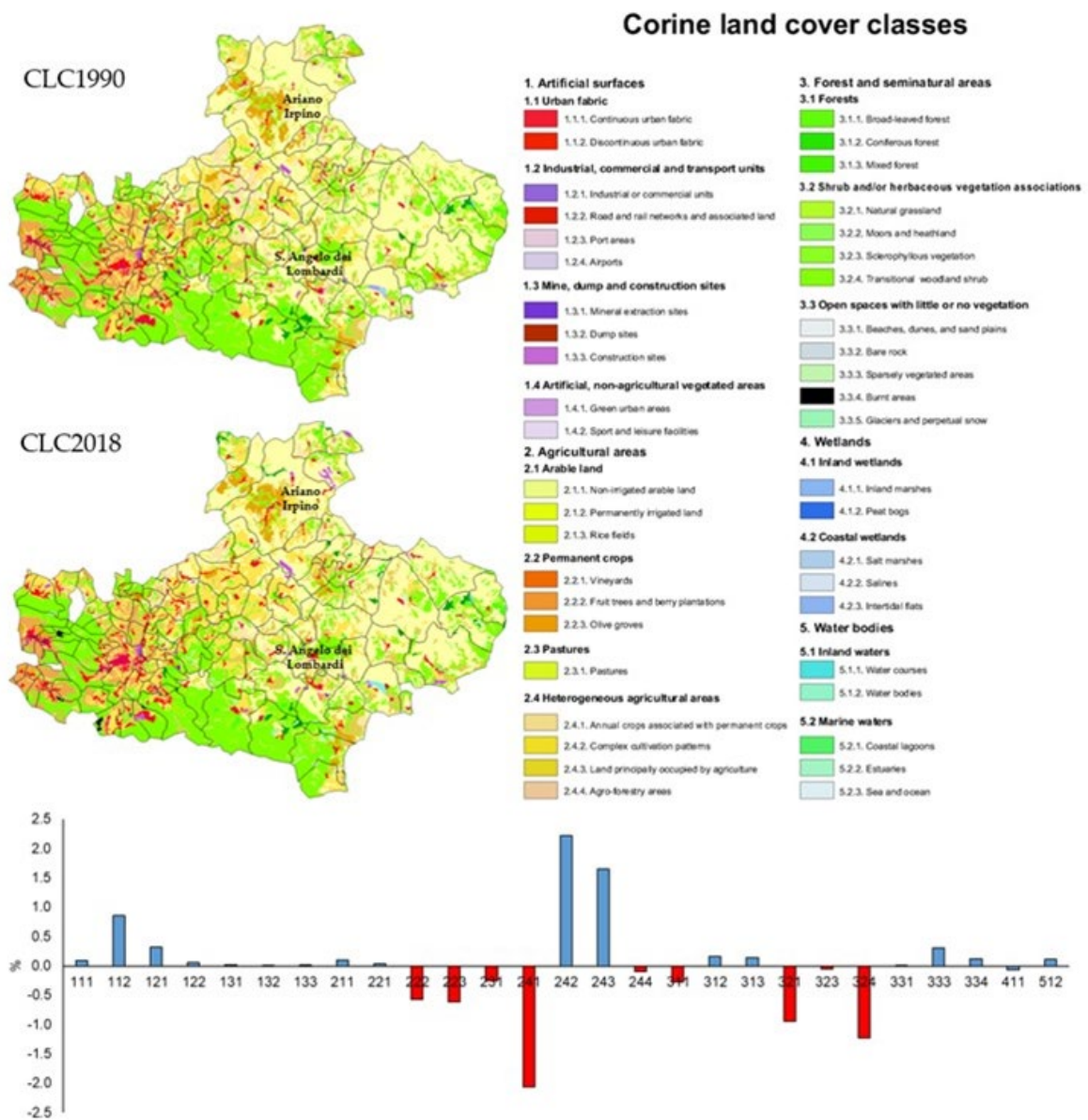


Figure 6. 1990 and 2018 CLC maps of the Province of Avellino and percentage variations for CLC classes (level 3) observed in the period 1990-2018 for the Province of Avellino.

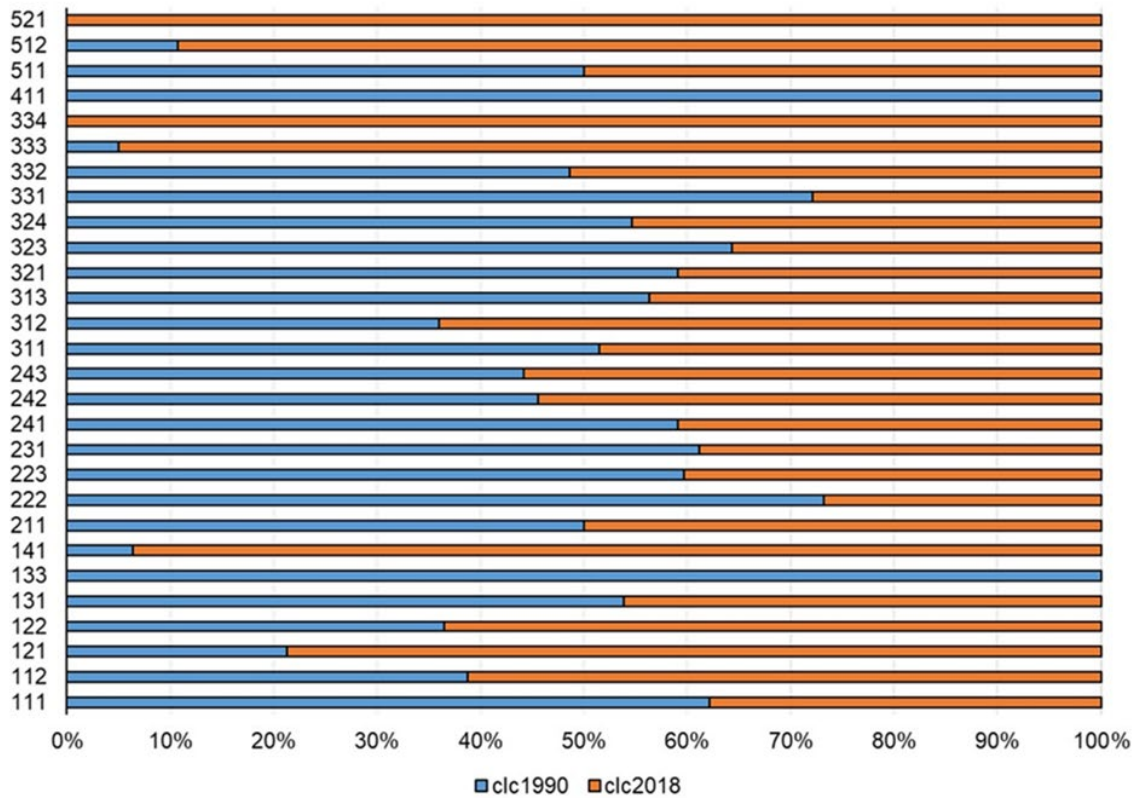


Figure 7. Proportion of CLC classes (level 3) between 1990 (in blue) and 2018 (in orange) for the Province of Avellino. See the legend of figure 6 to know the correct code.

crops (less than 2.3%). Specifically, non-significant transformations have interested areas within perennial crops (slight growth of orchards and olive groves to the detriment of vineyards) and heterogeneous agricultural classes (CLC 241-242-243-244).

As an example of the phenomena observed in the entire province of Avellino, we report the case of Sant'Angelo dei Lombardi, a municipality of 4,928 inhabitants in 1990 and 4,173 inhabitants in 2018. Despite the significant demographic contraction (about 15%), the sealed surfaces grow significantly (+73.7 ha corresponding to an increase of over 63%) with the contribution of the discontinuous urban fabric on the total urban coverage that goes from 69.7% in 1990 to about 100% in 2018. In other words, the whole town of Sant'Angelo dei Lombardi is characterized by a fragmented pattern of settlement which is typical of urban sprawl (Fig. 8).

As regards the agricultural component, very limited variations can be noted also in this specific case, with the reduction of class 211 (arable land), 231 (stable meadows), and 241 (annual crops associated with permanent crops) and a slight increase in 242 (crop systems and complex parcels) and 243 (areas mainly occupied by agricultural crops with the presence of important natural spaces).

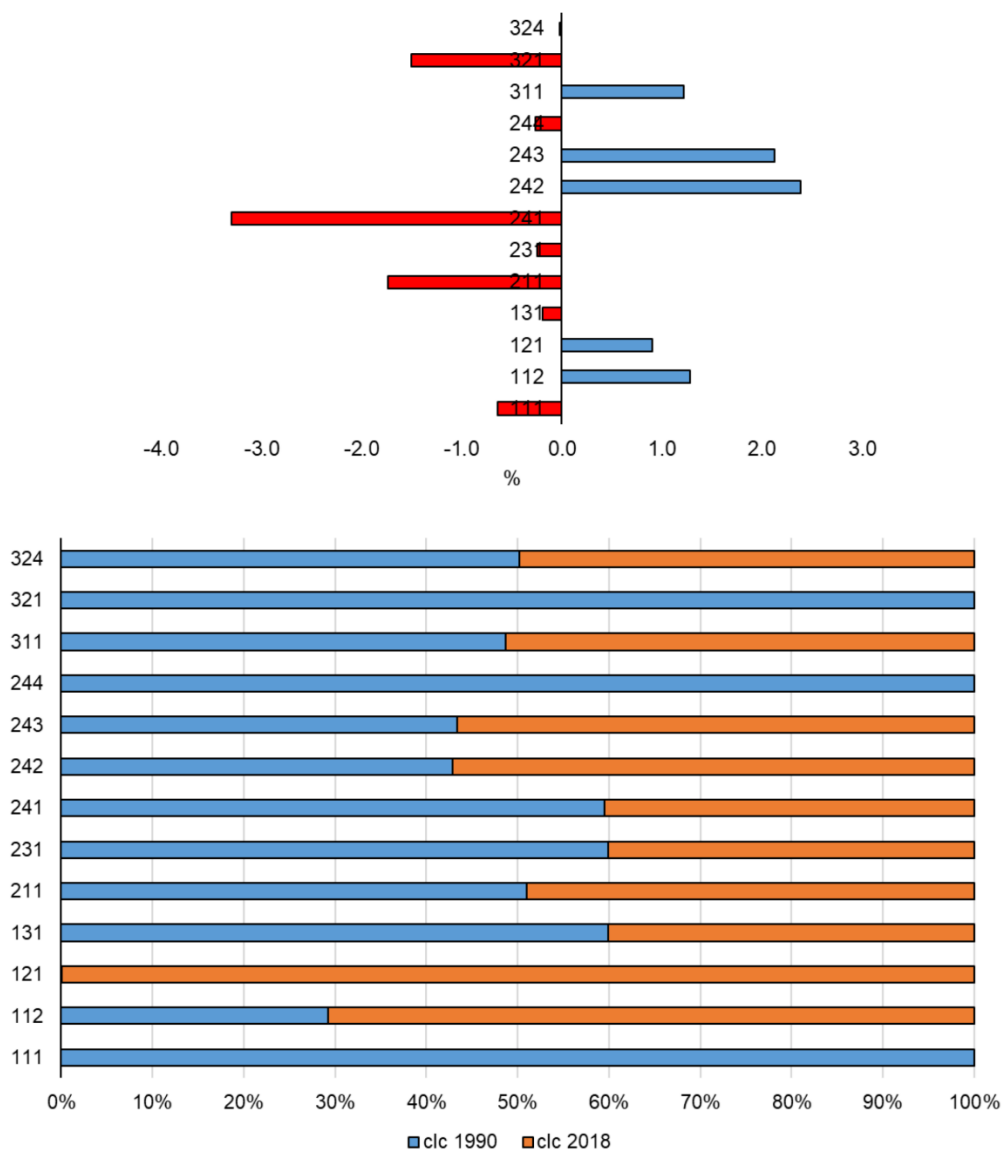


Figure 8. Percentage differences for CLC classes (level 3) observed in the period 1990-2018 for the municipality of Sant' Angelo dei Lombardi (Province of Avellino) and proportion of CLC classes (level 3) between 1990 (in blue) and 2018 (in orange) for the municipality of Sant' Angelo dei Lombardi (Province of Avellino). See the legend of figure 6 to know the correct code.

### 3.3. A focus on the municipality of Ariano Irpino

A detailed study has been carried out on the municipality of Ariano Irpino. Thanks to Keyhole KH-9 and Landsat historical satellite images, it has been possible to reconstruct the land cover map for 1975 (Fig. 9). The comparison between this map and the CLC 2018, after merging classes (the macro-categories are vegetation, agricultural areas/bare soil and urban areas), shows that the area was affected by an extraordinary increase in urbanized surfaces (about +175%) mainly concentrated in the period 1990-2018. Consequently, natural surfaces have undergone a considerable decrease (about -78%) over the entire period with a high rate of decrease in the time window 1975-1990 and a very low rate in the subsequent period 1990-2018 (Fig. 9). Finally, agricultural areas grow of about 29% in the period 1975-2018, but it worth noting that the entire expansion phase is limited to the first fifteen years, while the subsequent time segment (1990-2018) is characterized by an essential stability.

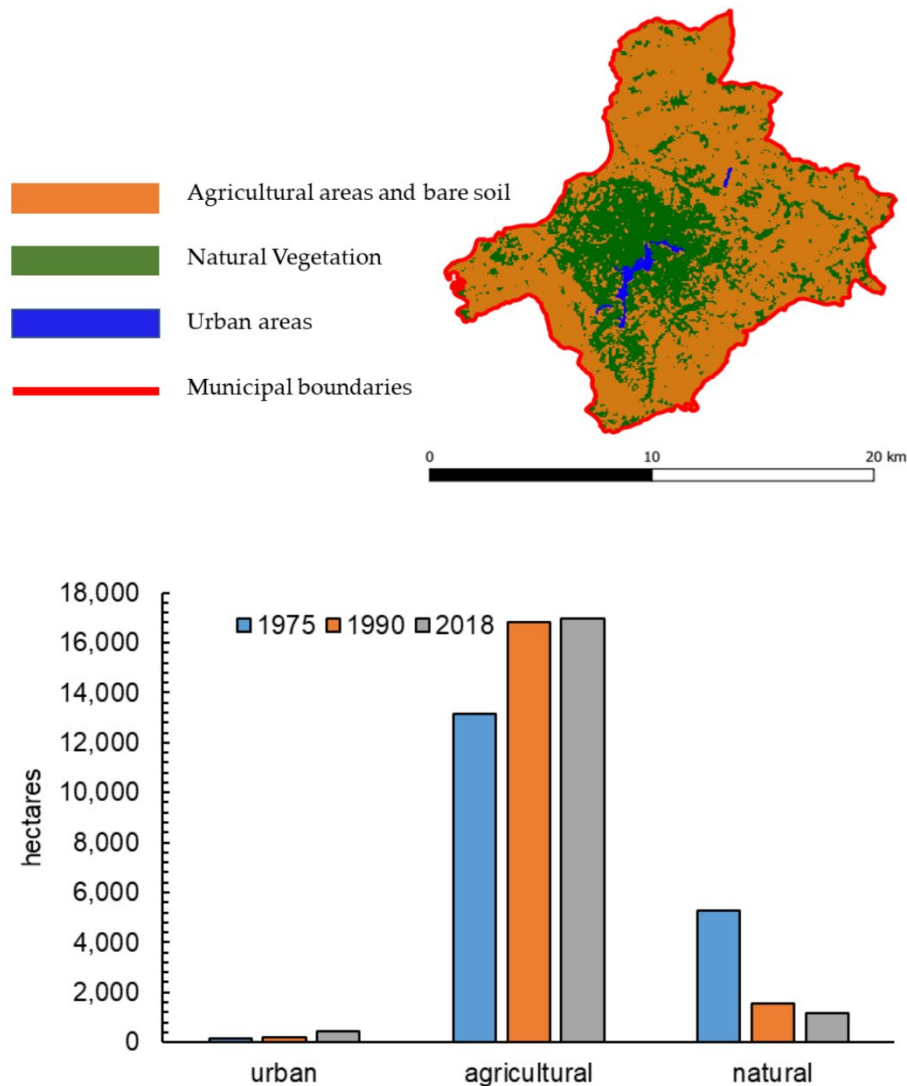


Figure 9. Ariano Irpino land cover map relative to the year 1975 extrapolated by processing the Keyhole KH-9 and Landsat MSS satellite data and diachronic trend of the main land cover (urban areas, agricultural and natural areas) in Ariano Irpino in the period 1975-2018.

The detailed analysis of the land cover carried out for the period 1990-2018 using the CLC maps (Fig. 10) suggests a further strengthening of the sprawl phenomenon, since the weight of the discontinuous urban fabric on the entire sealed surface increases from 79.5 % to 89.5%.

Furthermore, as observed in Figures 11 and 12 the urban surface in 2018 is largely made up (56.3%) of areas that were agricultural lands in 1990, while only 41.9% of the current urban area has conserved the same land use of 1990. Finally, 72% of the agricultural-urban transition formed new discontinuous urban fabric. Regarding agricultural areas, there are no significant variations. As usual, the trend is towards a reduction in arable land (class 211), olive groves (class 223) and annual associated with permanent crops (class 241), with an increase in the class 243 (agricultural crops with the presence of important natural spaces) with a more considerable presence of natural vegetation within heterogeneous agricultural areas.

### Corine land cover classes

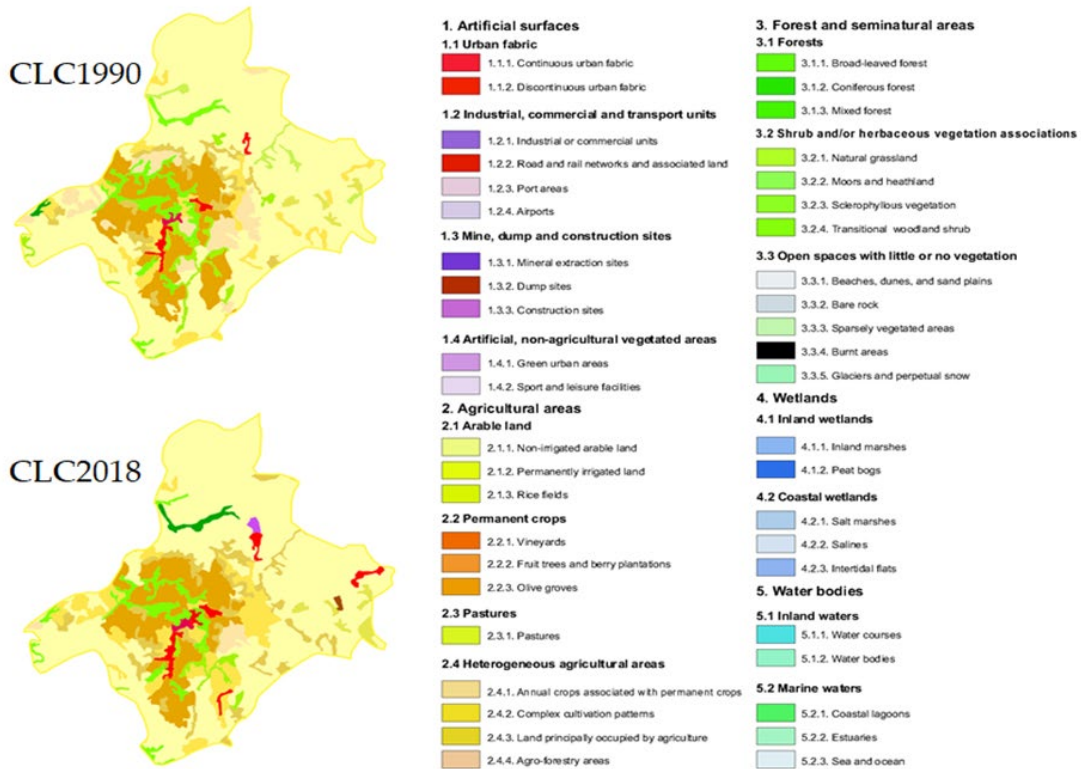


Figure 10. 1990 and 2018 CORINE Land Cover (CLC) maps of the municipality of Ariano Irpino.

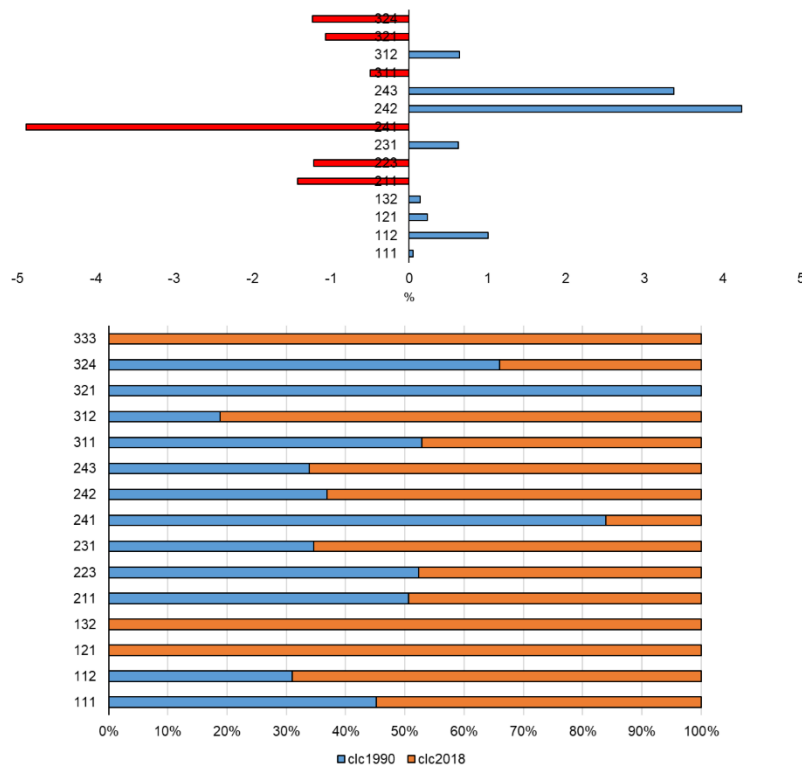


Figure 11. Percentage differences for CLC classes (level 3) observed in the period 1990-2018 for the municipality of Ariano Irpino and percentage of CLC classes (level 3) in 1990 (in blue) and in 2018 (in orange) in the municipality of Ariano Irpino. See the legend of figure 10 to know the correct code.

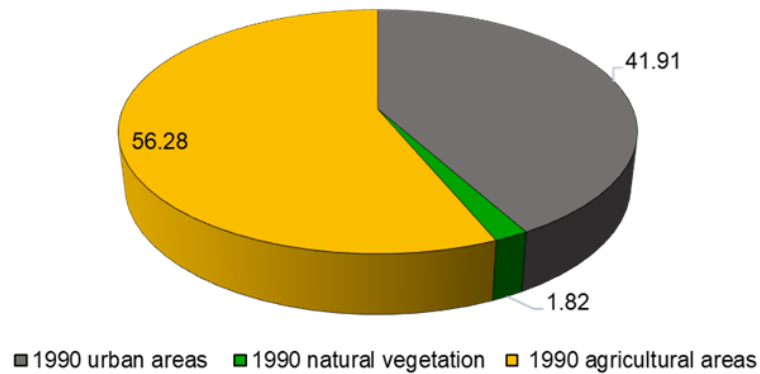


Figure 12. 1990 land cover classes which are urban areas in 2018 in the municipality of Ariano Irpino.

#### 4. Concluding remarks

The rural-urban pattern in the provinces of Avellino and Benevento has undergone important transformations in the period 1990-2018. In a context of stagnation and demographic contraction, under the grip of an economic crisis that pervades Mediterranean regions (Gallardo *et al.*, 2023) and especially the southern regions of Italy since the mid-2000s, we observed a significant increase in sealed surfaces in these areas through processes of urban and suburban expansion recognizable as sprawl that exceeds the real demand and carrying capacity of many areas of the analyzed districts (Punzo *et al.*, 2022). In fact, the weight of the discontinuous urban fabric on the total urban areas grows consistently and becomes, even in small towns, the dominant urban form. At the same time, in the period analysed, agriculture preserves approximately the same areal extension, but shows a tendency to replace arable land with an association of covers with a greater presence of perennial crops and natural vegetation patches. The loss of arable land is clearly attributable to the ageing of population and migration flows (Cardillo and Cimino, 2022, Santelli *et al.*, 2022). From the management point of view, we observed a peculiar condition marked by the crisis of the primary sector suggesting to farmers to differentiate their production rather than risking capitals on a single type of crop (Ronza *et al.*, 2013).

Also, more profitable crops, such as vineyards and orchards, record a general stability or a very slight decline, revealing the tendency to invest capitals in tourism activities based on experiential enjoyment encompassing speciality foods, cultural identity, natural areas (Bassano *et al.*, 2019). This has favoured the maintenance of those landscapes useful for these activities (just vineyards, olive groves and some types of orchards), as well as the production of food and wine of excellence driven by DOC (Denomination of Controlled Origin) and DCOG (Denomination of Controlled and Guaranteed Origin, see e.g., Cusano *et al.*, 2022). Lands combined with agritourist facilities also fall under this process, especially in the province of Avellino. Furthermore, farm density is notable in the study areas, i.e., both the number of farms and the average UAA (Utilized Agricultural Area) per farm are higher than the regional average, and in the face of the demographic trend and the wheat crisis, this suggests that agriculture is now an entrepreneurial reality, which would also help to explain, albeit marginally, the densification of services and infrastructure (see the report of Ciaravino *et al.*, 2021). The general picture does not change when examining the case of the municipality of Ariano Irpino. Here, an impressive urban growth can be observed, with an increase of sealed surfaces of over 137% in the period 1990-2018, which becomes 184% by extending the time window to 1975. The prevailing contribution of the discontinuous urban fabric becomes even more marked (from about 80% to 90%). Moreover, land cover trajectories towards urban land use are mainly generated by soils previously devoted to agriculture, with significant losses in terms of ecosystem goods and services (Assennato *et al.*, 2022). The atypical behaviour of urban expansion in Ariano Irpino is probably due to the close presence of both the highway Napoli-Bari and, most recently, the high-capacity railway line Napoli-Bari, favouring the concentrations of buildings and further infrastructures.

In conclusion, the analysis of the study area returns a picture where the expansion of the urban fabric and the consequent loss of soil is clearly decoupled from population growth and proceeds in parallel with a transformation of the agricultural sector projected toward a greater specialization (Fichera *et al.*, 2012). This confirms the need to enforce policies to contain the phenomenon of land consumption through the adoption of more effective planning tools including subsidies and incentives for the primary sector in the perspective of a sustainable agriculture able to halt depopulation phenomena and preserve Mediterranean landscapes (Di Gennaro, 2017).

## References

- Ahrens, A., Lyons, S., 2019. Changes in land cover and urban sprawl in Ireland from a comparative perspective over 1990–2012. *Land* 8(1), 16. <https://doi.org/10.3390/land8010016>
- Assennato, F., Smiraglia, D., Cavalli, A., Congedo, L., Giuliani, C., Riitano, N., Strollo, A., Munafò, M., 2022. The Impact of Urbanization on Land: A Biophysical-Based Assessment of Ecosystem Services Loss Supported by Remote Sensed Indicators. *Land* 11(2), 236. <https://doi.org/10.3390/land11020236>
- Bajocco, S., Dragoz, E., Gitas, I., Smiraglia, D., Salvati, L., Ricotta, C., 2015. Mapping forest fuels through vegetation phenology: The role of coarse-resolution satellite time-series. *PloS one* 10(3), e0119811. <https://doi.org/10.1371/journal.pone.0119811>
- Bajocco, S., Ceccarelli, T., Smiraglia, D., Salvati, L., Ricotta, C., 2016. Modeling the ecological niche of long-term land use changes: The role of biophysical factors. *Ecological Indicators* 60, 231-236. <https://doi.org/10.1016/j.ecolind.2015.06.034>
- Barakat, A., Ouargaf, Z., Khellouk, R., El Jazouli, A., Touhami, F., 2019. Land use/land cover change and environmental impact assessment in béni-mellal district (Morocco) using remote sensing and gis. *Earth Systems and Environment* 3(1), 113-125. <https://doi.org/10.1007/s41748-019-00088-y>
- Barattucci, C., 2004. *Urbanizzazioni disperse. Interpretazioni e azioni in Francia e Italia 1950-2000*. Roma: Officina Edizioni.
- Bassano, C., Barile, S., Piciocchi, P., Spohrer, J. C., Iandolo, F., Fisk, R., 2019. Storytelling about places: Tourism marketing in the digital age. *Cities* 87, 10-20. <https://doi.org/10.1016/j.cities.2018.12.025>
- Bencardino M., 2015. Consumo di suolo e sprawl urbano: drivers e politiche di contrasto. *Bollettino della Società Geografica Italiana* 13(8), 217-237.
- Bencardino, M., Valanzano, L., 2015. *Una misura dello sprawl urbano nelle aree interne della Campania: i casi di Benevento, Avellino e Battipaglia. Recuperiamo Terreno. Analisi e prospettive per la gestione sostenibile della risorsa suolo*, Franco Angeli, Milano, 73-88.
- Bianchini, L., Egidi, G., Alhuseen, A., Sateriano, A., Cividino, S., Clemente, M., Imbrenda, V., 2021. Toward a dualistic growth? Population increase and land-use change in Rome, Italy. *Land* 10(7), 749. <https://doi.org/10.3390/land10070749>
- Biasi, R., Brunori, E., Smiraglia, D., Salvati, L., 2015. Linking traditional tree-crop landscapes and agrobiodiversity in Central Italy using a database of typical and traditional products: A multiple risk assessment through a data mining analysis. *Biodiversity and Conservation* 24(12), 3009-3031. <https://doi.org/10.1007/s10531-015-0994-5>
- Bimonte, S., Stabile, A., 2017. Land consumption and income in Italy: a case of inverted EKC. *Ecological Economics* 131, 36-43. <https://doi.org/10.1016/j.ecolecon.2016.08.016>
- Blum, W.E.H., 2005. Functions of soil for society and the environment. *Rev. Environ. Sci. Biotechnol.* 4, 75-79. <https://doi.org/10.1007/s11157-005-2236-x>
- Bonfiglio, A., Cuomo, V., Lanfredi, M., Macchiato, M., 2002. Interfacing NOAA/ANHRR NDVI and soil truth maps for monitoring vegetation phenology at a local scale in a heterogeneous landscape of Southern Italy. *International Journal of Remote Sensing* 23(20), 4181-4195. <https://doi.org/10.1080/01431160110075811>

- Bonora, P., a cura di (2013). *Atlante del consumo di suolo per un progetto di città metropolitana, Il caso Bologna*, Bologna, Baskerville.
- Bruegmann, R., 2005. *Sprawl. A compact history*. Chicago: University Press.
- Büttner, G, Feranec J, Jaffrain G., 2002. Corine Land Cover Update 2000. Technical guidelines. *Technical Report 89*, European Environment Agency: Copenhagen.
- Cardillo, C., Cimino, O., 2022. Small Farms in Italy: What Is Their Impact on the Sustainability of Rural Areas? *Land* 11, 2142. <https://doi.org/10.3390/land11122142>
- Carlucci, C., Lucatelli S., 2013. Aree interne: un potenziale per la crescita economica del Paese. *Agriregionieuropa* 9(34).
- Carlucci, M., Chelli, F.M., Salvati, L., 2018. Toward a new cycle: Short-term population dynamics, gentrification, and re-urbanization of Milan (Italy). *Sustainability* 10(9), 3014. <https://doi.org/10.3390/su10093014>
- Cecchini, M., Zambon, I., Pontrandolfi, A., Turco, R., Colantoni, A., Mavrakis, A., Salvati, L., 2019. Urban sprawl and the ‘olive’ landscape: Sustainable land management for ‘crisis’ cities. *GeoJournal* 84(1), 237-255. <https://doi.org/10.1007/s10708-018-9848-5>
- Chelleri, L., Schuetze, T., Salvati, L., 2015. Integrating resilience with urban sustainability in neglected neighborhoods: Challenges and opportunities of transitioning to decentralized water management in Mexico City. *Habitat International* 48, 122-130. <https://doi.org/10.1016/j.habitatint.2015.03.016>
- Ciaravino, R., Salato, N., Chiara, S., 2021. *Analisi degli scenari agricoli in Campania. Interpretazione dei territori attraverso una diversa chiave di lettura*. CREA, Roma.
- Cieślak, I., Biłozor, A., Szuniewicz, K., 2020. The use of the CORINE land cover (CLC) database for analyzing urban sprawl. *Remote Sensing* 12(2), 282. <https://doi.org/10.3390/rs12020282>
- Ciommi, M., Chelli, F. M., Carlucci, M., Salvati, L., 2018. Urban growth and demographic dynamics in southern Europe: Toward a new statistical approach to regional science. *Sustainability* 10(8), 2765. <https://doi.org/10.3390/su10082765>
- Ciommi, M., Chelli, F.M., Salvati, L., 2019. Integrating parametric and non-parametric multivariate analysis of urban growth and commuting patterns in a European metropolitan area. *Quality & Quantity* 53(2), 957-979. <https://doi.org/10.1007/s11135-018-0798-2>
- Coluzzi, R., Fascetti, S., Imbrenda, V., Italiano, S. S.P., Ripullone, F., Lanfredi, M., 2020. Exploring the Use of Sentinel-2 Data to Monitor Heterogeneous Effects of Contextual Drought and Heatwaves on Mediterranean Forests. *Land* 9, 325. <https://doi.org/10.3390/land9090325>
- Coluzzi, R., Bianchini, L., Egidi, G., Cudlin, P., Imbrenda, V., Salvati, L., Lanfredi, M., 2022. Density matters? Settlement expansion and land degradation in Peri-urban and rural districts of Italy. *Environmental impact assessment review* 92, 106703. <https://doi.org/10.1016/j.eiar.2021.106703>
- Congedo, L., Marinosci, I., Ritano, N., Strollo, A., De Fioravante, P., Munafò, M., 2017. Monitoring of land consumption: An analysis of loss of natural and agricultural areas in Italy. *Annali di Botanica* 7, 1-9.
- Cusano, A., Russo, F., Guerriero, L., Colucciello, A., Ruzza, G., Guadagno, F. M., Revellino, P., 2022. Geotourism, traditions and typical products of Avellino Province. *Journal of Maps* 18(2), 133-141. <https://doi.org/10.1080/17445647.2021.2004941>
- D’Emilio, M., Coluzzi, R., Macchiato, M., Imbrenda, V., Ragosta, M., Sabia, S., Simoniello, T., 2018. Satellite data and soil magnetic susceptibility measurements for heavy metals monitoring: findings from Agri Valley (Southern Italy). *Environmental earth sciences* 77(3), 1-7. <https://doi.org/10.1007/s12665-017-7206-4>
- Di Feliciantonio, C., Salvati, L., Sarantakou, E., Rontos, K., 2018. Class diversification, economic growth and urban sprawl: Evidences from a pre-crisis European city. *Quality & Quantity* 52(4), 1501-1522. <https://doi.org/10.1007/s11135-017-0532-5>
- Di Gennaro, A., 2017. Il territorio rurale della Campania nelle nuove politiche regionali per l’agricoltura e il paesaggio. In: R. Del Prete, A.P. Leone, (a cura di) *Paesaggi rurali. Percezione, promozione, gestione, sviluppo sostenibile*, pp. 159–175. Regione Campania, Napoli.

- Diaz-Pacheco, J., Gutiérrez, J., 2014. Exploring the limitations of CORINE Land Cover for monitoring urban land-use dynamics in metropolitan areas. *Journal of Land Use Science* 9(3), 243-259. <https://doi.org/10.1080/1747423X.2012.761736>
- Duvernoy, I., Zambon, I., Sateriano, A., Salvati, L., 2018. Pictures from the other side of the fringe: Urban growth and peri-urban agriculture in a post-industrial city (Toulouse, France). *Journal of Rural Studies* 57, 25-35. <https://doi.org/10.1016/j.jrurstud.2017.10.007>
- Dymitrow, M., Stenseke, M., 2016. Rural-Urban Blurring and the Subjectivity Within. *Rural Landscapes* 3 (1). <https://doi.org/10.16993/rl.1>
- EC, 2006. *Thematic strategy for soil protection*. COM (2006)231 final. Commission of the European Communities, Brussels, Belgium.
- EC, 2016. *Science for Environment Policy (2016) No net land take by 2050? Future Brief 14*. Produced for the European Commission DG Environment by the Science Communication Unit, UWE, Bristol.
- Fekete, A., 2020. CORONA High-Resolution Satellite and Aerial Imagery for Change Detection Assessment of Natural Hazard Risk and Urban Growth in El Alto/La Paz in Bolivia, Santiago de Chile, Yungay in Peru, Qazvin in Iran, and Mount St. Helens in the USA. *Remote Sensing* 12(19), 3246. <https://doi.org/10.3390/rs12193246>
- Fichera, C. R., Modica, G., Pollino, M., 2012. Land Cover classification and change-detection analysis using multi-temporal remote sensed imagery and landscape metrics. *European Journal of Remote Sensing* 45(1), 1-18. <https://doi.org/10.5721/EuJRS20124501>
- Gallardo, M., Fernández-Portela, J., Cocero, D., Vilar, L., 2023. Land Use and Land Cover Changes in Depopulated Areas of Mediterranean Europe: A Case Study in Two Inland Provinces of Spain. *Land* 12(11), 1967. <https://doi.org/10.3390/land12111967>
- Goodarzi, M., Haghtalab, N., Saeedi, I., Moore, N. J., 2019. Structural and functional improvement of urban fringe areas: toward achieving sustainable built–natural environment interactions. *Environment, Development and Sustainability* 1-28. <https://doi.org/10.1007/s10668-019-00511-4>
- Horion, S., Ivits, E., De Keersmaecker, W., Tagesson, T., Vogt, J., Fensholt, R., 2019. Mapping European ecosystem change types in response to land-use change, extreme climate events, and land degradation. *Land Degradation & Development* 30(8), 951-963. <https://doi.org/10.1002/ldr.3282>
- Imbrenda, V., Coluzzi, R., Di Stefano, V., Egidi, G., Salvati, L., Samela, C., Simoniello, T., Lanfredi, M., 2022. Modeling spatio-temporal divergence in land vulnerability to desertification with local regressions. *Sustainability* 14(17), 10906. <https://doi.org/10.3390/su141710906>
- Irons, J. R., Dwyer, J. L., Barsi, J. A., 2012. The next Landsat satellite: The Landsat data continuity mission. *Remote Sensing of Environment* 122, 11-21. <https://doi.org/10.1016/j.rse.2011.08.026>
- Kosmas, C., Karamesouti, M., Kounalaki, K., Detsis, V., Vassiliou, P., Salvati, L., 2016. Land degradation and long-term changes in agro-pastoral systems: An empirical analysis of ecological resilience in Asteroussia-Crete (Greece). *Catena* 147, 196-204. <https://doi.org/10.1016/j.catena.2016.07.018>
- Lanfredi, M., Coluzzi, R., Imbrenda, V., Macchiato, M., Simoniello, T., 2020. Analyzing Space–Time Coherence in Precipitation Seasonality across Different European Climates. *Remote Sensing* 12 (1), 171. <https://doi.org/10.3390/rs12010171>
- Lanfredi, M., Egidi, G., Bianchini, L., Salvati, L., 2022. One size does not fit all: A tale of polycentric development and land degradation in Italy. *Ecological Economics* 192, 107256. <https://doi.org/10.1016/j.ecolecon.2021.107256>
- Lankao, P. R., Qin, H., 2011. Conceptualizing urban vulnerability to global climate and environmental change. *Current opinion in environmental sustainability* 3(3), 142-149.
- Marchetti, M., Marino D, Toni A, Giaccio V, Giannelli A, Mastronardi L, Vizzarri M., 2017. *Consumo di suolo, dinamiche territoriali e servizi ecosistemici*. Roma: ISPRA.
- Marquard, E., Bartke, S., Gifreu i Font, J., Humer, A., Jonkman, A., Jürgenson, E., Marto, N., Poelmans, L., Repe, B., Rybski, R., Schröter-Schlaack, C., Sobocká, J., Sorensen, M.T., Vejchodská, E., Yiannakou, A.,

- Bovet, J., 2020. Land Consumption and Land Take: Enhancing Conceptual Clarity for Evaluating Spatial Governance in the EU Context. *Sustainability* 12(19), 8269. <https://doi.org/10.3390/su12198269>
- Munafò, M., 2019. *Consumo di suolo, dinamiche territoriali e servizi ecosistemici*. Edizione 2019. Report SNPA 08/19.
- Nickayin, S. S., Salvati, L., Coluzzi, R., Lanfredi, M., Halbac-Cotoara-Zamfir, R., Salvia, R., Quaranta, G., Alhuseen, A., Gaburova, L., 2021. What Happens in the City When Long-Term Urban Expansion and (Un) Sustainable Fringe Development Occur: The Case Study of Rome. *ISPRS International Journal of Geo-Information* 10(4), 231. <https://doi.org/10.3390/ijgi10040231>
- Nickayin, S. S., Coluzzi, R., Marucci, A., Bianchini, L., Salvati, L., Cudlin, P., Imbrenda, V., 2022. Desertification risk fuels spatial polarization in 'affected' and 'unaffected' landscapes in Italy. *Scientific Reports* 12(1), 747. <https://doi.org/10.1038/s41598-021-04638-1>
- Perrin, C., Nougarede, B., Sini, L., Branduini, P., Salvati, L., 2018. Governance changes in peri-urban farmland protection following decentralisation: A comparison between Montpellier (France) and Rome (Italy). *Land Use Policy* 70, 535-546. <https://doi.org/10.1016/j.landusepol.2017.09.027>
- Punzo, G., Castellano, R., Bruno, E., 2022. Using geographically weighted regressions to explore spatial heterogeneity of land use influencing factors in Campania (Southern Italy). *Land Use Policy* 112, 105853. <https://doi.org/10.1016/j.landusepol.2021.105853>
- Quaranta, G., Salvia, R., Salvati, L., Paola, V. D., Coluzzi, R., Imbrenda, V., Simoniello, T., 2020. Long-term impacts of grazing management on land degradation in a rural community of Southern Italy: Depopulation matters. *Land Degradation & Development* 31(16), 2379-2394. <https://doi.org/10.1002/ldr.3583>
- Recanatesi, F., Clemente, M., Grigoriadis, E., Ranalli, F., Zitti, M., Salvati, L., 2016. A fifty-year sustainability assessment of Italian agro-forest districts. *Sustainability* 8(1), 32. <https://doi.org/10.3390/su8010032>
- Rodrigo-Comino, J., Salvia, R., Egidi, G., Salvati, L., Giménez-Morera, A., Quaranta, G., 2022. Desertification and Degradation Risks vs Poverty: A Key Topic in Mediterranean Europe. *Cuadernos de Investigación Geográfica* 48(1), 23-40. <https://doi.org/10.18172/cig.4850>
- Romano, B., Zullo, F., 2014. Land urbanization in Central Italy: 50 years of evolution. *Journal of Land Use Science* 9(2), 143-164. <https://doi.org/10.1080/1747423X.2012.754963>
- Ronza, M., Lapicciarella, V., Giglio, A., 2013. Aziende agricole tra diversificazione e innovazione. Resistenze e prospettive per il Mezzogiorno. In: V. Amato (a cura di). *Innovazione, impresa e competitività nel Mezzogiorno*, pp. 203-216. Aracne editrice, Roma
- Rouse, J. W., Haas, R. H., Schell, J. A., Deering, D. W., 1973. *Monitoring the vernal advancement and retrogradation (green wave effect) of natural vegetation*. Remote Sensing Center, Texas A&M University, College Station, Texas.
- Sailor, D. J., 2014. Risks of summertime extreme thermal conditions in buildings as a result of climate change and exacerbation of urban heat islands. *Building and Environment* 78, 81-88. <https://doi.org/10.1016/j.buildenv.2014.04.012>
- Salvati, L., 2014. Towards a Polycentric Region? The Socio-economic Trajectory of Rome, an 'Eternally Mediterranean' City. *Tijdschrift voor Economische en Sociale Geografie* 105(3), 268-284.
- Salvati, L., Zitti, M., 2007. Territorial disparities, natural resource distribution, and land degradation: a case study in southern Europe. *Geojournal* 70(2), 185-194. <https://doi.org/10.1007/s10708-008-9124-1>
- Salvati, L., Zitti, M., 2009. Substitutability and weighting of ecological and economic indicators: Exploring the importance of various components of a synthetic index. *Ecological Economics* 68(4), 1093-1099. <https://doi.org/10.1016/j.ecolecon.2008.07.017>
- Salvati, L., Petitta, M., Ceccarelli, T., Perini, L., Di Battista, F., Scarascia, M.E.V., 2008. Italy's renewable water resources as estimated on the basis of the monthly water balance. *Irrigation and Drainage: The Journal of the International Commission on Irrigation and Drainage* 57(5), 507-515. <https://doi.org/10.1002/ird.380>

- Salvati, L., Gemmiti, R., Perini, L., 2012. Land degradation in Mediterranean urban areas: an unexplored link with planning? *Area* 44(3), 317-325. <https://doi.org/10.1111/j.1475-4762.2012.01083.x>
- Salvati, L., Zitti, M., Sateriano, A., 2013. Changes in city vertical profile as an indicator of sprawl: Evidence from a Mediterranean urban region. *Habitat International* 38, 119-125. <https://doi.org/10.1016/j.habitatint.2012.05.006>
- Salvati, L., Ciommi, M. T., Serra, P., Chelli, F. M., 2019. Exploring the spatial structure of housing prices under economic expansion and stagnation: The role of socio-demographic factors in metropolitan Rome, Italy. *Land Use Policy* 81, 143-152. <https://doi.org/10.1016/j.landusepol.2018.10.030>
- Samela, C., Persiano, S., Bagli, S., Luzzi, V., Mazzoli, P., Humer, G., Reithofer, A., Essenfelder, A., Amadio, M., Mysiak, J., Castellarin, A., 2020. Safer\_RAIN: A DEM-Based Hierarchical Filling-&-Spilling Algorithm for Pluvial Flood Hazard Assessment and Mapping across Large Urban Areas. *Water*, 12, 1514. <https://doi.org/10.3390/w12061514>
- Samela, C., Imbrenda, V., Coluzzi, R., Pace, L., Simoniello, T., Lanfredi, M., 2022a. Multi-decadal assessment of soil loss in a Mediterranean region characterized by contrasting local climates. *Land* 11(7), 1010. <https://doi.org/10.3390/land11071010>
- Samela, C., Coluzzi, R., Imbrenda, V., Manfreda, S., Lanfredi, M., 2022b. Satellite flood detection integrating hydrogeomorphic and spectral indices. *GIScience & Remote Sensing* 59(1), 1997-2018. <https://doi.org/10.1080/15481603.2022.2143670>
- Santelli, F., Ragozini, G., Vitale, M. P., 2022. Assessing the effects of local contexts on the mobility choices of university students in Campania region in Italy. *Genus* 78(1), 5. <https://doi.org/10.1186/s41118-021-00144-4>
- Simoniello, T., Coluzzi, R., Imbrenda, V., Lanfredi, M., 2015. Land cover changes and forest landscape evolution (1985–2009) in a typical Mediterranean agroforestry system (high Agri Valley). *Natural Hazards and Earth System Sciences* 15(6), 1201-1214. <https://doi.org/10.5194/nhess-15-1201-2015>
- Song, D. X., Huang, C., Sexton, J. O., Channan, S., Feng, M., Townshend, J. R., 2015. Use of Landsat and Corona data for mapping forest cover change from the mid-1960s to 2000s: Case studies from the Eastern United States and Central Brazil. *ISPRS Journal of Photogrammetry and Remote Sensing* 103, 81-92. <https://doi.org/10.1016/j.isprsjprs.2014.09.005>
- Stratoulis, D., Kabadayı, M. E., 2020. Feature and information extraction for regions of Southeast Europe from Corona satellite images acquired in 1968. In *Eighth International Conference on Remote Sensing and Geoinformation of the Environment (RSCy2020)* (Vol. 11524, p. 115241R). International Society for Optics and Photonics.
- Tas, H. I., Lightfoot, D. R., 2005. Gecekonu Settlements in Turkey: Rural-Urban Migration in the Developing European Periphery. *Journal of Geography* 104(6), 263-271.
- Telesca, L., Coluzzi R., Lasaponara R., 2009. Urban Pattern Morphology Time Variation in Southern Italy by Using Landsat Imagery. In: B. Murgante, G. Borruso, A. Lapucci (eds) *Geocomputation and Urban Planning. Studies in Computational Intelligence*, vol 176. Springer, Berlin, Heidelberg. [https://doi.org/10.1007/978-3-540-89930-3\\_12](https://doi.org/10.1007/978-3-540-89930-3_12)
- UN, 2015. *Transforming our World: The 2030 Agenda for Sustainable Development*, A/RES/70/1, United Nations.
- Van Noorloos, F., Klaufus, C., Steel, G., 2018. Land in urban debates: Unpacking the grab–development dichotomy. *Urban Studies* 56(5), 855-867. <https://doi.org/10.1177/0042098018789019>
- Van Vliet, J., Birch-Thomsen, T., Gallardo, M., Hemerijckx, L.M., Hersperger, A.M., Li, M., Tumwesigye, S., Twongyirwe, R., van Rompaey, A., 2020. Bridging the rural-urban dichotomy in land use science. *Journal of Land Use Science* 15(5), 585-591. <https://doi.org/10.1080/1747423X.2020.1829120>
- Wang, X., Shi, R., Zhou, Y., 2020. Dynamics of urban sprawl and sustainable development in China. *Socio-Economic Planning Sciences* 70, 100736. <https://doi.org/10.1016/j.seps.2019.100736>

- Yu, L., Lyu, Y., Chen, C., Choguill, C. L., 2021. Environmental deterioration in rapid urbanisation: evidence from assessment of ecosystem service value in Wujiang, Suzhou (2021). *Environment, Development and Sustainability* 23, 331–349. <https://doi.org/10.1007/s10668-019-00582-3>
- Zambon, I., Colantoni, A., Carlucci, M., Morrow, N., Sateriano, A., Salvati, L., 2017. Land quality, sustainable development and environmental degradation in agricultural districts: A computational approach based on entropy indexes. *Environmental Impact Assessment Review* 64, 37-46. <https://doi.org/10.1016/j.eiar.2017.01.003>
- Zambon, I., Benedetti, A., Ferrara, C., Salvati, L., 2018. Soil matters? A multivariate analysis of socioeconomic constraints to urban expansion in Mediterranean Europe. *Ecological Economics* 146, 173-183. <https://doi.org/10.1016/j.ecolecon.2017.10.015>
- Zasada, I., Loibl, W., Berges, R., Steinnocher, K., Köstl, M., Piorr, A., Werner, A., 2013. Rural–urban regions: A spatial approach to define urban–rural relationships in Europe. In *Peri-urban futures: Scenarios and models for land use change in Europe*, pp. 45-68, Springer, Berlin, Heidelberg.
- Zhou, T., Kennedy, E., Koomen, E., van Leeuwen, E. S., 2020. Valuing the effect of land use change on landscape services on the urban–rural fringe. *Journal of Environmental Planning and Management* 63(13), 2425-2445. <https://doi.org/10.1080/09640568.2020.1726732>



---

## SHORT COMMUNICATION

---

# SOIL EROSION TRIGGERED BY THE ARCHEOLOGICAL EXCAVATION AND CONSERVATION OF TRENCHES. THE CASE OF “CERRO DE LAS TRINCHERAS” IN BAILÉN (JAÉN, SPAIN). AN OPEN DISCUSSION

JESÚS RODRIGO-COMINO<sup>1\*</sup> , JUAN JESÚS PADILLA FERNÁNDEZ<sup>2</sup> ,  
ARTEMI CERDÀ<sup>3</sup> 

<sup>1</sup>*Departamento de Análisis Geográfico Regional y Geografía Física, Facultad de Filosofía y Letras, Campus Universitario de Cartuja, Universidad de Granada, 18071 Granada, Spain.*

<sup>2</sup>*Grupo de Investigación Reconocido Estudios de Prehistoria en la Península Ibérica (GIR PrehUSAL), Dpto. de Prehistoria, Historia Antigua y Arqueología. Universidad de Salamanca, Spain.*

<sup>3</sup>*Soil Erosion and Degradation Research Group, Department de Geografia, Universitat de València, Blasco Ibàñez, 28, 46010, Valencia, Spain.*

**ABSTRACT.** Gully erosion is a landform developed due to accelerated soil erosion rates. Gullies can be identified by human impacts on geomorphological processes, as well as hydrological and erosional systems. In Spain, the trenches or "trincheras" from the Spanish Civil War (1936-1939) are considered of archaeological interest for several reasons. At Cerro de las Trincheras in Bailén (Jaén, Spain), a trench was built during the Spanish Civil War. In 2020, an archaeological excavation took place to restore the ruins, triggering the development of gullies and rills and a decrease in vegetation quality. We present a first approximation of the variations in vegetation cover and the decrease in quality (using NDVI, the normalized difference vegetation index) due to the trench acting as a gully (1956, 2005-2020) and the increase in rills and gullies after the excavation. We strongly advocate for future archaeological excavations to include a protocol (soil mapping, vegetation survey, and hydrological connectivity index) to reduce soil degradation and prevent damage to vegetation and associated ecosystems, thereby curbing the increase in soil erosion rates.

***Erosión del suelo provocado por la excavación arqueológica y conservación de trincheras. El caso del “Cerro de las Trincheras” (Bailén, Jaén, España). Una discusión abierta***

**RESUMEN.** Las cárcavas son formas de relieve desarrolladas por tasas aceleradas de erosión del suelo. Las cárcavas pueden identificar los impactos humanos sobre los procesos geomorfológicos y los sistemas hidrológicos y erosivos. En España, las trincheras pertenecientes a la Guerra Civil (1936-1939) se consideran de interés arqueológico por varias razones. En el Cerro de las Trincheras de Bailén (Jaén, España) se construyó una trinchera durante la Guerra Civil Española y en 2020 se llevó a cabo una excavación arqueológica para restaurar las ruinas, lo que desencadenó el desarrollo de cárcavas y regueros, y un empeoramiento del estado de la cubierta vegetal próxima. Presentamos una aproximación de las posibles variaciones de la cubierta vegetal y su disminución de calidad (mediante el NDVI, índice de vegetación de diferencia normalizada) debido a la presencia de la trinchera actuando como cárcava (1956, 2005-2020) y al aumento de surcos y cárcavas tras la excavación alrededor. Reclamamos firmemente que futuras

excavaciones arqueológicas deben incluir un protocolo (cartografía de suelos, estudio de vegetación y el uso de índices de conectividad hidrológica) para reducir la degradación del suelo y evitar el daño a la vegetación y a los ecosistemas asociados que provocan el aumento de las tasas de erosión del suelo.

**Keywords:** Trenches, soil conservation, land management, archeology, gullies, erosion.

**Palabras clave:** Trincheras, conservación del suelo; gestión del territorio, arqueología, cárcavas; erosión.

Received: 17 May 2023

Accepted: 30 October 2023

**\*Corresponding author:** Departamento de Análisis Geográfico Regional y Geografía Física, Facultad de Filosofía y Letras, Campus Universitario de Cartuja, Universidad de Granada, 18071 Granada, Spain. E-mail: [jesusrc@ugr.es](mailto:jesusrc@ugr.es)

## 1. The “trincheras” (trenches) as monuments defeating natural areas recovery and Enhancing gully erosion

Trenches were structures of warfare, where soldiers would dig long, narrow ditches in the ground to shield themselves from enemy fire. The trenches were frequently filled with mud and water, making living conditions extremely challenging for soldiers. They were often interconnected by a network of tunnels and heavily fortified with barbed wire, sandbags, and machine guns (Hutchinson *et al.*, 2008). The soldiers would spend weeks or even months in the trenches, facing constant danger from enemy fire, disease, and harsh living conditions (Dunkley *et al.*, 2011). The fighting in the trenches was often brutal and close quarters, with soldiers using bayonets, grenades, and other hand-to-hand combat techniques (Marshall *et al.*, 2016). Trench warfare was a significant factor in the stalemate of World War I, as neither side could make significant gains without suffering heavy casualties. The war eventually ended with the signing of the Armistice on November 11, 1918, bringing an end to the fighting and leading to the eventual collapse of the Central Powers (Gilbert, 2016).

The Spanish Civil War was an armed conflict that took place between 1936 and 1939 in Spain, and the use of trenches was widespread during the three years of war. The war was primarily fought between the forces of the Spanish Republican government and the Nationalist ones led by General Francisco Franco, who initiated the conflict with a "Coup d'État" involving part of the Spanish Army. The conflict was complex and multifaceted, with political, economic, and social factors contributing to its outbreak. The Spanish Civil War was a turning point in Spanish history, and its impact on the country's political, social, and cultural landscape was profound (Gonzalez Ruibal, 2023). The war resulted in the establishment of a military dictatorship under Franco, which lasted until his death in 1975. During the conflict, numerous defensive fighting positions (DFPs) were designed (González-Ruibal, 2007; 2023). One of the most famous types of defensive fighting positions (DFP) constructed as earthworks were the "trincheras" (translation of trenches). They were large enough holes to hide from one to a fire team unit. They are also similar to the *Tobruk*, defined by the Italian army in Libya, foxholes or fighting holes used by U.S. soldiers, fire trench by the British, and gun and fighting pits by the Australian or New Zealand forces, respectively.

As archaeological monuments, the “trincheras” from the Spanish Civil War have several advantages, including the preservation of historical heritage. These “trincheras” serve as a tangible reminder of a significant event in Spain's history. By conserving these monuments, future generations will be able to understand and appreciate the country's past. Moreover, they can promote tourism, as

many people may be interested in learning about history and visiting historical sites. Conserving the “trincheras” from the Spanish Civil War can attract tourists, thereby helping to boost local economies and provide employment opportunities (López Martínez *et al.*, 2020). On the other hand, they can foster national identity as they are part of Spain's cultural heritage, supporting a sense of national identity and pride among Spaniards. Finally, they could provide educational opportunities for schools and universities. By visiting these monuments, students can learn about the events of the war, the people who fought in it, and its impact on Spanish society, serving as memorials to those who lost their lives during the conflict. Preserving these remains can honor those who were involved in the Civil War.

Trenches are similar to a specific soil erosion feature: gullies. In geomorphology, a gully is a landform characterized by a steep-sided channel cut into the Earth's surface by the erosive action of water (Bocco, 1991; Castillo *et al.*, 2012). Gullies are typically found in areas with steep slopes and high intensity rainfall events on usually bare soils or modified by intensive human changes, where water runoff can rapidly erode the soil and create deep channels (Gómez-Gutiérrez *et al.*, 2009; Nadal-Romero *et al.*, 2014). Gullies can vary in size from small incisions in the soil to large channels that span several meters wide and deep (Arabameri *et al.*, 2019; Casalí *et al.*, 2003; De Ploey, 1991). Gullies can form through a variety of processes, including concentrated runoff, landslides, or the collapse of underground channels (pipes). Therefore, gullies can have significant implications for soil erosion, land degradation, and sediment transport. Gullies identify changes in the landscape and are formed when there are alterations in vegetation and soil properties (Amare *et al.*, 2019; Prosser and Soufi, 1998; Vanwalleghem *et al.*, 2005). The study of gullies and their formation processes are an important area of research in geomorphology, environmental science, and land management (Kirkby and Bracken, 2009; Rodrigo-Comino *et al.*, 2017). There is a lack of assessment and monitoring research on gully formation as a consequence of trenches and archaeological excavation.

Therefore, this note provides information about the “trincheras” (trenches) and their environmental impact. We use the example of the “Cerro de las Trincheras” located in the municipality of Bailén (province of Jaén, Spain) and demonstrate that archaeological excavation could be contributing to high soil erosion rates that should be controlled. We discuss the need to consider restoration (or not) of these archaeological sites and propose strategies to mitigate environmental impact, especially focusing on vegetation restoration and soil erosion, during and after archaeological restoration.

## 2. Cerro de las Trincheras (Bailén, Spain): Study site

We use Cerro de las Trincheras, Bailén (Andalusia), as a pilot area where cultural heritage and landscape management are under discussion. The study site is situated in the north of the province of Jaén within the municipalities of Bailén and Baños de la Encina, with an elevation of 400 m above sea level (Fig. 1).

The Rumblar River flows from the town of Baños de la Encina into the Guadalquivir River. Within the Rumblar River, a reservoir has been built, whose area presents archaeological remains of great importance, such as the Peñalosa site, or historical events of great magnitude in contemporary history, such as the Battle of Bailén (1808). This area is close to Sierra Morena and is considered the natural path to enter Andalusia from the Spanish altiplano (Meseta), serving as the gateway to communication routes from the north. It has geological formations of marly sandstones, marls, and conglomerates, as well as a large outcrop of metamorphic slates and sandstones in the area of the Rumblar basin, all oriented in a NE-SW direction. The vegetation is dominated by holm oaks (*Quercus Ilex*) and wild olives (*Olea europaea var. Sylvestris*), with extensive cultivation of olive trees of the Picual variety. The Cerro de las Trincheras is a small mountain located in the Dehesa de Burguillos, a public forest belonging to the municipality of Bailén, bordering with that of Baños de la Encina. This area covers 9.55 ha and is situated next to the Rumblar River. This location was a strategic point for controlling the passage of the upper course of the Rumblar River.

The “trincheras” found in the municipality of Bailén form a defensive system excavated into the rock, with a length of around 400 meters and an undulating route. It comprises two machine gun nests and lookout points, situated at the western end of the trench and another towards the middle, both currently filled with soil and featuring a circular plan delimited with a rock overlay area. They have a width of 1.60 meters and an estimated depth of 1.80 meters, according to fortification manuals on the battlefield. Various drains have been excavated inside the trenches, utilizing the terrain's inclination and also constructed directly into the rock (granite, sandstones, etc.) (López Martínez *et al.*, 2020).

The undulating route presented by the trench in question is designed to prevent a potential enemy overrun of the defensive line. In the event of having to engage in direct combat on the created parapet, this design ensures that there is no straight shot for enemy forces, reducing the likelihood of causing numerous casualties among the defending forces (Merino Chica, 2021). In addition, it is a place of shelter in case of artillery fire.

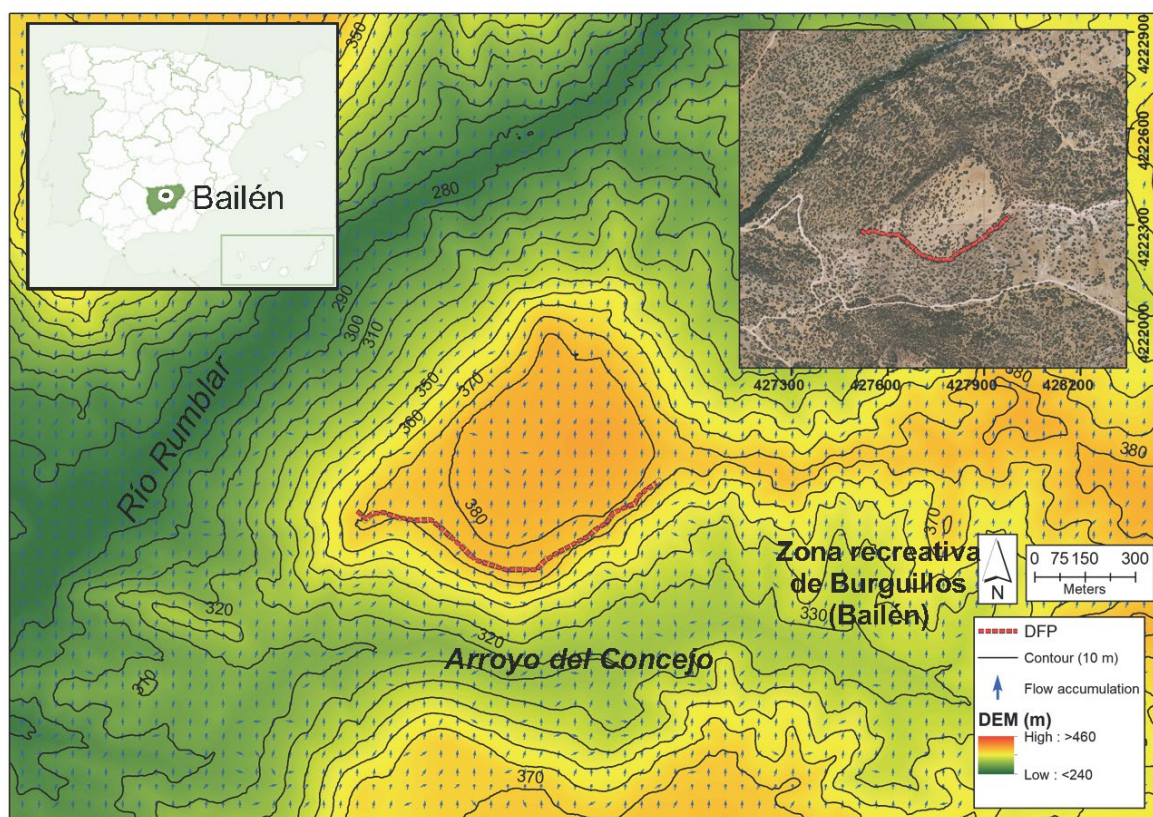


Figure 1. Location, topography, and hypothetical flow accumulation direction of the Cerro de las Trincheras and DFP (defensive fighting positions, “trinchera”).

### 3. Results obtained from a first approach

In figure 2, different historical aerial photos (1957, 2005, 2006, 2007, 2011 and 2020) are shown to inform about the evolution.

The latest available aerial photograph is from 2020, the year when the archaeological excavation commenced. In this last aerial photograph, it can be observed that the southern part of the area exhibits bare soil and barren vegetation cover compared to the northern part. The southern section of the gully remains bare, displaying soil erosion features. However, as shown in figure 3, soil erosion features are present near the trincheras with bare soils, rills, and gullies, forming a landscape resembling badlands. The lack of vegetation serves as evidence of land degradation processes, especially considering that this

area was managed under a restoration plan related to natural ecosystems by the township and province deputation. We utilized the Auravant app from Buenos Aires, Argentina (<https://www.auravant.com>) to assess the NDVI (normalized difference vegetation index) trends using Sentinel 2 images from 2015 to May 2023. The NDVI values range from 0 to 1, with lower values representing worse results and values close to 1 indicating better ones. We observed a decrease in vegetation status from 2015 to 2023, with this reduction intensifying from 2020 when the excavations began (Fig. 4). This decline serves as evidence of the impact of the excavation process.

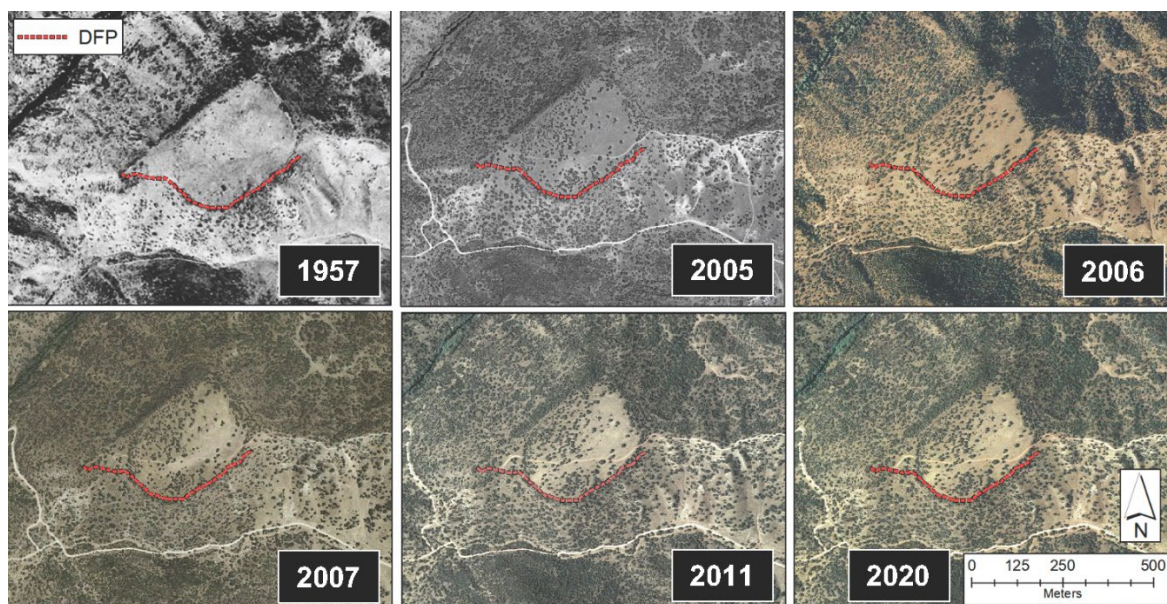


*Figure 2. Aerial photography dataset of the Cerro de las Trincheras and near areas. The length of the trincheras (DFP) is marked with red colour.*



*Figure 3. Rills triggered by the archeological excavation at the Cerro de las Trincheras.*

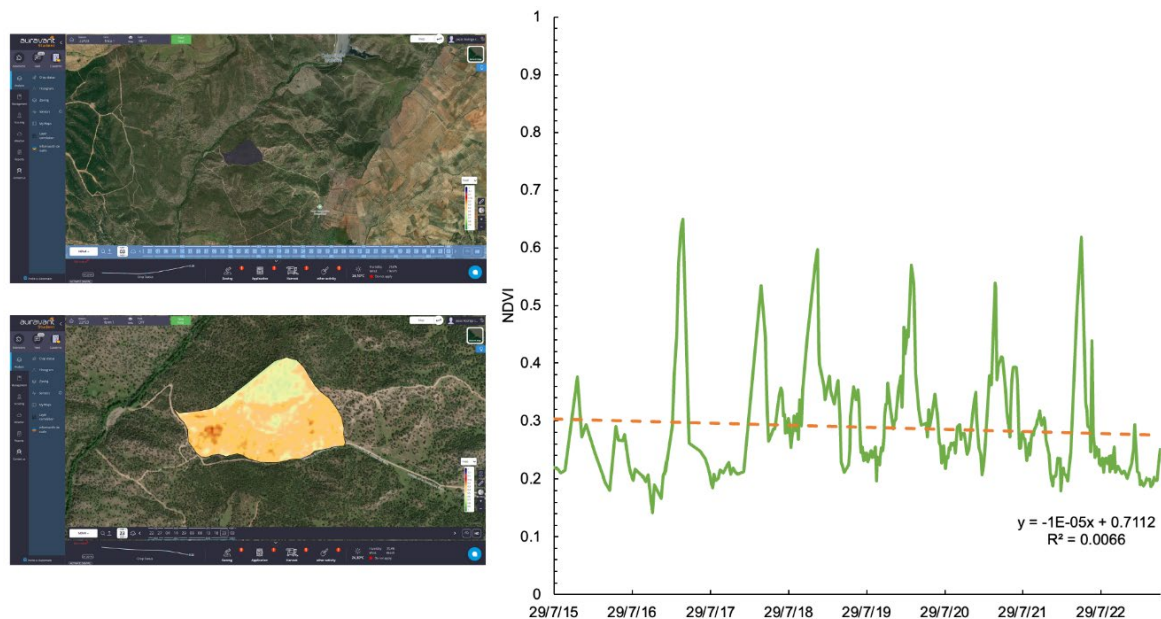


Figure 4. Screenshots of Auravant (Buenos Aires, Argentina) internet application and NDVI (normalized difference vegetation index) trend analysis.

#### 4. Final remarks: The restoration of war trenches. An open discussion

The question of whether it is ethical to conserve Spanish Civil War monuments is a complex and contentious issue that has been debated for many years (Owley and Phelps, 2018). On one hand, these monuments are important historical places, sites, and spaces belonging to the memorial landscape that serve as a reminder of a nation's past and should be preserved for future generations (Sheehan and Speights-Binet, 2019). Others may argue that these monuments are symbols of racism, oppression, and supremacy, and should be removed or destroyed (Evans, 2021). This debate is not unique to the Spanish Civil War, as other societies have also discussed this issue. As scientists, it is challenging to express opinions or beliefs without considering data or highlighting visual processes, as the impacts could be irreparable.

In Spain, many of the Civil War monuments were erected during the mid-20th century, a period when Spain was grappling with issues of racial inequality and segregation. These monuments were not only intended to commemorate the war but also to promote a particular view of history and reinforce specific types of supremacist ideas (Ferrándiz, 2019; González-Ruibal, 2007). For this reason, many people argue that these monuments are not simply historical artifacts but rather symbols of oppression that promote inequality (Delgado, 2015; Labanyi, 2007). In recent years, there has been a growing movement to remove these monuments from public spaces and place them in museums or other locations where they can be studied in their proper historical context. Ultimately, whether or not it is ethical to preserve Civil War monuments is a complex and multifaceted issue that involves considerations of history, culture, and social justice. There is no easy answer, and citizens have different opinions based on their own experiences, beliefs, and political opinions. It is clear that wars resulted in geomorphological changes due to the trenches, bombing, use of heavy vehicles, and the construction of infrastructures (Waga *et al.*, 2022). Valjavec *et al.*, (2018) found in the Kras Plateau (Slovenia) a hundred kilometers of I WW trenches. The recovery of this cultural heritage shows that some trenches and bomb craters are today gone due to sedimentation or human use of the land. Remote sensing and GIS become the most used methodology such as Koch and EL-Baz (1998) already claimed after the Gulf War in Kuwait. Most of the impact of a war on the landforms is lost after some decades due to natural processes such as erosion or soil development (Kiernan, 2015; Thestorf and Makki, 2022). The

impact of the war on vegetation cover and dynamics results in changes in soil erosion with higher erosion rates such as we found at the research site here and Abdo (2018) in Syria. Almohamad (2020) also studied in Syria the impact of the vegetation changes because of the war and conclude that there was a development of soil erosion features such as gullies and rill due to the lack of vegetation. Another recent example is the current Israel and Palestine or Ukraine war and Russian conflict is experiencing. The devastating consequences in a country on soil quality (Rawtani *et al.*, 2022) with previous land degradation issues (Stebelsky, 2015) can be environmentally irreparable.

In our research, we confirm that there is a lack of vegetation during the archaeological excavation that caused the increase in soil erosion, as evidenced by the gullies shown. It is already known that the lack of vegetation induces high erosion rates, and vegetation is commonly used to control soil erosion in agricultural land or reduce soil sealing, serving as a nature-based solution (Fini *et al.*, 2017; Keesstra *et al.*, 2018). We propose that during the archeological excavation, a cover of vegetation or mulches will be used to reduce the soil erosion rates, a solution that it was insisted to be considered since several years ago (Barnett *et al.*, 1967). Also, as Dmytruk *et al.*, (2023) mentioned the foreseen negative impacts of the Ukraine conflict, an accurate diagnosis pre- and post-excavations demands details at the scale at which war operated. They highlight a lack of information, coincident with Southern Spain, specifically the absence of a soil map at least 1:10000 scale, which is necessary to design a predictive model and be able to manage the land correctly (Rodrigo-Comino *et al.*, 2018). Therefore, we strongly propose that future archaeological excavations should include a protocol (soil mapping, vegetation survey, and hydrological connectivity) to reduce soil degradation and avoid damage to the vegetation and associated ecosystems, which can trigger an increase in soil erosion rates.

## Acknowledgements

The first author would like to thank his uncle, Mr. Francisco Javier Comino Oriola to organize the field excursion to the Cerro de las Trincheras and other ones around the wonderful landscapes of Jaén province.

## References

- Abdo, H.G., 2018. Impacts of war in Syria on vegetation dynamics and erosion risks in Safita area, Tartous, Syria. *Reg. Environ. Change* 18, 1707-1719. <https://doi.org/10.1007/s10113-018-1280-3>
- Almohamad, H., 2020. Impact of Land Cover Change Due to Armed Conflicts on Soil Erosion in the Basin of the Northern Al-Kabeer River in Syria Using the RUSLE Model. *Water* 12, 3323. <https://doi.org/10.3390/w12123323>
- Amare, S., Keesstra, S., van der Ploeg, M., Langendoen, E., Steenhuis, T., Tilahun, S., 2019. Causes and Controlling Factors of Valley Bottom Gullies. *Land* 8, 141. <https://doi.org/10.3390/land8090141>
- Arabameri, A., Cerda, A., Tiefenbacher, J.P., 2019. Spatial Pattern Analysis and Prediction of Gully Erosion Using Novel Hybrid Model of Entropy-Weight of Evidence. *Water* 11, 1129. <https://doi.org/10.3390/w11061129>
- Barnett, A.P., Diseker, E.G., Richardson, E.C., 1967. Evaluation of mulching methods for erosion control on newly prepared and seeded highway backslopes. *Agron. J.* 59, 83-85. <https://doi.org/10.2134/agronj1967.00021962005900010026x>
- Bocco, G., 1991. Gully erosion: processes and models. *Prog. Phys. Geogr. Earth Environ.* 15, 392-406. <https://doi.org/10.1177/030913339101500403>
- Casalí, J., López, J.J., Giráldez, J.V., 2003. A process-based model for channel degradation: application to ephemeral gully erosion. *Catena* 50, 435-447. [https://doi.org/10.1016/S0341-8162\(02\)00127-3](https://doi.org/10.1016/S0341-8162(02)00127-3)
- Castillo, C., Pérez, R., James, M.R., Quinton, J.N., Taguas, E.V., Gómez, J.A., 2012. Comparing the accuracy of several field methods for measuring gully erosion. *Soil Sci. Soc. Am. J.* 76, 1319-1332. <https://doi.org/10.2136/sssaj2011.0390>

- De Ploey, J., 1991. Gullying of drainage basins: analysis and predictions made by the Es model. *Bull. Soc. Geogr. Liege* 27, 69-76.
- Delgado, M.M., 2015. Memory, Silence, and Democracy in Spain: Federico García Lorca, the Spanish Civil War, and the Law of Historical Memory. *Theatre J.* 67, 177-196.
- Dmytruk, Y., Cherlinka, V., Cherlinka, L., Dent, D., 2023. Soils in war and peace. *Int. J. Environ. Stud.* 80, 380-393. <https://doi.org/10.1080/00207233.2022.2152254>
- Dunkley, R., Morgan, N., Westwood, S., 2011. Visiting the trenches: Exploring meanings and motivations in battlefield tourism. *Tour. Manag.* 32, 860-868. <https://doi.org/10.1016/j.tourman.2010.07.011>
- Evans, S.Z., 2021. The Removal of Confederate Monuments: Reflections on Power and Privilege in Shared Spaces. *Soc. Sci. Q.* 102, 1044-1055. <https://doi.org/10.1111/ssqu.12965>
- Ferrándiz, F., 2019. Unburials, Generals, and Phantom Militarism: Engaging with the Spanish Civil War Legacy. *Curr. Anthropol.* 60, S62-S76. <https://doi.org/10.1086/701057>
- Fini, A., Frangi, P., Mori, J., Donzelli, D., Ferrini, F., 2017. Nature based solutions to mitigate soil sealing in urban areas: Results from a 4-year study comparing permeable, porous, and impermeable pavements. *Environ. Res.* 156, 443-454. <https://doi.org/10.1016/j.envres.2017.03.032>
- Gilbert, M., 2016. *La Primera Guerra Mundial*. 15a Edición Aniversario. Madrid.
- Gómez-Gutiérrez, Á., Schnabel, S., Felicísimo, A.M., 2009. Modelling the occurrence of gullies in rangelands of southwest Spain. *Earth Surf. Process. Landf.* 34, 1894-1902. <https://doi.org/10.1002/esp.1881>
- González-Ruibal, A., 2007. Making things public: Archaeologies of the Spanish Civil War. *Public Archaeol.* 6, 203-226. <https://doi.org/10.1179/175355307X264165>
- Gonzalez Ruibal, A., 2023. *Tierra arrasada: Un viaje por la violencia del Paleolítico al siglo XXI*. Crítica. Barcelona.
- Hutchinson, D.J., Diederichs, M., Pehme, P., Sawyer, P., Robinson, P., Puxley, A., Robichaud, H., 2008. Geomechanics stability assessment of World War I military excavations at the Canadian National Vimy Memorial Site, France. *Int. J. Rock Mech. Min. Sci.* 45, 59-77. <https://doi.org/10.1016/j.ijrmms.2007.04.014>
- Keesstra, S., Nunes, J., Novara, A., Finger, D., Avelar, D., Kalantari, Z., Cerdà, A., 2018. The superior effect of nature based solutions in land management for enhancing ecosystem services. *Sci. Total Environ.* 610-611, 997-1009. <https://doi.org/10.1016/j.scitotenv.2017.08.077>
- Kiernan, K., 2015. Nature, Severity and Persistence of Geomorphological Damage Caused by Armed Conflict. *Land Degrad. Dev.* 26, 380-396. <https://doi.org/10.1002/ldr.2216>
- Kirkby, M.J., Bracken, L.J., 2009. Gully processes and gully dynamics. *Earth Surf. Process. Landf.* 34, 1841-1851. <https://doi.org/10.1002/esp.1866>
- Labanyi, J., 2007. Memory and Modernity in Democratic Spain: The Difficulty of Coming to Terms with the Spanish Civil War. *Poet. Today* 28, 89-116. <https://doi.org/10.1215/03335372-2006-016>
- López Martínez, J.J., Moreno Oronato, A., Arboleda Martínez, L., Padilla Fernández, J.J., 2020. Puesta en valor del patrimonio histórico y natural del Monte público de Burguillos (Bailén, Jaén). *Locuber* 25-39.
- Marshall, M.T., Petrelli, D., Dulake, N., Not, E., Marchesoni, M., Trenti, E., Pisetti, A., 2016. Audio-based narratives for the trenches of World War I: Intertwining stories, places and interaction for an evocative experience. *Int. J. Hum.-Comput. Stud., Data Sonification and Sound Design in Interactive Systems* 85, 27-39. <https://doi.org/10.1016/j.ijhcs.2015.08.001>
- Merino Chica, J.A., 2021. Estructuras defensivas de la Guerra Civil Española en la localidad de Bailén (Jaén). (Final degree thesis). University of Granada, Granada.
- Nadal-Romero, E., Petrlic, K., Verachtert, E., Bochet, E., Poesen, J., 2014. Effects of slope angle and aspect on plant cover and species richness in a humid Mediterranean badland. *Earth Surf. Process. Landf.* 39, 1705-1716. <https://doi.org/10.1002/esp.3549>
- Owley, J., Phelps, J., 2018. Understanding the Complicated Landscape of Civil War Monuments. *Indiana Law J. Suppl.* 93, 15.

- Prosser, I.P., Soufi, M., 1998. Controls on gully formation following forest clearing in a humid temperate environment. *Water Resour. Res.* 34, 3661-3671. <https://doi.org/10.1029/98WR02513>
- Rawtani, D., Gupta, G., Khatri, N., Rao, P.K., Hussain, C.M., 2022. Environmental damages due to war in Ukraine: A perspective. *Sci. Total Environ.* 850, 157932. <https://doi.org/10.1016/j.scitotenv.2022.157932>
- Rodrigo-Comino, J., Wirtz, S., Brevik, E.C., Ruiz-Sinoga, J.D., Ries, J.B., 2017. Assessment of agri-spillways as a soil erosion protection measure in Mediterranean sloping vineyards. *J. Mt. Sci.* 14, 1009-1022. <https://doi.org/10.1007/s11629-016-4269-8>
- Rodrigo-Comino, J., Senciales, J.M., Cerdà, A., Brevik, E.C., 2018. The multidisciplinary origin of soil geography: A review. *Earth-Sci. Rev.* 177, 114-123. <https://doi.org/10.1016/j.earscirev.2017.11.008>
- Sheehan, R., Speights-Binet, J., 2019. Negotiating strategies in New Orleans's memory-work: white fragility in the politics of removing four Confederate-inspired monuments. *Journal of Cultural Geography* 36, 346-367. <https://doi.org/10.1080/08873631.2019.1641996>
- Stebelsky, I., 2015. *Soil Management in Ukraine: Responding to Environmental Degradation*. Can. Slavon. Pap.
- Thestorf, K., Makki, M., 2022. Soils and landforms of war — Pedological investigations 75 years after World War II. *Geomorphology* 407, 108189. <https://doi.org/10.1016/j.geomorph.2022.108189>
- Valjavec, M.B., Zorn, M., Ribeiro, D., 2018. Mapping War Geoheritage: Recognising Geomorphological Traces of War. *Open Geosci.* 10, 385-394. <https://doi.org/10.1515/geo-2018-0030>
- Vanwalleghem, T., Poesen, J., Nachtergaele, J., Verstraeten, G., 2005. Characteristics, controlling factors and importance of deep gullies under cropland on loess-derived soils. *Geomorphology* 69, 76-91. <https://doi.org/10.1016/j.geomorph.2004.12.003>
- Waga, J.M., Szypuła, B., Fajer, M., 2022. Heritage of War: Analysis of Bomb Craters Using Lidar (kędzierzyn-Koźle, Poland) 593-608.





---

## BOOK REVIEW

---

Shit, P.K., Pourghasemi, H.R., Bhunia, G.S. (Eds.), 2020. *Gully Erosion Studies from India and Surrounding Regions*. Advances in Science, Technology & Innovation. Springer International Publishing. <https://doi.org/10.1007/978-3-030-23243-6>

It is well-known that erosion is a big concern for humankind because it threatens soils affecting fertility or biodiversity among other issues (Borrelli *et al.*, 2017; García-Ruiz *et al.*, 2015). The books published about this topic are diverse and try to focus on specific shapes or landforms, which is also helpful for the readers characterized by plenty of interest to learn and apply new geomorphological knowledge. However, the publications of materials devoted to covering land degradation processes focused on large territories such as a group of countries or specific continents are scarce and possibly also interesting for other scientists coming from other disciplines. Soil erosion should not be considered only at the hillslope or watershed scale, but also at a global process affecting large areas such as different countries that share among them similar environmental conditions or human activities (Lal, 2001; Poesen, 2018; Rodrigo-Comino *et al.*, 2018).

Under this above-mentioned consideration, I started to read this book recently published about one hot topic highly discussed nowadays, gully erosion (GE). Gullies and other associate processes such as rills, interrills, ravines or landslides among others are considered by scholars one of the most important manifestations of land degradation processes over the world, because they represent an extreme mobilisation of sediments, water and associated nutrients, irremediably, in many cases, irreparable (Arabameri *et al.*, 2020; Casali *et al.*, 2006; Martínez-Casasnovas *et al.*, 2009). However, GE also remarks on evidence of the past to understand the current landscapes. In chapter 26 (Hosseinalizadeh *et al.*, 2020), the authors insist that GE act as “one of the few geomorphological evidence of a past soil erosion which reflects the impacts of environmental changes on the landscape”. I fully agree that this is key for land managers and policymakers because it allows producing medium-scale erosion susceptibility maps that may help to mitigate the “environmental and socioeconomic-related challenges of soil erosion”, even contributing to achieving some SDGs (Sustainable Development Goals) such as SDSs 1 (No poverty), 2 (Zero hunger), 3 (Good health and well-being), 6 (Clean water and sanitation), and 11 (sustainable cities and communities) (Abdulkadir *et al.*, 2020).

I was surprised to read the alarming statement by Kumar *et al.* (2020) for Indian ravines on the need to pay attention to the "realistic assessment of the policy gap by a dedicated agency especially related to tenure provision, illegal land occupation and land use policy". It is disappointing to observe how this book presents the negative impacts of GE affecting, for example, aquatic environments (Kar *et al.*, 2020; Mahala, 2020) or plant biodiversity (Kala *et al.*, 2020) and the lack of governmental plans to solve them. Therefore, I can understand that one of the most important conclusions of this book is that further research and more work related to awareness is necessary. Fortunately, I consider that this book probably contains brilliant material to introduce, review and give context about the detection and remediation of areas affected by GE, considering India and surrounding countries as examples that can be extrapolated for other countries over the world. Therefore, I would strongly encourage policymakers and land planners to read this book too.

I will not go into too much detail, but shortly I would want to pick out the most important parts of the book, some conclusions and novel topics discussed. Firstly, it is highly appreciated that the authors

include a wide range spectrum of modelling techniques to show how GE can be assessed. Random forest model, diverse-based runoff-sediment yield modelling, Bayesian weight of evidence, machine learning algorithms or the traditional RUSLE, SWAT or MARS models among others. On the other hand, I also consider that they are well-performed experiments and in situ measurements that present novel results. One example is presented in chapter 18 using flume experiments. The results give new insights on how to assess GE and understand plant responses that could be included to develop control measures paying special attention to the roots of about <1 mm in diameter with unequal impact on soil anti-scourability (Shit *et al.*, 2020a). It is also impressive the field measurements conducted by Islam *et al.*, (2020) and Joshi (2020) using pins or a self-made microprofilometer to estimate the cross-sectional profiles of several gullies inserted into an expanding gully network.

On the other hand, I also want to discuss some aspects to be mentioned in future editions or further research conducted by the authors and editors. Dedicating a chapter related to gullies intentionally built for agricultural drainages (e.g. Agri-spillways; Rodrigo-Comino *et al.*, 2017) or urban areas (e.g. Informal urban patterns; Adediji *et al.*, 2013) would fill an important gap. Discussing how well the authors can deal with it using these well-explained modelling techniques and *in situ* measurements would be appreciated from my point of view. As a geographer, I also miss a final or introductory chapter related to the whole studied area, summarizing the differences or similarities among countries and regions. It would give a global perspective for potential solutions or policies to be designed in Southern and Western Asia. This idea could also be materialised in the form of a review paper joining all the results obtained in this book.

To conclude, I consider that if you liked other books such as “Gully Erosion Under Global Change” (Li *et al.*, 2004), “Gully Erosion and Management Methods and Application: A field Manual” (Singh and Dubey, 2002), the book chapters written by Rădoane and Rădoane, (2017), Aber *et al.* (2010) and Poesen *et al.* (2006), or the review papers by Bocco, (1991), Castillo and Gómez (2016) and Kertész and Gergely (2011), you will highly appreciate the read of Gully Erosion Studies from India and Surrounding Regions by (Shit *et al.*, 2020b) as scientist, policymaker or land planner.

## References

- Abdulkadir, T.S., Muhammad, R.U.M., Okeola, O.G., Khamaruzaman, W.Y., Adelodun, B., Aremu, S.A., 2020. Spatial Analysis and Prediction of Soil Erosion in a Complex Watershed of Cameron Highlands, Malaysia. In: P.K. Shit, H.R. Pourghasemi, G.S. Bhunia (Eds.), *Gully Erosion Studies from India and Surrounding Regions*. Advances in Science, Technology & Innovation. Springer International Publishing, Cham, pp. 461-477. [https://doi.org/10.1007/978-3-030-23243-6\\_31](https://doi.org/10.1007/978-3-030-23243-6_31)
- Aber, J.S., Marzloff, I., Ries, J.B., 2010. Chapter 13 - Gully Erosion Monitoring. In: J.S. Aber, I. Marzloff, J.B. Ries (Eds.), *Small-Format Aerial Photography*. Elsevier, pp. 193-200, Amsterdam. <https://doi.org/10.1016/B978-0-444-53260-2.10013-4>
- Adediji, A., Jeje, L.K., Ibitoye, M.O., 2013. Urban development and informal drainage patterns: Gully dynamics in Southwestern Nigeria. *Applied Geography* 40, 90-102. <https://doi.org/10.1016/j.apgeog.2013.01.012>
- Arabameri, A., Cerda, A., Pradhan, B., Tiefenbacher, J.P., Lombardo, L., Bui, D.T., 2020. A methodological comparison of head-cut based gully erosion susceptibility models: Combined use of statistical and artificial intelligence. *Geomorphology* 359, 107136. <https://doi.org/10.1016/j.geomorph.2020.107136>
- Bocco, G., 1991. Gully erosion: processes and models. *Progress in Physical Geography: Earth and Environment* 15, 392-406. <https://doi.org/10.1177/030913339101500403>
- Borrelli, P., Robinson, D.A., Fleischer, L.R., Lugato, E., Ballabio, C., Alewell, C., Meusburger, K., Modugno, S., Schütt, B., Ferro, V., Bagarello, V., Oost, K.V., Montanarella, L., Panagos, P., 2017. An assessment of the global impact of 21st century land use change on soil erosion. *Nature Communications* 8. <https://doi.org/10.1038/s41467-017-02142-7>

- Casalí, J., Loizu, J., Campo, M.A., De Santisteban, L.M., Álvarez-Mozos, J., 2006. Accuracy of methods for field assessment of rill and ephemeral gully erosion. *CATENA* 67, 128-138. <https://doi.org/10.1016/j.catena.2006.03.005>
- Castillo, C., Gómez, J.A., 2016. A century of gully erosion research: Urgency, complexity and study approaches. *Earth-Science Reviews* 160, 300-319. <https://doi.org/10.1016/j.earscirev.2016.07.009>
- García-Ruiz, J.M., Beguería, S., Nadal-Romero, E., González-Hidalgo, J.C., Lana-Renault, N., Sanjuán, Y., 2015. A meta-analysis of soil erosion rates across the world. *Geomorphology* 239, 160-173. <https://doi.org/10.1016/j.geomorph.2015.03.008>
- Hosseinalizadeh, M., Alinejad, M., Mohammadian Behbahani, A., Khormali, F., Kariminejad, N., Pourghasemi, H.R., 2020. A Review on the Gully Erosion and Land Degradation in Iran. In: P.K. Shit, H.R. Pourghasemi, G.S. Bhunia, (Eds.), *Gully Erosion Studies from India and Surrounding Regions*. Advances in Science, Technology & Innovation. Springer International Publishing, Cham, pp. 393-403. [https://doi.org/10.1007/978-3-030-23243-6\\_26](https://doi.org/10.1007/978-3-030-23243-6_26)
- Islam, A., Sarkar, B., Das, B.C., Barman, S.D., 2020. Assessing Gully Asymmetry Based on Cross-Sectional Morphology: A Case of Gangani Badland of West Bengal, India. In: P.K. Shit, H.R. Pourghasemi, G.S. Bhunia (Eds.). *Gully Erosion Studies from India and Surrounding Regions*. Advances in Science, Technology & Innovation. Springer International Publishing, Cham, pp. 69-92. [https://doi.org/10.1007/978-3-030-23243-6\\_5](https://doi.org/10.1007/978-3-030-23243-6_5)
- Joshi, V.U., 2020. Application of Field-Monitoring Techniques to Determine Soil Loss by Gully Erosion in a Watershed in Deccan, India. In: P.K. Shit, H.R. Pourghasemi, G.S. Bhunia (Eds.). *Gully Erosion Studies from India and Surrounding Regions*. Advances in Science, Technology & Innovation. Springer International Publishing, Cham, pp. 109-131. [https://doi.org/10.1007/978-3-030-23243-6\\_7](https://doi.org/10.1007/978-3-030-23243-6_7)
- Kala, S., Singh, A.K., Rao, B.K., Meena, H.R., Rashmi, I., Singh, R.K., 2020. Bamboo-Based Technology for Resource Conservation and Management of Gullied Lands in Central India. In: P.K. Shit, H.R. Pourghasemi, G.S. Bhunia (Eds.). *Gully Erosion Studies from India and Surrounding Regions*. Advances in Science, Technology & Innovation. Springer International Publishing, Cham, pp. 307-319. [https://doi.org/10.1007/978-3-030-23243-6\\_19](https://doi.org/10.1007/978-3-030-23243-6_19)
- Kar, A., Chini, D.S., Bhattacharya, M., Das, B.K., Patra, B.C., 2020. Impacts of Gully Erosion on River Water Quality and Fish Resources: A Case Study. In: P.K. Shit, H.R. Pourghasemi, G.S. Bhunia (Eds.), *Gully Erosion Studies from India and Surrounding Regions*. Advances in Science, Technology & Innovation. Springer International Publishing, Cham, pp. 345-355. [https://doi.org/10.1007/978-3-030-23243-6\\_22](https://doi.org/10.1007/978-3-030-23243-6_22)
- Kertész, Á., Gergely, J., 2011. Gully erosion in Hungary, review and case study. *Procedia - Social and Behavioral Sciences, The 2nd International Geography Symposium-Mediterranean Environment 2010* 19, 693-701. <https://doi.org/10.1016/j.sbspro.2011.05.187>
- Lal, R., 2001. Soil degradation by erosion. *Land degradation & development* 12, 519-539. <https://doi.org/10.1002/ldr.472>
- Li, Y., Poesen, J., Valentin, C., 2004. *Gully Erosion Under Global Change*. Sichuan Science and Technology Press.
- Mahala, A., 2020. Land Degradation Processes of Silabati River Basin, West Bengal, India: A Physical Perspective. In: P.K. Shit, H.R. Pourghasemi, G.S. Bhunia (Eds.), *Gully Erosion Studies from India and Surrounding Regions*. Advances in Science, Technology & Innovation. Springer International Publishing, Cham, pp. 265-278. [https://doi.org/10.1007/978-3-030-23243-6\\_16](https://doi.org/10.1007/978-3-030-23243-6_16)
- Martínez-Casasnovas, J.A., Ramos, M.C., García-Hernández, D., 2009. Effects of land-use changes in vegetation cover and sidewall erosion in a gully head of the Penedès region (northeast Spain). *Earth Surface Processes and Landforms* 34, 1927-1937. <https://doi.org/10.1002/esp.1870>
- Poesen, J., 2018. Soil erosion in the Anthropocene: Research needs. *Earth Surface Processes and Landforms* 43, 64-84. <https://doi.org/10.1002/esp.4250>
- Poesen, J., Vanwalleggem, T., Vente, J. de, Knapen, A., Verstraeten, G., Martínez-Casasnovas, J.A., 2006. Gully Erosion in Europe. In: *Soil Erosion in Europe*. John Wiley & Sons, Ltd, pp. 515-536. <https://doi.org/10.1002/0470859202.ch39>

- Rădoane, M., Rădoane, N., 2017. Gully Erosion. In: M. Radoane, A. Vespremeanu-Stroe (Eds.), *Landform Dynamics and Evolution in Romania*. Springer Geography. Springer International Publishing, Cham, pp. 371-396. [https://doi.org/10.1007/978-3-319-32589-7\\_16](https://doi.org/10.1007/978-3-319-32589-7_16)
- Rodrigo-Comino, J., Senciales, J.M., Cerdà, A., Brevik, E.C., 2018. The multidisciplinary origin of soil geography: A review. *Earth-Science Reviews* 177, 114-123. <https://doi.org/10.1016/j.earscirev.2017.11.008>
- Rodrigo-Comino, J., Wirtz, S., Brevik, E.C., Ruiz-Sinoga, J.D., Ries, J.B., 2017. Assessment of agri-spillways as a soil erosion protection measure in Mediterranean sloping vineyards. *J. Mt. Sci.* 14, 1009-1022. <https://doi.org/10.1007/s11629-016-4269-8>
- Shit, P.K., Pourghasemi, H.R., Bhunia, G.S., 2020a. Role of Plant Roots to Control Rill-Gully Erosion: Hydraulic Flume Experiment. In: P.K. Shit, H.R. Pourghasemi, G.S. Bhunia (Eds.), *Gully Erosion Studies from India and Surrounding Regions*. Advances in Science, Technology & Innovation. Springer International Publishing, Cham, pp. 295-306. [https://doi.org/10.1007/978-3-030-23243-6\\_18](https://doi.org/10.1007/978-3-030-23243-6_18)
- Shit, P.K., Pourghasemi, H.R., Bhunia, G.S. (Eds.), 2020b. *Gully Erosion Studies from India and Surrounding Regions*. Advances in Science, Technology & Innovation. Springer International Publishing. <https://doi.org/10.1007/978-3-030-23243-6>
- Singh, S., Dubey, A., 2002. *Gully Erosion and Management Methods and Application: A Field Manual*. New Academic Publishers.

**JESÚS RODRIGO-COMINO** 

*Departamento de Análisis Geográfico Regional y Geografía Física,  
Facultad de Filosofía y Letras, Campus Universitario de Cartuja,  
Universidad de Granada, 18071 Granada, Spain*

## **Administración / Administration**

---

Universidad de La Rioja  
Servicio de Publicaciones  
Piscinas, 1, 26006 LOGROÑO (España)  
Tel.: (+34) 941299187 Fax: (+34) 941299193  
Correo-e: publicaciones@unirioja.es

## **Edición electrónica / E-Journal**

---

EISSN: 1697-9540  
<http://publicaciones.unirioja.es/revistas/cig>  
cig@unirioja.es

## **Indización y Calidad / Indexation and Quality Analysis**

---

Bases de Datos y Recursos para el análisis de la calidad de las revistas científicas /  
Databases and Resources for the analysis of the Scientific Journal's Quality:

CARHUS Plus+ 2018	Latindex (Catálogo)
CIRC (EC3 Metrics)	MIAR (Matriz de Información para el Análisis de Revistas)
Dialnet Métricas (Fundación Dialnet)	Periodicals Index Online (ProQuest)
DOAJ (Directory of Open Access Journals)	SCIMAGO Journal & Country Rank (SJR)
ERIH Plus (European Science Fundation)	Scopus (Elsevier)
ESCI, Emerging Sources Citation Index (Web of Science™, Clarivate Analytics)	Sello de Calidad FECYT
Fuente Académica Plus (EBSCO)	

## **Política del editor sobre copyright y autoarchivo**

---

- Sólo se puede archivar la versión final del editor/PDF.
- En el sitio web del autor o repositorio institucional o cualquier repositorio designado por los organismos financiadores a petición de dichos organismos o como resultado de una obligación legal desde el momento de su publicación.
- El uso debe ser no comercial, no permitiéndose obras derivadas.
- La fuente editorial debe reconocerse. Debe incluirse la declaración establecida por el editor: “Publicado originalmente en *Cuadernos de Investigación Geográfica / Geographical Research Letters* en [volumen y número, o año], por la Universidad de La Rioja (España)”.
- Debe enlazar a la versión del editor con la inclusión del número DOI a partir de la siguiente frase: “La publicación original está disponible en *Cuadernos de Investigación Geográfica / Geographical Research Letters* a partir de [http://doi.org/\[DOI\]](http://doi.org/[DOI])”.

## **Publisher copyright & self-archiving policies**

---

- Authors may self-archive publisher's version of the article (final PDF version) on their own websites.
- Authors may also deposit this version of the article in institutional or funder repositories, at the request of the fundind organizations or as a result of legal obligation after publication.
- The final published version can only be used for non-commercial purposes. Derivative work is not allowed.
- Acknowledgement to the original source of publication must be given as follows: “First published in *Cuadernos de Investigación Geográfica / Geographical Research Letters* in [volume and number, or year] by Universidad de La Rioja (Spain)”.
- A link must be inserted to the published article on the journal's website by including the DOI number of the article in the following sentence: “The final publication is available at *Cuadernos de Investigación Geográfica / Geographical Research Letters* via [http://doi.org/\[DOI\]](http://doi.org/[DOI])”.

---

**Cuadernos de Investigación Geográfica / *Geographical Research Letters***  
*A scientific journal of Physical Geography*

---



CUADERNOS DE INVESTIGACIÓN GEOGRÁFICA  
GEOGRAPHICAL RESEARCH LETTERS

TOMO 49 (2), Año 2023

*Número monográfico: Riesgos de degradación del suelo: temas clave para afrontar en el mundo*

**Special issue: Land degradation risks: Key topics to be faced over the world**

**Jesús Rodrigo-Comino, Casandra Muñoz-Gómez, Mohammad Reza Rahdari, Luca Salvati.** Land degradation risks: Key topics to be faced over the world

**Masoud Masoudi, Elham Asrari, Somaye Razaghi, Fatemeh Karimi, Artemi Cerdà.** A new proposed model of EMOLUP for assessing of ecological capability of different utilizations and land use planning in Sepidan Township, Iran

**Jesús Rodrigo-Comino, José María Senciales-González, Ana Pérez Albarracín, Erick R. Bandala, Francisco Escrivá Saneugenio, Saskia D. Keesstra, Artemi Cerdà.** Circulation weather types as a key factor on runoff initiation and sediment detachment in Mediterranean shrublands

**Ahmed Abed Gatea Al-Shammery, Nabil Raheem Lahmod, Jesús Fernández-Gálvez, Andrés Caballero-Calvo.** Effect of tillage systems combined with plastic film mulches and fertilizers on soil physical properties in a wheat-agricultural site in southern Iraq

**Abdessamed Derdour, Antonio Jodar-Abellán, Amparo Melian-Navarro, Ryan Bailey.** Assessment of land degradation and droughts in an arid area using drought indices, modified soil-adjusted vegetation index and Landsat remote sensing data

**Pedro Simón Lamprea-Quiroga, Omar Jaramillo-Rodríguez, Wladimir Mejía Ayala.** Soil erosion due to rainfall and the impacts of climate change in an Andean Highland in Colombia

**Nazanin Mohammadzade Miyab, Ramin Fazloul, Manouchehr Heidarpour, Ataollah Kavian, Jesús Rodrigo-Comino.** Surveying three-dimensional perspectives of the flow structure around the bridge pile depending on the vegetation pattern distribution

**Rafael Córdoba Hernández, Federico Camerin.** Assessment of ecological capacity for urban planning and improving resilience in the European framework. An approach based on the Spanish case

**Vito Imbrenda, Casandra Muñoz Gomez, Mariagrazia D'Emilio, Caterina Samela, Luca Salvati, Nadia Matarazzo, Maria Lanfredi, Rosa Coluzzi.** Remote sensing and spatial databases for investigating latent urban-rural dynamics in rural, inland districts of Southern Italy

**COMUNICACIONES CORTAS / SHORT COMMUNICATIONS**

**Jesús Rodrigo-Comino, Juan Jesus Padilla Fernández, Artemi Cerdà.** Soil erosion triggered by the archeological excavation and conservation of trenches. The case of "Cerro de las trincheras" in Bailén (Jaén, Spain). An open discussion

**RECENSIONES / BOOK REVIEW**

